

EXPERIMENTAL DESIGN AND MODELING OF A  
CONTINUOUS COUNTERFLOW SOLID-SOLID  
HEAT TRANSFER PROCESS

BY

SHYH-JYE CHERN

Bachelor of Science in Chemical Engineering  
National Taipei Institute of Technology  
Taipei, Taiwan  
1978

Master of Engineering in Chemical Engineering  
West Virginia Institute of Technology  
Montgomery, West Virginia  
1985

Submitted to the Faculty of the  
Graduate College of the  
Oklahoma State University  
in Partial Fulfillment of  
the Requirements for  
the Degree of  
Doctor of Philosophy  
July 1989

Thesis  
1989D  
CSSI &  
Cop. 2

EXPERIMENTAL DESIGN AND MODELING OF A  
CONTINUOUS COUNTERFLOW SOLID-SOLID  
HEAT TRANSFER PROCESS

Thesis Approved:

Arland H. Johannes

Thesis Advisor

KAMBASO

John C. Cline

Mark L. ...

Norman R. Durham

Dean of the Graduate College

## ACKNOWLEDGEMENTS

I would like to take this opportunity to express my deep appreciation to my advisor, Dr. A.H. (A.J.) Johannes, for his valuable guidance and long-term support and help in enabling me to complete my PH.D. requirements. His great patience and encouragement has always been a constant source of inspiration to me and he makes me feel like family. I also would like to express my appreciation to Dr. M.L. Stone for suggesting this interesting topic to me, providing support to build the experimental apparatus and laboratory as well as the helpful advice given me during this research work. Other committee members performed a different and important role in my PH.D. program and I like to express my appreciation to them. Members of my committee other than Professor Johannes and Professor Stone, were Dr. K.J. Bell, Dr. M.M. Johnson, and Dr. B. Clary. I would also like to thank Dr. K.G. Gasem and Dr. R. Erbar for agreeing to be on my final examination committee.

Since the design and construction of an experimental apparatus was an integral portion of this research, a great amount of construction, and maintenance work needed to be done at the agricultural engineering laboratory. I would like to thank the following people for their help during

these experimental studies: Wen, for managing whatever I needed whenever I needed it; Van Swift, for construction of the experimental apparatus; Bruce Lambert, for development of the instrumentation and electronic devices required for this experiment; and other people in the laboratory for helping in whatever was required.

A special note of thanks is due to Mr. Chatis Herabut, one of my best friends, for the unforgettable friendship, encouragement and his help in taking the photos of the experimental apparatus. I am also thankful to Mr. Charles Baker, laboratory manager, for his help given to me during the experimental work, and to all the wonderful secretaries in my department for their kindness in all things. Special thanks are due to my department for the financial support I received over the period of my studies. I feel I have made many friends during my stay here and I appreciate the support of these friendships. In addition, I like to express my appreciation for their encouragement and assistance I have received during the course of this work.

Family always plays a very important role in any long-term effort such as this. I would like to express my deep gratitude to my parents, my sister, my brother and my uncle as well as all the other family members for their love, encouragement, and constant support throughout my stay in Stillwater. A special thanks is due to my girl friend for her encouragement and love. In addition, I would like to dedicate this work and the honor to my mother. I would not

have today's accomplishments without her greatest love and encouragement to me at all times.

## TABLE OF CONTENTS

Chapter	Page
I. INTRODUCTION .....	1
II. LITERATURE REVIEW .....	7
Various Process Designs on solid-solid heat transfer .....	7
Fundamental Studies of Heat Transfer in Solids .....	18
Studies of Residence Time Distribution. Models Applicable to Residence Time Distribution .....	31
Residence Time for Rotary Drums...	38
Recent studies of the RTD with the Heat Transfer.....	41
III. EXPERIMENTAL SYSTEM DESIGN .....	44
Bench Scale Experimental Design with Initial Conceptual Ideas .....	44
Experimental Apparatus and Materials ..	48
Central Component .....	52
Accessory Components .....	55
Heat Transfer Materials .....	57
Computerized Measurement System .....	57
Instrumentation Design for Temperature Measurement.....	58
Data Acquisition System Design ...	61
Experimental Variables .....	66
Experimental Procedures .....	67
Methods .....	67
Residence Time Test.....	70
Heating Test.....	71
IV. MATHEMATICAL MODEL DEVELOPMENT .....	74
Residence Time Model .....	75
Heat Transfer Model .....	77
Modeling Approach with Computer Algorithms.....	82

Chapter	Page
V. RESULTS AND DISCUSSIONS .....	88
Experimental Findings and Analyses for Residence Time.....	88
Heat Transfer System .....	95
Experimental Findings .....	97
Modeling Findings and Analyses ...	115
VI. CONCLUSIONS AND RECOMMENDATIONS .....	124
Conclusions .....	124
Recommendations .....	128
BIBLIOGRAPHY .....	134
APPENDIXES.....	140
APPENDIX A - EQUATIONS USED FOR MODELING CALCULATIONS .....	141
APPENDIX B - LISTINGS OF COMPUTER SOURCE PROGRAMS .....	144
APPENDIX C - CALCULATIONS FOR OPERATING VARIABLES .....	157
APPENDIX D - EXPERIMENTAL DATA GRAPHS .....	159



## LIST OF TABLES

Table	Page
I. The Experimental Stimulus-Response Data for Drum Speeds of 2, 1, 0.5, and 0.25 rpm ....	89
II. The Moment and Model Analysis for Drum Speeds of 2, 1, 0.5, and 0.25 rpm .....	89
III. Experimental Conditions for the Runs Performed .....	95
IV. System Operating Parameters for the Selected Runs Performed .....	115
V. The Results of System Parameters for the Modeling Tests Performed .....	116

## LIST OF FIGURES

Figure	Page
1. A Counterflow Solid-Solid Heat Exchanger Using a Third Stream of Solid as the Media .....	15
2. A Counterflow Solid-Solid Heat Exchanger Using a Third Stream of Liquid as the Media .....	16
3. A Counterflow Solid-Solid Heat Exchanger Using Heat Pipes as the Media .....	17
4. Schematic Diagram of the Fractional Tubularity Model .....	33
5. Schematic Diagram of the Tanks-in-Series Model..	34
6. Schematic Diagram of Tanks-in-Series with Backflow Model .....	35
7. Flow Patterns in a Stirred Tank and Related Circulation Model .....	37
8. Angle of Repose of Particles in a Flighted Rotary Drum .....	40
9. Coverage of Drum by Falling Particles .....	42
10. Conceptual Representation of a Counterflow Solid Heating Process with Heat Recovery .....	46
11. Physical Representation of a Counterflow Heat Exchanger Using an Inclined Drum .....	47
12. Physical Representation of a Counterflow Heat Exchanger Equipped with Fixed Plates .....	49
13. Schematic Flow Diagram of a Counterflow Solid-Solid Heat Transfer Process .....	50
14. Detail Drawings of the Components for the Counterflow Heat Transfer Process .....	51

Figure	Page
15. A Bench-Scale Counterflow Heat Exchanger .....	53
16. Thermocouples' Locations Inside the Drum .....	59
17. Schematic Diagram for a Data Acquisition System .....	62
18. A Drawing for the DT-707T Terminal Panel .....	64
19. A Physical Representation for the Stagewise Heat Transfer Process .....	79
20. The Experimental Residence Time for a Drum Speed of 2 rpm .....	91
21. The Experimental Residence Time for a Drum Speed of 1 rpm .....	91
22. The Experimental Residence Time for a drum Speed of 0.5 rpm .....	92
23. The Experimental Residence Time for a Drum Speed of 0.25 rpm .....	92
24. The Experimental Plot of Dimensionless Variance and Mean Residence Time vs. Drum Speed .....	93
25. The Temperature Profiles of Prop as a Function of Time Along the Axial Direction for Run #2 ....	98
26. The Temperature Profiles of Prop as a Function of Time Along the Axial Direction for Run #2 ....	98
27. The Temperature Profiles of Prop as a Function of Time Along the Axial Direction for Run #2 ....	99
28. The Temperature Profiles of Prop as a Function of Time Along the Axial Direction for Run #2 ....	99
29. The Temperature Profiles of Prop as a Function of Time Along the Axial Direction for Run #2 ....	100
30. The Temperature Profiles of Prop as a Function of Time Along the Axial Direction for Run #2 ....	100
31. The Temperature Profiles of Prop as a Function of Time Along the Axial Direction for Run #2 ....	101
32. The Temperature Profiles of Prop as a Function of Time Along the Axial Direction for Run #7 ....	102

Figure	Page
33. The Temperature Profiles of Prop as a Function of Time Along the Axial Direction for Run #7 ....	102
34. The Temperature Profiles of Prop as a Function of Time Along the Axial Direction for Run #7 ....	103
35. The Temperature Profiles of Prop as a Function of Time Along the Axial Direction for Run #7 ....	103
36. The Temperature Profiles of Prop as a Function of Time Along the Axial Direction for Run #7 ....	104
37. The Temperature Profiles of Prop as a Function of Time Along the Axial Direction for Run #7 ....	104
38. The Temperature Profiles of Prop as a Function of Time Along the Axial Direction for Run #7 ....	105
39. The Temperature Profiles of Prop as a Function of Time Along the Axial Direction for Run #7 ....	105
40. The Temperature Profiles of Prop as a Function of Time Along the Axial Direction for Run #7 ....	106
41. The Temperature Profiles of Prop as a Function of Time Along the Axial Direction for Run #7 ....	106
42. Temperatures of Prop vs. Time Inside the Hopper and Inlet Port of Drum for Run #2 .....	107
43. Temperature of Prop vs. Time Inside the Hopper and Inlet Port of Drum for Run #7 .....	107
44. Outlet Temperatures of Soybean vs. Time for Run #1 .....	108
45. Outlet Temperatures of Soybean vs. Time for Run #2 .....	108
46. Outlet Temperatures of Soybean vs. Time for Run #3 .....	109
47. Outlet Temperatures of Soybean vs. Time for Run #4 .....	109
48. Outlet Temperatures of Soybean vs. Time for Run #5 .....	110
49. Outlet Temperatures of Soybean vs. Time for Run #6 .....	110

Figure	Page
50. Outlet Temperatures of Soybean vs. Time for Run #7 .....	111
51. Feed Rates of Prop vs. Time for Run #2 .....	112
52. Feed Rates of Prop vs. Time for Run #7 .....	112
53. Average Soybean Outlet Temperature Profile vs. Conveyer Speed .....	117
54. Average Soybean Outlet Temperature Profile vs. Drum Speed .....	117
55. Temperature Profiles for the Modeling Performed( One Phase, Drum at 2 rpm ).....	119
56. Temperature Profiles for the Modeling Performed( One Phase, Drum at 0.25 rpm ).....	119
57. Temperature Profiles for the Modeling Performed (Two Phase, Drum at 2 rpm, at 3 Min. ).....	120
58. Temperature Profiles for the Modeling Performed (Two Phase, Drum at 2 rpm, at 30 Min. ).....	120
59. Temperature Profiles for the Modeling Performed (Two Phase, Drum at 0.25 rpm, at 3 Min. ) ....	121
60. Temperature Profiles for the Modeling Performed (Two Phase, Drum at 0.25 rpm, at 30 Min. ) ...	121
61. Schematic Drawing of a Modified Fixed Plates Inside the Drum.....	131
62. Experimental Temperature Profiles for Run #1 ...	160
63. Experimental Temperature Profiles for Run #1 ...	160
64. Experimental Temperature Profiles for Run #1 ...	161
65. Experimental Temperature Profiles for Run #1 ...	161
66. Experimental Temperature Profiles for Run #1 ...	162
67. Experimental Temperature Profiles for Run #1 ...	162
68. Experimental Temperature Profiles for Run #1 ...	163
69. Experimental Temperature Profiles for Run #1 ...	163
70. Experimental Temperature Profiles for Run #1 ...	164

Figure	Page
71. Experimental Temperature Profiles for Run #1 ...	164
72. Experimental Temperature Profiles for Run #1 ...	165
73. Experimental Temperature Profiles for Run #1 ...	165
74. Experimental Temperature Profiles for Run #1 ...	166
75. Experimental Temperature Profiles for Run #1 ...	166
76. Experimental Temperature Profiles for Run #1 ...	167
77. Experimental Temperature Profiles for Run #1 ...	167
78. Experimental Temperature Profiles for Run #1 ...	168
79. Experimental Temperature Profiles for Run #1 ...	168
80. Experimental Temperature Profiles for Run #1 ...	169
81. Experimental Temperature Profiles for Run #1 ...	169
82. Experimental Temperature Profiles for Run #1 ...	170
83. Experimental Temperature Profiles for Run #1 ...	170
84. Experimental Temperature Profiles for Run #1 ...	171
85. Feed Rates of Prop for Run #1 .....	171
86. Experimental Temperature Profiles for Run #3 ...	172
87. Experimental Temperature Profiles for Run #3 ...	172
88. Experimental Temperature Profiles for Run #3 ...	173
89. Experimental Temperature Profiles for Run #3 ...	173
90. Experimental Temperature Profiles for Run #3 ...	174
91. Experimental Temperature Profiles for Run #3 ...	174
92. Experimental Temperature Profiles for Run #3 ...	175
93. Experimental Temperature Profiles for Run #3 ...	175
94. Experimental Temperature Profiles for Run #3 ...	176
95. Feed Rates of Prop for Run #3 .....	176
96. Experimental Temperature Profiles for Run #4 ...	177

Figure	Page
97. Experimental Temperature Profiles for Run #4 ...	177
98. Experimental Temperature Profiles for Run #4 ...	178
99. Experimental Temperature Profiles for Run #4 ...	178
100. Experimental Temperature Profiles for Run #4 ...	179
101. Experimental Temperature Profiles for Run #4 ...	179
102. Experimental Temperature Profiles for Run #4 ...	180
103. Experimental Temperature Profiles for Run #4 ...	180
104. Experimental Temperature Profiles for Run #4 ...	181
105. Experimental Temperature Profiles for Run #4 ...	181
106. Experimental Temperature Profiles for Run #4 ...	182
107. Experimental Temperature Profiles for Run #4 ...	182
108. Experimental Temperature Profiles for Run #4 ...	183
109. Experimental Temperature Profiles for Run #4 ...	183
110. Experimental Temperature Profiles for Run #4 ...	184
111. Experimental Temperature Profiles for Run #4 ...	184
112. Experimental Temperature Profiles for Run #4 ...	185
113. Feed Rates of Prop for Run #4 .....	185
114. Experimental Temperature Profiles for Run #5 ...	186
115. Experimental Temperature Profiles for Run #5 ...	186
116. Experimental Temperature Profiles for Run #5 ...	187
117. Experimental Temperature Profiles for Run #5 ...	187
118. Experimental Temperature Profiles for Run #5 ...	188
119. Experimental Temperature Profiles for Run #5 ...	188
120. Experimental Temperature Profiles for Run #5 ...	189
121. Experimental Temperature Profiles for Run #5 ...	189
122. Experimental Temperature Profiles for Run #5 ...	190

Figure	Page
123. Experimental Temperature Profiles for Run #5 ...	190
124. Experimental Temperature Profiles for Run #5 ...	191
125. Experimental Temperature Profiles for Run #5 ...	191
126. Experimental Temperature Profiles for Run #5 ...	192
127. Feed Rates of Prop for Run #5 .....	192
128. Experimental Temperature Profiles for Run #6 ...	193
129. Experimental Temperature Profiles for Run #6 ...	193
130. Experimental Temperature Profiles for Run #6 ...	194
131. Experimental Temperature Profiles for Run #6 ...	194
132. Experimental Temperature Profiles for Run #6 ...	195
133. Experimental Temperature Profiles for Run #6 ...	195
134. Experimental Temperature Profiles for Run #6 ...	196
135. Experimental Temperature Profiles for Run #6 ...	196
136. Experimental Temperature Profiles for Run #6 ...	197
137. Experimental Temperature Profiles for Run #6 ...	197
138. Experimental Temperature Profiles for Run #6 ...	198
139. Feed Rates of Prop for Run #6 .....	198



## LIST OF SYMBOLS

A	: cross sectional area, ft <sup>2</sup>
C <sub>PB</sub>	: heat capacity of big particles (soybean), btu/lb °F
C <sub>PS</sub>	: heat capacity of small particles (prop), btu/lb °F
d	: particle size, ft
D	: dispersion coefficient, ft <sup>2</sup> /min
D <sub>S</sub>	: diameter of screw, inches
D <sub>P</sub>	: Diameter of pipe, inches
D/uL	: dispersion number
E	: exit age, 1/min
E <sub>θi</sub>	: dimensionless exit age
F	: flow rate, ft <sup>3</sup> /hr
F <sub>0</sub>	: Fourier number
h	: heat transfer coefficient, btu/ft <sup>2</sup> min °F
H <sub>C</sub>	: contact resistance, btu/ft <sup>2</sup> min °F
H	: bed height, ft
k	: particle thermal conductivity, btu/min ft °F
K	: percent trough loading
k <sub>g</sub>	: gas thermal conductivity, btu/min ft °F
L	: length of the drum, ft
L'	: length of the screw, ft
L <sub>P</sub>	: coverage length of the drum by falling particles, ft
m	: mass flow rate of small particles, lb/min

$M$  : mass flow rate of big particles, lb/min  
 $N$  : equivalent stage or tank numbers  
 $N_u$  : Nusselt number  
 $q_{in}$  : heat flow into the system, btu/min  
 $q_{out}$  : heat flow out from the system, btu/min  
 $q_{loss}$  : heat loss to the environment due to convection  
and conduction heat transfer, btu/min  
 $r$  : distance of particle from axis of drum, ft  
 $P$  : pitch of screw, inches  
 $R$  : radius of drum, ft  
 $t$  : time, min  
 $T$  : surface temperature of small particles, °F  
 $T'$  : surface temperature of big particles, °F  
 $T_i$  : Initial temperature of small particles, °F  
 $T'_i$  : Initial temperature of big particles, °F  
 $T_{air}$  : surrounding air temperature, °F  
 $u$  : velocity, ft/min  
 $UA$  : lumped heat transfer coefficient, btu/min °F  
 $UA'$  : lumped heat loss term, btu/min °F  
 $V_B$  : equivalent thermal mass of the system , lb  
 $V_m$  : mass volume of small particles, lb  
 $V_M$  : mass volume of big particles, lb  
 $W_i$  : the mass of particles collected at the drum  
outlet at time period  $\Delta t_i$ , lb  
 $W_T$  : the total mass of particles dumped into the drum  
as an impulse input, lb

Greek letters:

$\sigma^2$	: variance
$\sigma_\theta^2$	: dimensionless variance
$\tau$	: mean residence time, min
$\theta$	: dimensionless time
$\lambda$	: angle of repose, degrees
$\mu$	: coefficient of friction
$\Omega$	: speed of rotation, rpm
$\omega$	: speed of rotation, radians/sec
$\rho$	: density, lb/ft <sup>3</sup>
$\phi$	: angle defining position of particle in drum
$\gamma$	: accommodation coefficient
$\Lambda$	: mean free path of gas molecules, ft
$\alpha$	: thermal diffusivity, ft <sup>2</sup> /min
$\chi$	: contact resistance parameter
$\epsilon$	: bed porosity

## CHAPTER I

### INTRODUCTION

For the purpose of energy saving, it is necessary to economically and uniformly exchange large quantities of heat in a variety of heat transfer processes such as drying, heat treating, freezing, or roasting. Conventional methods using convective air heat exchange and fluidized beds, have been the principal solutions to these problems but have not been necessarily to reach the goals of uniformity and economy.

Air is an attractive heat transfer medium since it can be handled easily and does not contaminate most of the processed materials. However, the thermal conductivity of air is too low to produce high heat transfer rates compared with liquids and solids. In view of this constraint, it is desirable to find an alternate heat transfer method to improve the heat transfer rates, while retaining many of the desirable characteristics associated with gaseous system, such as fluidity, ease of handling, free of contamination, etc.

One possibility to fulfill these requirements is a fluidized bed system. Intensive agitation inside the fluidized bed can be obtained which will reduce temperature gradients to negligible proportions through the bulk of the

bed, thus ensuring uniform temperature control. Many studies (1-4) have shown that high heat transfer rates from the fluid to the particles are obtained and accompanied with a high mass transfer rate. Although fluidized bed systems appear to be a promising alternative because of their high heat transfer rates, They have limited application to the continuous heating or cooling of particulate materials which are encountered in drying, cooling, and thermal disinfection processes. The major shortcoming of applying this technique to heating certain particles of large size ( $>1$  mm) is the high air velocity and relatively high power consumption required to deal with these large and dense particles. It is also difficult to control the residence time uniformity, and separate the particulate materials being heat processed.

Various investigators (5-7) have explored different systems other than the fluidized bed to improve heat transfer efficiency using such methods as spouted beds (5), vibrating beds (6), and rotating beds (7). A new heat transfer method using solid heating medium which can exchange heat uniformly and rapidly with the surfaces of objects immersed in it has been widely investigated by many researchers (7, 8, 9, 10) and appears to be a promising method of heat exchange. The basic principle used for this system is to immerse the particles to be processed in a hot/cold granular material via contact-dominated conduction heat exchange; and to provide continuous agitation and

mixing by means of a mechanical device such as a rotary drum. In this type of system, particles are in direct contact and the interstitial gas has no significant relative motion with respect to the solids. This is substantially different from a fluidized bed where agitation is accomplished by gas movement. In addition, the processed materials can be separated from the heating medium by a sieving process and the entire operation can be made as a batch or continuous flow process. This system is particularly well suited as a heating process for coarse particles of food products due to non-contaminating properties, and ease of residence time control. The same degree of system simplicity, uniformity, low power required for mixing, as well as contact time control would be difficult to duplicate in a fluidized bed system.

In order to optimize the design of a solid-solid heat exchange process, a certain number of parameters must be investigated such as the mechanical properties of the agitating devices, and the fundamental mechanism of particle-particle contact heat exchange. In addition, the porosity of the bed, the type of particles used and the contact times between two particle groups as well as the mixing rate and the residence time are of importance in the heat transfer behavior of the system. The design of the drum itself in terms of the width, length and the presence of the flights, helix or other means of agitation as well as other operating variables such as rotating speed, tilt of

the drum, etc. will control the mixing rate and the residence time directly and thus further influencing the performance of this heat exchange system.

Due to the uniqueness and importance of the solid-solid heat transfer system, a variety of processes utilizing this idea have been explored, designed and constructed. To date, research on this type of heat transfer has concentrated on controlled flow situations. Akpaetok (11) in 1973 built a small dryer to study the effect of hot sand on the performance of the heating process. Raghavan and Harper (12) tested a continuous flow dryer using salt as the heat transfer medium. Teisser and Raghavan (13) also designed and tested a newer version of a particulate bed dryer and used hot sand to dry corn. Recently a new machine design based on the principle of solid heating medium in conduction heat transfer was constructed and tested(7). This process was built with 3 concentric sections to accomplish all the steps of heating, mixing, separating and recirculation in a continuous flow operation. All of the operating designs above can be classified as co-current flow processes which do not have the potential for heat recovery. No work is reported on the counterflow type until the work of Simonton and Stone (9). They explore the potential of a particle-particle heat exchanger in a counterflow discrete manner.

Although a number of solid medium heating units have been built and tested, few have the potential for commercial use, implying that more research and development work is

required in this field. In this study a flighted rotary drum equipped with an inner rotary screw conveyer covered with mesh screen was designed and tested for its performance as a major component of a continuous counterflow solid-solid heat transfer process. The transient temperature profiles of the heating medium along the drum with hot medium immersed and mixed with cold medium were measured. A residence time distribution (RTD) test was conducted to examine the flow pattern of the hot medium inside the rotary drum. In addition, a heat transfer model and a RTD model for this particular process was developed and tested with the experimental data.

A continuous counterflow heat exchanger has the potential for heat recovery and such use is typical in a conventional shell-and-tube heat exchanger system. The major objective of this research was to design, construct and model a bench scale continuous counterflow solid-solid heat exchanger and to evaluate the potential of this new process. Investigations included determining the feasibility of the concept, qualifying performance criteria and comparing the experimental results with those obtained from a theoretical model developed for this research.

The scope of this research emphasized the investigation of the behavior of the rotary drum in terms of particle flow patterns and heat transfer characteristics. Specifically the major goals of this research are:

(i) To design and construct a unique continuous counterflow



solid-solid heat exchanger;

(ii) To obtain transient temperature profiles on the heating medium, trademark of the Norton Alcoa Corp., Ft. Smith, Arkansas (interprop), along the drum and at the inlet and outlet, and of the processed material (soybean);

(iii) To obtain the residence time information of the heating medium inside the rotary drum at a variety of drum speeds;

(iv) To develop a theoretical heat transfer model and a RTD model for this system to determine the transient characteristics in terms of temperature and residence time;

(v) To compare the experimental data with the models to evaluate the primary system parameters such as the lumped heat transfer coefficient, equivalent thermal mass and the lumped heat loss due to convection loss;

(vi) To identify important parameters of this process and quantify the impact of these parameters on the performance of this heating process;

(vii) To determine the feasibility of the concept, quantifying performance criteria and future research directions.

## CHAPTER II

### REVIEW OF LITERATURE

A survey of the recent articles and several related books concerning topics in the previous process designs on the solid-solid heating system, the fundamental heat transfer theories behind this system and the residence time studies has been done for this investigation. This survey of the latest articles was used as a guide for this investigation.

#### Various Process Designs on Solid-Solid Heat Transfer

The heating and cooling of particulate solids is a common process throughout the chemical and food industries. The idea of using solid-solid heat transfer for processing food products came from attempts to use conduction heat transfer for drying grain. Some of the physical devices which perform the heating or cooling actions are based on this mechanism. Of these devices, a great majority are of the indirect heat exchanger type. One of the earlier indirect heating machines is the heated steel plate which was used to heat a thin layer of corn to determine the characteristics of conduction drying at a maximum

temperature of 100 °C by Hall and Hall (14). They found that the rate of drying was directly proportional to the surface temperature of the plate. Finney et al.(15) conducted similar investigations with different heating temperatures(38-77 °C). A conduction heat process composed mainly of horizontal metal plates placed over a fire pit heated to 93 °C for drying rice was reported by Chancellor (16, 17). He suggested that the use of a granular medium such as sand would avoid the problems of localized heating. Khan et al.(18) designed both laboratory and full scale dryers which using a horizontal metal plate for transmitting heat to a stirred bed of grain. In addition, vibrated beds have been investigated by Thomas et al.(6) as heat transfer devices because of the excellent heat transfer characteristics observed between a vibrated bed and its immersed heating surface.

Direct solid-solid heat transfer has been investigated by several researchers(19-21). Huber (19) presented a system to process cereal using a roll mill as the heat transfer device. Aspegran (20) developed a direct solid-solid heat transfer process. In this device heated balls and cool particles are mixed and conveyed by means of rotation, and it separates the solids at the outlet with recirculating and reheating of the balls. Benson (21) designed a solid-solid co-current flow device for processing cereal grains. The machine uses an inclined barrel with an internal perforated screw attached. The heating medium

stays inside the device at all times and is heated through the shell of the barrel. Grain is fed to the lower layer of the barrel, then transported out by the screw, with the heating medium falling back through the screw perforations.

Lengar et al.(22) used hot sand for roasting peas. They also developed a continuous dryer for drying rice using hot sand at 150 °C. Akpaetok (11) tested a batch dryer and a continuous flow dryer and investigated the mechanical parameters of these machines. The influence of flight angle and rotating speed of the drum on residence time using a simple unflighted drum was reported in this work. He concluded that the residence time was roughly proportional to the rotating speed and particle size.

Bateson and Harper (23) designed a solid-solid heat transfer system to process food products. A mixing barrel was used and the mixture was dumped into a vibratory, screened conveyer. The heating medium was separated and was conveyed by a screw back to the barrel. Reheating of the medium was done in the screw conveyer using electrical resistance heating bands.

Raghavan and Harper(12) built a small continuous flow dryer using heated granular salt. The dryer consists of an inclined rotary drum 61 cm in diameter, and 76 cm long, fitted with a perforated helix inside the drum for conveying and separating the grain from the salt. The hot salt falls through the perforations on the helix down to the bottom of the drum. This system thus co-currently performs agitation,

conveying and separation. Salt bed temperatures were varied from 274 to 525 °F, and the residence time was regulated from 4.2 to 21.8 seconds.

Lapp et al. (24-26) investigated drying of rapeseed, wheat and rice. Their experiments involved comparison between particulate media, different temperatures and other parameters. Lapp (27) used heated fine sand and steel balls to investigate the feasibility of drying rapeseed. Initial experimental results suggested that the process was feasible and a continuous flow dryer was developed by Lapp and Manchur (24) to investigate the drying of cereal grains using hot sand. A small bench scale dryer consisting of a rotating drum 18 inches long and 12 inches diameter was originally built to assess the potential for drying. The prototype consists of a rotary drum with a screened separating section at middle-length and 2 hoppers, one for seed and one for sand. This rotating cylinder is 12 ft long, 18 inches in diameter and provides a 4 ft length of insulated drying section, a 2 ft screened separating section and a 4 ft cooling and dry delivery section. Sand and grain were metered into the barrel and this mixture was conveyed along to the center section at which point the heating medium was separated from the mixture and returned to a heated hopper. The outlet section cooled the grain with ambient air. The problem in these systems is to minimize heat loss to the surroundings in the conveying operation since the medium is heated at the exterior of the drum.

Khan et al. (18) designed and built a solid-solid heat transfer device using hot sand at 204 °C to dry rice. This process is similar to the one described above, but neither an external heating hopper nor a cooling section were used. External sweeps on the barrel were used to push the heat transfer medium back to the front after separation at the end of the device. The medium was also reheated during the recirculation. Lapp et al.(25) also investigated the feasibility of applying the principle of a solid heat transfer medium to the drying of rice. A six stage experiment using a maximum temperature of 150 °C, a sand to rice mass ratio of 16:1, and a 2 minute drying time in each stage was conducted.

The drying of wheat with solid heat transfer medium was investigated by Mittal (28). A batch and a continuous flow dryer were designed and used with hot sand as heating medium. Comparative performance tests of different sand sizes and other heating medium were conducted on the batch dryer. The major component of the batch dryer was an aluminum drying bucket 29.3 cm in diameter and 22.9 cm deep. The bucket assembly was mounted on a supporting yoke and the yoke had an angular adjustment to permit selected positioning of the bucket. The bucket was normally positioned upward for loading horizontally and inclined downward for dumping. The continuous dryer consisted of a rotating drum 3.05 m long with a 43.2 cm diameter. The length of dryer was divided into 3 sections: a 1.22 m

insulated drying section, a 0.61 m screened separating section and a 1.22 m cooling and delivery section. The cylinder was driven by a small gear meshing with a larger gear fitted on the rotating cylinder. Adjustable legs were installed on the frame of the machine to control the angle of inclination of the drum. The residence time of the sand and grain in the drying section could be regulated by varying the drum slope, and the rotating speed. Mixing and axial movement of the mixture were assisted by spiral flights fixed to the internal surface of the drum in the drying and cooling section. The screened separation section consisted of steel wire cloth used to separate the sand from the grain. The sand hopper contained electrical heating elements which were used for heating the recycled sand particles.

Mittal et al.(29) described wheat drying using a prototype continuous flow dryer employing a solid heat transfer medium to assess the commercial potential of the process at different grain flow rates. The design of this dryer is similar to that used by Mittal (28).

Richard and Raghavan (30) studied heat transfer mechanisms in rotary units using sand as the heating medium. Tessier and Raghavan (13) tested a newer version of a particulate bed dryer and used hot sand to dry corn. Experimental tests were carried out in a continuous flow unit to determine the potential of this design for drying corn. This unit consists of a rotary drum, 0.69 m in

diameter and 1.8 m long. An annular space of 0.05 m was provided to allow recirculation by gravity of the sand along its length. A second spacing of 0.05 m was provided to allow for the heat transfer between the hot air flow stream and the sand by conduction through the walls. Sand recirculation and separating were achieved by a set of sieves located at each end of the drum. Some of the shortcomings of their drum design such as dealing with water vapor, slow heat transfer from hot air to the sand, etc. was mentioned and possible solutions to the problems were noted in their report.

A new heating process utilizing the principle of continuous operation to dry grains by conductive heat transfer was designed and constructed by Pannu and Raghavan (7). This machine consists of 3 concentric sections: one for heating the medium directly using a hot air stream, another drum for mixing and separation of the two medium, and the one for recirculation. In this process, sand was heated and metered into a closed annular space along with a regulated mass of grain. The mixture was then mixed for a period of time and separated. Heated grain was dispersed into a tank and sand was recirculated for reheating. This machine was designed to accomplish all the above steps in a co-current continuous flow operation. It was reported that the separation was complete for drum angular velocities between 1.6 and 2.6 rad/s.

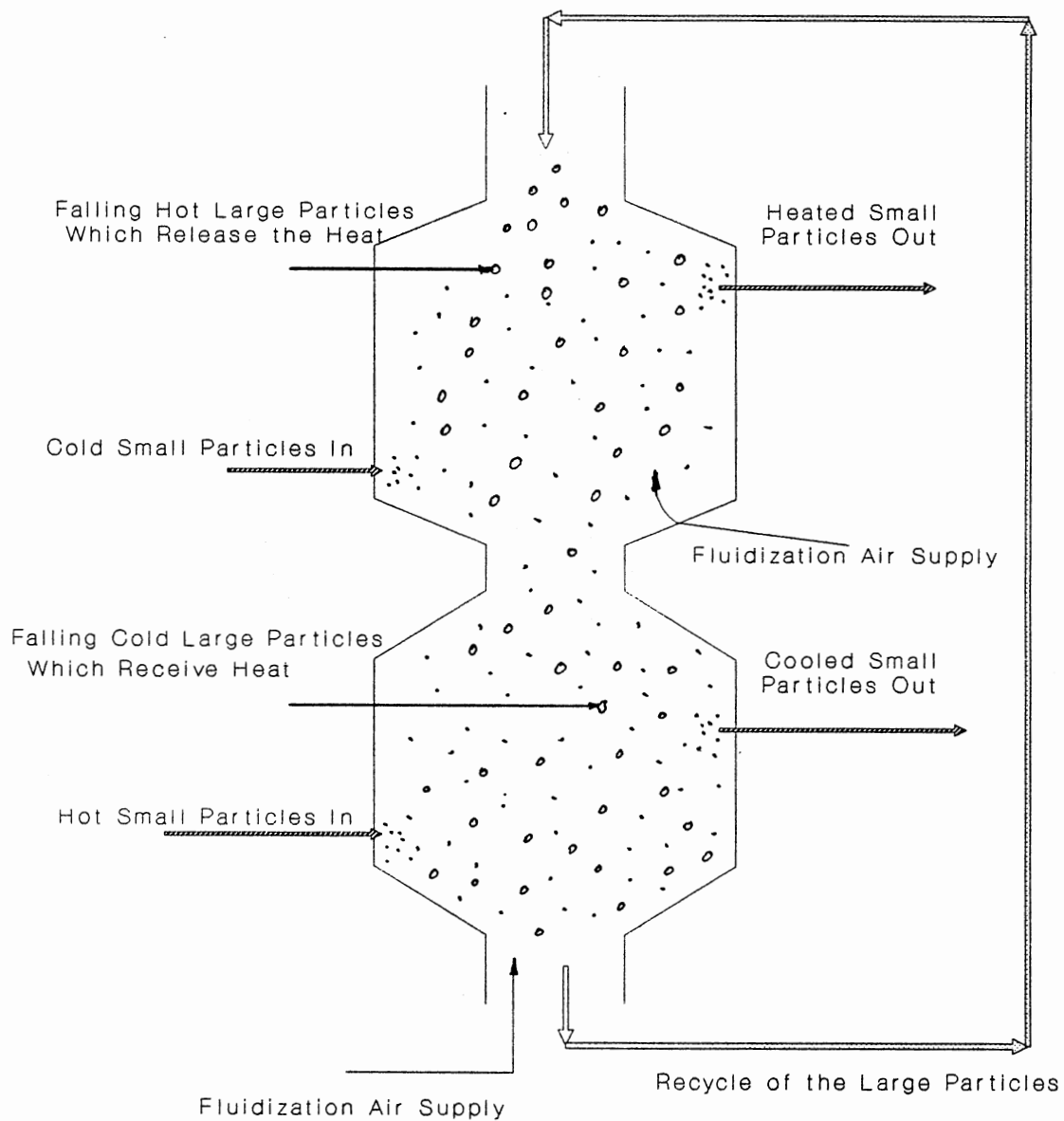
All of the above researchers indicate that a hot



particulate medium can be used to process grains. However, there is no work which has been reported on the design of a counterflow process. One of the possibilities in such a process is that a third stream could be used as a go-between to take up the heat from the hot stream and then deliver it to the cold stream in a countercurrent operation. Figure 1 shows the SPHER process which uses a recirculating solid falling countercurrent through two smaller particles in separate fluidized beds (31). The vigorous backmixing of solids in the fluidized beds results in deviations from the desirable plug flow pattern of solids. Another design uses either highly efficient heat pipes or a liquid stream as a go-between in an arrangement which yields a counterflow heat exchanger as shown in figures 2 and 3 respectively (31).

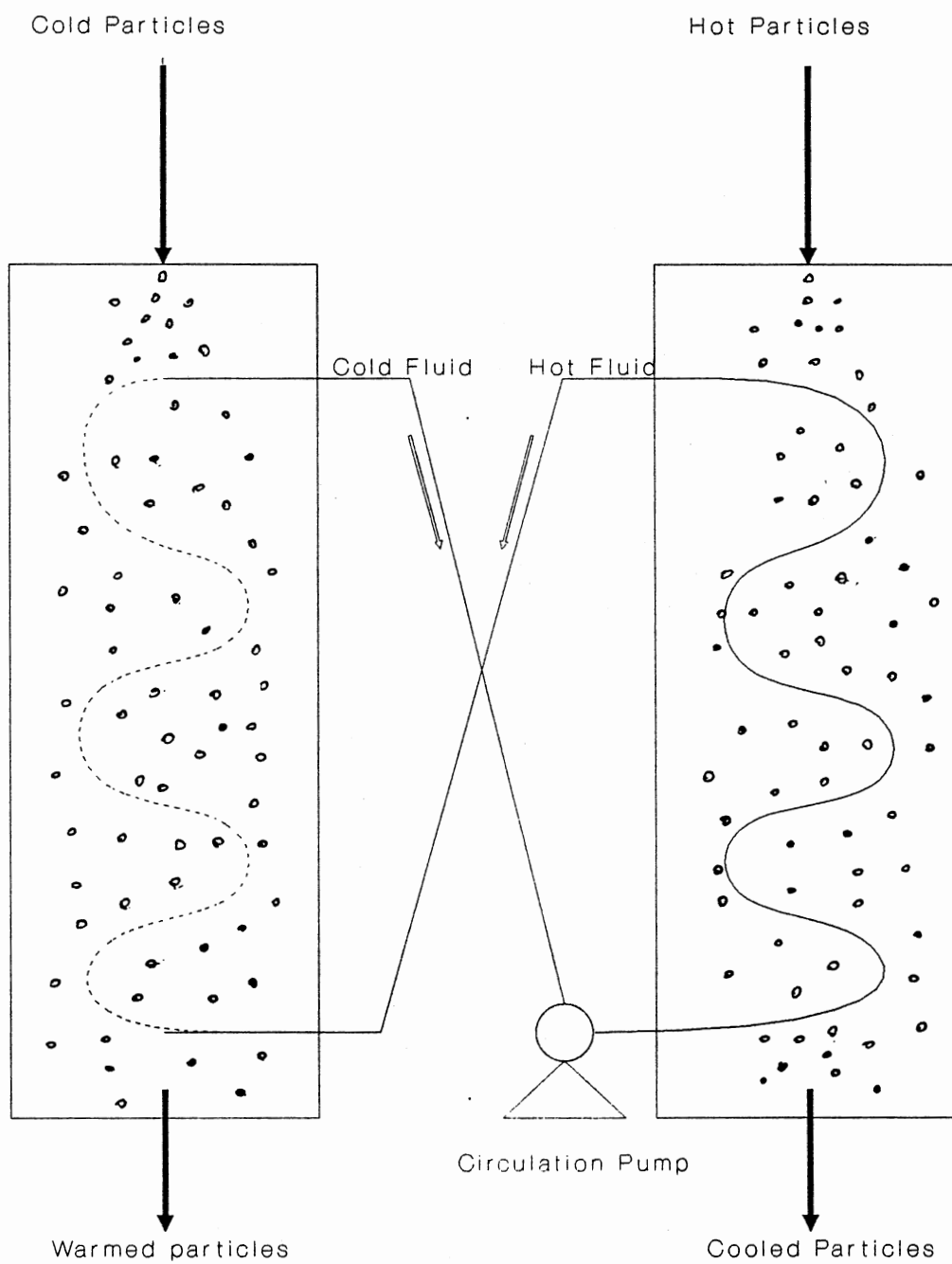
Lapp et al.(32) also developed a counterflow heat exchanger for counterflow thermal treatment of infested grain. However, it is a liquid-solid indirect heat transfer process. Although the processes mentioned above are designed to operate in a counterflow mode, they are not true solid-solid heat exchangers since they are not based on direct thermal contact of two particles.

A heat exchanger which discretely mixes and separates grain from a high density heating medium in a counterflow configuration was developed by Simonton and Stone (9). This process was divided into 3 stages: one for heating grain, one for recovering energy from the grain and one for providing energy to the heating medium. From their



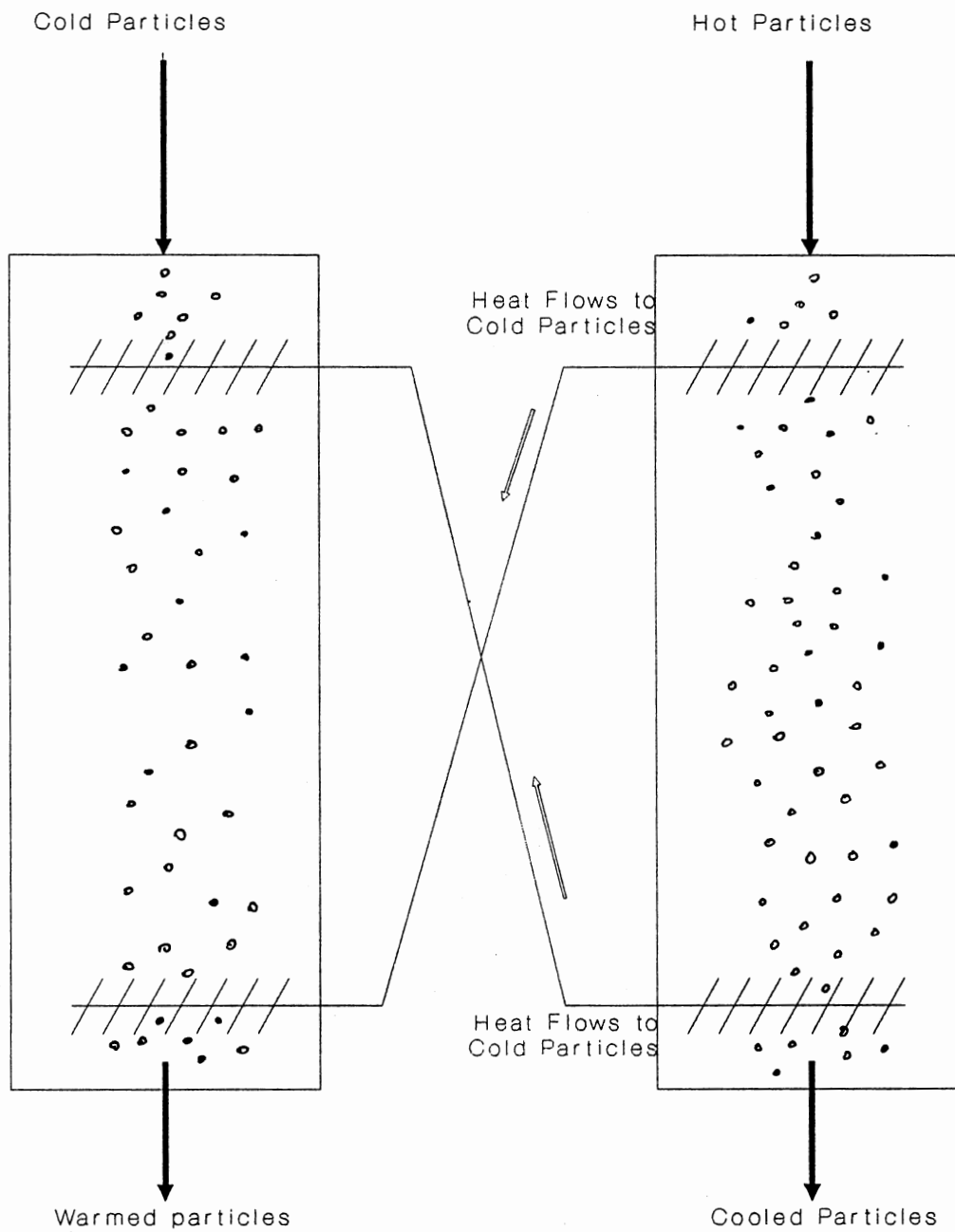
Source: Levenspiel, O., Engineering Flow and Heat Exchange,  
New York: Plenum Press (1984).

Figure 1. A Counterflow Solid-Solid Heat Exchanger Using  
a Third Stream of Solid as the Media



Source: Levenspiel, O., Engineering Flow and Heat Exchange,  
New York: Plenum Press (1984).

Figure 2. A Counterflow Solid-Solid Heat Exchanger Using  
a Third Stream of Liquid as the Media



Source: Levenspiel, O., Engineering Flow and Heat Exchange,  
New York:Plenum Press (1984).

Figure 3. A Counterflow Solid-Solid Heat Exchanger Using  
Heat Pipes as the Media

experimental studies on a 5 cell per stage process, the thermal efficiency of 84% and 68% heat recovery were reported. However, this batch operated heat exchanger has a mass of about 30 times the mass of the processed materials, and is not likely to be implemented into a full scale process. They also found that salt was superior to interprop (high density aluminum oxide) with respect to heating efficiency within their process. However, the corrosion properties of salt was a major problem in the process.

Past research has led to the design of heat exchangers using solid media, however, none of these have been commercially successful, partly due to a lack of fundamental design information on both the configuration of a continuous counterflow process and the heat transfer mechanisms.

#### Fundamental Studies of Heat Transfer in Solids

Considerable literature dealing with heat transfer in stationary packed beds(33-38) has shown that conduction through the contact of the particles is the major contribution to the effective thermal conductivity of the bed. A number of efforts have been made to model solid heat transfer either from a theoretical approach or from an empirical fitting approach. One theoretical model was developed by Otake and Tone (39) and was based on the assumption that there are 2 heat transfer processes

operating in parallel: heat transfer from the heating surface to a bed of solid particles; and heat transfer from the heated particles to non-heated particles. The use of this equation is limited since the equations apply only to a specific geometry.

Mery (40) developed an empirical model for a cut-flight screw-type agitator and demonstrated that the thermal conductivity had a direct impact on the rate of heat transfer. The high heat transfer rate is mainly due to the phenomenon of backmixing.

Uhl and Root(41) described two batch models: one model was based on a Bessel function solution of a differential heat balance equation and the other was based on a dimensional analysis.

Otake and Tone(39), Mery(40), Horzella(42), and Uhl and Root (41) all have shown that particle thermal conductivity, specific heat and bulk density affect the rate of heat transfer. All of these works suggest that particle properties play an important role in the solid-solid heat transfer area.

The empirical findings offer insight into the operation of solid-solid heat transfer systems. However, fundamental theories behind these systems should also be investigated in order to improve the design of such systems. The environment inside the drum can be viewed as follows: The product and the medium are not moving at the same speed, and a cluster of particles from the medium comes into contact

with the product surface. This medium is then replaced by another cluster and so on. The heat transfer of each cluster will depend on the time of contact. This type of model is similar to one developed by Mickley and Fairbanks (43) for fluidized beds. However, the situation in the drum is different from that in a fluidized bed since the interstitial gas in the bed of the drum is assumed to move passively with the particles.

Several workers have investigated the heat transfer coefficient produced when a stream of particles flows past a sphere. Brinn et al. (44) set up an experiment in which a bed of sand was flowing down a vertical tube. This tube was heated and gave off heat to the sand through its surface. They found that the sand bed could be considered as a continuous medium, moving in rodlike flow in the tube. In contrast, Kurochkin (45) investigated the heat transfer between a stream of granular material and tubes placed perpendicular to the flow. Various tube geometries were tested to find the relationship between the heat transfer coefficient and the size of the material. The heat transfer coefficient was found to be inversely proportional to the material size and therefore, solid beds can not be considered as a continuous medium.

Heat transfer coefficients for a moving bed of fine particles with various interstitial gases were measured by Harakas and Beatty(46). Heat transfer to the particle bed was provided from an electrically heated surface which was

immersed in the rotating bed tangentially to the radius of rotation. Velocities of the bed relative to the heat transfer surface were varied from 6 to 46 ft/min. Good agreement was found between the experimental data and a simple conduction model which was based on a continuous phase assumption and depends on the thermal conductivity of the interstitial fluid, the velocity of the bed, the length of the heat transfer surface as well as the particle size. They concluded that the heat transfer rate for a moving bed of fine particles may be predicted by a simple conduction model, and the granular bed of particles could be represented by a continuum or homogeneous model under certain circumstances. The criteria for this is dependent on the thermal conductivity of the interstitial fluid, the velocity of the bed, and the length of surface as well as the particle size.

In solid-solid heat transfer, the main mode of heat transfer is by conduction through contacts between solid granular materials at different temperatures. Experimental data were taken using a metal ball as the large particle and different size particles of salt as the small particle by Raghavan et al.(47). They developed both theoretical and empirical models for particle-particle heat transfer. The theoretical model was based on the assumptions that the heat transfer rate is proportional to the number of impacts between particles, and that all particles crossing the cross-sectional area of the sphere will strike the sphere.



However, the thermal properties of the particulate materials were not included in the model or the experimental study. A regression model was developed from the data which showed a linear relation between the rate of heat transfer and the inverse of the relative velocity between large and small particles. The heat transfer coefficients were experimentally determined and varied from 35 to 75  $\text{btu/hr}\cdot\text{ft}^2\cdot^{\circ}\text{F}$ . These values increased with smaller particle sizes and higher particle velocity. They also determined that the surface heat transfer coefficient was not affected by changes in the diameter of the large particles considered in their study but did vary with flow rates as well as the porosity of the bed.

Sullivan and Sabersky (48) studied the heat transfer mechanism between granular solids and other adjacent objects. Several assumptions were made in the analytical development of their first model, including infinite particle thermal conductivity and an orderly array heat flow. Their second model considered the bed as a one-component continuum, and the contact between the plate and the bed was assumed imperfect, creating a finite thermal resistance. With such assumptions, a heat transfer model in terms of Nusselt number ( $N_u$ ), which was based on particle diameter and gas conductivity, was proposed (48).

They found that the granular materials function as a single component continuum and heat transfer from plates is governed only by the bulk thermal properties of the bed at

low modified Peclet number. This also implies that the heat transfer coefficient does not vary with particle size and gas thermal conductivity as described in their second model at long contact times. Conversely, heat transfer is dominated by the thermal resistance at the wall at high modified Peclet number. The film coefficient is inversely proportional to the particle size and proportional to the gas conductivity. In between these two extremes of modified Peclet numbers is a transitional region where the heat transfer will be influenced by both the bulk and structural properties of the medium.

Richard and Raghavan (30) examined the heat transfer process between flowing particulate solids and objects immersed in the flow path. An analytical equation was derived for the transfer coefficient for flow past either a flat or a curved surface. The result was nearly identical to that reported by Sullivan and Sabersky(48) except a Nusselt number based on particle conductivity rather than gas conductivity.

$$h = [ H_C^{-1} + k^{-1} (\pi \alpha t / 4)^{\frac{1}{2}} ]^{-1} \quad (1)$$

or,

$$N_u = [ 1/N_{uC} + (\pi F_0 / 4)^{\frac{1}{2}} ]^{-1} \quad (2)$$

where  $N_{uC} = H_C \cdot d / k$ ,  $F_0 = \alpha t / d^2$ ,  $N_u = h \cdot d / k$  and  $H_C = k_g / \chi d$ .

The second term of equation (2) will become important as the Fourier number ( $F_0$ ) becomes large. This is the solution for the first model mentioned above where a perfect conductance at the bed-plate interface is assumed. Another

interesting aspect of equation (2) is that it is equivalent to adding in series the contact resistance at the plate to the resistance created within the bed which was treated as a continuum media.

The equivalence of equation (1) for a general geometry can be expressed in the form:

$$h_{av} = [ H_C^{-1} + h_{\text{continuum}}^{-1} ] \quad (3)$$

where  $h_{av}$  is the heat transfer coefficient of general objects. Equation (3) implies that approximate values of  $h$  can be estimated if it is possible to calculate a heat transfer coefficient for a similar situation where there is perfect thermal contact between the heating and processed material. The contact resistance is often explained in terms of the presence of gas film between the plate and granular bed, and can be expressed in terms of the thermal conductivity of the gas,  $k_g$ , and the resistance parameter,  $\chi$  (30).

$$H_C = k_g(d \cdot \chi)^{-1} \quad (4)$$

where  $k_g$  is the gas conductivity,  $d$  is the particle size and  $\chi$  is a contact resistance parameter.

The authors (30) also attempted to determine an empirical model for the value of  $\chi$  using a regression technique. They found that beds of irregular particles tend to have a greater porosity than the regular particles. An empirical equation which relates  $\chi$  with porosity,  $\epsilon$ , was

fitted as:

$$\chi = 5.16 \epsilon^{5.06} \quad (5)$$

They also concluded that when the contact time is long, like that observed by Brinn et al. (44), the Fourier number is large and the bed behaves like a continuum. Conversely, the contact resistance becomes important and can be predicted by the bed porosity when the contact time is short. This also implies that heat transfer can be controlled as long as the contactor can be built in a way that the porosity of the bed and the contact time can be controlled. The main difficulty left is the lack of the knowledge about the mechanical motion of the rotary contactor which could be used in determining the contact time of the particles.

Downs et al. (8), presented four dimensionless empirical equations for particle-particle heat transfer. Metal balls were used to transfer heat to sand, salt and glass beads. Data were taken over a variety of conditions and dimensional analysis was used to develop the equations. The equations gave a theoretical Nusselt number in terms of a group of dimensionless terms and their individual exponents. Among these dimensionless groups, the diameter ratio, internal angle of friction and shape factors were the dominant factors, while the poorest correlation was for the Froude number. In order to determine surface heat transfer coefficients, an experimental model was developed by Downs et al. (8) based on the Newton's Law of Cooling.

$$h = - \frac{\ln [1 - (1 + C_{pB}/C_{ps}) \cdot (T_i' - T') / (T' - T)_i]}{(A_B/C_{pB}) \cdot (1 + C_{pB}/C_{ps}) \cdot t} \quad (6)$$

where  $T'$ ,  $T_i'$ ,  $T$ , and  $t$  are measured and the rest of variables are the physical properties of particles.

A heat transfer experiment using a solid medium in a flighted inclined rotary drum was conducted using different media, bead materials and sizes by Tessier and Raghavan (49). An algorithm describing the mixing process was developed and tested with the experimental data. Heat transfer coefficients between granular media and glass or aluminum beads were experimentally determined. The heat transfer coefficient, varied from 325 to 650  $\text{w/m}^2\text{k}$  and was a function of the drum speed, bead size, and the media. In addition, the dimensionless contact resistance parameter,  $\chi$ , was found to be affected by the bead size, medium static porosity and the density. The contact time of a particle in the sliding layer and the bulk layer as well as the residence time in both layers were computed based on the original design information (13). The value of sliding velocity and  $\chi$  were unknown and estimated numerically through an iteration procedure which minimized the residual sum of squares between the predicted and experimental observed heat transfer coefficients, using equations (1), (4) and (6) with the mixing algorithm.

Heat transfer from a heated surface to the packing is the rate-determining step in a number of thermal and

chemical processes. It has long been known that heat transfer from a heated surface to packing can be improved if the packing is intensively mixed. During mixing, temperature gradients are confined to the region close to the wall, and only the thermal resistance of this layer near the wall remains. In contrast to this situation, a stationary condition, the heat flow has to overcome a considerable resistance in the entire path through the packing. The heat transfer rate is therefore considerably slower and represents a minimum value to a mixed case.

Heat transfer from a horizontal, electrically heated plate to a packing of spheres of polystyrene, glass, tin and bronze was investigated experimentally and theoretically by Wunschmann and Schluender (50). The concept of an apparent resting time applied to a moving bed was proposed and was used with the equations, developed for a stationary bed to calculate the heat transfer coefficient in a mixed bed. The authors (50) proposed two asymptotic equations to calculate the heat transfer coefficient of a quasi-homogeneous packing at short contact time and long contact time, respectively as,

$$h = \frac{2 \cdot k}{(\pi \cdot \alpha \cdot t)^{\frac{1}{2}}} \quad \text{short time} \quad (7)$$

$$h = 3 \cdot k/H \quad \text{long time} \quad (8)$$

where  $k$  is the thermal conductivity,  $H$  is the bed height,

and  $\alpha$  is the thermal diffusivity. Equation (7) may become invalid at very short contact time, since the packing can no longer be assumed to be a homogeneous material. The following equation was proposed by the author (51) to estimate the maximum value of heat transfer coefficient as the contact time approaches zero.

$$h_{\max} = \frac{2 \cdot k_g}{d} \left[ \left( \frac{\sigma}{d} + 1 \right) \cdot \ln \left( \frac{d}{\sigma} + 1 \right) - 1 \right] \quad (9)$$

where  $\sigma = 2 \cdot \Delta \cdot (2 - \gamma) / \gamma$ ,  $\gamma$  is the accommodation coefficient, and  $d$  is the particle size. The first term in equation (9) describes heat conduction through the gas, while the second term describes the radiation exchange between the heating surface and the first particle layer. Equation (9) depends on the particle diameter and the properties of the gas, while equation (8) depends on the thermal properties of the particles. These equations are consistent with previous findings (30, 48).

Heat transfer between particles and submerged surfaces takes place in numerous industrial processes, such as heating, cooling and drying of particulate material as well as chemical reactions in fixed, moving and fluidized beds. Modeling of heat transfer between particle beds and immersed surfaces has been the subject of experimental and theoretical investigations for the past 2 decades. The state of the art was reviewed by Schluender(52).

Two different limiting cases, unmixed and a homogeneous mixed bed, in the theoretical modeling of heat transfer to particles were formulated by Molerus and Scheuring(53). In the unmixed bed, the mechanism was viewed as a gradual transfer of heat via a repeated sequence of heat transfer in the gap between adjacent particles and conduction in the particulate material. In the mixed bed, heat was assumed to be transferred to the interior of the bed by the mixing of particles which had previously attained the temperature of the heating surface. The mixing motion in the bed thus maintains a homogeneously lower temperature throughout the bed.

The theory developed by Molerus and Scheuring (53) predicts a difference in the behavior of heat transfer coefficients for the 2 regimes at long contact times,  $t$ , such that the heat transfer coefficient is proportion to  $t^{1/2}$  in unmixed bed, and is proportional to  $t$  in mixed bed. For short contact times,  $t$ , the heat transfer coefficient is independent of  $t$  in both regimes. In addition, the heat transfer rate is dominated by the heat transfer from the particles to particles instead of the heating surface to adjacent particle at longer contact times, in the unmixed bed. These results are also consistent with the findings of previous investigations(30, 48).

When moving particles impact on a stationary surface or when two particles impact, heat conduction occurs through the contact area of the particles. Usually it is believed



that this conduction contribution to the overall heat transfer is very small due to the small contact area and short contact times (54). However, a recent model (55) reported that this conduction effect becomes predominant as particles become small. The study of this problem was pioneered by Soo (57) in 1967 by using the theory of elasticity to evaluate the area and duration of contact between the particles. Later work by Sun and Chen(56) can be considered an extensive evaluation of the basic concepts originated by Soo(57). A quantitative evaluation of direct conduction heat transfer between particles and surfaces in suspension flows was described in their report. The mechanism investigated was conduction through time varying contact area during impaction. They reported that the impaction Fourier number based on the maximum contact area radius and the contact duration is inversely proportional to the particle Peclet number and independent of mechanical properties. The theoretical equations for heat transfer coefficients during impaction in particle-particle and in particle-surface heat transfer was also reported in the paper. The following assumptions were made: perfect thermal contact, semi-infinite media, and the surfaces outside the contact area are flat and insulated. Their results were similar to those reported by Raghavan et al.(47). The heat transfer coefficient had a strong dependence on the impact velocity. This implies that impacts with the highest velocities make the greatest

contribution to heat transfer. In addition, they concluded that the mechanism they proposed was expected to be dominate for highly conductive particles or at low pressures in a heat contact device, where the relative contribution of the fluid is small.

### Studies of Residence Time Distribution

#### Models Applicable to Residence Time Distribution

The experimental determination of the age-distribution functions is accomplished for a particular process by a stimulus-response technique using a tracer material in the inlet stream. The injection is the stimulus and the response is the tracer concentration measured in the outlet stream. Flow patterns with a relatively small degree of mixing are not too difficult to treat. Probably the best approach to characterize mixing is to use a simple model whose parameters are then easy to correlate for broad classes of processes.

Many chemical engineering operations can be classified as a tank or a column operation. Empirical mixing models are constructed to represent particular pieces of equipment or kinds of operation. Those models may be classified as tank or column models are zero-parameter models. It is generally useful to consider 1-parameter models which will represent a mixing condition with variance between 0 and 1. The simplest model is a stirred tank in series or in

parallel with a piston flow vessel. The series arrangement is commonly used and is known as the fractional tubularity model (shown in figure 4).

Chemical engineering has long been concerned with stirred tank processes, and the second model is that for  $N$  stirred tanks of equal volume in series (shown in figure 5). This model has so far been designed only for integral values of  $N$ . There is a need for a method having an extension to non-integral  $N$ , especially when the tanks-in-series model is to be used to model small deviations from the exponential distribution of a single stirred tank. Two such extensions have been proposed, the gamma function model and the fractional tank model (58). The simplest extension of the tank-in-series model is the gamma function model. The value of  $N$  needs not be an integer and it is treated as an adjustable index of mixing performance. A major use of this model is to deal with small departures from the exponential distribution of a simple stirred tank. This model has the advantage of mathematical simplicity, but lacks a physical interpretation of the  $N$  parameter. The alternative method to this model overcomes this problem. The fractional tank model treats the system as consisting of  $I+1$  stirred tanks in series,  $I$  of the tanks have identical volumes and one of the tanks has a smaller volume. In this model  $I$  is an integer less than or equal to  $N$ .

Another way of extending the tank-in-series model is to add backflow between the vessels (shown in figure 6). The

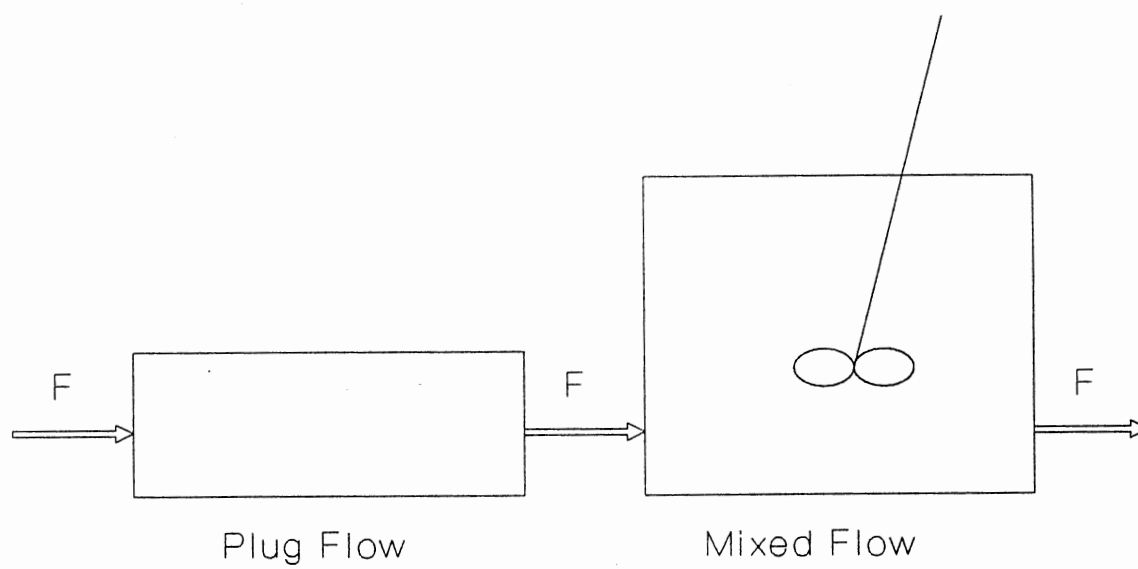


Figure 4. Schematic Diagram of the Fractional Tubularity Model

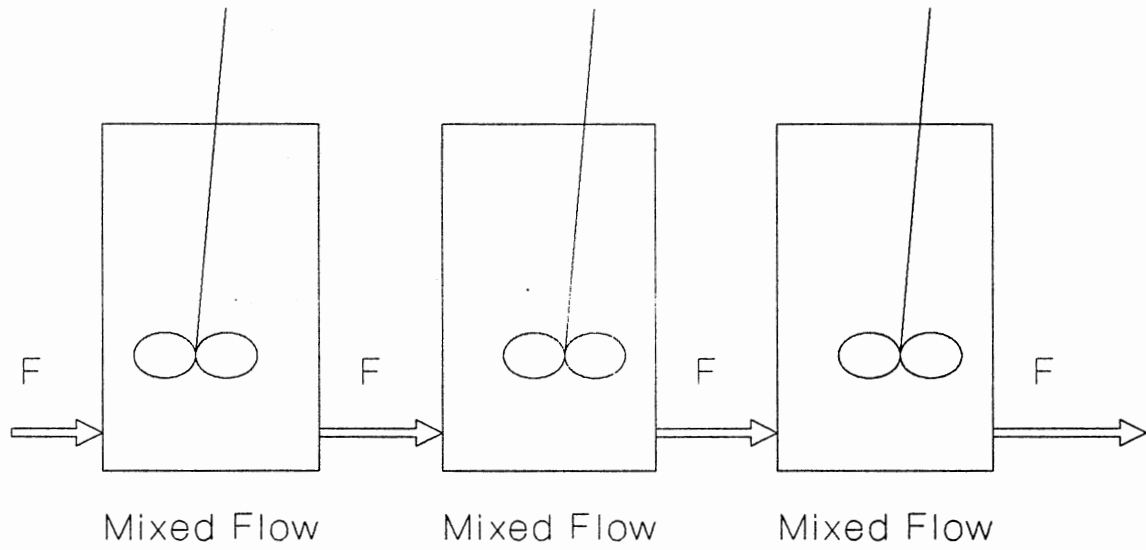


Figure 5. Schematic Diagram of the Tanks-in-Series Model

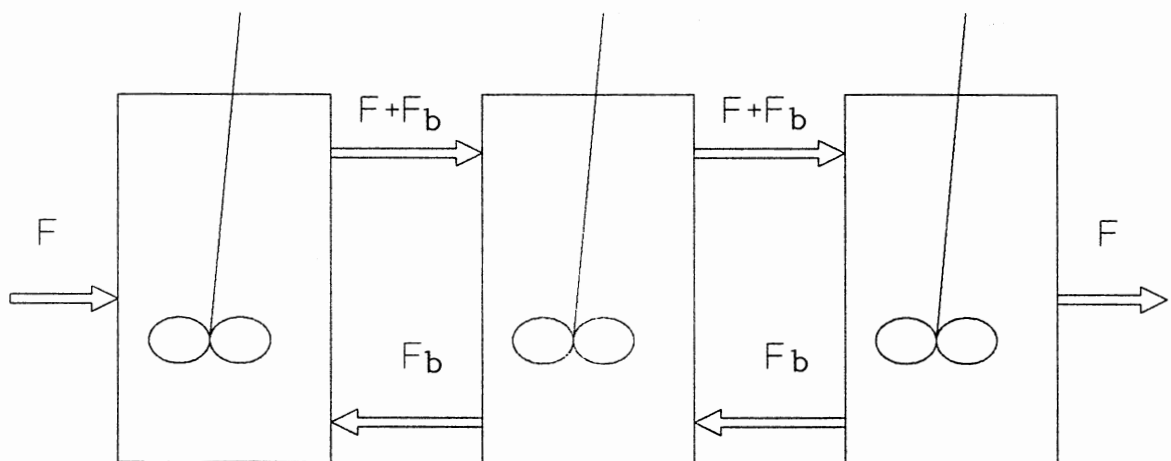
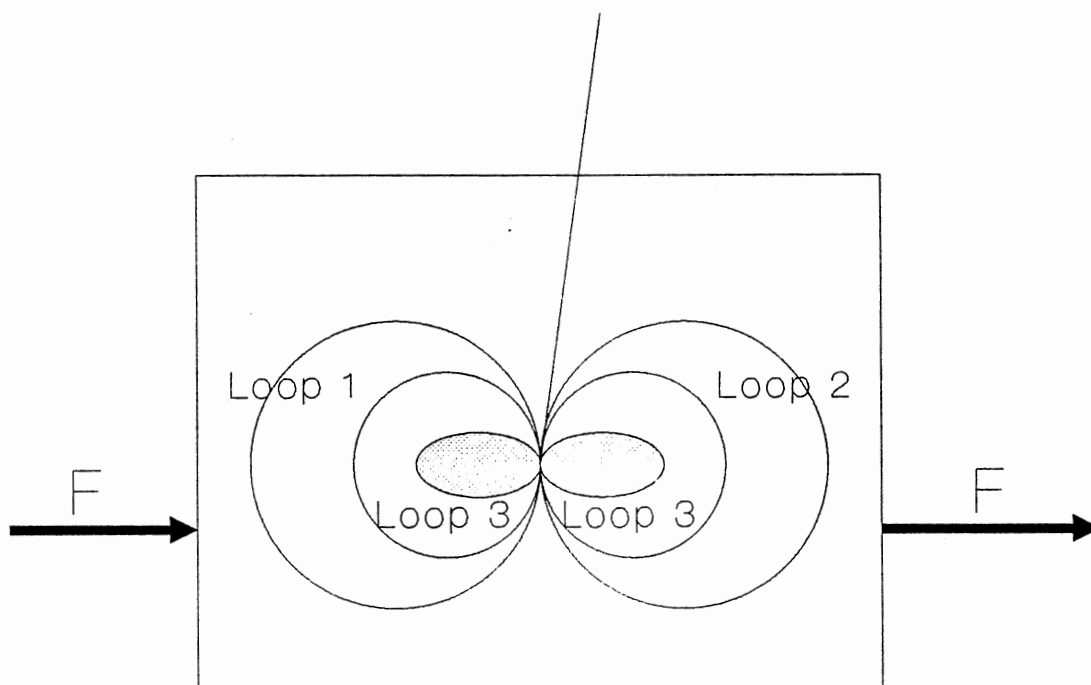


Figure 6. Schematic Diagram of Tanks-in-Series with Backflow Model

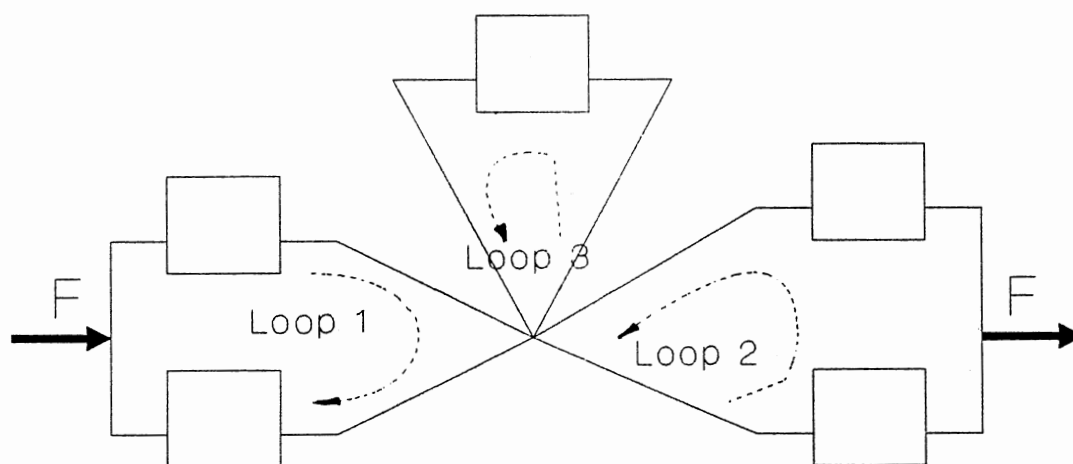
ordinary tank-in-series model can account for a spreading of residence times, but is limited by spatial mixing. This limitation can be removed by incorporating backflow. A comprehensive treatment of this model has been given by Mecklenburgh and Hartland(59).

Another method is to add regions that are more-or-less stagnant. This enhances the ability of the simple model to handle mixing in the radial direction for more complicated mixing conditions than dead space or bypassing. It is probably most useful to utilize some type of flow model for the total vessel made up of small regions of the simpler types of mixing, such as uniform mixing, dead space, bypassing. These combined models have been found useful for many problems.

Van de Vusse(60) proposed a type of circulation model in which there were basically 3 main loops circulating in the reactor: one loop receives the feed stream, another loop delivers to the outflow stream, and all the other internal streams combined to form a third loop, as shown schematically in figure 7. Models having these characteristics can be applied to interpret the non-ideal flow of the system being considered based on the actual flow situation present such as in the pyrolysis fluidized bed reactor (61). A physical diagram for the circulating model consisting of 3 loops as shown in figure 7 can be fitted to the experimental results of Berruti et al.(61).



(a) A Typical Stirred Tank System



(b) Its Related Model

Figure 7. Flow Patterns in a Stirred Tank and Related Circulation Model



### Residence Time for Rotary Drums

In order to obtain a clear picture of the factors which influence the performance of a flighted or an unflighted rotary drum tumble, it is desirable to examine the motion of the particles within the rotating cylinder. It is the object of this section to review previous work related to this field and to enhance understanding of the dynamics and eventually the heat transfer mechanism.

The report of Downs et al.(8), included a detailed description of the flow regions of a mixture of particles inside an unflighted rotary drum. It offers a good insight into the flow situation in such an apparatus. These fundamental flow regions are referred to as slipping, slumping, rolling, showering, and centrifuging.

Knowledge of the movement of particles in a rotary drum is required for a fundamental study of the heat transfer occurring inside the drum. Earlier studies (62, 63) for a residence time equation related the residence time to the principal parameters, such as effective drum diameter, length, slope, drum speed, drum loading, flight profile, properties of processed material and particle distribution from the flight.

Kelly et al.(62) investigated the phenomena affecting behavior of particles within a rotary drum system with a view to develop a more fundamental basis for process analysis and equipment design. The dynamics of particles in rotary drum was considered in two sections and experimental

studies were carried out to test the model. In the first part, radioactive tracer experiments were used to determine the mean cycle time of a cascading particle in a small horizontal closed rotary drum at different levels of holdup but without throughput. In the second part, equations of motion were developed for particles undergoing a cascade cycle in an inclined rotary drum with counter air flow. The momentum balance equations were solved numerically to give the mean axial advance of particles within the drum leading to an evaluation of their mean residence time. The model proposed by Kelly et al.(62) gave an insight into the fundamental operation of a rotary drum and the model performs satisfactory at normal operating condition, except at the region of high air velocity or in overloaded conditions.

Another method of designing rotary machines for heat transfer between particulate solids and a gas is reported by Porter et al.(63). A logical basis of flight design was introduced in this work. The instantaneous angle of repose of particles at any position in the flight,  $\lambda$ , which is a function of the flight position, drum speed, and the properties of the solid is given by Porter et al.(63) as:

$$\lambda = \tan^{-1} \left[ \mu + \frac{\nu(\cos\phi - \nu\sin\phi)}{1 - \nu(\mu\cos\phi + \sin\phi)} \right] \quad (10)$$

where  $\nu = r\omega^2/g$  and  $\mu$  is the coefficient of friction, with the other symbols shown in figure 8. The angle of the tip

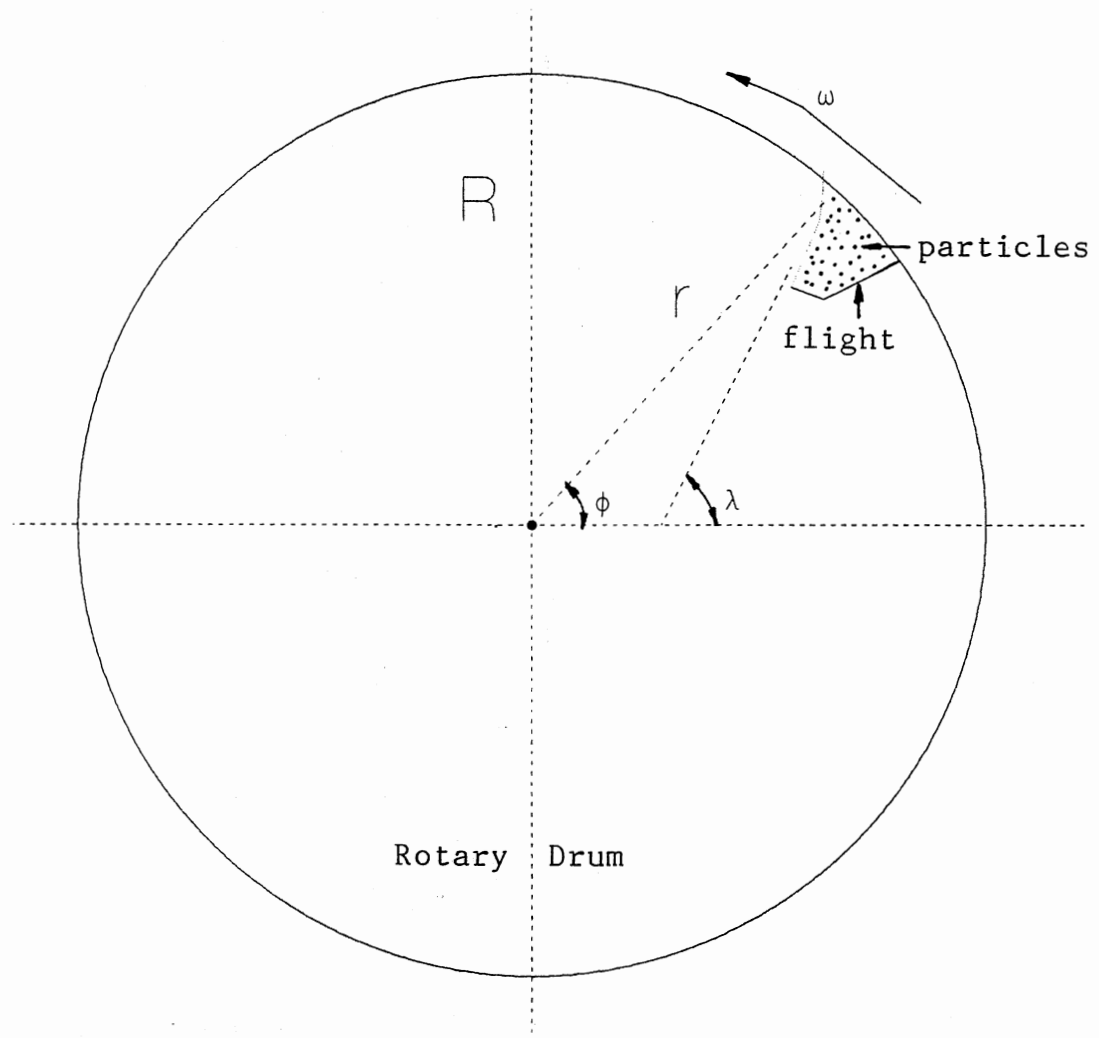


Figure 8. Angle of Repose of Particles in a Flighted Rotary Drum

of the flight governs the position at which the last particles fall. In addition, the particles falling from the flight in a position will cross the horizontal axis of the drum at a distance from the center of the drum,  $L_p$ , as shown in figure 9.

$$L_p = R - R \left\{ 1 + \cos\phi - \sin\phi - \sin\phi \left[ \nu \cos\phi + (\nu^2 \cos^2\phi + 2\nu \sin\phi)^{1/2} \right] \right\} \quad (11)$$

### Recent Studies of the RTD with the Heat Transfer

The particle dispersion coefficient is a measure of the movement of particles relative to the bulk flow of solids. The influence of solid dispersion on the heat transfer profile in a shallow axial flow fluidized bed has been investigated by Nilsson (64). An experimental system was designed and built to measure the temperature profile along the axial-bed direction with two different materials, four different particle sizes, different bed velocities, and different bed heights. Their results showed that a certain flattening of the temperature profiles could be explained by the solid dispersion effect, and it is also clear that there is a correspondence between the width of the residence time distribution and the flatness of the temperature profile.

Rotational effects on natural convection in a horizontal cylinder has been investigated by Yang et al.(65). The rotational effect is examined with the region

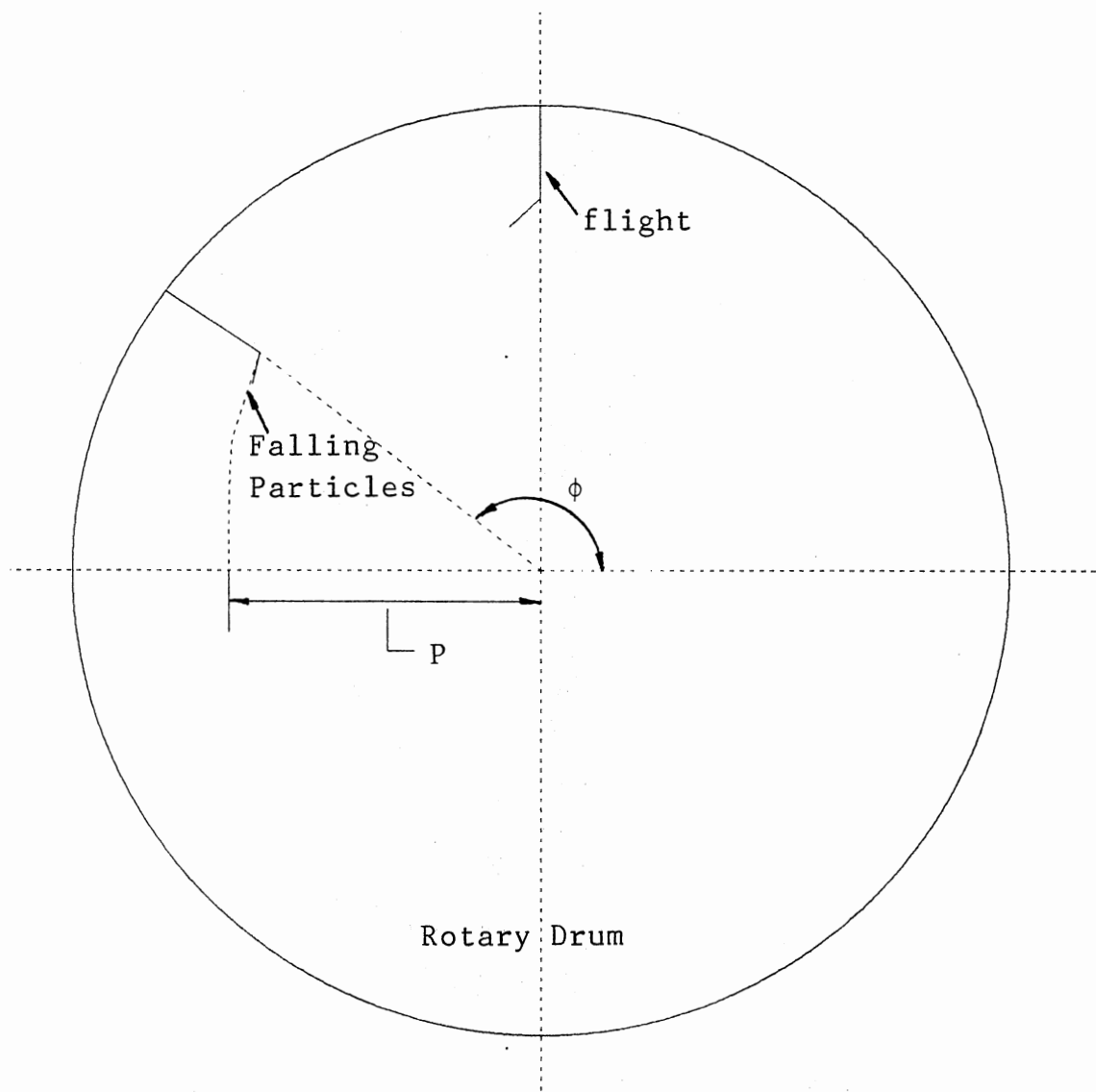


Figure 9. Coverage of Drum by Falling Particles

ranging from rotational dominant to natural convection dominant regions. They found that the effect of rotation is to render the spatial heat flux distribution more uniform at small rotational speed. However, the heat transfer distribution on the end surface is more homogeneous with a lower heat transfer rate due to reduced buoyancy driving force at high rotational speed, and the entire flow stream acts like a rigid body at sufficiently high rotational speed.

In conclusion, an extensive review of the literature showed that a limited amount of previous work has been done on particle-particle heat transfer systems, and no work has been reported on the design and modeling of a continuous counterflow particle-particle heat transfer process which is feasible to be implemented and scaled-up to a commercial-level process. The lack of the knowledge in design and modeling of this new process, provides the motivation for the research described in the following chapters.

## CHAPTER III

### EXPERIMENTAL SYSTEM DESIGN

The concept of particle-particle heat exchange appears promising with respect to heat transfer capability as shown in the literature review. An extensive review of the literature has shown little previous work on particle-particle heat exchanger systems operating in countercurrent flow. Although a number of experimental grain drying units have been built and tested, none is available on the market, implying that more research and development work is required in this field. Due to a lack of knowledge on the design and modeling of a continuous counterflow particle-particle heat exchange process, a decision was made to develop, design, construct and test such a new process in order to obtain information which would be helpful in the following modeling task.

#### Bench-Scale Experimental Design with Initial Conceptual Ideas

The objectives of this research necessitate an experimental design and study of a new heat transfer process which depends on the contact mechanism for its performance. The experiment was designed so that one of the two materials

would be heated in an external heating device, then mixed with a cooler material. The heat transfer medium which moved to the left hand-side is mixed with grain coming from the left hand-side during a time step. The mixture is then separated into two components, each having been forced to flow in opposite axial directions of the contactor. The two materials are again contacted and separated in a repetitive sequence resulting in a continuous counterflow heat exchanger which is shown conceptually in figure 10. The same idea applies to the heat recovery section also shown in figure 10.

For simplicity, the experiment was designed, constructed and carried out only for the heating stage since both stages (heating and heat recovery) are operated in a similar manner. The heat transfer coefficients in both stages should be similar provided that differences in thermal properties of the materials and the operating conditions are accounted for. The approach taken to design a counterflow heat exchange device using particulate solids was that of continuous and repeated mixing, heating and separating as mentioned above. In order to implement the conceptual idealized design into a realistic operating system, many possible mechanical configurations were considered. An approach which combines two rotating cylinders together in a concentric arrangement was taken as shown in figure 11. The outer rotating cylinder is used to transport the heating medium down to one end by gravity, while the inner rotating



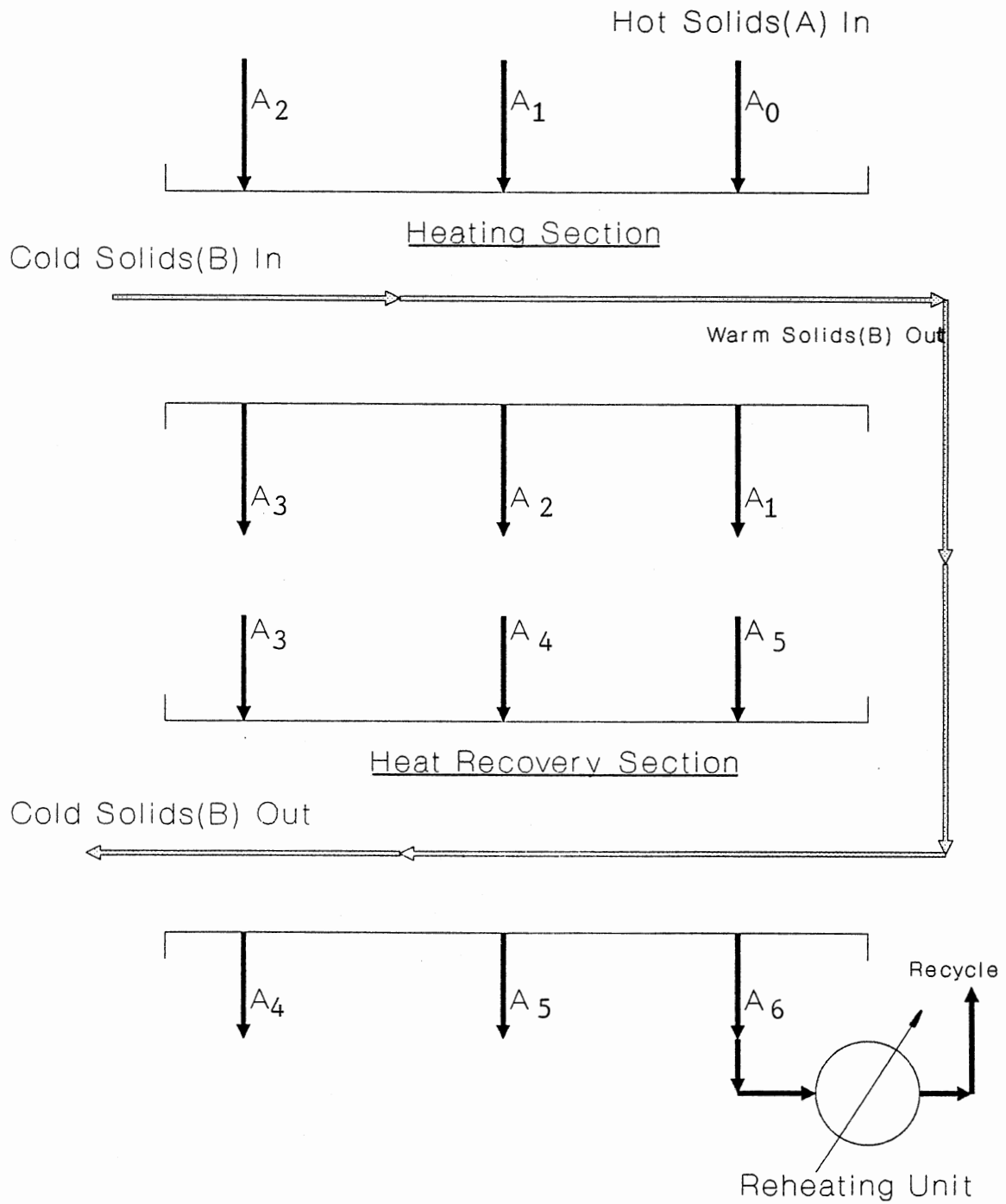


Figure 10. Conceptual Representation of a Counterflow Solid Heating Process with Heat Recovery

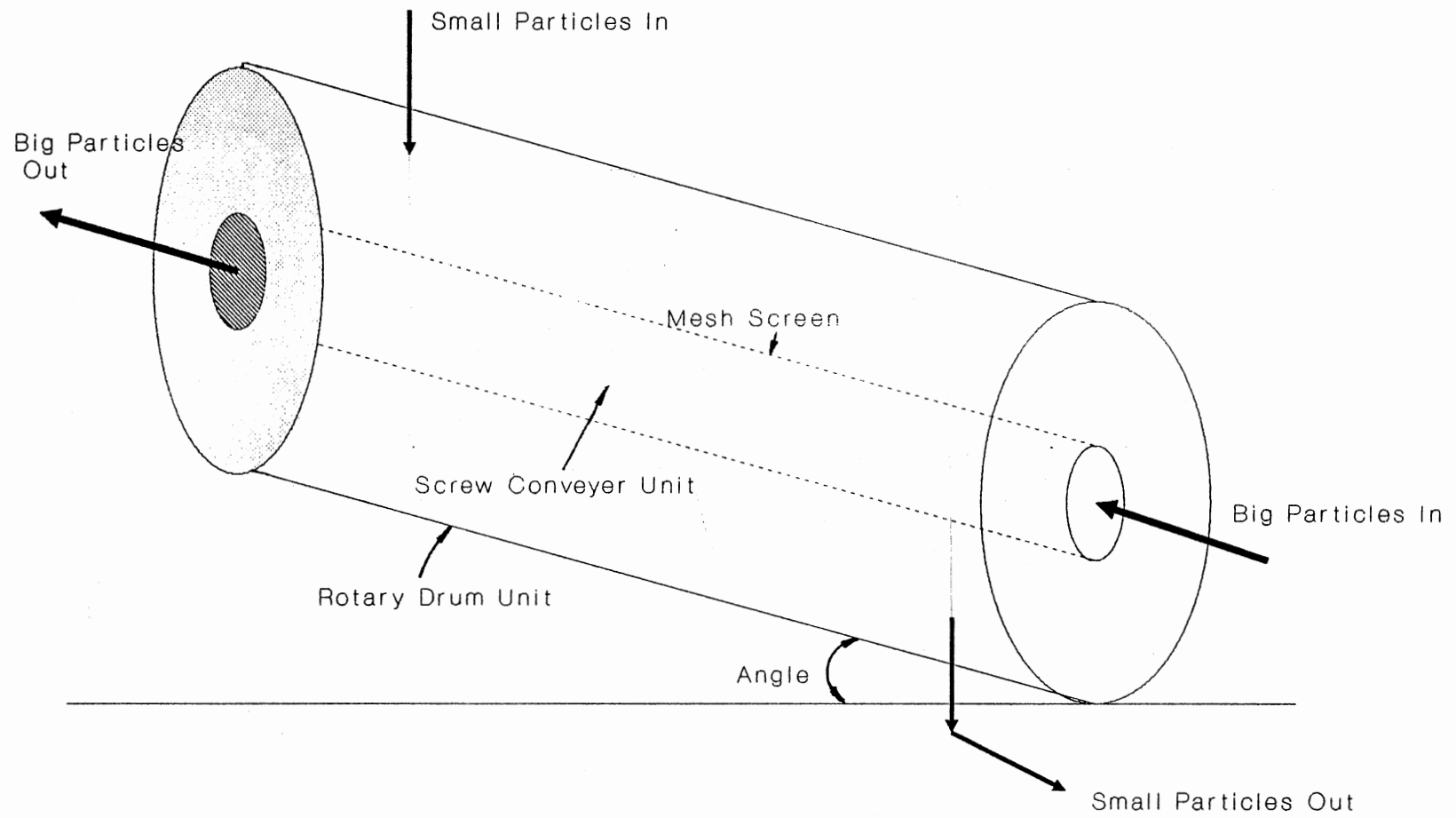


Figure 11. Physical Representation of a Counterflow Heat Exchanger Using an Inclined Drum

cylinder is used to transport the processed material up to another end of the drum using a screw conveyer. The screw conveyer was covered with a screen of correct mesh-size and used to allow the heating medium to fall through, mix and exchange heat with the cool particles via thermal contact. After contact the screen allows the two materials to separate. Furthermore, to better control the mixing process, heating time and residence time without inclination of the drum, several additional metal plates were installed in series above the inner screen and inclined at an angle of  $53^\circ$  to the horizontal inside the drum as shown in figure 12. The purpose of the metal plates is to guide the heating particles through the screen and force these particles to move forward along the axial direction of the drum during horizontal operation. The continuous counterflow particle-particle heat transfer process is shown schematically in figure 13. Several different views of the major components, rotary drum, and some detail drawings for the fluidized bed, interprop hopper, and other components in the process are shown in figure 14.

#### Experimental Apparatus and Materials

An experimental continuous flow heat transfer process using heated interprop (prop) with mixing, separating, and recycling capabilities was built for this research. Operation of this process showed that prop could be heated, mixed with soybeans conveyed in a rotary drum, and separated

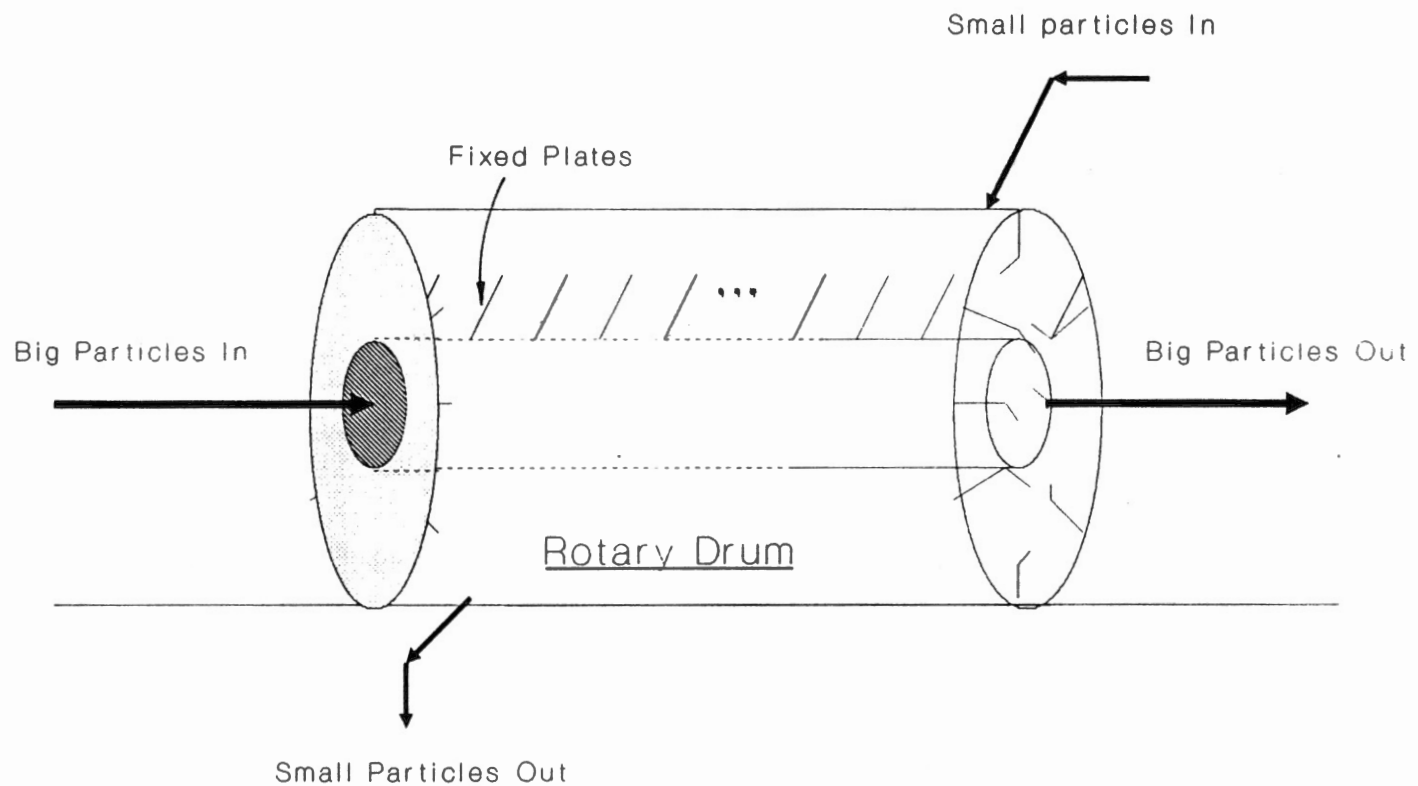


Figure 12. Physical Representation of a Counterflow Heat Exchanger Equipped with Fixed Plates

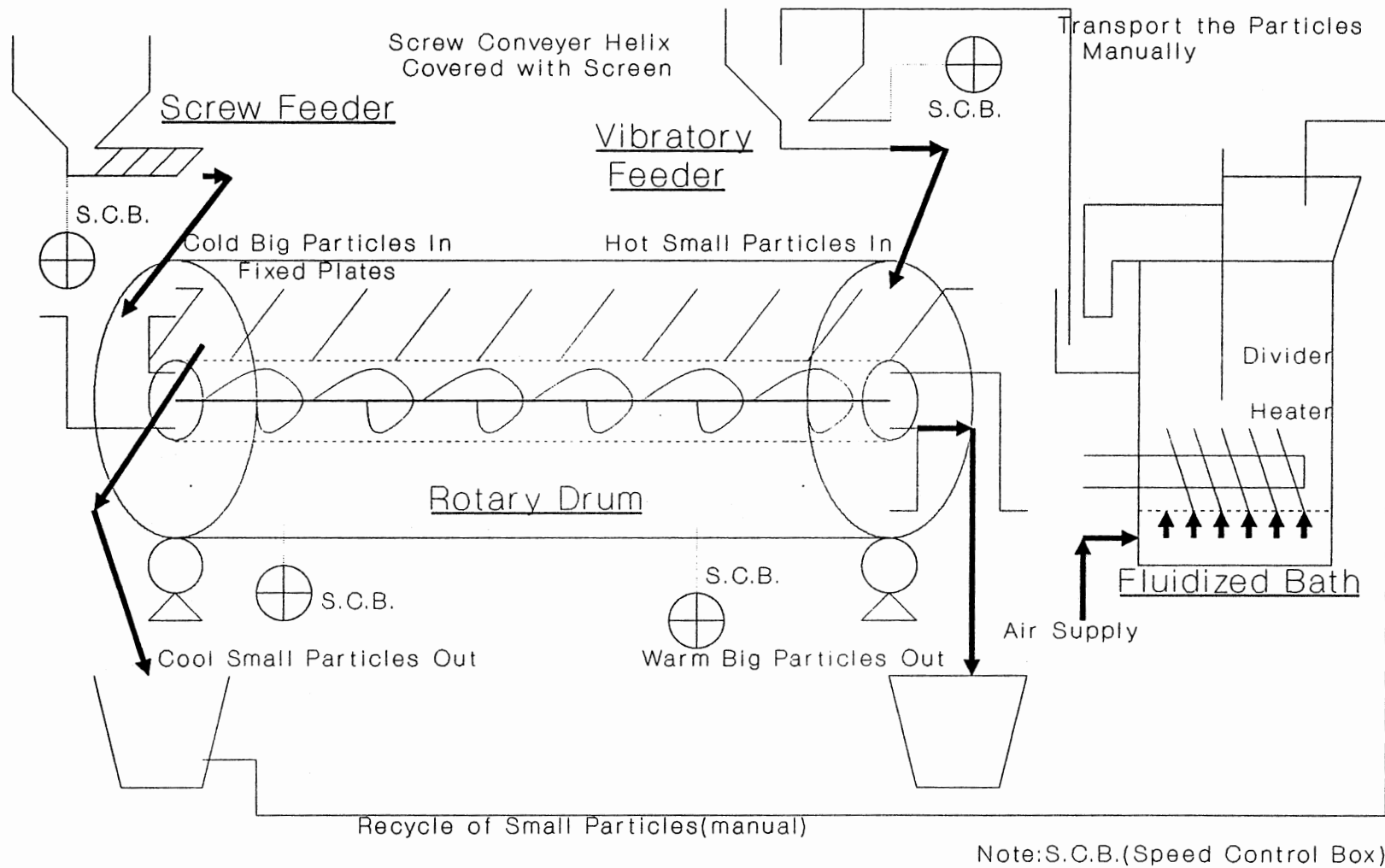


Figure 13. Schematic Flow Diagram of a Counterflow Solid-Solid Heat Transfer Process

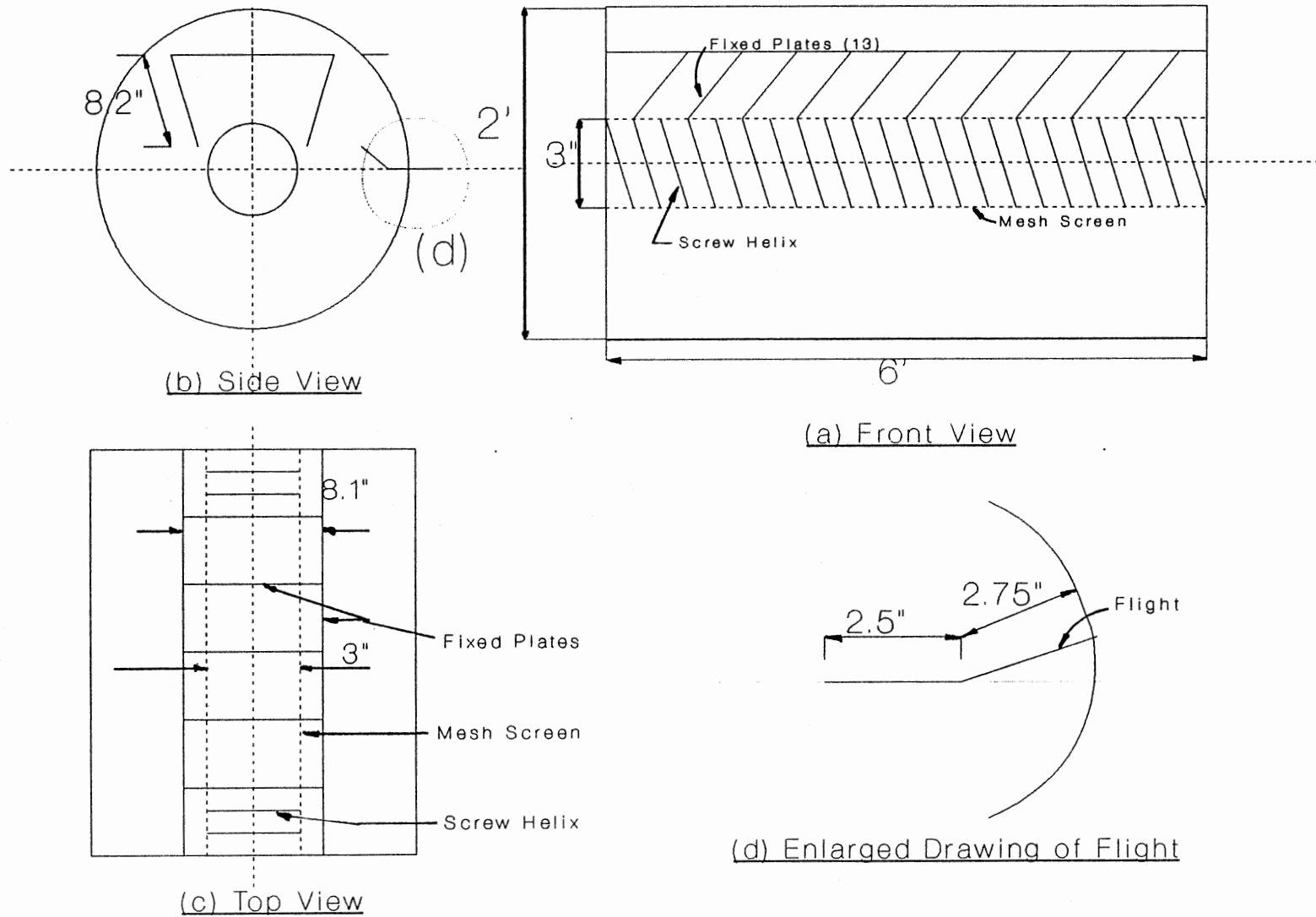


Figure 14. Detail Drawings of the Components for the Counterflow Heat Transfer Process

from the grain by a rotating screen, all in a continuous counterflow heat exchange sequence. The bench scale unit as shown schematically in figure 13, consists of two hoppers, one for prop and one for soybeans, an outer rotating cylindrical drum equipped with 8 longitudinal flights, an inner rotating screened cylinder covered with 12 mesh screen, 13 inclined fixed plates, a fluidized bath, a vibratory feeder, a screw feeder, and the motors, with speed control boxes for the vibratory feeder, rotary drum, inner screen screw and screw feeder.

#### Central component

A rotating contacting drum was designed and built to be the central component of the hardware system, and allows mixing and exchange of heat between the prop and soybeans. The contactor consists of a tin drum 2 ft in diameter, and 6 ft long, horizontally mounted on a fixed frame as shown in figure 15. The angle of the flights and the rotating speed were designed to allow the angle of repose to fall in a range which would correspond with the opening of the fixed metal plates. Thirteen metal plates in series inclined at an angle of 53 degrees to the horizontal were installed between the outer cylinder and the inner screened cylinder and were fixed at both ends of the drum. The function of the flights is to carry the heating medium up the top of the drum before dropping onto the fixed metal plates. The function of these fixed plates is to serve as a guide to

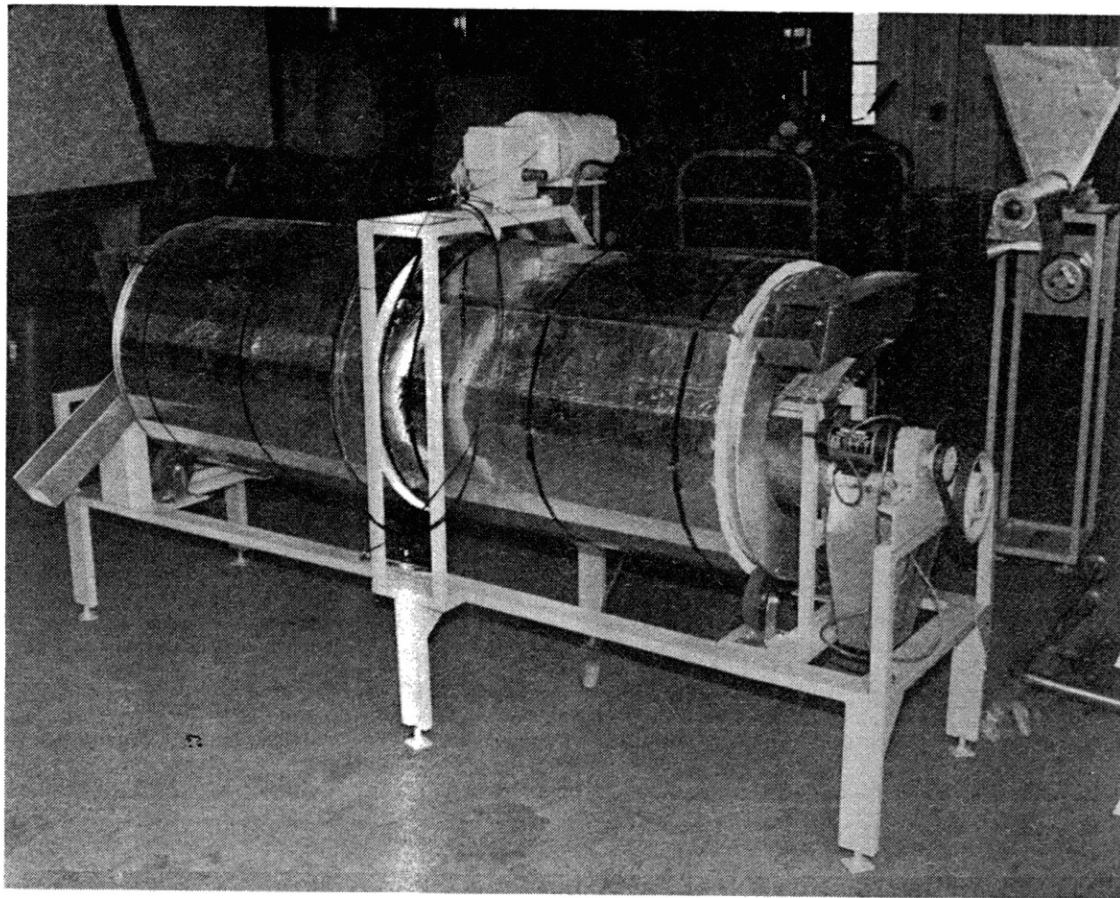


Figure 15. A Bench-Scale Counterflow Heat Exchanger



ensure that the heating medium falls through the inner screen to mix with grain and also to force the heating particles to move forward gradually from one end of the drum to another end without an inclined drum. The inner surface of the drum is smooth and equipped with 8 flights. The drum is covered with insulation 1 inch thick except at the ends.

A 0.56 kw dc motor connected through a gear box and chain drive rotates the drum. The angular speed of the drum can be regulated using a variable speed reduction system driven by a 250-w electric motor. The residence time of the heating medium inside the drum was controlled by varying the rotating speed of the drum. Two hoppers were used to store prop and soybeans. One of the hoppers, for the heating medium, prop, is mounted on a vibratory feeder, which is used to deliver and control the feeding rate of the medium. The other hopper is used for the grain and is mounted on a screw feeder, and used to control the feeding rate of the grain into the inner screw conveyer. The maximum output rate from the vibratory feeder is in the range of 100-250 lb/hr, while the maximum output rate from the screw feeder is about 275 lb/hr (at 6.4 rpm). The residence time of the heating medium inside the drum and the grain inside the screw conveyer is controlled by varying the rotational speed of the drum and the screw conveyer respectively. The heating medium after collection in the outlet port of the drum, was recirculated manually and put back into the fluidized bath for reheating. Reheated particles were

transported to the feed hopper manually to keep the hopper full during the experiment.

#### Accessory components

The prop heating device, a fluidized bath, (SBL-2 from Techne Inc.) shown in figure 13 was modified and used to uniformly heat the prop by acting as a shallow fluidized bed heater. Cool material was placed into one end of the divider and hot material flowed out from the other side of the divider inside the fluidized bed steel vessel. This apparatus is a cylindrical stainless vessel of welded construction with an inside diameter 9 inches. The vessel is thermally insulated by an outer container. A porous plate made of stainless steel is mounted across the vessel between compression flanges. Three, 1-kw electric heating elements are mounted above the porous plate. An air control valve is mounted on the right side of the bath. Temperature control is achieved through a manually operated energy regulator. A rotary switch is used for the selection of 1 kw, 2 kw, or 3 kw heat input but only the initial 1 kw is controlled by the energy regulator. A pneumatically operated safety switch is provided to switch off the heating elements in case of failure of the air supply. Each heater has its own Neon light indicator to show when it is working. This heating device provides a working volume in the shape of a cylinder 8.5 inches in diameter and around 18 inches deep.

Small solid particles can be readily fluidized by means of a suitable air stream. Clean, dry air at a constant pressure of about 3 lb/in<sup>2</sup> is normally supplied via a control chamber beneath a porous plate. The porous plate is required to ensure a uniform air flow and to provide support for the fluidized bed. Since the prop particles used in the fluidized bed have a larger particle size than the original material (sand) used for this device, a larger air compressor was needed to provide a sufficient volumetric flow rate of air to reach the minimum fluidization velocity of the bed. Based on fluidization theory (66), the minimum velocity required is proportional to the square of particle size, and therefore 16 ft<sup>3</sup>/min of air was needed for fluidization of prop. A large capacity Diesel engine air compressor was used for this purpose to generate enough air flow rate for this experiment. An air filter with a water trap was installed before the fluidized bed to provide a clean and dry air supply. The compressed air also served as a means to push the hot particles out of the vessel for feeding purposes.

Screw conveyers are bulk material transporting devices capable of handling a great variety of materials which have relatively good flowability. This characteristic is important in screw conveyer operation as the screw helix mounted on a central pipe or shaft, rotates within a fixed trough or tube and pushes the material along the bottom and sides. A shearing motion on the material in the radial

clearance between the helix and trough and causes the material to tumble upon itself as the moving face of the helical flight tends to lift the material. A screw conveyer of 6 inches in diameter with a pitch of 3 inches and standard flights was chosen for this experiment. Screw conveyers are very adaptable for volumetric control of material from the bottom of hoppers. In this use they are termed screw feeders and as such fill an important role in this experiment. A 3-inch screw feeder with a standard type of pitch and flights was chosen for this experiment. The equations for computing the flow rate and residence time of a screw conveyer are shown in appendix A.

#### Heat Transfer Materials

Soybeans were used as the grain and Norton-Alcoa interprop was used as the heat transfer media. Interprop, an aluminum oxide product with a bulk density of approximately  $118 \text{ lb/ft}^3$  and specific heat of  $0.24 \text{ btu/lb } ^\circ\text{F}$  is utilized by the oil industry in well fracturing. Interprop has a sphericity of 0.95 and 98% of the particle size lies in the range of 40 to 60 mesh. Soybeans were chosen for their high sphericity and have a bulk density of around  $45 \text{ lb/ft}^3$  and specific heat of  $0.49 \text{ btu/lb } ^\circ\text{F}$ .

#### Computerized Measurement System

The determination of the unsteady temperature profiles of both particles is a major subject of this investigation.

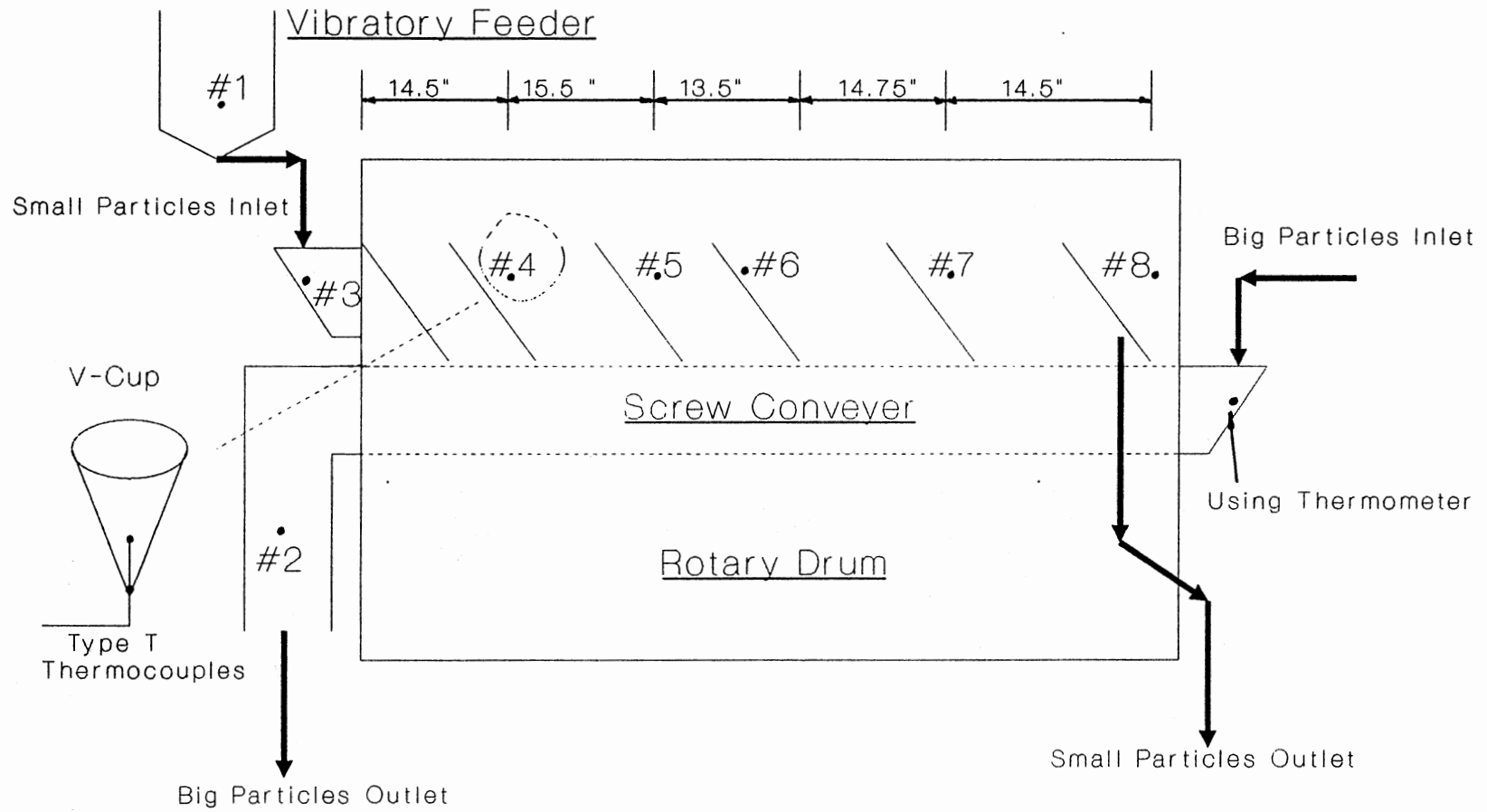
In order to collect this information efficiently with the least effort on the part of the operator, a computerized measurement system was set up for this experiment.

Interfacing for data acquisition was achieved by using an analog to digital converter. Analog signals were converted into digital signals and stored on disk for latter analysis. A complete single board data acquisition system (Data Translation Inc., DT-2805) and an IBM-PC compatible micro-computer were chosen for this experiment.

### Instrumentation design for Temperature

#### Measurement

Type T thermocouples were chosen as the temperature sensors for this experiment to measure the surface temperatures of particles because of their low cost and suitability. Eight copper-constantan (T-type) thermocouples were fixed in place within the heating section and not affected by the machine's rotation as shown in figure 16. Thermocouple #1 was located inside the hopper of vibratory feeder to monitor the interprop temperatures. Thermocouple #2 was located at the outlet of the grain stream from the screw conveyer to measure soybean outlet temperatures. Thermocouple #3 was located at the inlet of the outer rotary drum to measure the prop temperatures. In addition, four more thermocouples (#4-#7) were mounted at approximately equal spacing along the length of the drum and just above the fixed plates. Thermocouple #8 was located near the exit



Note: #1 - #8 is the thermocouples' no.  
 (\*0 - \*7 is the Channel no. of A/D Board)

Figure 16. Thermocouples' Locations Inside the Drum

of rotary drum to determine the outlet temperature of the prop. A V-shape slot, with an embedded thermocouple, was installed at each end of drum to collect prop samples for temperature measurement. 4 V-shape cups were designed to allow the prop stay inside long enough for the embedded thermocouples (#4-#7) to collect the prop samples for temperature measurement. A small cup was used to collect a soybean sample at the outlet of the screw conveyer for temperature measurement.

A calibrated digital temperature read-out device was used to monitor the temperature at each location to ensure a correct temperature measurement. A high-precision glass thermometer ( $\pm 0.1$  °C) was used to monitor both the room temperature and the soybean inlet temperatures. In addition, the temperatures inside the fluidized bed was monitored with a digital temperature read-out device. In order to reduce the manpower on the repetitive data collection work and to be able to make 8 temperatures measurements simultaneously, a real-time experimental data bank, a microcomputer-based system for data logging and data analysis was designed and implemented to improve the laboratory productivity and process monitoring.

Thermocouples #1 through #8, all are connected to a DT707-T screw terminal panel which was used to send all the analog voltage signals into a DT-2805 A/D board to convert the signal to a digital format that the computer read. An IBM personal computer-AT with 2 floppy disk drives and one

hard drive served as the data collecting device. A BASIC program was written to store the digital data. The greatest advantage of a language like Basic is its ease in writing and editing small programs and the ability to run an experiment within the time allowed.

#### Data acquisition system design

The data acquisition system contains three major components as shown in figure 17. Part I. contains the heat transfer apparatus which consists of the thermocouples and the experimental apparatus. The Type T thermocouples are used as the temperature sensors for this experiment, and they are affixed inside the drum. Part II contains an analog input board. The Data Translation model 2805 with DT707-T terminal panel is used for the A/D signal conversion. The A/D board uses 12-bit, 8 differential input channels, unipolar and 0-20 mv input signal range with an amplification ratio of 500.

This board has four different measurement ranges from 0 V to +10 V. The temperature range encountered in this experiment is approximately from 0 to 200 °C which corresponds to a voltage output of 0 to 10 mv from the type T thermocouples. The 0-20 mv range of the A/D board was selected for this experiment.

The board can accept 8 input signal channels from the thermocouples and can be programmed by an external device, such as a microcomputer. The microcomputer can retrieve the



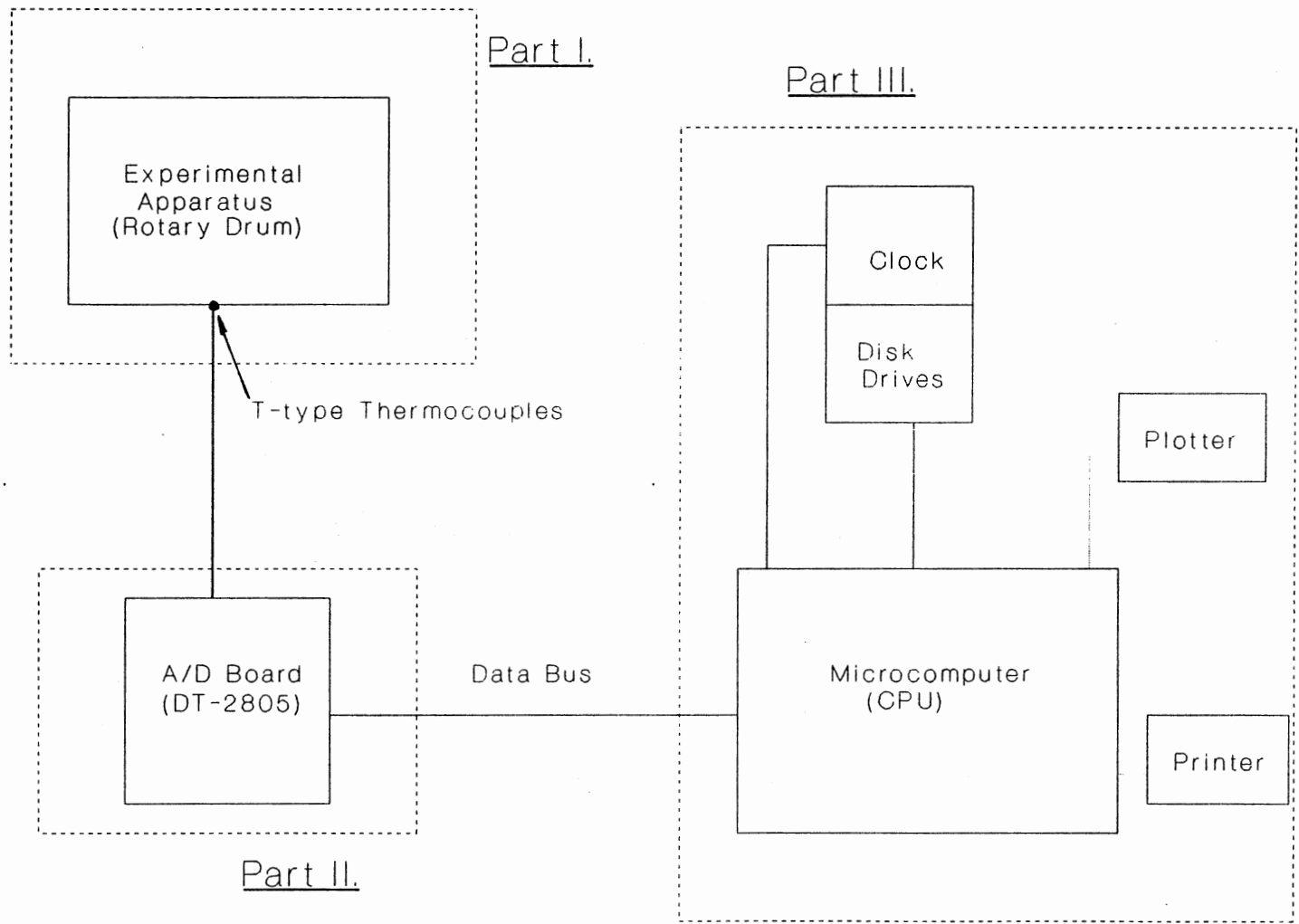


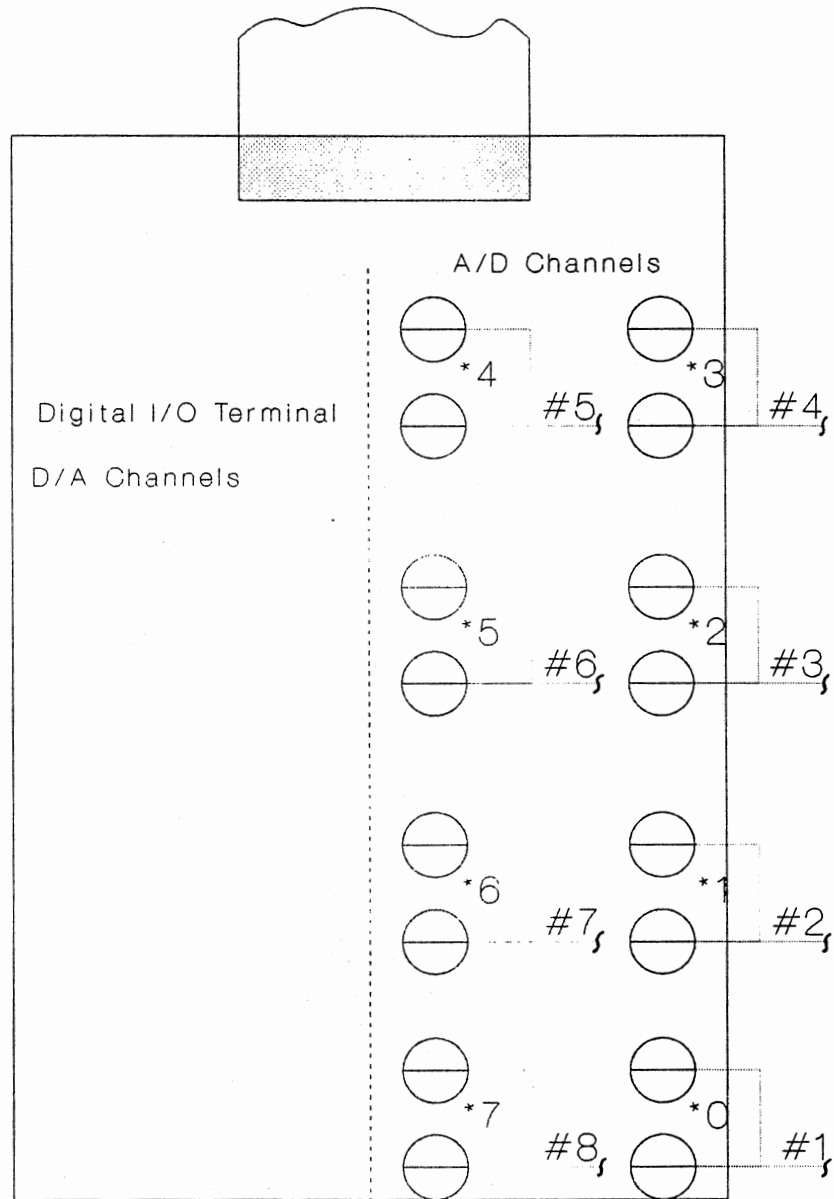
Figure 17. Schematic Diagram for a Data Acquisition System

digital information on the selected channel from the A/D board. The A/D board is designed to select one of 8 input channels to scale the input signal according to the selected full-scale range, and to read this input signal. It returns with a number proportional to the input signal for storage in the memory location of the computer. The desired analog signal is selected by an 8-channel multiplexer when a reading is requested. The input signal is sampled for a short time interval, then held constant by a sample and hold amplifier. The conversion is limited once the signal is fixed.

The DT-2805 board has 12 bit of resolution, which assumes 4096 different states. A 12-bit converter can therefore resolve differences in analog input as small as 0.024% of the selected analog input range. Unipolar input ranges accept positive signals only. On the board, they can be used with input signals ranging from 0-20 mv to 0-10 v depending on the programmable gain setting. The board also contains an on-board programmable clock, which can be used to provide clock pulses to control the operation of the board's A/D subsystems. On this board, a clock is an electronic frequency source which is used to initiate repetitive data conversions, and this internal clock can be set any period from 5.0 microseconds to .1638 seconds, in increments of 2.5 microseconds.

All the channels for analog to digital are easily accessible through a screw terminal as shown in figure 18.

## Cable to A/D Board in One Slot of PC



Note: \* = Channel Number of A/D Board

# = Numbering of Thermocouples

Figure 18. A Drawing for the DT-707T Terminal Panel

This panel is an accessory product which permits the user connections to the DT-2805 board to be made on screw terminals. The DT707 panel plugs into a connector on the A/D board via an integral one meter ribbon cable. In addition, DT707-T is a DT707 panel equipped with a thermocouple cold-junction compensation circuit. The DT707-T contains a thermocouple cold-junction compensation circuit (CJC). The CJC provides a means by which the user can determine the temperature of the DT707-T panel. A short program used to compensate for the cold-junction thermocouple formed at the DT707-T panel, was embedded in the main program developed for data logging. When the CJC is used, it occupies differential input channel zero and channels 1 through 7 can be used for the thermocouple inputs.

Part III contains a personal computer. Peripheral devices, such as a plotter, can be used to plot a graph for presentation of the results of the experiment. The real-time software simulates the actual time and forces the microcomputer to follow events in the real world. The IBM-PC programmed in the BASIC language is sufficiently powerful for this application.

A computer language program written in BASIC, named ADBLOCK, is used to read a block of A/D channels under program control at a rate of 10 conversions per second and is listed in appendix B. It sets the DT-2805 on-board clock to operate at a frequency of 10 Hz. This program requests

that the user to provide information interactively such as the A/D input channels to be sampled, the total number of A/D conversions which will occur, etc. For proper completion of the program, legal values must be entered for these inputs.

The program will then perform the block of A/D conversions. It calculates the voltage input values from the converted data, and prints out these values for the entire block. In addition, a regression fitting procedure was used to obtain an equation which will correlate the relationship between the voltage and temperature for type T thermocouples. This program was written in FORTRAN and is listed in appendix B. The equation obtained from this procedure is used with the data logging program to convert the voltage into its corresponding temperature values.

#### Experimental Variables

The variables in this study were: (i) rotational speed of drum, (ii) rotational speed of screw conveyer, and (iii) soybean flow rate. The range of these rates was selected to determine the limits of the present design with respect to heat transfer coefficients. The dependent variables measured were: (i) unsteady temperature profile of prop inside the drum, (ii) soybean outlet temperature, (iii) the temperature of the prop inside the hopper, and (iv) feed rate of prop. Other readings including rotational speed of drum, screw conveyer and soybean feeder; fluidized bed

temperature; outlet flow rates of prop and soybean as well as room temperatures were occasionally checked by means of a stop watch, a scale and a digital temperature read-out device to ensure the experiment is operated as desired. The inlet temperatures of soybean and prop as well as the prop feed rate was kept constant during the experiment.

## Experimental Procedures

### Methods

A continuous counterflow particle-particle heat exchange process as described was designed and built to take experimental data. Unsteady state heating tests were designed in order to evaluate the performance of this process as a heat exchanger. Soybean temperatures, and prop temperatures as a means to represent the efficiency of this process were chosen as output variables of primary importance. Variable process inputs include the rotational speed of drum and screw conveyer as well as soybean feed rates. Temperature data on the ambient condition, soybean stream, and prop stream were recorded every 5 minutes. The time was also recorded, along with true machine speed, flow rate, fluidized bed temperature. Each test was continued until a steady state was reached. In general, this requirement took around two hours.

Before taking experimental data, a few preliminary tests were carried out which included measurement and determination of the operating ranges of the apparatus, such

as rotary speed of drum and screw conveyer, feed rates of soybean and prop, and the heating capacity of the fluidized-bed vessel, etc. Preliminary tests of this process revealed several adjustments that could be made in order to improve performance. These were:

(i) The outlet fluidized bed was connected to the inlet of drum directly, by feeding the cool prop into the fluidized bed at constant flow rate using the vibratory feeder in the original design. The output rate from the fluidized bed, however, was not constant because of slug flow inside the vessel. An alternative method was used by switching the fluidized bed and the vibratory feeder operating sequence, i.e. feeding the cool prop into the fluidized bed instead of the vibratory feeder. Hot prop inside the fluidized bed was then pumped out using the compressed air provided by the compressor and manually feed into the vibratory feeder periodically. In this alternative arrangement, the outlet of vibratory feeder was connected to the inlet port of the drum directly.

(ii) The second problem that occurred was that the vibratory feeder was not able to function normally to provide a constant feed rate of hot prop, and the flow rate varied in a range of 172 lb/hr to 439 lb/hr at its maximum scale. From experimental observation, the output rate of the feeder was found to be inversely proportional to the prop level inside the hopper due to excessive vibration. In order to overcome this problem, a decision was made to add

some heavy lead blocks on the top of the hopper to keep it from vibrating. This method reduced variation in the prop feed rates to a tolerable range, but was not perfect.

(iii) Finally, a large amount of heat loss was found in this system. In order to minimize the heat loss, insulating materials were added on the prop hopper and vibratory feeder. Since the fluidized media was changed from sand to prop the SBL-2 fluidized bath temperature could no longer heat up to 600 °C. Because of the limitation on heating capacity of this device, a decision was made to fix the flow rate of prop at about 75 lb/hr, and the flow rate of soybeans was fixed at 25 or 35 lb/hr.

The rotational speed of the drum was set at 2.0, 1.0, 0.5 and 0.25 rpm for the experiment. The working volume in each pitch inside the screw conveyer can be varied by changing the rotational speed of the screw helix, provided that the feed rate of the soybeans was kept constant. In order to provide a more reliable system for temperature measurement, a computerized data acquisition system was designed and built. One initial difficulty that developed was that the available channels on the A/D board was limited. Therefore, the channel for temperature measurement of soybeans at the inlet was disconnected and reserved to monitor the temperature inside the prop hopper. Initially channel 0 was assigned to CJC circuit to compensate for changes in room temperature, instead this activity was executed inside the main computer program.



The distribution of the residence time of solids in a rotary drum can be determined by a stimulus-response technique. For this technique a unit impulse of particles is injected into a simple, closed system, and a measurement is taken of the distribution of the particles in the outlet stream. A perfect tracer should have exactly the same flow properties as the particles it represents, and yet it is sufficiently different in some attribute that it can be detected by an analytical method. In this particular system, the prop particles were used as a tracer to determine the residence time distribution of the particles inside the rotary drum. Further experimental investigation on choosing a suitable tracer and detector for this system is strongly encouraged.

After the preliminary tests were completed and the adjustments noted above were made, 7 experimental runs were conducted to evaluate this new process.

#### Residence Time Test

The specific experimental procedures to measure the residence time distribution of prop inside the drum are listed below:

- (1) The drum was started and rotated at a desired speed.
- (2) A known amount of prop was dumped into the inlet port of the drum, and stop watch was started.
- (3) Discrete sample of prop were collected at the output port of the drum at fixed time intervals.

- (4) The weight and time were record continuously, until all the prop was collected.
- (5) The experiment was repeated for another set of experimental conditions.
- (6) Data from this experiment were plotted and analyzed at the conclusion of the experiment.

### Heating Test

In order to properly carry out experimental data collection, the following procedures were used for this research:

- (1) Check the oil and motor oil level of the diesel engine compressor.
- (2) Connect the rubber hose to the inlet port of the fluidized bed, and start up the compressor outside the building.
- (3) Set both the energy regulator and heater switch control knobs to OFF position on the fluidized bed.
- (4) Connect the fluidized bed to the correct electrical supply (220/250 volts, 50 Hz) ensuring correct polarity and turn on the heaters. Connect electricity to all other units.
- (5) Slowly open the air control valve until the bed appears to be continuously boiling.
- (6) Set the heater switch to high(3 kw) and set the energy regulator knob to a high value, 10, then as the desired temperature (220 °F) is approached the knob should be

slowly turned counter-clockwise to a lower reading until the desired temperature is achieved.

- (7) With increasing bed temperature the air control valve must be adjusted to reduce the flow, but the bed still must be kept in a boiling state.
- (8) Connect the DT2805 with DT707-T to the IBM-PC and turn on the power. The A/D board and the thermocouples should be tested to ensure that the whole system is working.
- (9) Running the BASIC interpreter and load the data logging program (ADBLOCK) into the memory.
- (10) Fill up the prop hopper with heated prop from the fluidized bed. Start the drum rotating at the desired speed. Fill up the soybean hopper.
- (11) Start a stop watch and the vibratory feeder at same time, and set the feeder at the desired flow rate for prop feeding into the drum.
- (12) Run the ADBLOCK program and answer the key questions from keyboard, such as the room temperature, how many channels to scan, etc.
- (13) Take temperature measurements every 5 minutes by hitting the enter key on the keyboard. The experimental data will be saved on the floppy disk automatically.
- (14) Collect the prop at the outlet of the drum and put these particles back into the fluidized bed vessel for reheating; Check the level of the prop hopper.
- (15) When the temperatures of the prop reach steady state

( $\pm 2$  °F), turn on the screw conveyer and the soybean feeder. Set the rotational speed to obtain the desired flow rates of soybean and the desired working volume inside the conveyer.

- (16) Take the temperature measurements of prop and soybean every 5 minutes.
- (17) Make occasional measurements of the rotational speed of the drum, screw conveyer, screw feeder; fluidized bed temperatures; output rates of soybeans and prop as well as the input rates of the prop.
- (18) When the soybean outlet temperature reach steady state, change the operating variables such as drum speed, conveyer speed, soybean feed rate to another operating level with the same procedures described above.
- (19) Data from the text files which are stored on the floppy disk during the experiment can be plotted and analyzed at the conclusion of the experiment.

## CHAPTER IV

### MATHEMATICAL MODEL DEVELOPMENT

Mathematical models are important tools for design and analysis. Theoretical and/or empirical models are particularly useful to process engineers in that a certain idea or operation can be analyzed prior to the physical experiment. The use of solid heat transfer media as a mechanism for thermal disinfestation is a prime target for initial investigation through established model analysis. The general method of attack on this kind of analysis is to split the heat transfer problem into a heat conduction problem and a particle motion problem. Once the particle motion problem is solved, the heat conduction problem can be solved by the application of analytical methods with information provided from the particle motion.

The residence time distribution (RTD) model for the prop particles inside the drum will be investigated and developed, based on the characteristics of the heating medium flow pattern inside the rotary drum. Consequently a mathematical model was developed that predicts both the steady state and transient response of the temperature profiles of a continuous counterflow solid-solid heat exchange process. Due to a lack of knowledge on the

performance of a device which accomplishes this type of heat transfer, experimental work was carried out as described in the previous chapter. In order to predict the effect of system parameters on performance of this new heat exchanger, an analytical tool of some nature is required. The model was developed based on a theoretical viewpoint first and then this model was modified into a more realistic model based on the experimental observations.

#### Residence Time Model

It may be postulated that deviation of the residence times from the mean arise from a large number of random variations in the local velocities as they pass through the rotary drum. These disturbances on the flow are statistical in nature and may be treated mathematically in the same way as heat conduction in solids and the molecular diffusion of particles.

Many different types of models could be used to characterize non-ideal flow patterns within the rotary drum. Some draw on the analogy between mixing in actual flow and mixing in diffusional processes, others visualize various flow regimes connected in series. Models vary in complexity, but generally one parameter models can adequately represent flow patterns for mixing.

The analysis of the present system was carried out by considering the simplest mono-dimensional models, in terms of the dispersion model and the tanks-in-series model to

describe the random movement of the particles inside the system. The dispersion model is based on the generalized equation:

$$E_{\theta} = \frac{1}{2 \cdot [\pi(D/uL)]^{\frac{1}{2}}} \exp \left[ \frac{-(1-\theta)^2}{4(D/uL)} \right] \quad (12)$$

where  $D/uL$  is the dispersion number, which is characterized by the mean and variance of the residence time of the medium within the drum. The axial dispersion number uniquely characterizes the degree of dispersion in the medium flow. The system will approach plug flow if this number becomes zero, and the system approaches mixed flow if this number becomes very large. This dispersion number can be computed from the experimental results as a function of the variance.

In the experimental rotary drum, dispersion of the medium occurs neither upstream of the drum inlet nor downstream of the outlet thus the flow regions corresponds to the "close-close" situation described by Wen and Fan (67). The following relationship between variance, mean residence time, and dispersion is given by those authors as:

$$\sigma_{\theta}^2 = 2(D/uL) - 2(D/uL)^2 [1 - \exp(-uL/D)] \quad (13)$$

If the dispersion effect is small, equation (13) can be simplified to:

$$\sigma_{\theta}^2 = 2(D/uL) \quad (14)$$

In the case of the tanks-in-series model, the flow is considered to pass through a series of equal-size ideal

stirred tanks, and the one-parameter of the model is the number of tanks. The number of tanks may be determined by measuring the amount of medium in the outlet stream of the drum at fixed time intervals in a pulsed test. In the series model, the relationship between exit age distribution and time is given as follows:

$$E_{\theta} = \frac{N(N\theta)^{N-1}}{(N-1)} \exp(-N\theta) \quad (15)$$

N can be computed from the experimental results either by a comparison of the RTD curve given by equation (12) for various values of N with the experimental data or by using the simple relationship,  $N = 1/\sigma_{\theta}^2$ . The results of both these one-parameter models in terms of dispersion number and tank number will be discussed in the Chapter of Results and Discussions.

#### Heat Transfer Model

An objective of the research was to develop a model capable of relating the heat transfer coefficient,  $h$ , to the transient temperature profile, and to the various operating parameters of a unique continuous counterflow solid-solid heat transfer system. Such a model could be used to predict the heat transfer efficiency, heat loss to the environment and the time constant at different operating conditions. The model would therefore serve as a tool for improving the contactor design. The following heat transfer equations are



focused only for this specific system.

Beginning with a general form of the thermal energy equation for a free flow process, several assumptions are made as follows: (1) negligible viscous flow and reversible work (2) constant thermal conductivity, (3) one dimensional flow without heat generation, and (4) negligible second partial derivatives:

$$\rho c_p \left[ \frac{\partial T}{\partial t} + u_z \frac{\partial T}{\partial z} \right] = 0 \quad (16)$$

where  $u_z$  is the velocity of the stream in the z-direction, This is an ideal thermal equation with one phase flow.

Lumping of distributed parameter models is an important technique in obtaining a mathematical solution, particularly for the solution of a model involving a partial differential equation as is in equation (16). In order to develop a lumped parameter model equivalent to the distributed parameter model of equation (16), the spatial variation of temperature must be eliminated, leaving only a continuous time dependence. Suppose a system is set up as shown in figure 19, each of which is represented by an unsteady state macroscopic model, i.e. a lumped parameter model. The total length of the exchanger is divided up into N equal segments so that  $\Delta z = L/N$ . The macroscopic energy balance of this continuous particle-particle heat transfer process at the n-th stage will be derived with the following assumptions:

- (1) the overall process was equally divided into N stages;
- (2) the cold-stream flow is close to plug flow ;

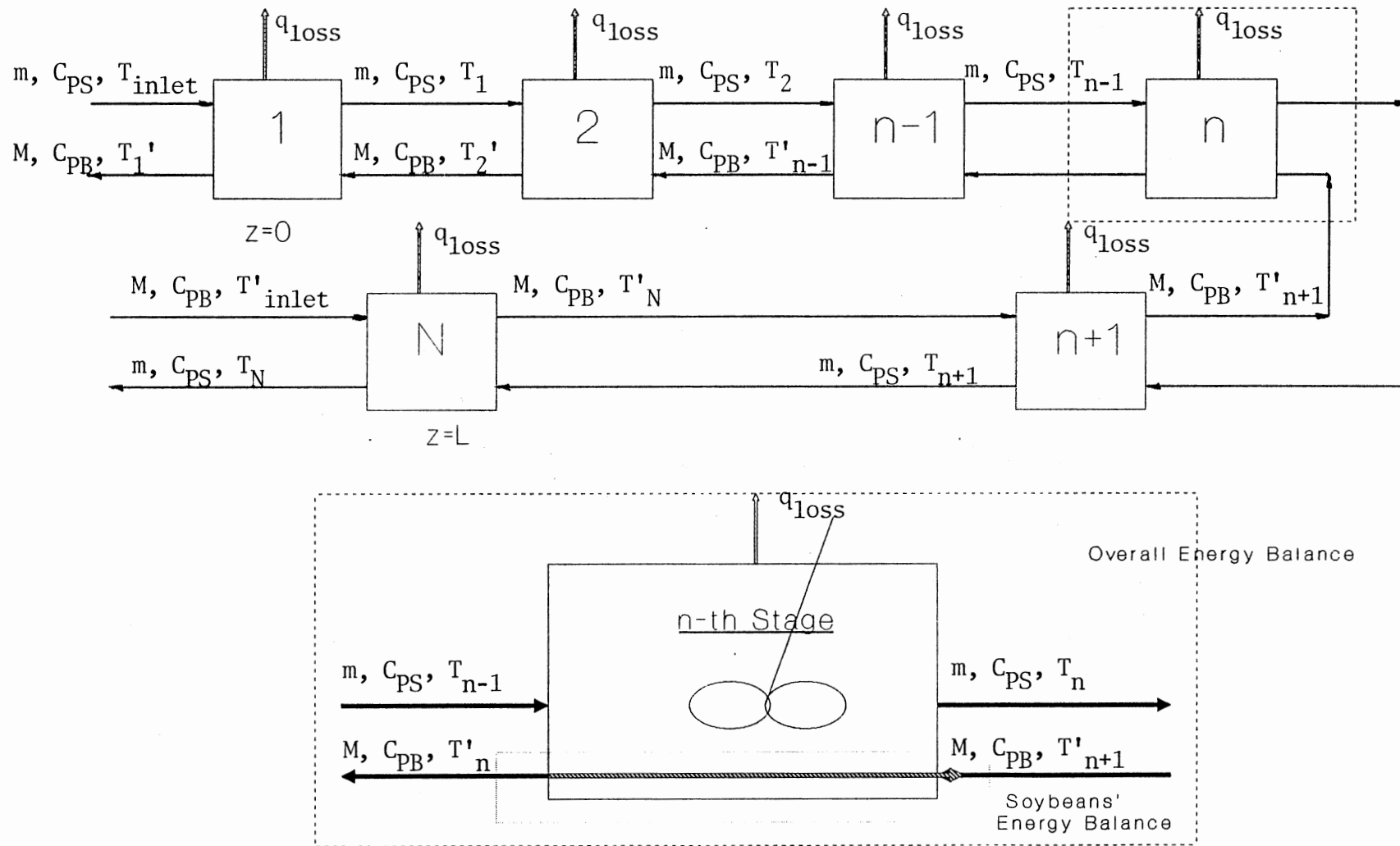


Figure 19. A Physical Representation for the Stagewise Heat Transfer Process

- (3) the mass flow is at steady state in both phases;
- (4) the heat transfer coefficient between the big particles and the small particles is assumed constant at each stage;
- (5) the heat capacity for both particles is assumed constant;
- (6) no chemical reaction, no heat generation by shaft work or no heat consumption occurs in this system;
- (7) each stage is well mixed in the small particle phase;
- (8) heat loss to the air between the second stage and the (n-1)-th stage is at the same level;
- (9) thermal radiation and any heat related to phase changes is neglected;
- (10) the heat loss term for the large particles (soybeans) is embedded in the 'UA' term, which is related to the system efficiency;
- (11) the equivalent thermal mass of the apparatus is lumped with the processed materials term.

The overall energy balance at n-th stage is:

$$q_{in} - q_{out} - q_{loss} = \text{accumulation} \quad (17)$$

$$q_{in} = m \cdot C_{ps} \cdot T_{n-1} + M \cdot C_{pB} \cdot T'_{n+1} \quad (18)$$

$$q_{out} = m \cdot C_{ps} \cdot T_n + M \cdot C_{pB} \cdot T'_n \quad (19)$$

$$q_{loss} = UA' \cdot (T_n - T_{air}) \quad (20)$$

$$\text{Accumulation} = (V_m + V_B) \cdot C_{ps} \cdot \frac{dT_n}{dt} \quad (21)$$

Substituting into equation (17), and rearranging gives:

$$\frac{dT_n}{dt} = \frac{1}{(V_m + V_B) C_{PS}} \left[ m \cdot C_{ps} (T_{n-1} - T_n) + M \cdot C_{pB} (T'_{n+1} - T'_n) - UA' (T_n - T_{air}) \right] \quad (22)$$

with initial conditions,  $T_{inlet} = 180 \text{ }^\circ\text{F}$ ,  $(T_1 \sim T_n)_i = 70 \text{ }^\circ\text{F}$ .

The energy balance of soybeans at n-th stage is:

$$q_{in} = M \cdot C_{pB} \cdot T'_{n+1} + UA \cdot \Delta T; \quad \text{let } \Delta T \cong T_n - T'_n \quad (23)$$

$$q_{out} = M \cdot C_{pB} \cdot T'_n \quad (24)$$

$$q_{loss} = 0 \quad (25)$$

$$\text{Accumulation} = V_M \cdot C_{pB} \cdot \frac{dT'}{dt} \quad (26)$$

Substituting into equation (17) and rearranging, gives,

$$\frac{dT'_n}{dt} \cong \frac{1}{(V_M \cdot C_{pB})} \left[ M \cdot C_{pB} (T'_{n+1} - T'_n) + UA (T_n - T'_n) \right] \quad (27)$$

with initial conditions  $T'_{inlet} = (T'_1 \sim T'_n)_i = 70 \text{ }^\circ\text{F}$ .

At steady state, i.e.  $\frac{dT'_n}{dt} \cong 0$ , equation (27) becomes,

$$M \cdot C_{pB} \cdot (T'_n - T'_{n+1}) = UA \cdot (T_n - T'_n) \quad (28)$$

Letting  $m = \rho A u$ ,  $M=0$ ,  $(V_m + V_B) = \rho A \Delta z$ , equation (29) can be obtained by combining equations (22) and (27) provided no heat loss and heat transfer occurred ( $UA=UA'=0$ ) within the

system, then,

$$\frac{dT_n}{dt} + \frac{u}{\Delta z} (T_n - T_{n-1}) = 0 \quad (29)$$

Comparison of equation (16) and equation (29) the lumped-parameter model, shows the fact that equation (29) is a finite difference analog of equation (16). In fact, equation (29) should become equation (16) as  $n$  approaches infinity, or  $\Delta z$  approaches zero. The lumping procedure changes the spatial derivative in equation (16) to a finite difference form leading to equation (29).

#### Modeling Approach With Computer Algorithms

In the current experimental process as designed and developed, there are 13 stages inside the rotary drum. Thus  $N=13$  will be used in the mathematical equations(22) and (27) for the purpose of modeling. The numerical method for solving a set of first order ordinary differential equation for initial value problems will be employed. The experimental procedures developed as described in previous chapters were: (1) use of hot media to heat up the drum itself without soybean input until steady state is reached; and then (2) use of hot media for heat exchange with the soybeans in a well warmed environment. Based on these experimental procedures, a strategy to approach this problem was to divide the modeling task into 2 major steps: (1) heat exchange with only one phase flow (prop); (2) heat

exchange with two phase flow (prop and soybean).

The important system parameters included model and operating parameters such as  $UA$ ,  $UA'$  ( $UA'_{in}$ ,  $UA'_{int}$ ,  $UA'_{out}$  represent the heat loss at inlet, intermediate and outlet position in the drum, respectively ),  $V_B$ ,  $m$ ,  $C_{ps}$ ,  $M$ ,  $C_{pB}$ ,  $V_m$ , and  $V_M$ . Among these key parameters, the numerical values of the operating parameters ( $m$ ,  $C_{ps}$ ,  $M$ ,  $C_{pB}$ ) were adopted from the experimental data directly; while the values of  $V_m$ ,  $V_M$  could be computed based on the information of mean residence time provided from the experimental data of the RTD tests. Values of the model parameters ( $UA$ ,  $UA'$ , and  $V_B$ ) are to be determined through this work. The strategy taken to approach this problem is to estimate values for these model parameters using a trial-and-error methodology. Initial guess values are assigned from previous researchers (8, 9, 13, 30, 55, 68, 69). The values of  $UA$ ,  $UA'$ , and  $V_B$  were determined numerically through an iteration procedure by minimizing temperature differences between the predicted and observed temperature profiles. The correct values of  $UA$ ,  $UA'$ , and  $V_B$  for this particular system should be obtained once the temperature profile predicted from this model is compares with that of the experimental observations. Therefore the criterion of this methodology is determined on the temperature profile difference between the model predictions and the experimental data, and this algorithm is used to find the values of  $UA$ ,  $UA'$ , and  $V_B$  for various operating conditions.

The impact of the operating parameters on the performance of this new process in terms of  $UA$ ,  $UA'$ , and  $V_B$  thus could be examined and evaluated.

Several primary key parameters affected by the system operating variables are  $V_m$ ,  $V_M$ ,  $V_B$ ,  $UA$ , and  $UA'$ .  $V_m$  is the unit working mass of prop in each stage which assumes the total working mass inside the drum is divided into 13 stages equally.  $V_m$  is determined by the drum speed.  $V_M$  is the unit mass of soybean in each stage. This also assumes the total mass inside the conveyer is divided into 13 parts equally, and is determined by the conveyer speed. While  $V_B$  represents the thermal mass of the whole apparatus and is transformed into the equivalent thermal mass of the prop and lumped together with  $V_m$ .

The values of  $UA$  and  $UA'$  deserve a further explanation and examination. An extensive review of previous works has shown that only a limited information is available on the determination of the heat transfer coefficient, the contact areas, and the contact time of two particle groups in direct thermal contact. Yet none of these seem particularly suitable for the current process. Therefore, a decision was made to lump the heat transfer coefficient ( $U$ ) and contact area ( $A$ ) together to serve as an index of heat transfer efficiency. The same idea applies to the heat loss term. Both the values of  $UA'$  and  $V_B$  were determined in the heat transfer experiment and modeling without soybean input, and consequently, the values of  $UA$  will be estimated in the same

manner with soybean input. In addition, an overall analysis of these model parameters can be summarized by:

- (1) the operating parameters:  $m$ ,  $C_{ps}$ ,  $M$ ,  $C_{pB}$ , rotational speed of drum and conveyer;
- (2) the criterion variables: temperature profiles;
- (3) the system parameters:  $V_m$ ,  $V_M$  and  $V_B$ ;
- (4) the performance parameters:  $UA$  and  $UA'$ ;

The computer program named MODEL, used to solve equations (22) and (27) with initial conditions, was developed for a PC and is shown in appendix B. The algorithm with the IVP solver DGEAR was implemented in Fortran on both an IBM-AT microcomputer and the IBM mainframe at the OSU computer center. A data file to store the temperature profiles is created when this program is running, and this data file can be used with other software, such as LOTUS, Havard Graphics, etc. to plot out the data in any form the user desires. Further development of this simulation program into a package with automatic plotting capability is encouraged in future work. It usually took less than 3 minutes to complete the program running on an 8 MH<sub>z</sub> AT-microcomputer provided there was no errors found at the compile and linkage stages. Thus, the cost to run this program on a PC is minimum by being reasonably fast enough to satisfy the user needs.

The specific procedures to run this Fortran program are as follows:

- (1) obtain values of  $m$ ,  $C_{ps}$ ,  $M$ ,  $C_{pB}$  from the experimental



- operating settings and set up the initial conditions;
- (2) compute values for  $V_m$  and  $V_M$  with the mean residence time provided from the RTD test;
  - (3) set  $V_B$  at zero, and obtain the value for the heat loss term ( $UA'$ ), as the initial guess for program input. This loss is mainly due to air convection at both ends of drum ( $UA'_{in}$ ,  $UA'_{out}$ ) and at intermediate sections along the drum ( $UA'_{int}$ );
  - (4) set the values of  $M$  and  $UA$  equal to zero temporarily;
  - (5) run the program for the one phase flow condition to determine the heat loss and the equivalent thermal mass of the process by comparing the predicted temperature profile and the experimental data. Rerun this step by changing the values of  $UA'$  to minimize the difference between the predicted values and the experimental values. Change values of  $V_B$  to minimize the difference in the time needed to reach steady state between the predicted data and experimental observations;
  - (6) Final values for  $UA'$  and  $V_B$  are estimated once the criterion is met;
  - (7) Change to the correct value of  $M$  as obtained in step 1, and set up the initial conditions of prop temperature profiles from the data obtained from step 6;
  - (8) input numerical values for  $UA$  (from Simonton and Stone (9)), and compute the surface area of soybeans, Lump  $U$  and  $A$  together as the initial guess of this trial-and-error input;

- (9) run the program again for 2 phases flow conditions with  $V_B$  equal to zero as the initial guess to determine the lumped heat transfer parameter (UA) of this process. Change the value of UA until the difference between the predicted outlet soybean temperatures and the experimental observations are minimized.
- (10) values for UA are to be estimated once the criterion is met.

The parameters used for this work and the model results are tabulated and shown in the following chapter. Detailed calculations for  $V_m$  and  $V_M$  at different operating conditions are given in appendix C.

## CHAPTER V

### RESULTS AND DISCUSSIONS

#### Experimental Findings and Analyses for Residence Time

Experimental stimulus-response data from the RTD tests at 2, 1, 0.5, and 0.25 rpm are shown in table I. The two quantities most often measured for describing tracer response curves are: the mean residence time (first moment about the origin), which locates the center of gravity of the response; and the variance (second moment about the mean), which describes how the response is spread out in time. A given distribution of tracer residence time can be completely defined mathematically by the moments of the distribution.

The results of the moment analysis, based on the given information from table I, are shown in table II. Table II shows the mean residence time, variance and dispersion number as well as equivalent tank numbers which were computed based on equations (A3-A8) and (13-15) in Appendix A and Chapter IV respectively. In models, it is usual convenient to measure time in units of mean residence time. The experimental RTD plots of rotational speed of the drum

TABLE I  
THE EXPERIMENTAL STIMULUS-RESPONSE DATA FOR DRUM  
SPEEDS of 2, 1, 0.5, AND 0.25 RPM

#1		#2		#3		#4	
2 rpm		1 rpm		0.5 rpm		0.25 rpm	
t	w	t	w	t	w	t	w
(min.)	(lb)	(min.)	(lb)	(min.)	(lb)	(min.)	(lb)
0	0	0	0.00	0	0.00	21.7	0.00
3	0.04	5.6	0.04	10.5	0.02	25.7	0.06
4	0.76	6.6	0.27	13.5	0.18	29.7	0.15
5	0.75	7.6	0.40	16.5	0.55	33.7	0.27
6	0.21	8.6	0.38	19.5	0.45	37.7	0.30
7	0.04	9.6	0.25	22.5	0.18	41.7	0.22
9.9	0.04	10.6	0.1	25.5	0.07	45.7	0.13
		11.6	0.06	30.5	0.03	49.7	0.07
		12.6	0.02			53.7	0.03
		18.7	0.06			59.9	0.03

TABLE II  
THE MOMENT AND MODEL ANALYSIS FOR DRUM SPEEDS of  
2, 1, 0.5, AND 0.25 RPM

experiment number	$\tau$ (min.)	$\sigma_{\theta}^2$ (dimensionless)	D/uL	N
#1	4.83	0.05	0.025	19
#2	8.74	0.07	0.037	13
#3	18.4	0.038	0.019	26
#4	38.3	0.034	0.017	29

at 2, 1, 0.5, 0.25 rpm are shown in figures 20-23. The various distribution curves based on dimensionless time units are denoted by the subscript  $\theta$ .

A plot of prop variance vs. rotational speed of the drum is shown in figure 24. It is interesting that the maximum value of  $\sigma_{\theta}^2$  occurs at 1 rpm. This phenomenon can be attributed to the angle of repose and the angle of the fixed metal plates since the apparatus was designed to run at approximately 1 rpm. Figure 24 also shows the experimentally determined values of the prop residence time vs. the drum speed. The two curves behave differently. As the rotational speed increases, the residence time of the prop decreases, but the randomness measure (dimensionless variance) increased slightly and had a maximum value at 1 rpm. This implies that the prop particles are mixed the best at this drum speed. An overall view of this graph, however, does not show a significant difference in terms of the variance as a function of the rotational speed of the drum.

The purpose of the RTD study was two fold. First, the experimentally determined mean residence time at various rotational speeds provides information for the calculation of the model parameter ( $V_m$ ) of the heat transfer model. Second, it provides insight into the flow characteristics of the prop. The flow characteristics can be used to explain the behavior of the axial temperature distributions obtained from the heat transfer model in terms of axial dispersion

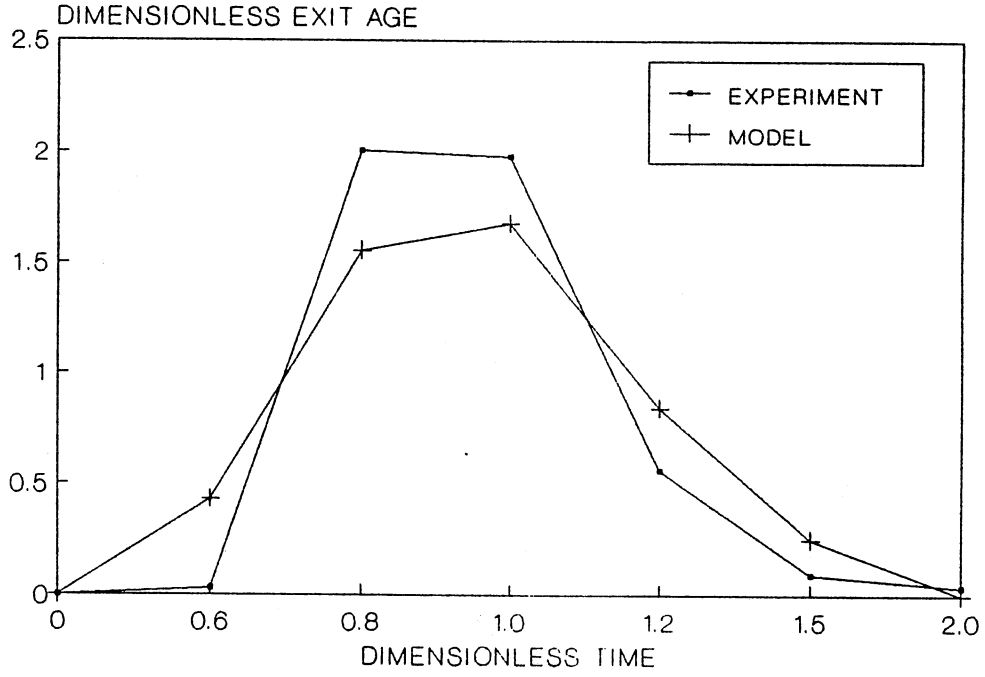


Figure 20. The Experimental Residence Time for a Drum Speed of 2 rpm

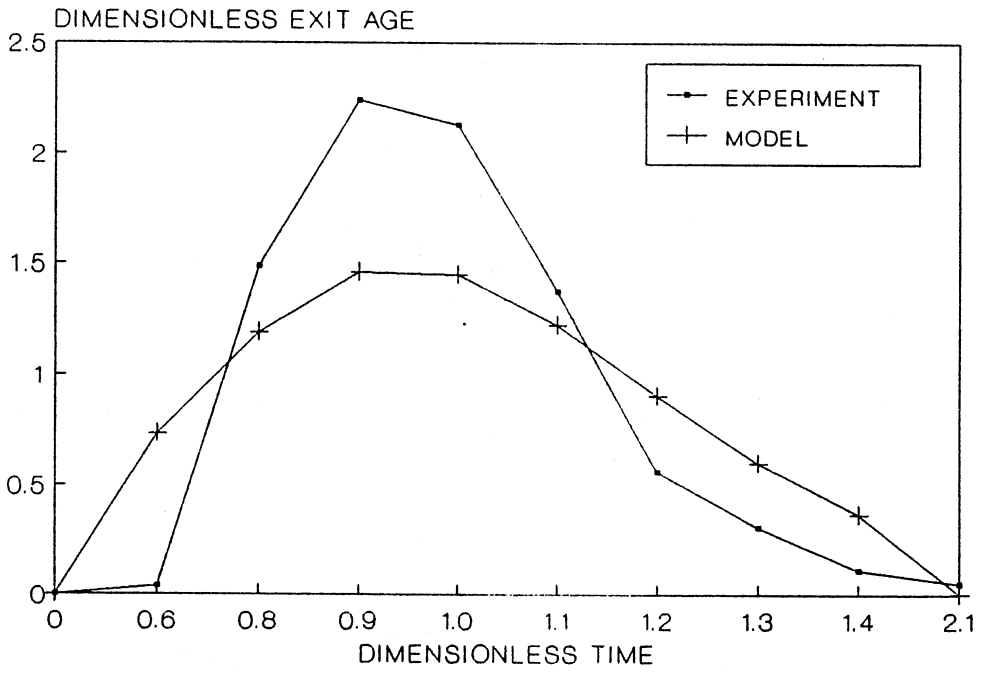


Figure 21. The Experimental Residence Time for a Drum Speed of 1 rpm

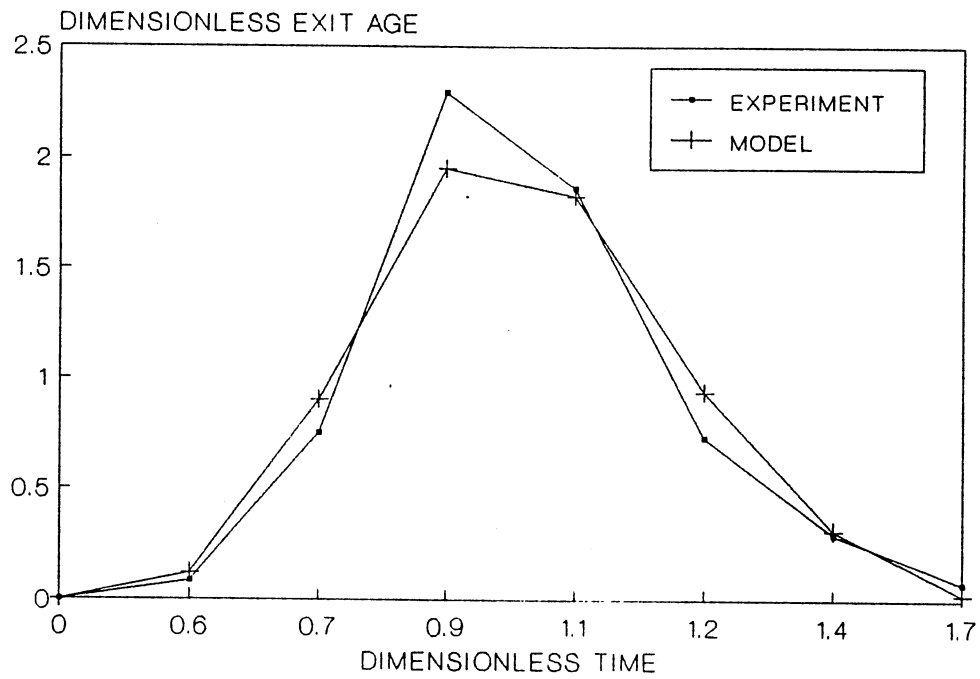


Figure 22. The Experimental Residence Time for a drum Speed of 0.5 rpm

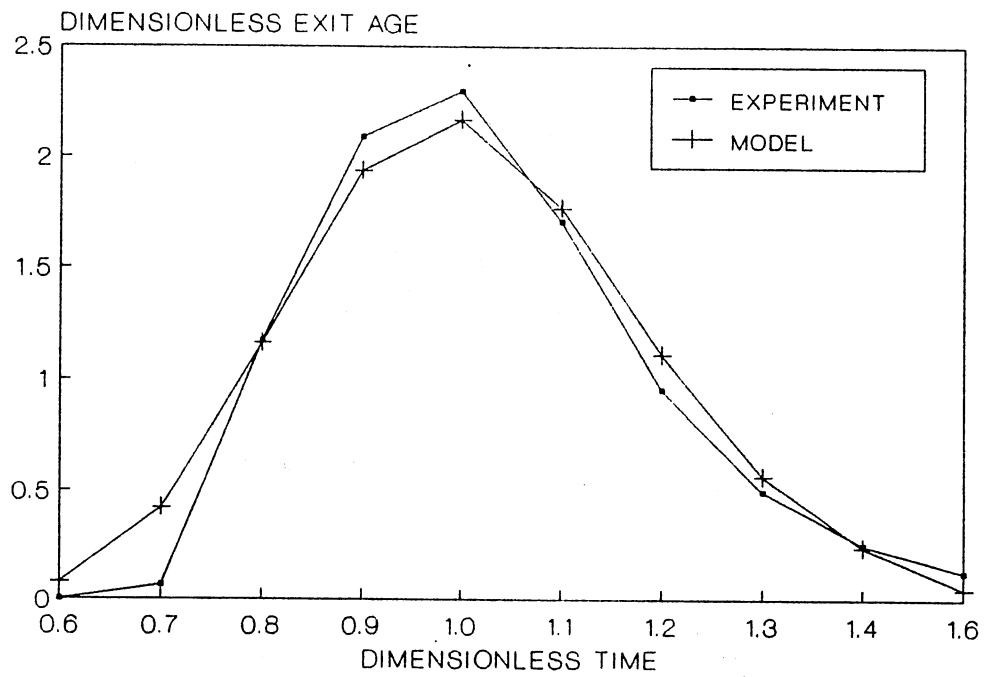


Figure 23. The Experimental Residence Time for a Drum Speed of 0.25 rpm

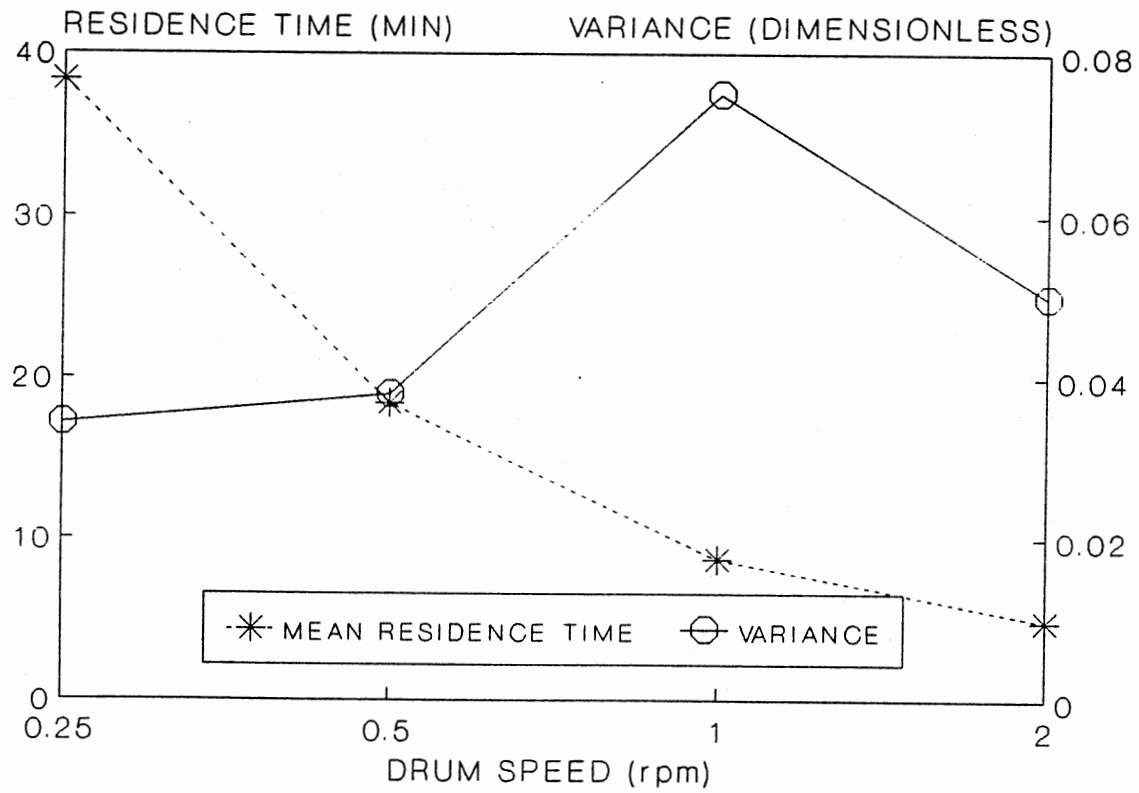


Figure 24. The Experimental Plot of Dimensionless Variance and Mean Residence Time vs. Drum Speed



from the RTD model, similar to the previous work Nillson (64) in a shallow fluidized bed study.

As mentioned in previous chapters, there are many both theoretical and empirical models for the residence time distribution. In the experimental design of this heat exchanger the flow path was divided into 13 cells by means of fixed metal plates. Due to this staged design, use of the semi-empirical equation, tanks-in-series, is most likely to be the best model to use to describe this process. The equivalent tank number is computed based on the compartment model at a variety of drum rotational speeds and was shown in table II. A comparison between the actual measured values and those predicted from the model shown in figures 20-23. It can be seen that the model results fit the experimental data except at 1 rpm. Differences between the model results and the experimental data at 1 rpm can be described by:

- (1) The model parameter,  $N$ , may not be suitable when obtained from the simplified equation,  $N = (\sigma_{\theta}^2)^{-1}$  derived from the compartment model and the dispersion model.
- (2) The model does not account for a longer tail which existed in this particular set of experimental data.

If a fitting procedure is used instead of using the relation,  $N = (\sigma_{\theta}^2)^{-1}$ , an equivalent tank number for this set of data at 1 rpm was determined to be  $N= 20$ . Future research on this subject is needed to develop a new experimental technique to obtain a more accurate estimate of

RTD. In addition, axial and/or radial dispersion effects on the pattern of axial temperature distributions should be examined. The data from this RTD study was used to calculate the mean residence time which is needed to compute one of the key process parameters,  $V_m$ , for the heat transfer modeling. This is described in the following section.

### Heat Transfer System

A series of preliminary performance tests using this new system to exchange heat between interprop and soybeans were run. After many preliminary tests were completed and adjustments were made, seven final experimental runs were carried out to evaluate this new process. Each run consists of four or more tests under different operating conditions and are summarized in table III. The feed rate of the prop was kept as constant as possible, at an average value of 75 lb/hr which will be used in this work.

TABLE III  
EXPERIMENTAL CONDITIONS FOR THE RUNS PERFORMED

Test run (#)	drum speed (rpm)	screw speed (rpm)	soybean feed rate (lb/hr)	time duration (min.)
#1	2.2	n.a.	n.a.	0-265
	2.2	5.57	35	265-332
	1.5	5.57	35	332-360
	1.1	5.57	35	360-397
	0.5	5.57	35	397-445

TABLE III (Continued)

Test run (#)	drum speed (rpm)	screw speed (rpm)	soybean feed rate (lb/hr)	time duration (min.)
#2	2.2	n.a.	n.a.	0-86
	2.2	5.53	35	86-121
	2.2	2.75	35	121-160
	2.2	1.85	35	160-196
#3	0.24	n.a.	n.a.	0-120
	0.24	2.75	35	120-150
	2.2	n.a.	n.a.	0-51
	2.2	2.75	35	51-85
#4	1.1	n.a.	n.a.	0-106
	1.1	5.57	35	106-147
	1.1	2.78	35	147-180
	1.1	1.86	35	180-212
	1.1	3.77	24	212-253
	1.1	1.88	24	253-297
	1.1	1.26	24	297-338
	1.1	2.86	18	338-387
	1.1	1.43	18	387-424
	1.1	0.95	18	424-460
#5	0.5	n.a.	n.a.	0-100
	0.5	5.57	35	100-120
	0.5	n.a.	n.a.	0-77
	0.5	2.78	35	77-118
	0.5	1.86	35	118-154
	0.5	3.77	24	154-191
	0.5	1.88	24	191-224
	0.5	1.26	24	224-291
#6	2.2	n.a.	n.a.	0-87
	2.2	5.57	35	87-126
	2.2	2.79	35	126-161
	2.2	1.86	35	161-197
	2.2	3.77	24	197-232
	2.2	1.88	24	232-267
	2.2	1.26	24	267-320
#7	0.25	n.a.	n.a.	0-101
	0.25	3.77	24	101-141
	0.25	1.88	24	141-174
	0.25	1.26	24	181-213
	0.25	5.57	35	222-247
	0.25	2.79	35	247-287
	0.25	1.86	35	287-347

n.a.: not available

### Experimental Findings

The experimental data from runs #2 and #7 coupled with the plots of soybean outlet temperatures from the rest of the experimental runs are shown in this section to represent typical performance for this system. The rest of the experimental data are seen in appendix D.

Temperature profiles of prop and soybeans along the drum are shown in figures 25-41. The temperature variations of both the prop inside the hopper and the inlet port of the drum with respect to the time elapsed during the experiment are shown in figures 42-43. Figures 44-50 show the temperatures of soybeans at the outlet of the conveyer with respect to time under various operating conditions used in the experiment. Figures 51-52 show the variation of the prop flow rates from the vibratory feeder with respect to time during the experiment.

The data shown in figures 25-52 reveal several important aspects of the system performance. Figures 25-41 show the resulting transient temperature profiles within the heat transfer system using various rotational drum speed ( 0.25 and 2.0 rpm) while the conveyer speed was either varied from 5.5 rpm to 1.8 rpm or from 3.7 to 1.3 rpm depending on the soybean feed rate. From these plots a large temperature difference can be seen between inlet port and first temperature measuring point inside the drum. This shows that a large amount of heat was lost to the environment between these two points due to air convection heat loss.

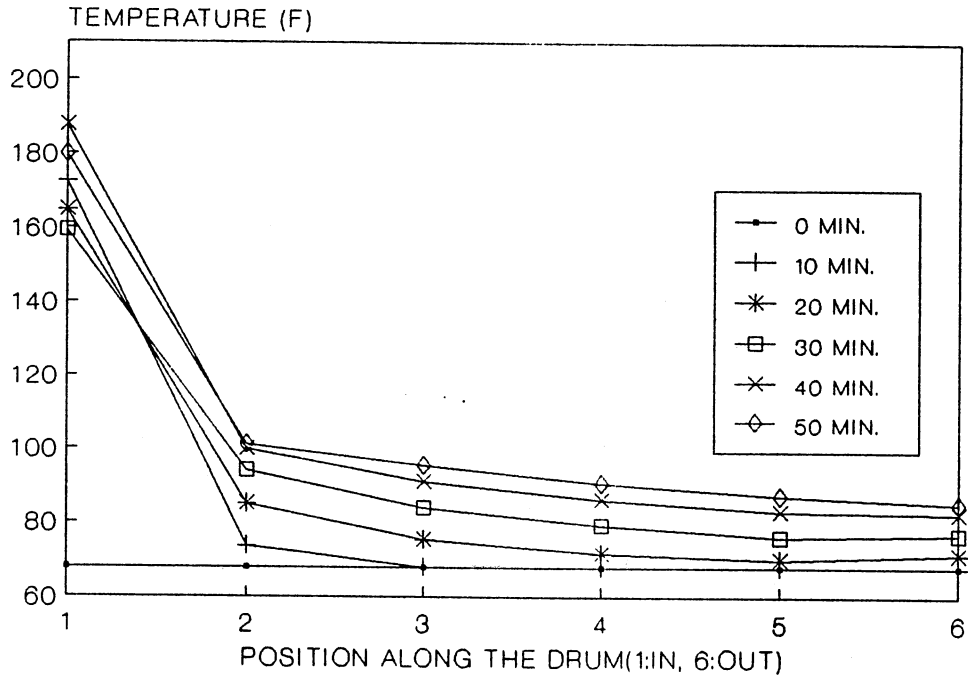


Figure 25. The Temperature Profiles of Prop as a Function of Time Along the Axial Direction for Run #2

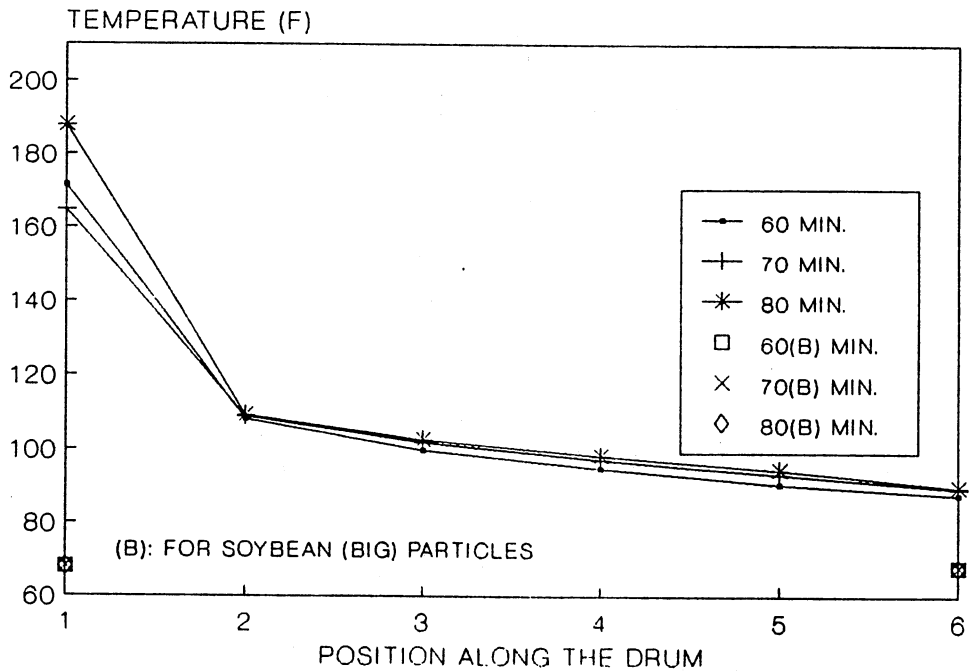


Figure 26. The Temperature Profiles of Prop as a Function of Time Along the Axial Direction for Run #2

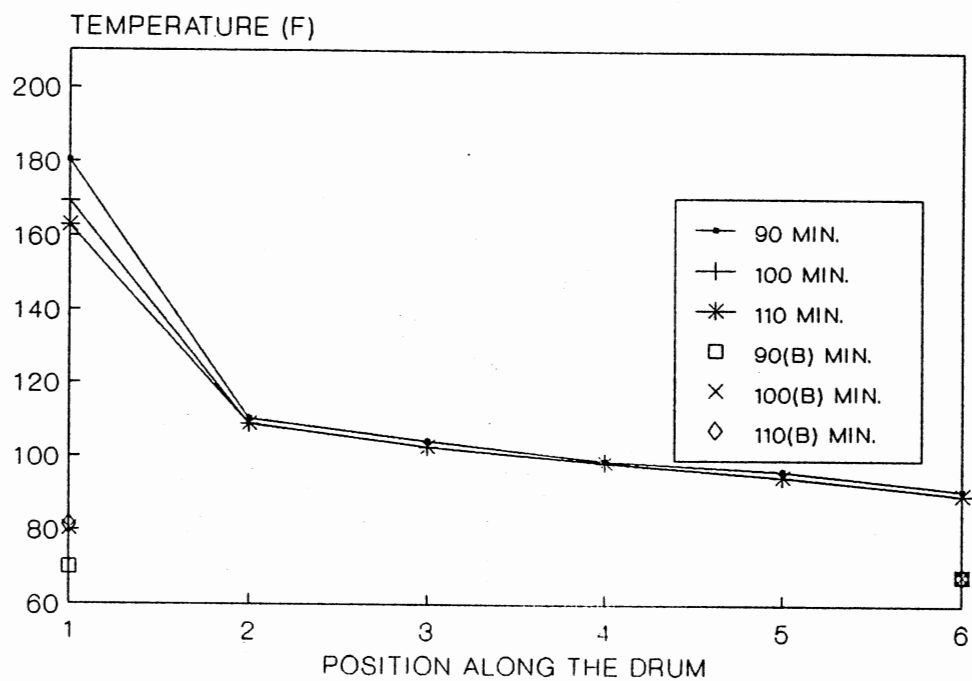


Figure 27. The Temperature Profiles of Prop as a Function of Time Along the Axial Direction for Run #2

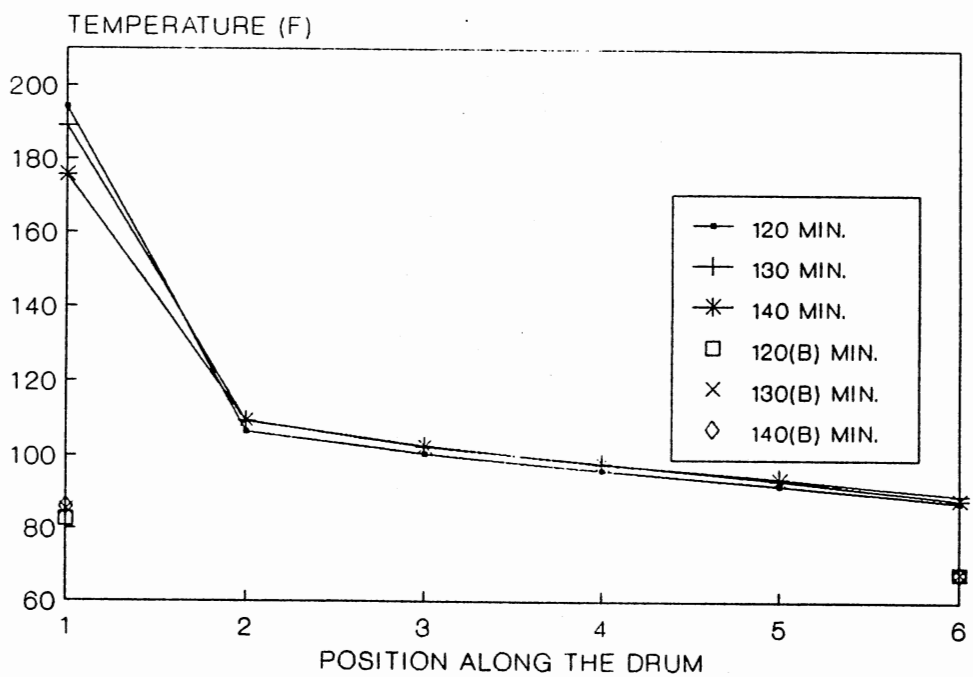


Figure 28. The Temperature Profiles of Prop as a Function of Time Along the Axial Direction for Run #2

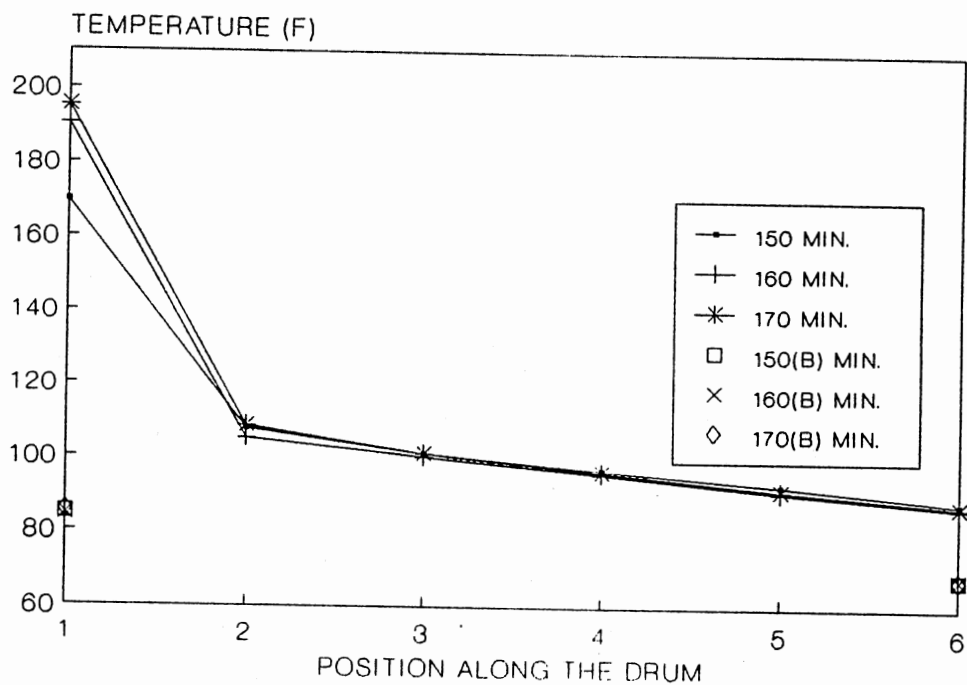


Figure 29. The Temperature Profiles of Prop as a Function of Time Along the Axial Direction for Run #2

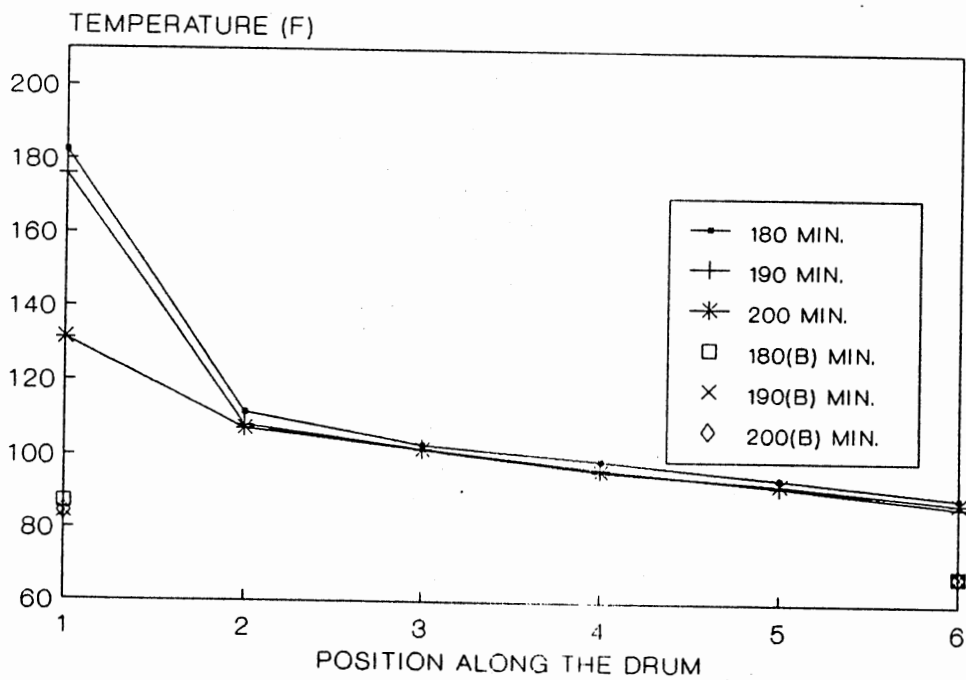


Figure 30. The Temperature Profiles of Prop as a Function of Time Along the Axial Direction for Run #2

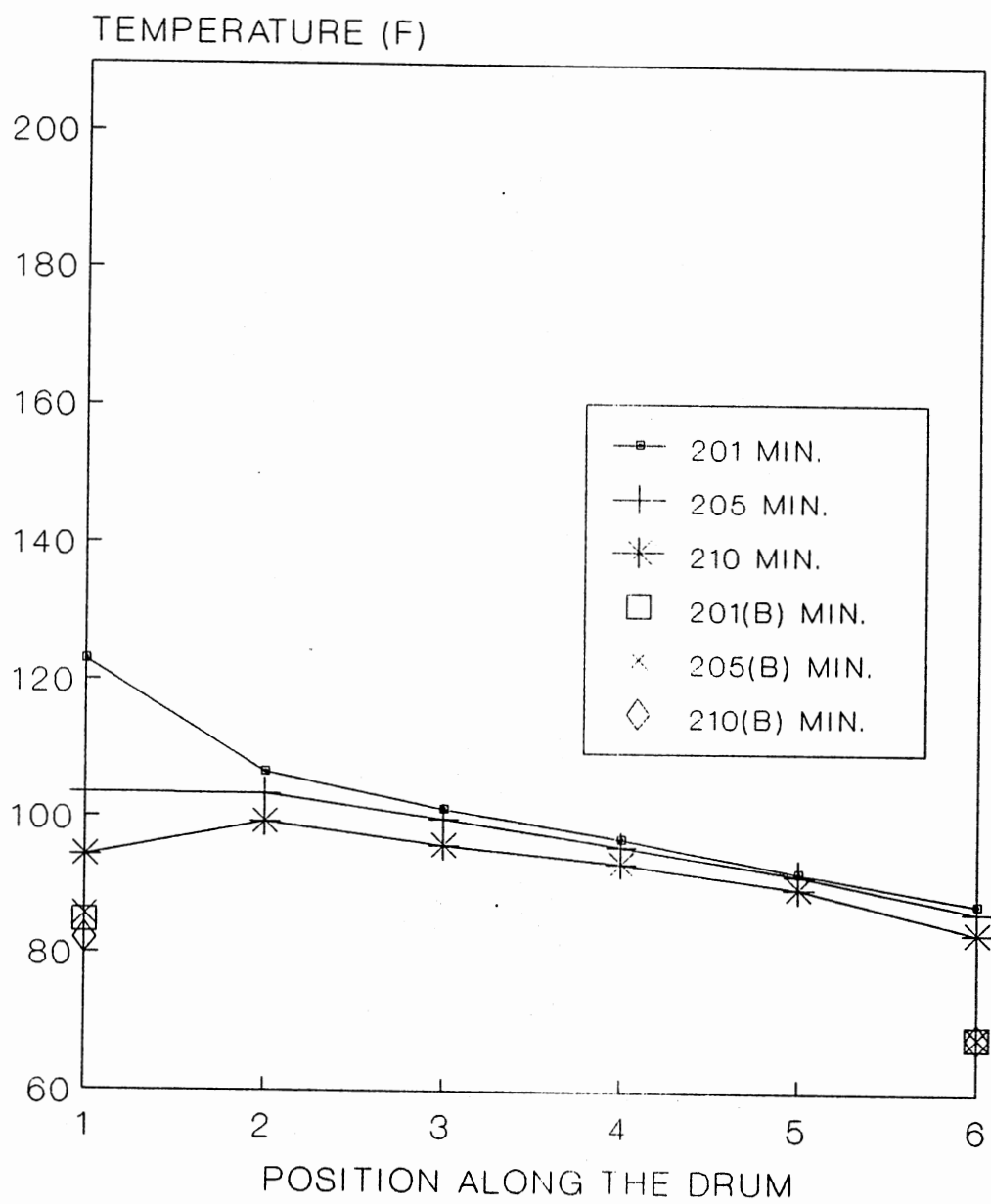


Figure 31. The Temperature Profiles of Prop as a Function of Time Along the Axial Direction for Run #2



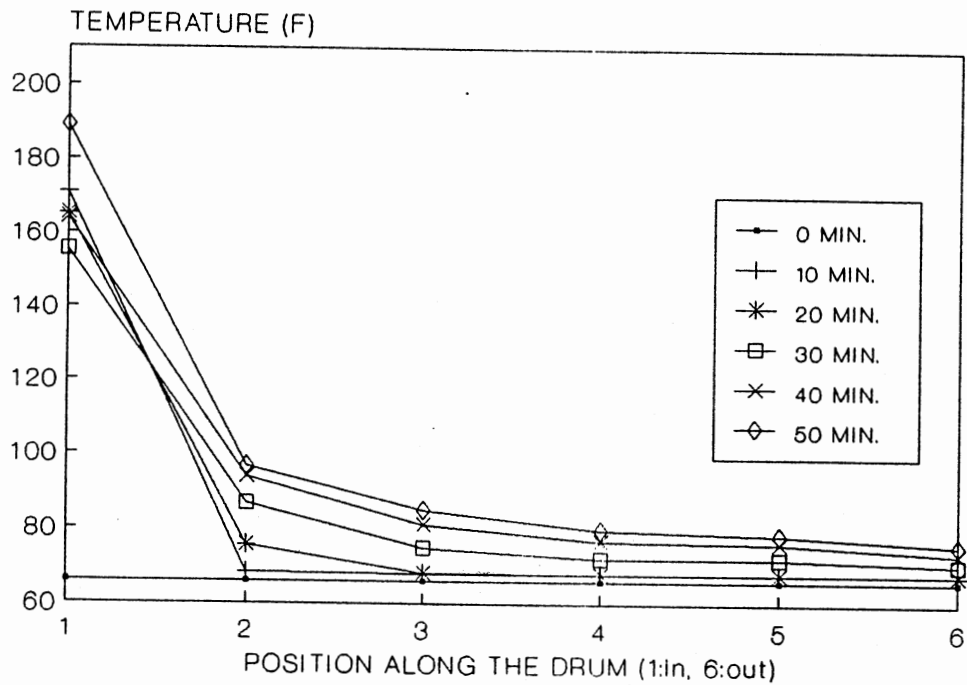


Figure 32. The Temperature Profiles of Prop as a Function of Time Along the Axial Direction for Run #7

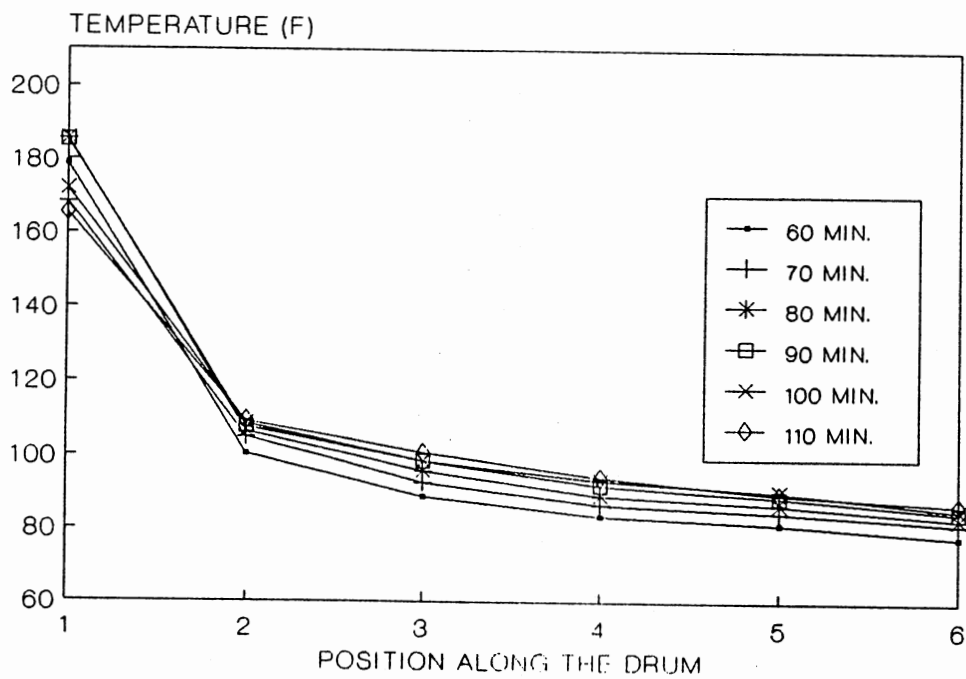


Figure 33. The Temperature Profiles of Prop as a Function of Time Along the Axial Direction for Run #7

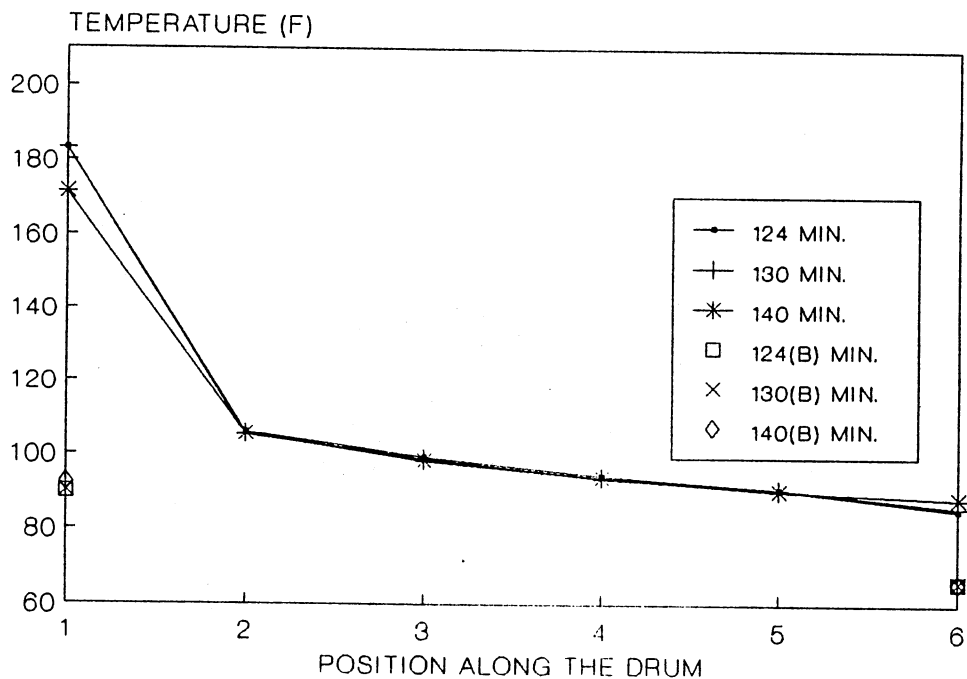


Figure 34. The Temperature Profiles of Prop as a Function of Time Along the Axial Direction for Run #7

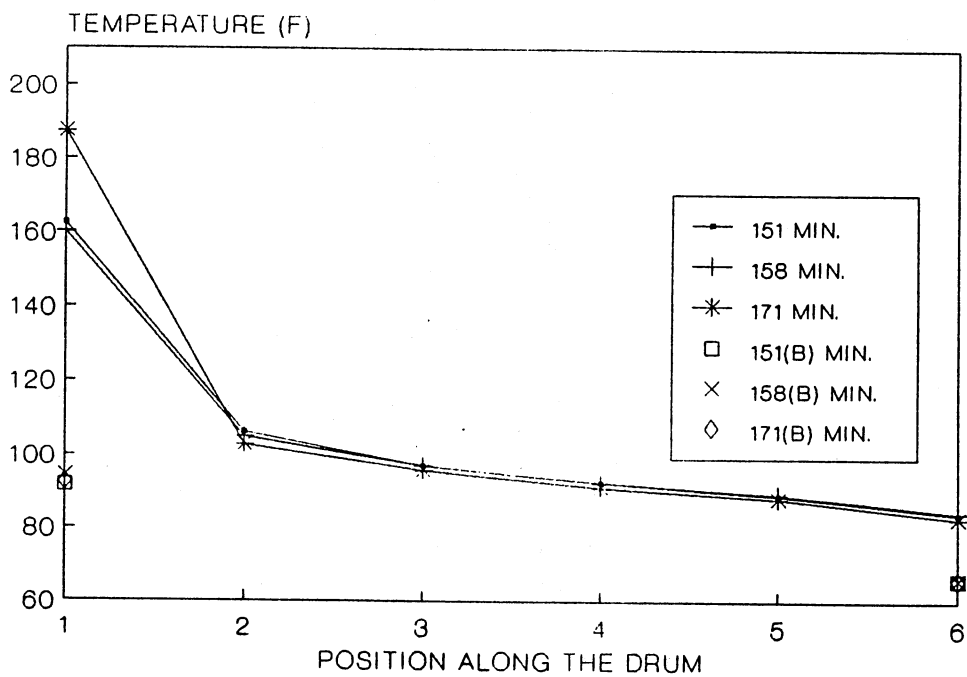


Figure 35. The Temperature Profiles of Prop as a Function of Time Along the Axial Direction for Run #7

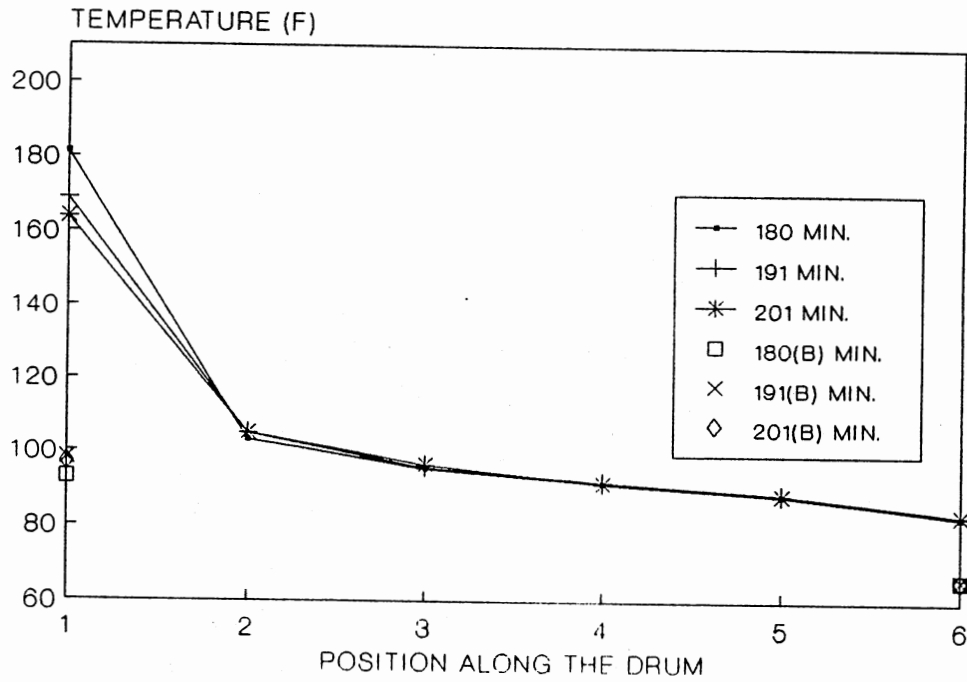


Figure 36. The Temperature Profiles of Prop as a Function of Time Along the Axial Direction for Run #7

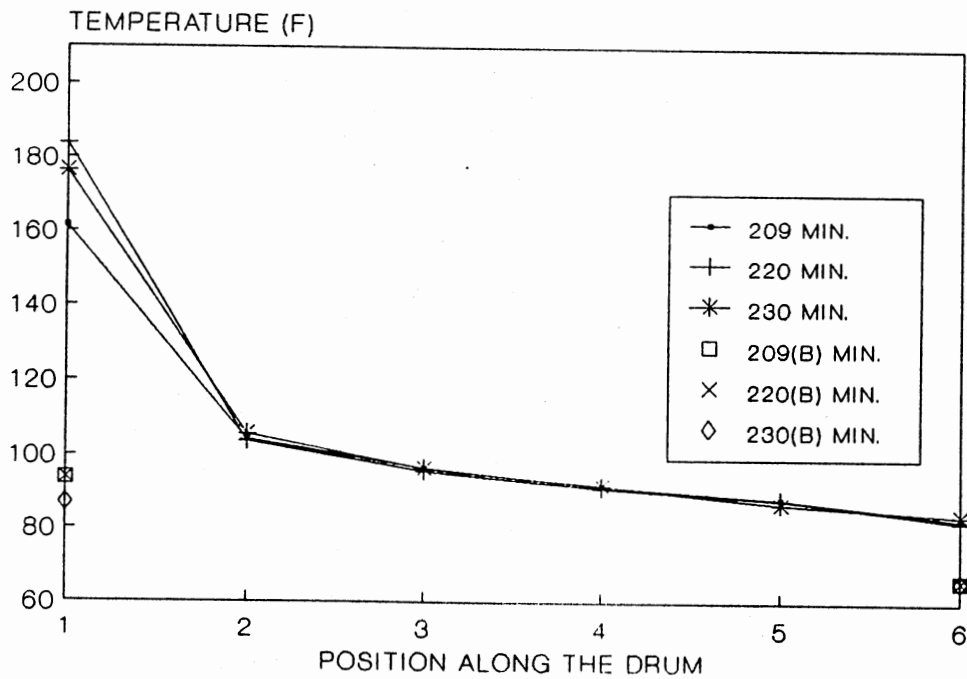


Figure 37. The Temperature Profiles of Prop as a Function of Time Along the Axial Direction for Run #7

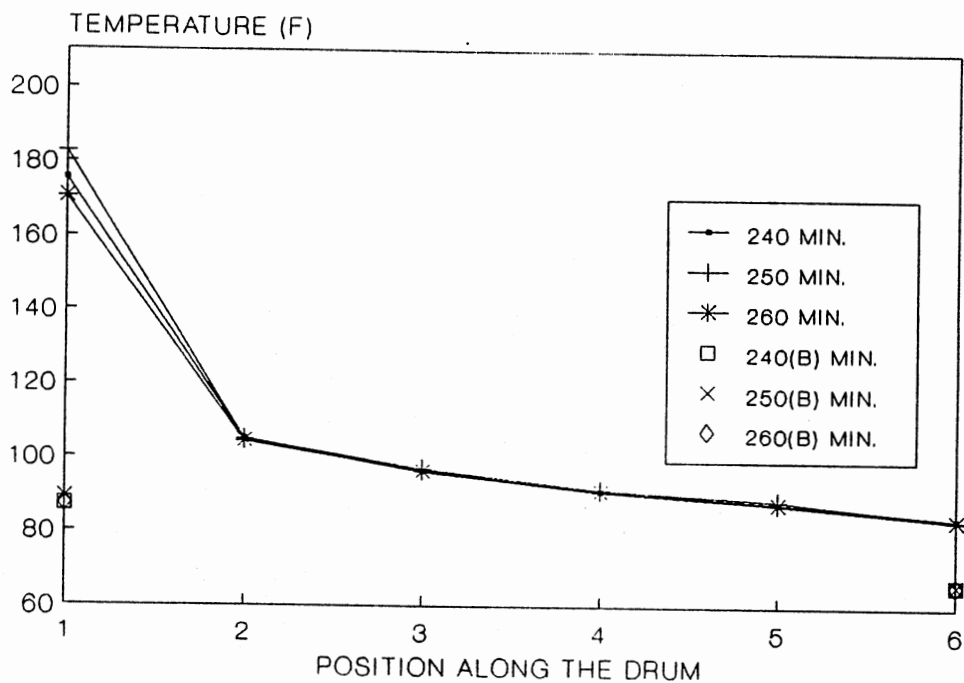


Figure 38. The Temperature Profiles of Prop as a Function of Time Along the Axial Direction for Run #7

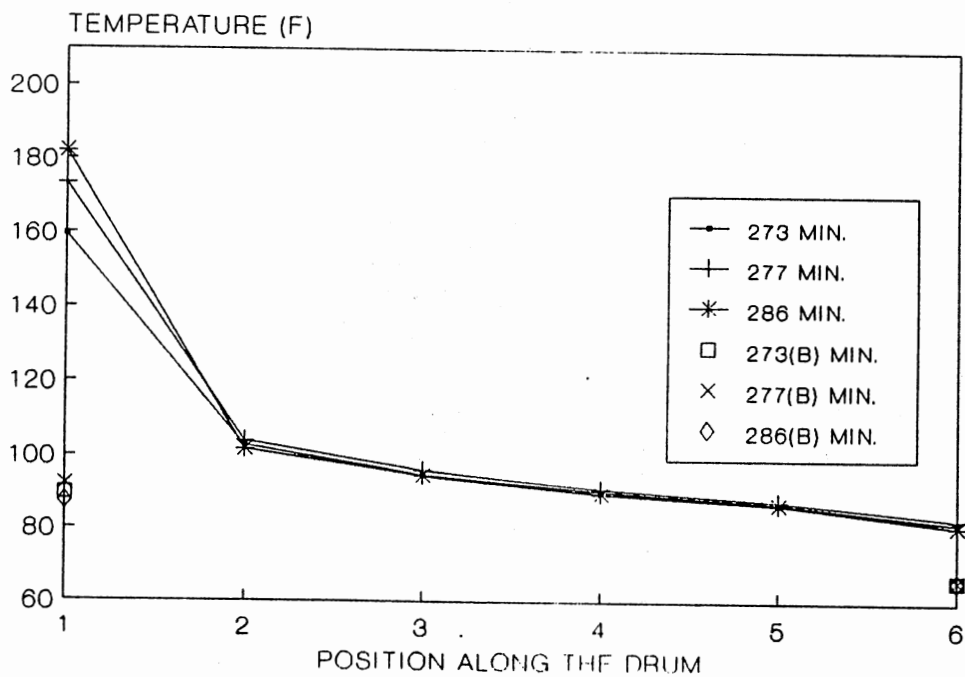


Figure 39. The Temperature Profiles of Prop as a Function of Time Along the Axial Direction for Run #7

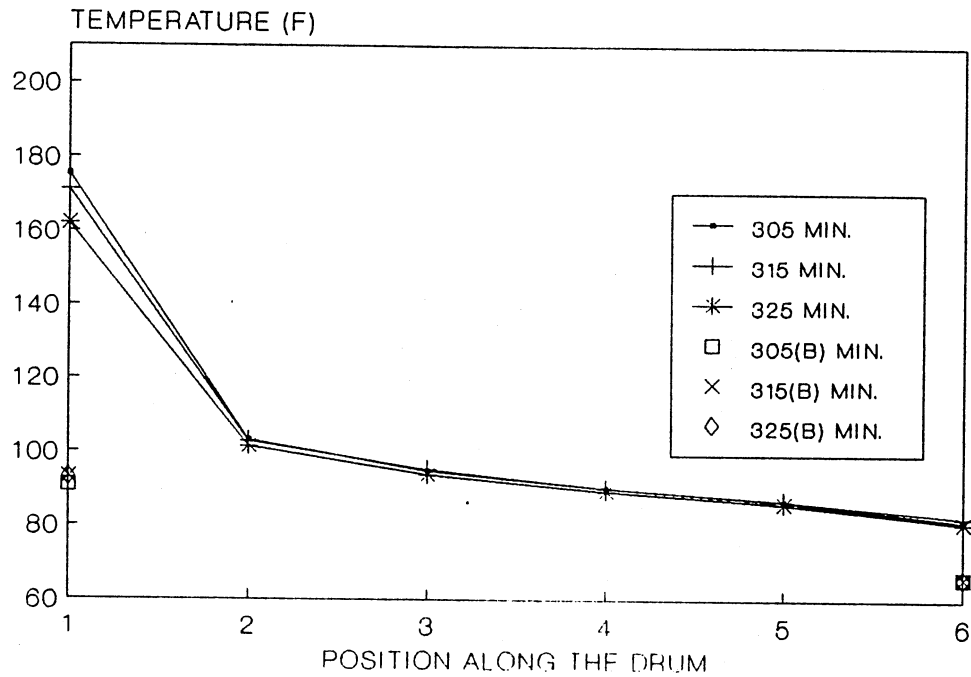


Figure 40. The Temperature Profiles of Prop as a Function of Time Along the Axial Direction for Run #7

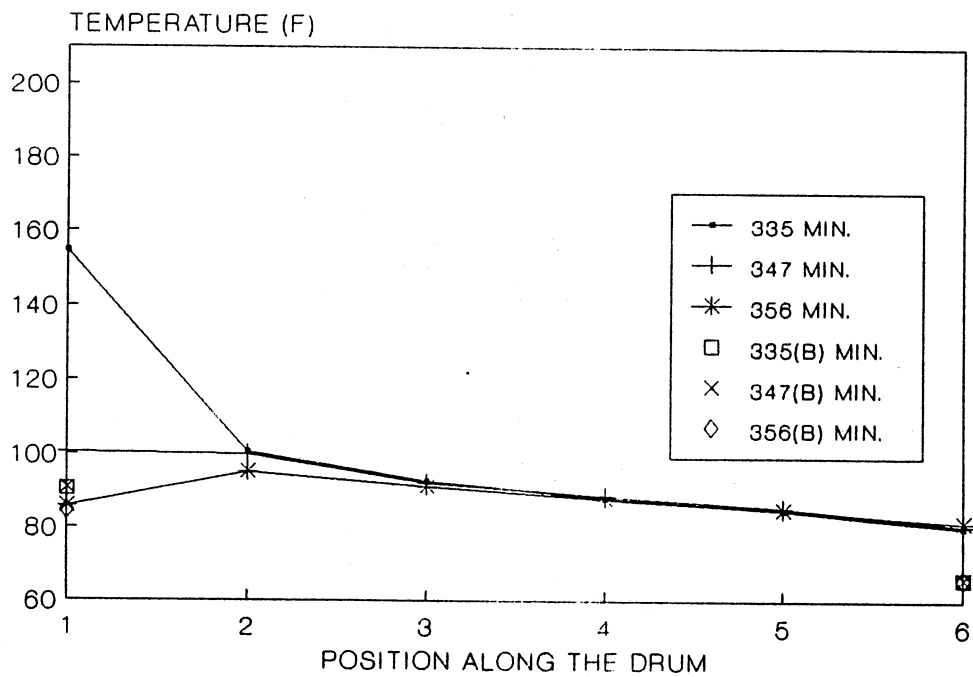


Figure 41. The Temperature Profiles of Prop as a Function of Time Along the Axial Direction for Run #7

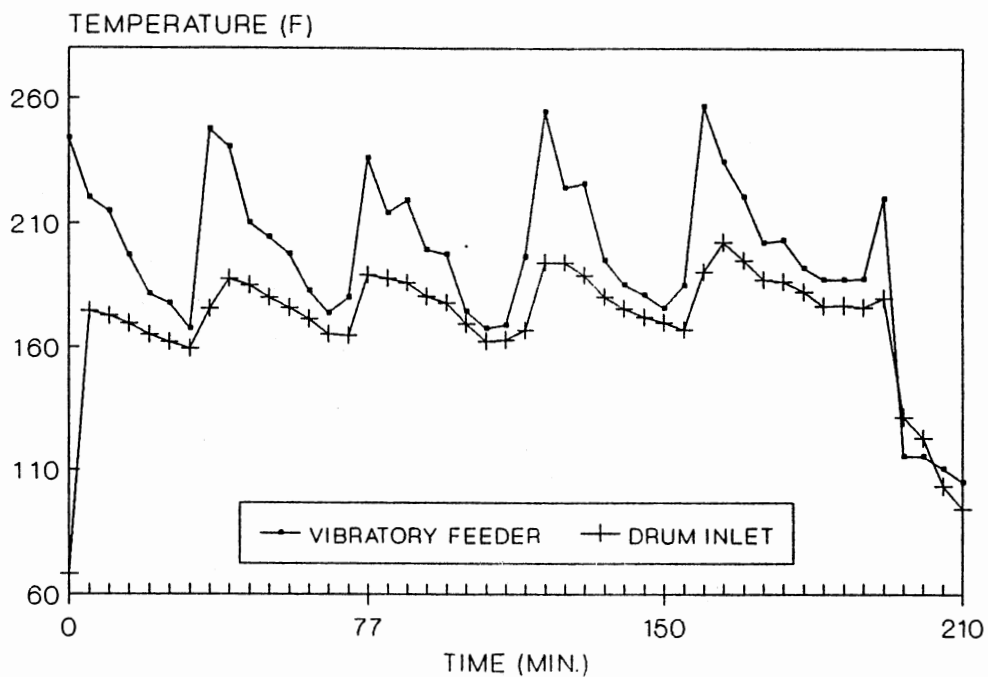


Figure 42. Temperatures of Prop vs. Time Inside the Hopper and Inlet Port of Drum for Run #2

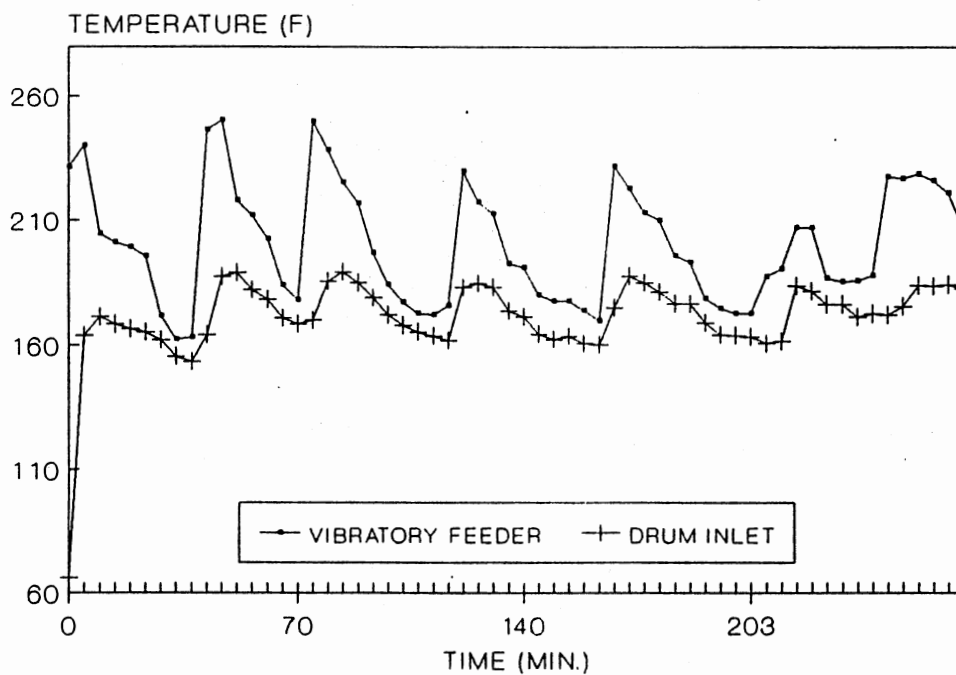


Figure 43. Temperatures of Prop vs. Time Inside the Hopper and Inlet Port of Drum for Run #7

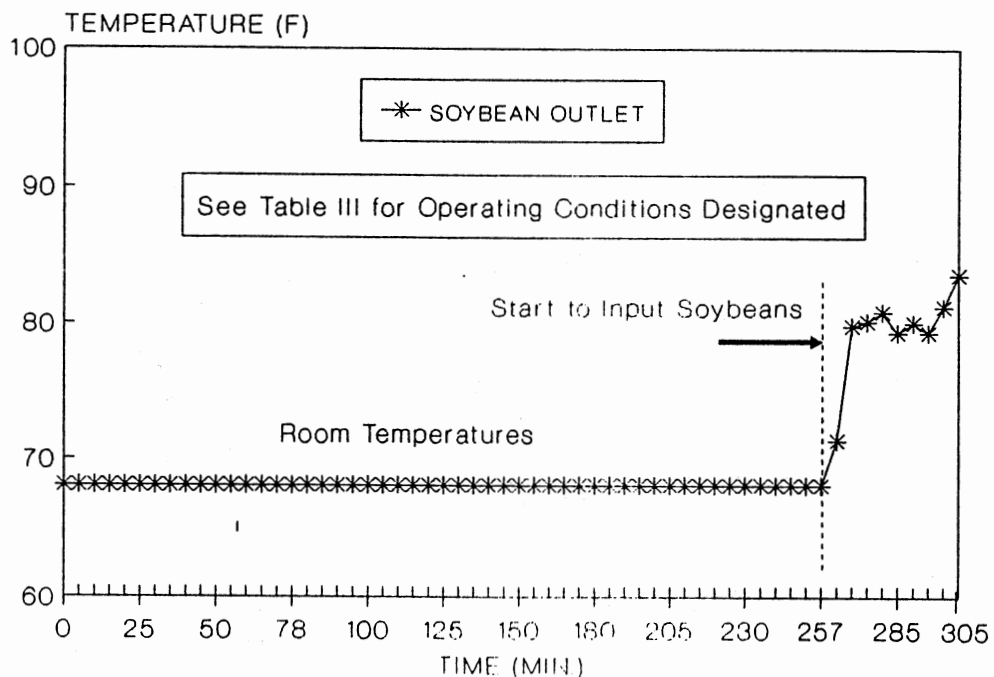


Figure 44. Outlet Temperatures of Soybean vs. Time for Run #1

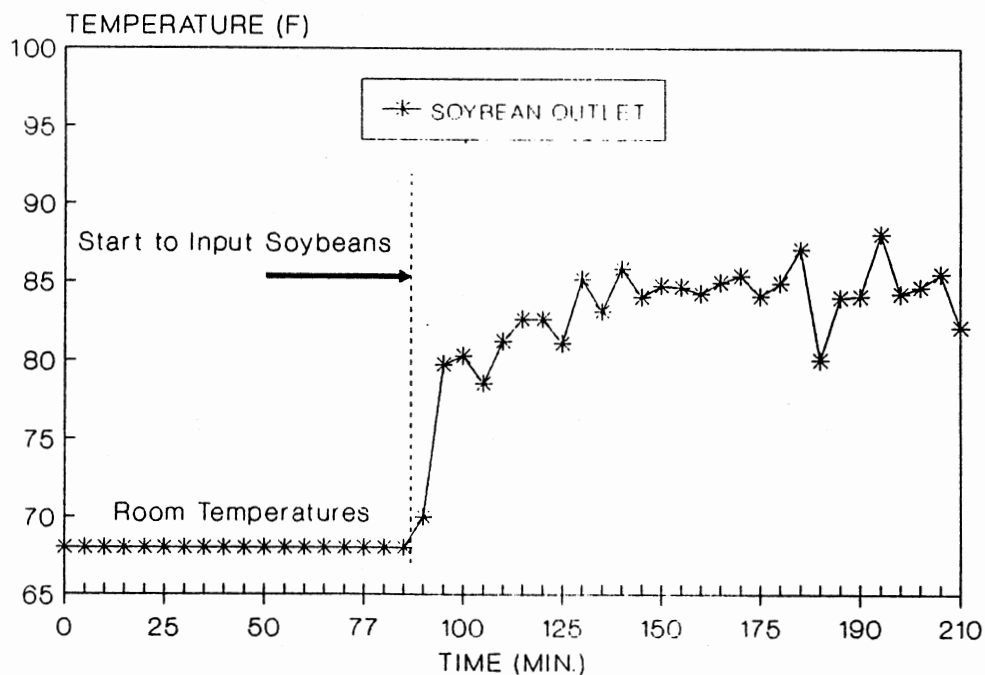


Figure 45. Outlet Temperatures of Soybean vs. Time for Run #2

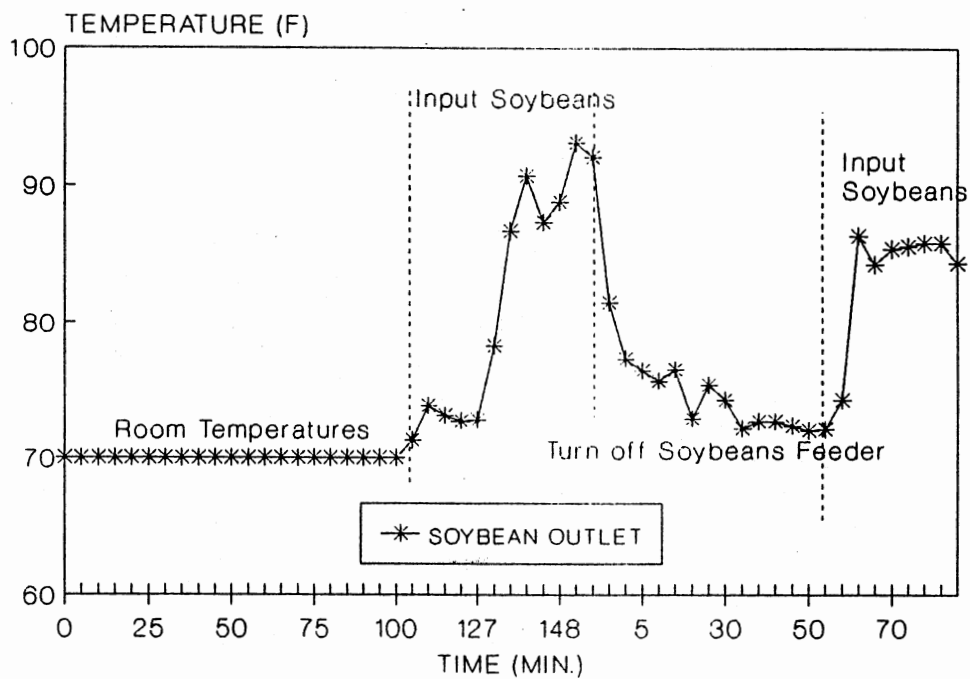


Figure 46. Outlet Temperatures of Soybean vs. Time for Run #3

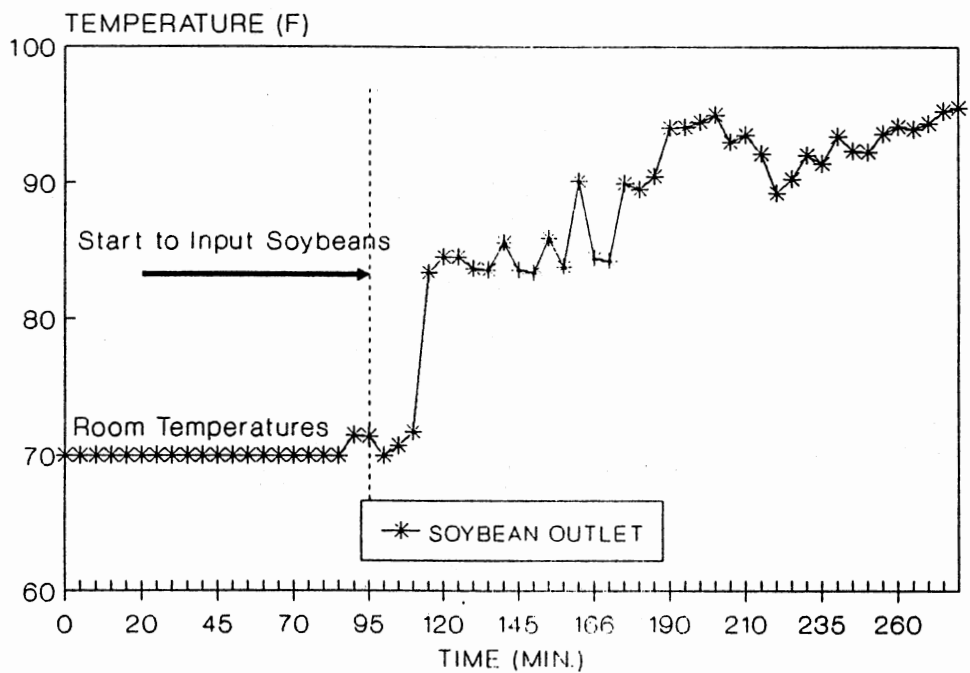


Figure 47. Outlet Temperatures of Soybean vs. Time for Run #4



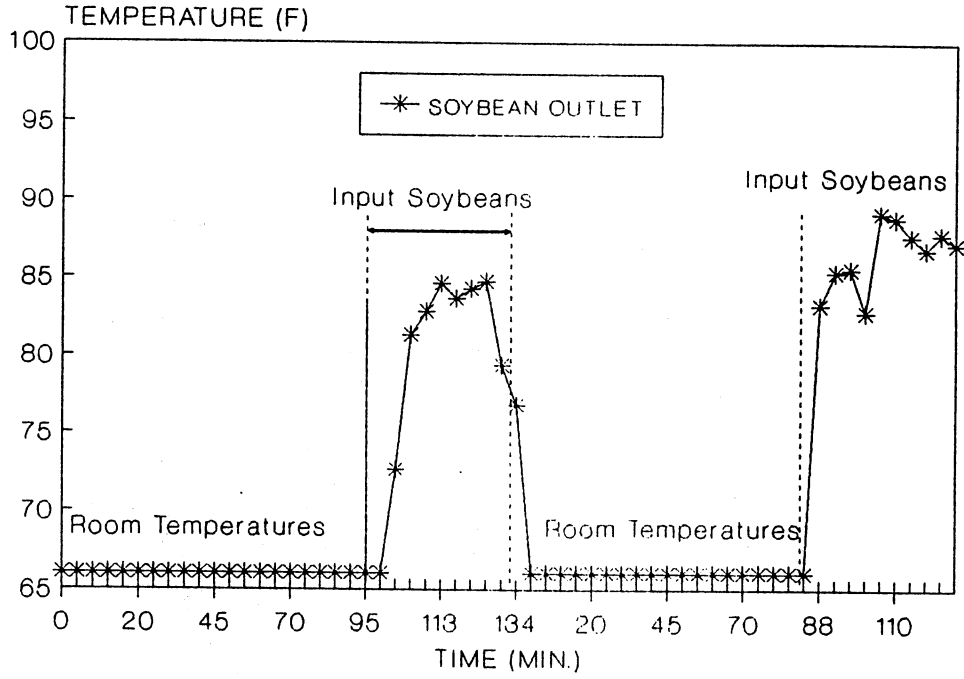


Figure 48. Outlet Temperatures of Soybean vs. Time for Run #5

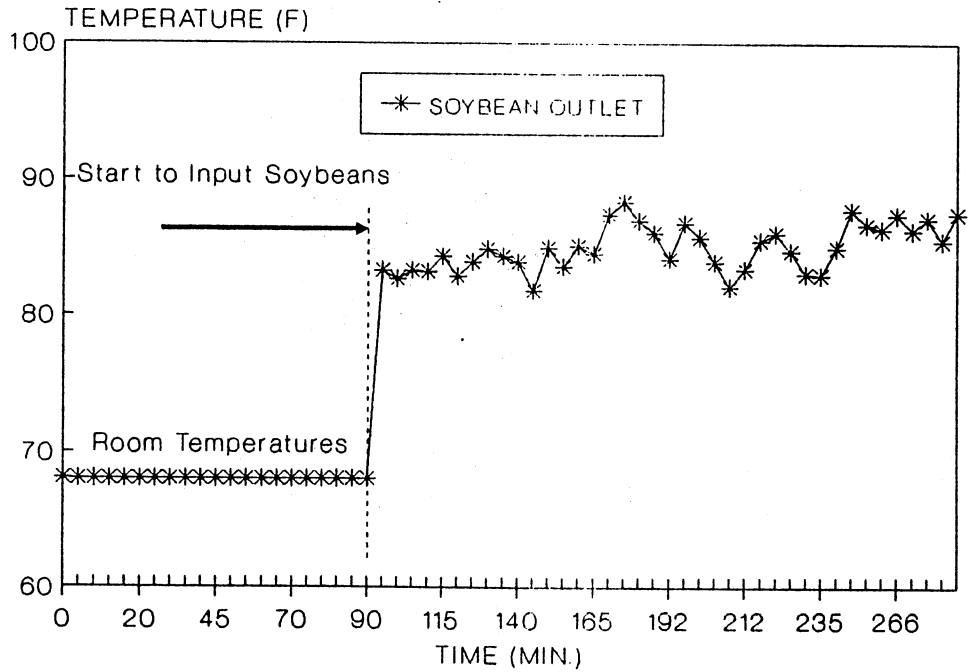


Figure 49. Outlet Temperatures of Soybean vs. Time for Run #6

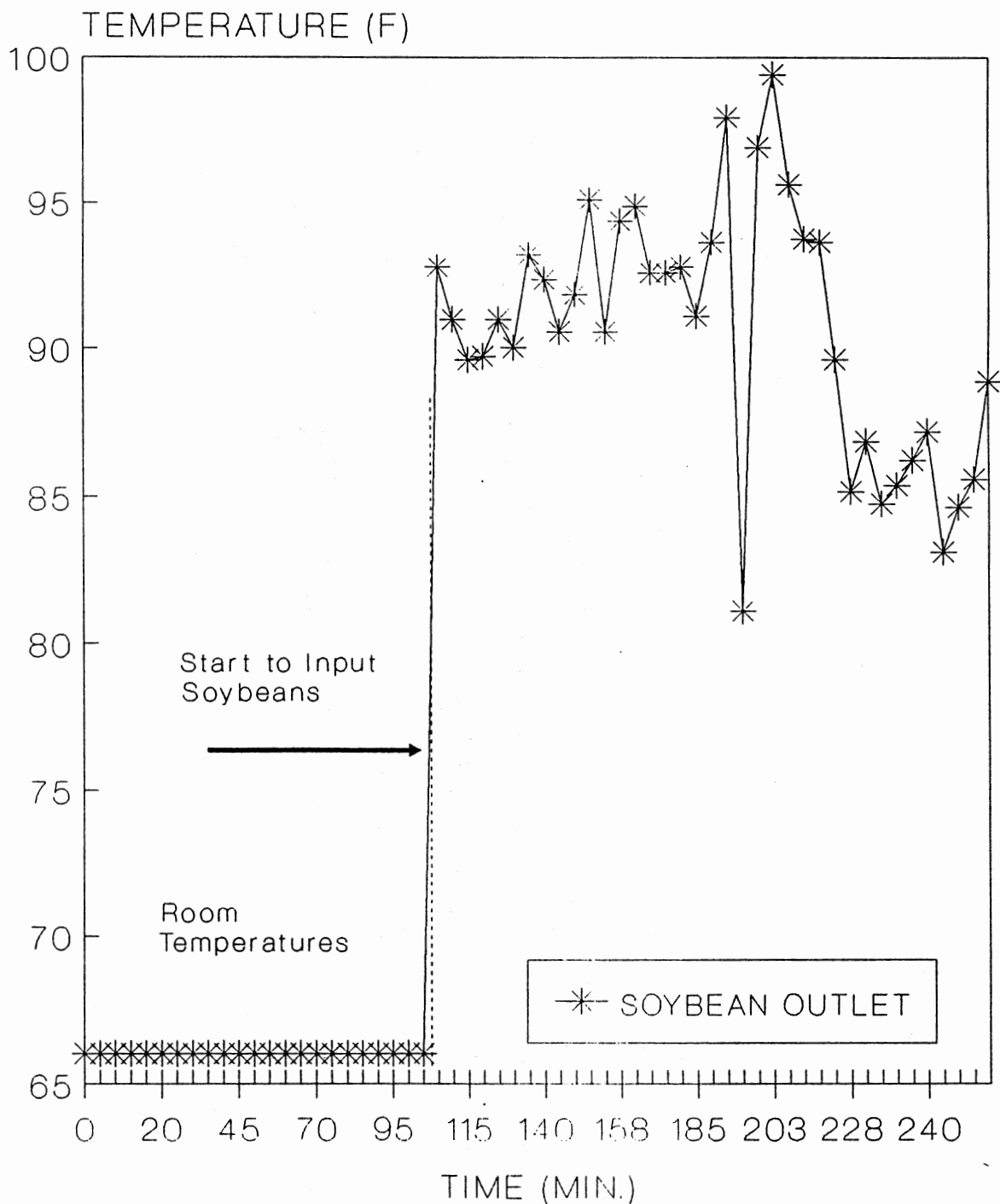


Figure 50. Outlet Temperatures of Soybean vs. Time for Run #7

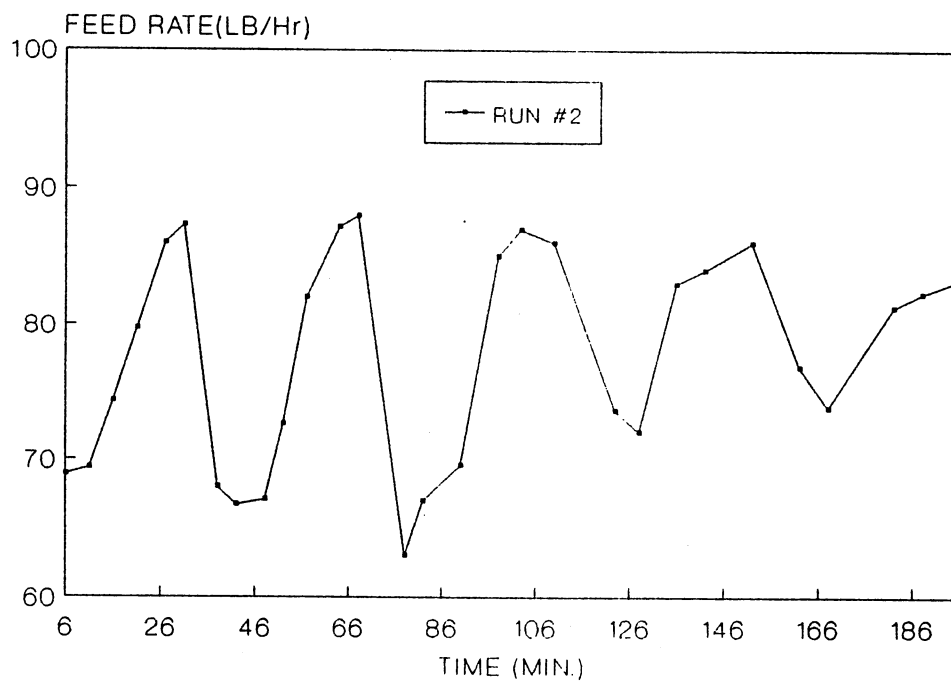


Figure 51. Feed Rates of Prop vs. Time  
for Run #2

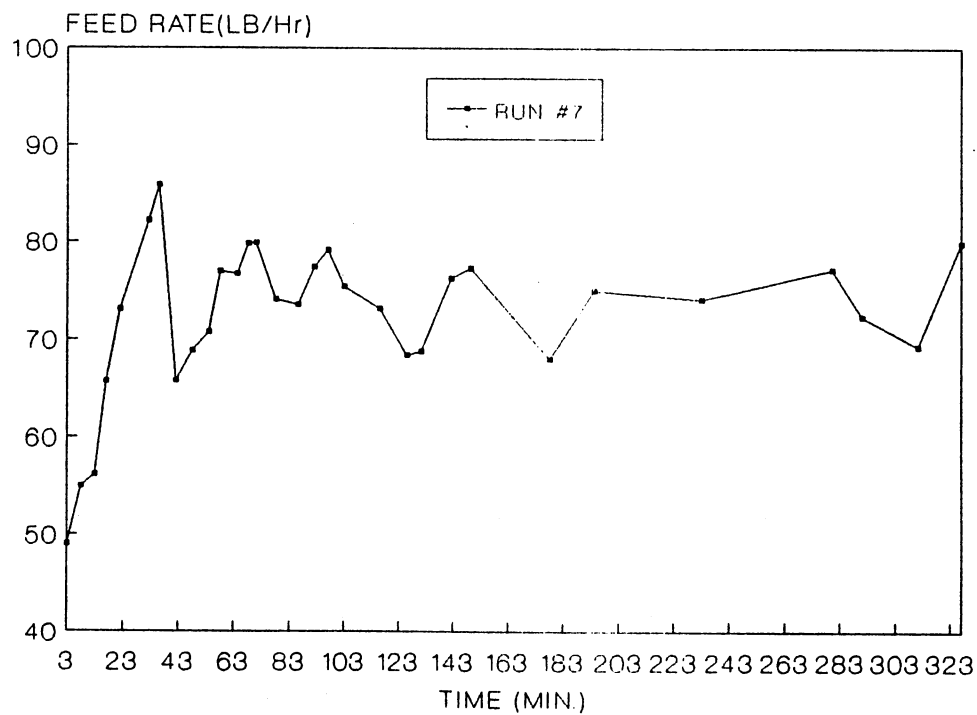


Figure 52. Feed Rates of Prop vs. Time  
for Run #7

The figures also show that it generally required approximately 80-100 minutes to reach steady state, without any soybean input. This phenomenon can be attributed to the existence of the thermal mass of the apparatus. The fluctuations in the feed rate and in the inlet temperature of prop are shown in figures 42, 43, 51 and 52.

The effect of the drum rotational speed on the maximum outlet soybean temperatures can be seen from figures 44-50. It can clearly be seen that a trend exists such that the soybean outlet temperature will increase if the drum speed is decreased. This observation results due to an increase in residence time.

The somewhat uneven fluctuations in the temperature measurements for the outlet soybeans is due to a combination of uneven mixing and difficulty in measuring the true soybean surface temperatures as the grain moves continuously to the outside of conveyer. From the experimental observations, one can see that more hot medium will fall through the screw conveyer and have direct contact and mixing with the soybean stream at a lower drum speed than at a higher speed. This phenomenon is partially due to the design of the angle of repose. Also a gap existed between the inner rotating screen and the fixed plates. This results in the prop slipping through by the small slot instead of passing through the inside of the conveyer. This was a major problem and is discussed along with other problems in the chapter on recommendations.

From plots shown in figures 25-41, it can be seen that the temperatures of the prop did not drop significantly when soybeans were fed into the system. This can probably be explained by: (1) the soybean feed rate is quite small, and (2) most of the soybean heating was provided by the thermal mass of the apparatus. The effect of the rotational speed of the conveyer on the maximum soybean outlet temperature can be seen from figures 44-50. These show that the lower speed of the conveyer, the higher the maximum temperature of soybeans. This is attributed to the fact that a longer contact time results at lower rotational speeds.

From the experimental observations, there are several problems which existed in this designed experimental bench-scale apparatus. The major factors which affect the performance of this process are convection heat loss and unsteady prop feed rates coupled with temperature fluctuations. Heat exchanger performance has been evaluated in terms of the maximum soybean temperatures reached. A more important criterion for process evaluation may be the value of heat transfer coefficient. The heat transfer coefficient still remains an unknown process parameter for this system, and it will be discussed and estimated utilizing a combination of experimental data and theoretical model predictions for the temperature profiles in the following section.

### Modeling Findings and analyses

There are a total of 32 experimental data sets with two phase flow and 4 sets without soybean input in the 7 experimental runs. Since most of the runs involve duplicates, a representative set of data was chosen and analyzed with the heat transfer model. The numerical values of the process parameters ( $m$ ,  $C_{ps}$ ,  $M$ ,  $C_{pB}$ ,  $V_m$ ,  $V_M$ ,  $T_{inlet}$  and  $T'_{inlet}$ ) and the assigned initial guesses ( $UA$ ,  $UA'$ ,  $V_B$ ) used for system modeling and analysis were selected from the 7 runs and are summarized in table IV. The results of system parameters for this particular analysis performed are shown in Table V. For convenience in experimental data analysis, the average soybean outlet temperature data were selected for conveyer speeds ranging from 5 to 1.8 rpm with the rotational speed of the drum kept constant.

TABLE IV  
SYSTEM OPERATING PARAMETERS FOR THE SELECTED RUNS  
PERFORMED

model test	$m$ (lb/min)	$M$	$C_{ps}$ (Btu/lb °F)	$C_{pB}$	drum speed (rpm)	$V_m$	$V_M$ (lb)
#1	1.25	0.0	0.24	0.49	2.0	0.46	n.a.
#2	1.25	0.0	0.24	0.49	0.25	3.67	n.a.
#3	1.25	.58	0.24	0.49	2.0	0.46	0.19
#4	1.25	.58	0.24	0.49	0.25	3.67	0.19
#5	1.25	.58	0.24	0.49	2-.25	2.0	0.19
#6	1.25	.58	0.24	0.49	2-.25	2.0	0.57

The resulting average temperatures of soybeans as a function of conveyer speed are shown in figure 53. In a similar manner, the average soybean outlet temperatures at drum speeds ranging from 0.25 to 2.0 rpm with the conveyer speed fixed, are shown in figure 54. Soybean feed rate and prop feed rate were kept at constant 35 lb/hr and 75 lb/hr respectively.

TABLE V  
THE RESULTS OF SYSTEM PARAMETERS FOR THE MODELING TESTS PERFORMED

Test no	$V_B$ (lb)	in.	UA' inter.	out.	UA (Btu/min °F)
#1	5.6	.4	.03	.03	n.a.
#2	5.6	.4	.03	.03	n.a.
#3	n.a.	.4	.03	.03	0.03
#4	n.a.	.4	.03	.03	0.06
#5	n.a.	.4	.03	.03	0.03
#6	n.a.	.4	.03	.03	0.05

Note: in-inlet; inter-intermediate; out-outlet of the drum.

The simulation program called MODEL, written in Fortran, can be run either on an IBM-PC with a PC-version of DGEAR or on the IBM Mainframe at the OSU Computer Center using the IMSL subroutine package. The approach taken as mentioned previously, was a kind of empirical fitting, in other words, it means that the resulting temperature profiles between the data from the model and the data from the experiment were compared. Values for UA, UA' and  $V_B$

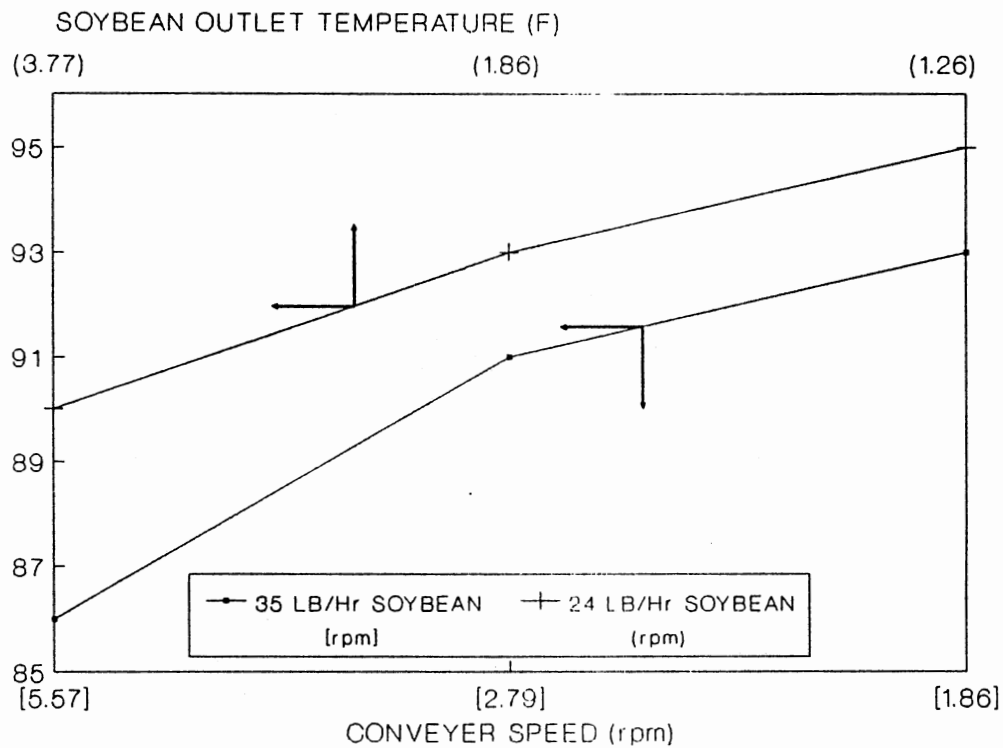


Figure 53. Average Soybean Outlet Temperature Profile vs. Conveyer Speed

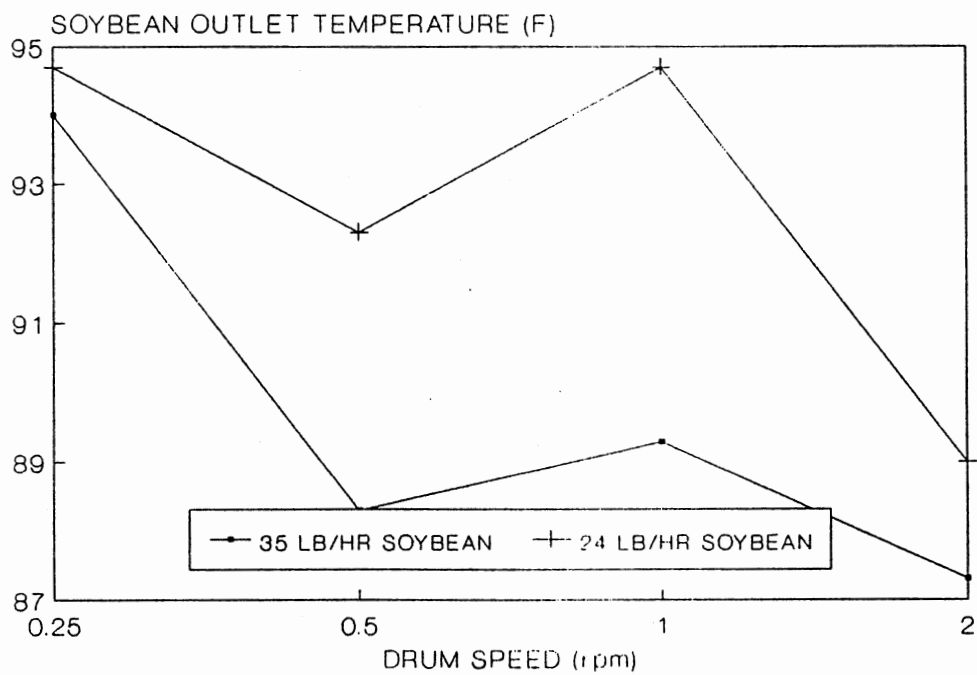


Figure 54. Average Soybean Outlet Temperature Profile vs. Drum Speed



were estimated by minimizing the differences of these two profiles. Representative results of these modeling tests as described above are shown in table V, and the corresponding steady and unsteady state temperature profile plots are shown in figures 55-60. Since the experimental system had problems in controlling the inlet temperature of prop, the experimental data and the predicted data were not plotted together. The major purpose of this work is to demonstrate the usefulness of the model for predicting the transient temperature profile, heat loss, thermal mass, and the heat transfer coefficient at a variety of operating conditions.

The graphs shown in figures 55 and 56 indicate that both the predicted temperature profiles of the prop from the model for drum speeds of 2 and 0.25 rpm, respectively, did not exactly fit the experimental ones. This results because the model assumes that heat loss to the environment is independent of the axial position along the drum except at the inlet and outlet location of the drum and assigns the same values of  $UA'$  to the intermediate section of the drum. It can also be seen from the experimental data and model results that the time required to reach steady state in the prop temperature profiles at different rotational speeds is not very different (70 minutes at 2 rpm and 100 minutes at 0.25 rpm ). This observation is explained by the large difference in thermal mass that exists between the apparatus and the processed material, as shown in table V. Therefore,

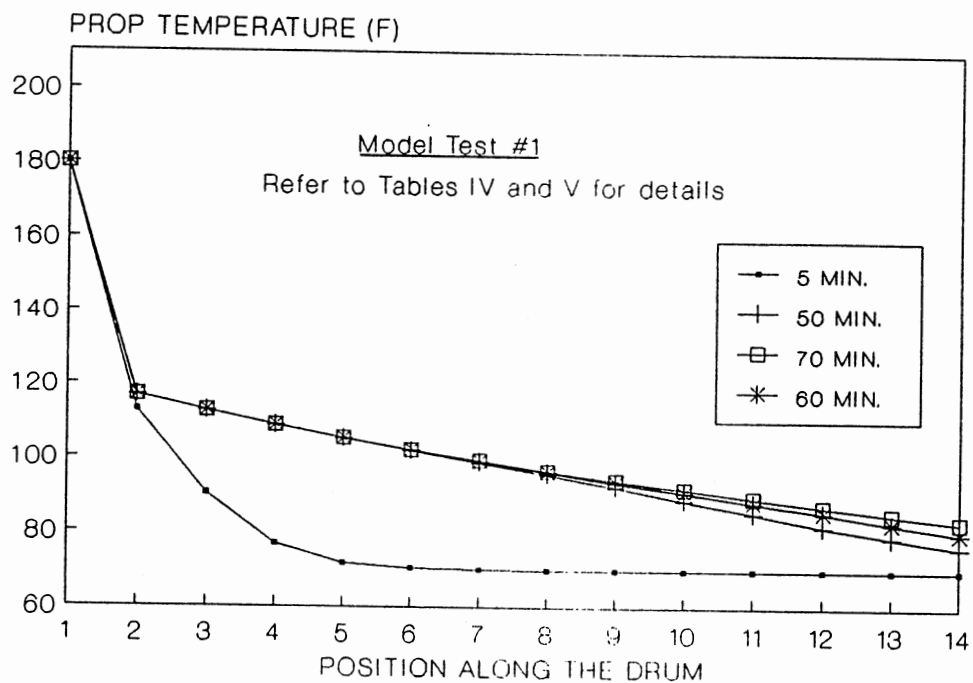


Figure 55. Temperature Profiles for the Modeling Performed( One Phase, Drum at 2 rpm )

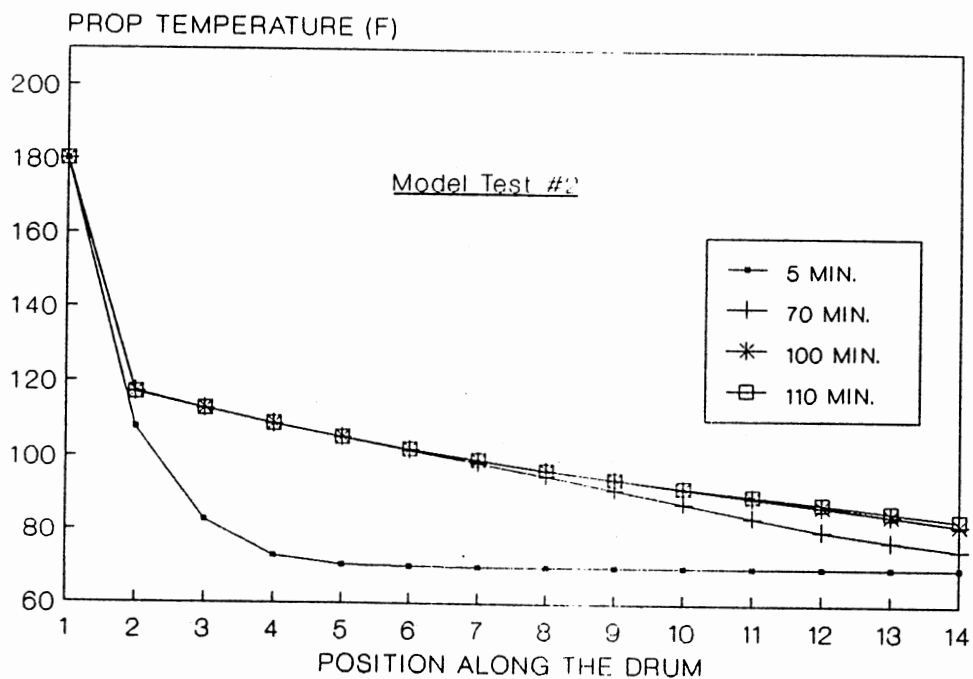


Figure 56. Temperature Profiles for the Modeling Performed( One Phase, Drum at 0.25 rpm )

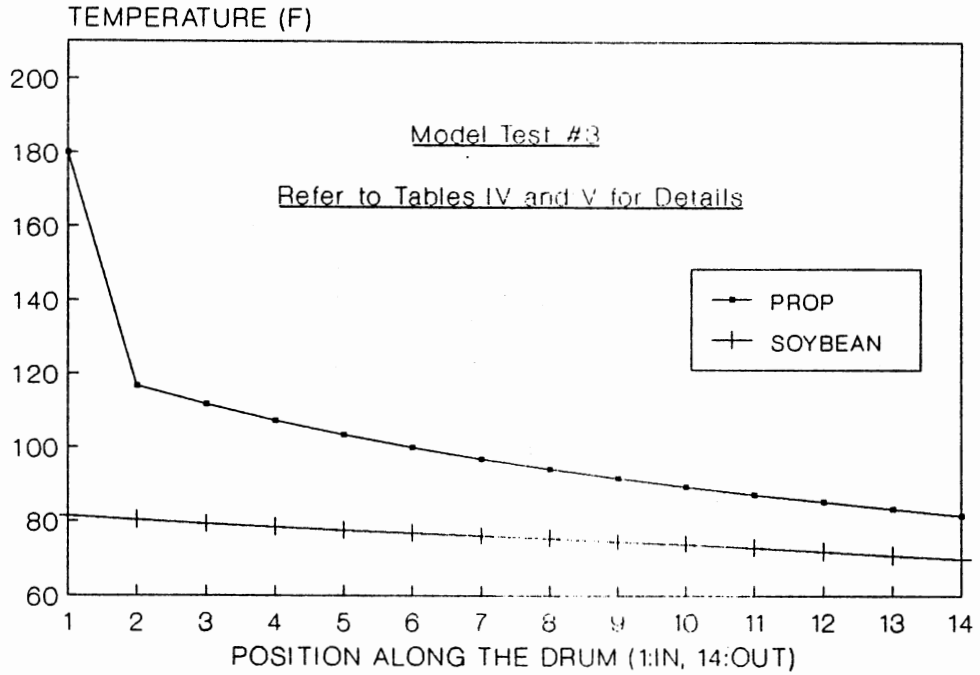


Figure 57. Temperature Profiles for the Modeling Performed (Two Phase, Drum at 2 rpm, at 3 Min. )

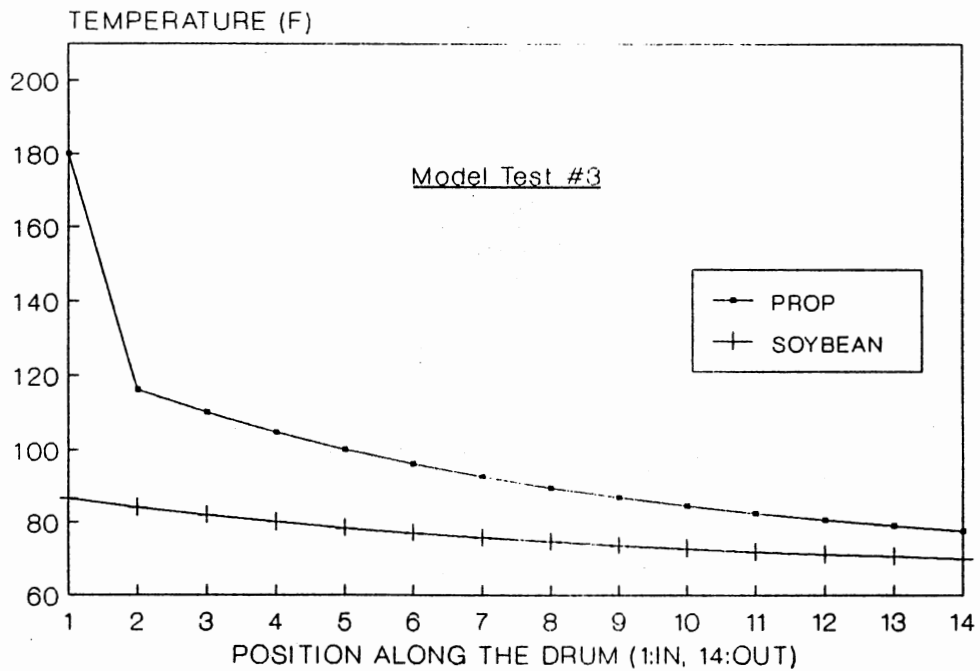


Figure 58. Temperature Profiles for the Modeling Performed (Two Phase, Drum at 2 rpm, at 30 Min. )

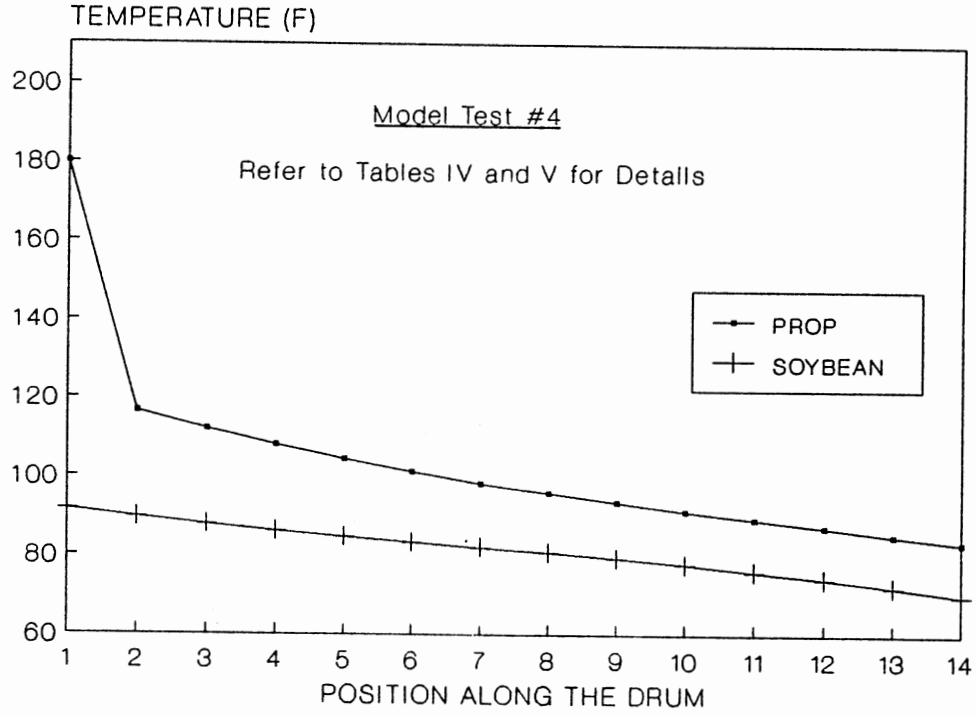


Figure 59. Temperature Profiles for the Modeling Performed (Two Phase, Drum at 0.25 rpm, at 3 Min. )

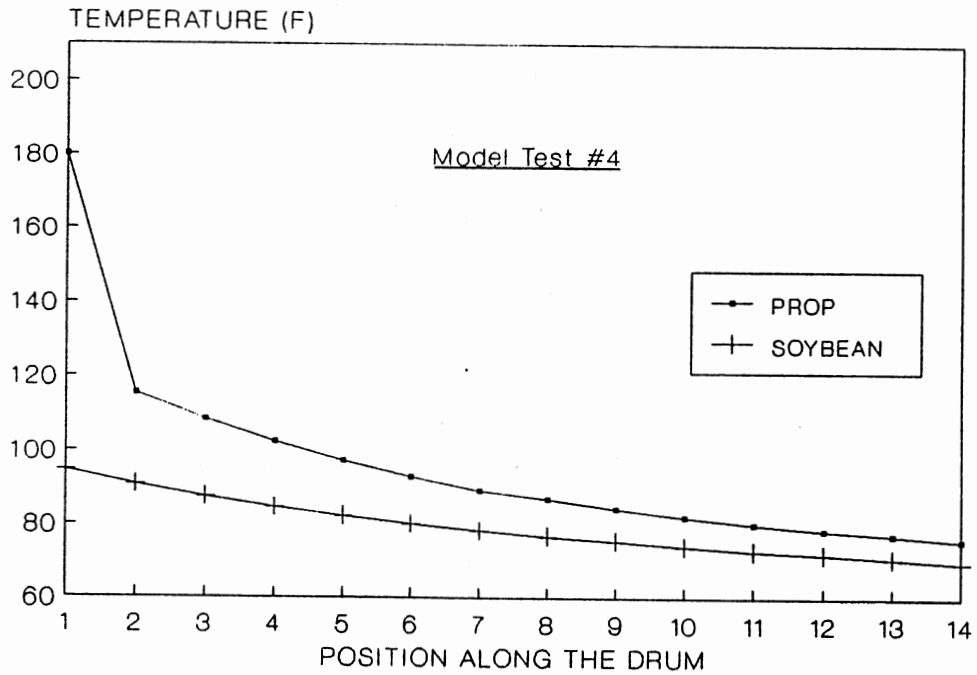


Figure 60. Temperature Profiles for the Modeling Performed (Two Phase, Drum at 0.25 rpm, at 30 Min. )

the time needed to reach steady state is determined mainly by the thermal mass of the apparatus, which is equivalent to about 5.6 lb per stage of processed particles.

The lumped heat transfer loss value ( $UA'$ ) can be estimated about 0.04 Btu/min °F at the inlet and 0.03 Btu/min °F elsewhere along the drum for this system due to air convection heat loss and conduction loss. Figures 57-60 show the predicted temperature profile of prop and soybeans operated at the conditions of test 3 and test 4, (see Tables IV and V), respectively. The lumped heat transfer term for this system can be estimated ranging from 0.03 Btu/min °F (at 2 rpm) to 0.06 Btu/min °F (at 0.25 drum) speed as the conveyer speed is averaged from 5 to 1 rpm, In addition, the lumped heat transfer term is found ranging from 0.03 Btu/min °F to 0.05 Btu/min °F depends on the conveyer speed as the drum speed is averaged from 2 to 0.25 rpm, as shown in table V. The lumped heat transfer term ( $UA$ ) was assumed to be independent of the axial position along the drum for model input, which is probably not very accurate.

Heat transfer coefficients ranging from 17 to 38 Btu/min ft<sup>2</sup> °F at different operating conditions was calculated based on the area of one soybean particle. Undoubtedly, these values should be much higher than calculated in the present work due to problems with heat loss, unstable hot medium flow, and fluctuating temperatures. Future refinements of this process design should provide a constant prop feed rate with constant

temperature. New thermocouples should be installed inside the conveyer for soybean temperature profile measurements. In addition, utilizing experimental data obtained from the modified system coupled with the model equations developed from this work and the theoretical equations developed by previous investigators (8, 30, 49, 53, and 56), a more accurate heat transfer coefficient could be obtained without using the lumped heat transfer terms. It is also possible to evaluate the impact of rotational speed of the drum and the conveyer as well as other operating variables on the performance of this process in terms of heat transfer coefficient, contact area, and contact time. A transparent drum design for flow visualization should be constructed and tested to understand the dynamic motion of the particles inside the drum. These observation could be utilized to compare with the information predicted from several theoretical equations developed by Downs et al.(8) or Kelly and O'Donnell(62).

## CHAPTER VI

### CONCLUSIONS AND RECOMMENDATIONS

Due to the problems associated with previous process designs and models of solid-solid heat exchangers (7, 9, 13), knowledge concerning an alternative method of the process design is desirable. The general objective of this study is to design and analyze a thermal-based process that might be used to economically perform heat treatment of grain. The process developed and studied was a continuous counterflow solid-solid heat exchanger, used to transfer heat using small solid particles such as prop to large solid particles such as soybeans. An experimental apparatus was designed, constructed and tested to determine the feasibility and performance. Simplified mathematical models for heat transfer and RTD were developed and along with the experimental test information used in a simulation mode to estimate potential heat exchanger characteristics in terms of lumped heat transfer coefficients, lumped heat losses, and equivalent thermal mass of the system.

#### Conclusions

The major conclusion of this investigation is that the continuous solid-solid heat exchanger appears to be a

promising heat transfer device, and yet has some shortcomings which needs to be remedied. Specific conclusions drawn from the results of this investigation can be summarized as follows:

(1) The experimental heat transfer process using a solid-solid mechanism, has shown potential as a good heat transfer device based on the observed time-temperature profiles.

(2) Models developed for heat transfer analysis predict the experimental data provided that the correct values for the model parameters(  $UA$ ,  $UA'$ ,  $V_B$ ) are used. According to the model, an equivalent thermal mass of approximate ranging from 1.5 to 11.2 times the thermal mass of the processed particles (prop), was calculated and was dependent on the rotational speed of the drum.

(3) For this particular design, the effect of rotational speed of the drum and the conveyer and the mass ratios of the two particle groups in terms of flow rate, on the performance of this system was studied experimentally and theoretically. From experimental observations, it was observed that the process has a large heat loss to the environment due to air convection effect.

(4) The lumped heat transfer coefficient,  $UA$ , between the granular media and soybeans was determined by comparison of the temperature profiles between the experimental data and the modeled values. The value of  $UA$  was assumed independent of axial position and was found to range from 0.03 to 0.06 Btu/min °F under a variety of operating conditions. These



values were found to be influenced mainly by the drum speed and the conveyer speed. These values correspond to values of the heat transfer coefficient (U) in a range of 0.027 to 0.045 Btu/min ft<sup>2</sup> °F provided that the total surface area of the soybeans at each stage was used as the value for the heat transfer area (A).

(5) From the experimental data and modeling of residence time distribution, it was shown that the flow pattern of the prop particles inside the drum was influenced by the drum speed (as expected). It was also shown that the flow pattern of prop could be characterized using plug flow assumptions for drum speeds of 2, 0.5 and 0.25 rpm. At 1 rpm the flow pattern had a long tail response. These tests also showed an increasing trend of randomness of the flow pattern along with an increase in the rotational speed of the drum.

(6) From model predictions and experimental observations, the heat transfer coefficient was found to be a slight function of drum speed. This is probably due to the fact that drum speed can only be varied over a small range. It is also limited by the capacity of the heating device, heat loss, as well as the unstable feed rates.

(7) The soybean outlet temperature would be much higher than in the present case and the thermal efficiency would be improved if fluctuations of the hot medium feed rates, medium temperatures and heat losses could be minimized.

(8) From the experimental observations, a large amount of

heat was lost to the environment due to the lack of proper insulation. Longer time periods than expected were required to reach steady state due to the existence of the large thermal mass of the whole apparatus. It can also be seen that the soybean outlet temperatures increased as the drum speed decreased. This could be attributed to the fact that more hot medium falls through the conveyer and has direct thermal contact with the soybeans at a lower drum speed than that of running at higher speed, except at 1 rpm (which can be explained by the results of the RTD tests).

(9) From the dynamic motion model of the particles inside the drum developed in previous work (63), the particles falling range will widen if the drum speed decreases as shown in equation(11). This coupled with the increase in the prop volume at each stage at lower drum speed, could explain why more particles fall inside of the conveyer at a lower speed rather than at a higher speed.

(10) The uneven fluctuation of the outlet soybean temperature measurements is due to a combination of uneven mixing and the difficulty which exists in measuring the true soybean surface temperature.

(11) The lower the speed of conveyer, the higher the outlet temperature of the soybeans, this is explained by longer contact time at lower speed.

(12) The mathematical model developed not only can be used to predict process parameters as in the present investigations, but also could be used as a tool to study

and analyze the system behavior primarily in terms of temperature profiles for this type of process.

(13) In the mathematical model development, the assumptions to use the mathematical average temperature difference between the prop and the soybean particles instead of using a log-mean was justified by the experimental findings both from the RTD tests and the heat transfer tests.

(14) The experimental design of this process is not ideal and there are several problems which need to be solved. These will be covered in the following sections.

#### Recommendations

The mode of heat transfer in the granular bed appears to be conductive through the contact areas between the dissimilar particles. Conduction and convection through the gas trapped between the particles is of lesser importance. Further work related to the contact areas between the dissimilar particles would appear particularly useful in refining and improving heat transfer models in agitated granular bed heat exchange. The following tasks are recommended based on the results of the experimental observations and the mathematical modeling work. Further experimental work should be aimed at fixing the problems which exist in the current system and applying the models and information from this work to the modified system. Several areas in particular should be investigated, and some of the shortcomings of the present design and its possible

solutions, will be noted.

(1) Other potential heat transfer media such as steel balls or glass beads should be studied. Such studies would involve using a combination of the models developed in this research and the models developed by previous investigators (8, 9, 30, 49) to examine the effect of particle size on the performance of this new heating process.

(2) A multiplexer should be built for use with A/D board and thermocouples should be installed along the conveyer at each stage to measure the temperatures of soybeans. This information would be useful in computing the local heat transfer coefficient as a function of time and location, based on the models developed from this work and previous work (8, 9, 30, 49). However, there is a technical bottleneck which needs to be overcome to obtain the actual temperature measurements of the soybeans. A flexible measuring device must be built which could change for different operating conditions. Another alternative is to find new locations for the temperature measurements of soybeans and prop which would not need to be varied along with the change of the operating conditions.

(3) The separation of the prop and the soybeans would be improved if the static electricity between these particles could be eliminated.

(4) The drum's rotational direction and the fixed metal plates should be redesigned to force the hot particles to fall through the conveyer and mix with the soybean

particles. One idea is to modify the plates into multiple stages in the radial direction by welding several baffles into it. This would increase the opportunity for the particles to fall through instead of slipping by the conveyer as shown in figure 61. In addition, the effect of the rotational direction between the drum and conveyer on the amount of particles falling through instead of slipping by should be investigated.

(5) A flexible, adjustable angle of flight inside the drum should be investigated to meet the requirements of different operating conditions.

(6) One of the more important things to investigate is a new heating device which could provide a constant feed rate of heated particles at uniform temperatures. One possibility is to modify the current heating device, the fluidized bath, into a structure similar to the design of Nillson (64), by adding additional baffles inside the fluidized bed. This would create a multiple-stage flow path and reduce the undesirable channeling inside the fluidized bath. With these improvements a true continuous operation instead of semi-continuous operation could be obtained.

(7) A new device such as a screw feeder should be used to provide a constant feed rate of prop particles.

(8) The advantage and disadvantage of using different types of temperature sensors should be investigated to determine response time, accuracy, and the effect of noise.

(9) The suitability of the screw conveyer formula should be

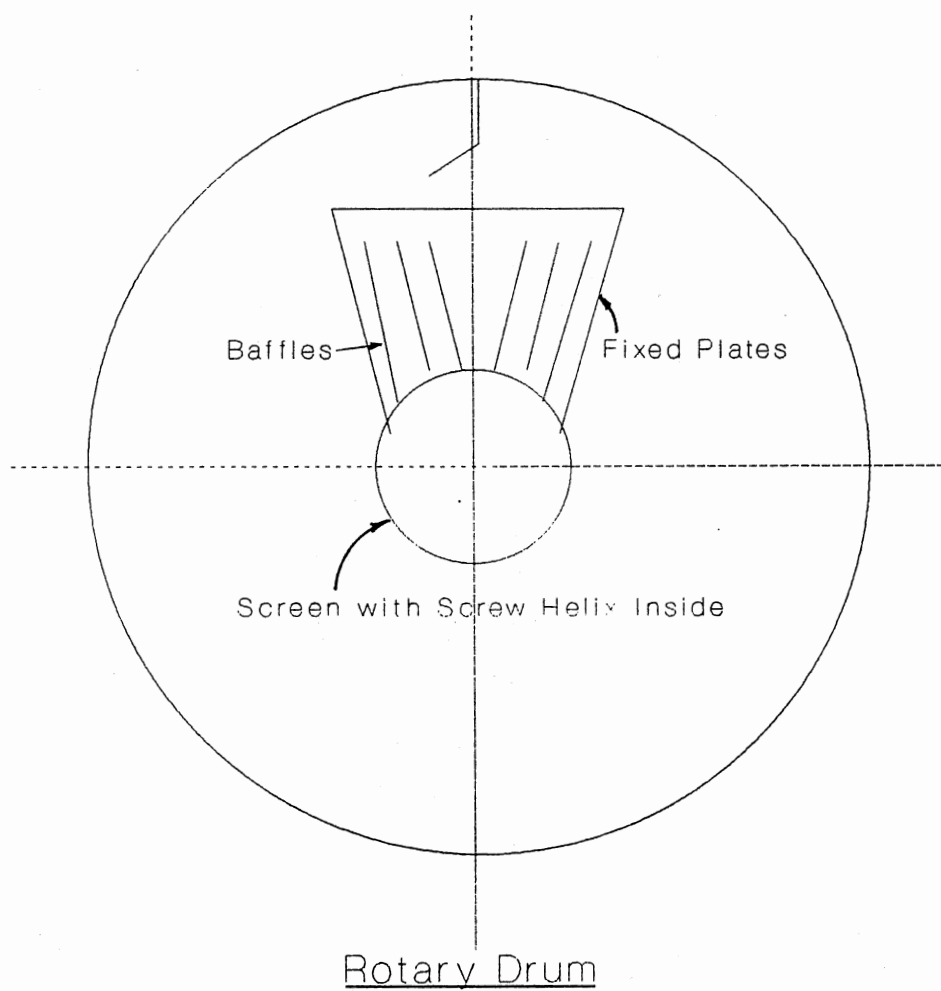


Figure 61. Schematic Drawing of Modified Fixed Plates Inside the Drum

checked on the current conveyer.

(10) The heat loss should be reduced in the system by insulating the apparatus and also closing both ends of the current rotary drum.

(11) Design the drum for flow visualization and compare the visual data with the predicted data from theoretical equations developed by several authors (8, 49, 62, 63).

(12) Use a better adjustable dial for the motor speed control of the soybean feeder.

(13) Redesign or enhance the seal between the screen and the sheet metal at the soybean inlet port to prevent leakage.

(14) Seal most of the connections or moving parts of the drum to prevent leakage of the prop particles.

(15) Investigate a new experimental technique for obtaining a more accurate RTD of the prop by finding a suitable tracer and detector for this particular system. Dye may be a potential tracer for soybean measurement.

(16) Characterize the overall flow pattern in this process by running RTD tests at different drum and conveyer speeds and different feed rates of prop and soybean. Correlate the behavior of the heat transfer rate to the RTD tests in terms of axial dispersion, dead space, bypassing, etc.

(17) Investigate the mass transfer effect on the performance of this heat exchanger by coupling the heat transfer mechanism with the mass balance for this process.

(18) Study the thermal death model(kinetic) which could provide important information on design of this system as a

thermal disinfestation device.

(19) Build another similar device to study the heat recovery capability of this particular design and analyze the economic potential.

(20) Scale up and optimize the heat transfer model using a sensitivity analysis of the model parameters.

I hope that the results from this investigation will encourage other workers in the field to continue so that the phenomenon of solid-solid heat transfer may be more fully understood.



## BIBLIOGRAPHY

1. Evans, D.E., G.R. Thorpe and T. Dermott, " The Disinfestation of Wheat in a Continuous Flow Fluidized Bed", J. Stored Prod. Res., 19:125-137 (1983).
2. Dermott, T., and D.E. Evans, " An Evaluation of Fluidized Bed Heating As a Means of Disinfestating Wheat", J. Stored Prod. Res., 14:4-12 (1978).
3. Ziegler, E.N., and W.T. Brazelton, " Mechanism of Heat Transfer to a Fixed Surface in a Fluidized Bed", I and E.C. Fund., 3:94-98 (1964).
4. Petrie, J.C., W.A. Freeby, and J.A. Buckham, " In-bed Heat Exchangers", Chem. Engr. Prog., 64:45-51 (1968).
5. Claflin, J.K., D.E. Evans, A.G., Fane, and R.J. Hill, " The Thermal Disinfestation of Wheat in a Spouted Bed", J. Stored Prod. Res., 22:153-161, (1986).
6. Thomas, B., Y.A. Liu, M.O. Mason, and A.M. Squires, " Vibrated Beds: New Tools for Heat Transfer", Chem. Engr. Prog., 65-75 (June, 1988).
7. Pannu, K.S., G.S.V. Raghavan, " A Continuous Flow Particulate Medium Grain Processor", Canadian Agr. Engr., 29:39-43 (1987).
8. Downs, H.W., J.D. Kellerby, J.M. Harper, and R.D. Haberstroh, " Heat Transfer by Contact Between Agitated Particles", Final Report to National Science Foundation, NSF Grant no. ENG-7418150 (1977).
9. Simonton, W. and M. Stone, " Counterflow Particle-Particle Heat Exchange, Part II. Design and Performance of a Prototype", Trans. ASAE, 29:874-880 (1986).
10. Mittal, G.S., M.M. Lapp, and J.S. Townsend, " Feasibility of Drying Wheat with Various Solid Heat Transfer Media", Canadian Agr. Engr., 27:121-125 (1985).

11. Akpaetok, O.I., " Shell Corn Drying with Heated Sand", M.Sc. Thesis, University of Wisconsin, Madison, Wis. (1973).
12. Raghavan, G.S.V., and J.M. Harper, " High Temperature Drying Using a Heated Bed of Granular Salt", Trans. ASAE., 17:108-111 (1974).
13. Tessier, S. and G.S.V. Raghavan, " Performance of a Sand Medium Dryer for Shelled Corn", Trans. ASAE., 27:1227-1232 (1984).
14. Hall, G.E., and A.W. Hall, " Drying Shelled Corn by Conduction Heating", Agric. Eng., 42:186-187 (1961).
15. Finney, E.E., N.N. Mohsenin, and J.D. Hovanesian, " Thermal Efficiency of Conduction Drying of Shelled Maize and Effects of Temperature and Kernel Injury on Drying Rate", J. Agric. Eng. Res., 8:62-69 (1963).
16. Chancellor, W.J., " A Simple Grain Drying Using Conducted Heat", Trans. ASAE., 11:857-862 (1968).
17. Chancellor, W.J., " Characteristics of Conducted Heat Drying and Their Comparison with Those of Other Drying Methods", Trans. ASAE., 11:863-867 (1968).
18. Khan, A.U., A. Amilhussin, J.R. Arboleda, A.S. Manalo, and W.J. Chancellor, " Accelerated Drying of Rice Using Heat-Conduction Media", Trans. of ASAE., 949-955 (1974).
19. Huber, L.J. " Process of Preparing a Puffed Cereal Product and the Resulting Product", US Patent no. 2701200 (1955).
20. Aspegren, O.E.A., " Heat Treatment of Piece-Shaped Material", US Patent no. 2872386 (1959).
21. Benson, J.O., " Puffed Food Products", US Patent no. 3253533 (1966).
22. Lengar, N.G., C.R. Bhaskar and P. Dharamarajan, " Studies on Sand Parboiling and Drying of Paddy", J. Indian Soc. Agric. Eng., 851-854 (1971).
23. Bateson, R.N., and J.M. Harper, " Apparatus and Process for Puffing Food Products", US Patent no. 3746546 (1973).
24. Lapp, H.M., and L.R. Manchur, " Drying Oilseeds with a Solid Heat Transfer Medium", Canadian Agri Eng., 16:54-59 (1974).

25. Lapp, H.M., and P.S.K. Leung, and J.S. Townsend, " Solid Heat Transfer Mediums for Processing Grains and Oilseeds", Paper no. NC 75-302, ASAE., St. Joseph, MI (1975).
26. Lapp, H.M., G.S. Mittal, and J.S. Townsend, " Cereal Grain Drying and Processing with Solid Heat Transfer Media", Paper no. 76-3524, ASAE., St. Joseph, MI (1976).
27. Lapp, H.M., " Drying Oilseeds Employing a Solid Heat Transfer Medium", Proc. Manitoba Agron. Ann. Conf., 22-26 (1973).
28. Mittal, G.S., " Wheat Drying with Solid Heat Transfer Media", M.Sc. Thesis, University of Manitoba, Winnipeg, Manitoba, Canada (1977).
29. Mittal, G.S., H.M. Lapp and J.S. Townsend, " Continuous Drying of Wheat with Hot Sand", Canadian Agri. Eng. 24:119-122 (1982).
30. Richard, P. and G.S.V. Raghavan, " Heat Transfer Between Flowing Granular Materials and Immersed Objects", Trans. ASAE., 1564-1572 (1980).
31. Levenspiel, Octave, Engineering Flow and Heat Exchange, New York:Plenum Press (1984).
32. Lapp, H.M., F.J. Madrid, and L.B. Smith, " A Continuous Thermal Treatment to Eradicate Insects from Stored Wheat", Paper no. 86-3008, ASAE, St. Joseph, MI (1986).
33. Agro, W.B., and J.M. Smith, " Heat Transfer in Packed Beds", Chem. Engr. Prog., 49:433-451 (1953).
34. Masamune, S. and J.M. Smith, " Thermal Conductivity of Beds of Spherical Particles", I. and E.C. Fund., 2:136-142, (1963).
35. Ofuchi, K. and D. Kunii, " Heat Transfer Characteristics of Packed Beds with Stagnant Fluids", Intl. J. Heat Mass Transfer, 8:749-757 (1965).
36. Singer, E. and R.H. Wilhelm, " Heat Transfer in Packed Beds- Analytical Solution and Design Methods", Ind. Engr. Chem., 46:343 (1950).
37. Yagi, S. and D. Kunii, " Studies on Effective Thermal Conductivities in Packed Beds", AIChE J., 3:373-381 (1957).

38. Gorring, R.L., and S.W. Churchill, " Thermal Conductivity of Heterogeneous Materials", Chem. Engr. Prog., 57:53-59 (1961).
39. Otake, T. and S. Tone, " Mechanism of Heat Transfer in Solid Particle Beds", Chem Engr. (Japan), 24:156-159 (1960).
40. Mery, M.S., " Heat Transfer in Porcupine Processor", Report no. 204, the Bethlehem, Corp., Bethlehem, PA (August, 1965).
41. Uhl, V.W., and W.L. Root, " Heat Transfer to Granular Solid in Agitated Units", Chem. Engr. Prog., 63:81-92 (1967).
42. Horzella, T. " Practical Indirect Heating of Solids", Chem. Engr. Prog., 59:90-92 (1963).
43. Mickley, H.S., and Fairbanks, D.F., " Mechanism of Heat Transfer to Fluidized Beds", AIChE J., 1:374-384 (1955).
44. Brinn, M.S., S.J. Friedman, F.A. Gluckert, and R.L. Pigford, " Heat Transfer to Granular Materials", Industrial and Eng. Chemistry, 1050-1061 (June 1948).
45. Kurochkin, Y.P., " Heat Transfer Between Tubes of Different Sections and a Stream of Granular Material", J. Eng. Phys., 10:447-449 (1966).
46. Harakas, N.K., and K.O. Beatty, " Moving Bed Heat Transfer", Chem. Engr. Prog. Symp. Series, 59:122-128 (1963).
47. Raghavan, G.S.V., J.M. Harper and R.D. Haberstroh, " Heat Transfer Study Using Granular Media", Trans. ASAE., 589-592 (1974).
48. Sullivan, W.N. and R.H. Sabersky, " Heat Transfer to Flowing Granular Media", Int. J. Heat Mass Transfer, 18:97-107 (1975).
49. Tessier, S. and G.S.V. Raghavan, " Heat Transfer by Mixing in Solid Media with a Flighted Rotating Drum", Trans. ASAE., 1233-1238 (1984).
50. Wunschmann, J. and E.U. Schluender, " Heat Transfer from Heated Surfaces to Spherical Packings", Intl. Chem. Engr., 20:555-563 (1980).

51. Schluender, E.U. " Heat Transfer to Moving Spherical Packings at Short Contact Times", Intl Chem Engr., 20:550-554 (1980).
52. Schluender, E.U., " Heat Transfer to Packed and Stirred Beds from the Surface of Immersed Bodies", Chem Eng. Process, 18:31-53 (1984).
53. Molerus O. and H. Scheuring, " Heat Transfer Between Particle Beds and Submerged Surfaces", Chem Eng. Technol., 126-138 (1988).
54. Saxena, S.C., N.S. Grewal, and J.D. Gabor, " Heat Transfer Between a Gas Fluidized Bed and Immersed Tubes", Adv. Heat Transfer, 14:149-247 (1978).
55. Schluender, E.U., " Particle Heat Transfer", Heat Transfer, Proc. Seventh Int. Heat Transfer Conf., 1:195-211 (1982).
56. Sun, J. and M.M. Chen, " A Theoretical Analysis of Heat Transfer Due To Particle Impact", Int. J. Heat Mass Transfer, 31:969-975 (1988).
57. Soo, S.L., " Fluid Dynamics of Multiphase Systems", Blais Dell Waltham, Massachusetts (1967).
58. Stoke, R.L., and E.B. Nauman , " Residence Time Distribution Function for Stirred Tanks in Series", Can. J. Chem. Eng., 48:723-725 (1970).
59. Mecklenburgh, J.C., and S. Hartland, The Theory of Backmixing, London:Wiley (1975).
60. Van De Vusse, J.G., " A New Model for the Stirred Tank Reactor", Chem. Eng. Sci., 17:507-521 (1962).
61. Berruti, F., A.G. Liden, and D.S. Scott, " Measuring and Modeling Residence Time Distribution of Low Density Solid in a Fluidized Bed Reactor of Sand Particles", Chem. Eng. Sci., 43:739-748 (1988).
62. Kelly, J.J. and P. O'Donnell, " Residence Time Model for Rotary Drum", Trans. I. Cheme., 55:243-252 (1977).
63. Porter, S.J., " The Design of Rotary Dryers and Coolers", Trans. Instn. Chem. Engrs., 41:272-280 (1963).
64. Nillson, L., " Influence of Solid Dispersion on the Heat Transfer Process in a Longitudinal Flow Fluidized Bed ", Chem Eng. Sci., 43:3217-3223 (1988).

65. Yang, H.G., K.T. Yang, J.R. Lloyd, " Rotational Effects on Natural Convection in a Horizontal Cylinder" , AIChE J., 34:1627-1633 (1988).
66. Yates, J.G., Fundamentals of Fluidized-Bed Chemical Processes, Boston:Butter Worths (1983).
67. Wen, C.Y. and L.T. Fan, Models for Flow Systems and Chemical Reactors, Marcel Dekker, (1975).
68. Holman, J.P., Heat Transfer, 5th ed., McGraw-Hill (1981).
69. McComick, P.Y., " The Key to Drying Solids ", Chem Engr., 113-122 (August 15, 1988).

**APPENDIXES**

APPENDIX A  
EQUATIONS USED FOR MODELING  
CALCULATIONS



The equations used for computing the flow rates and residence time inside a screw conveyer as well as the residence time inside the drum are summarized and shown as follows:

The capacity, cubic feet per hour per revolution per minute:

$$\frac{F}{\Omega} = \frac{0.7854 (D_S^2 - D_P^2) PK 60}{1728} \quad (A.1)$$

The mixing time inside the conveyer :

$$t = \frac{12 (L')}{P (\Omega)} \quad (A.2)$$

where F = cubic feet per hour

$\Omega$  = revolutions of screw per minute

$D_S$  = diameter of screw, inches

$D_P$  = diameter of pipe, inches

P = pitch of screw, inches

K = per cent trough loading

L' = length of the screw, feet

t = mixing time, min

$$E_i = (W_i\% / \Delta t_i) \quad (A.3)$$

$$\tau = \sum_{i=1}^J W_i\% * t_i \quad (A.4)$$

$$\sigma^2 = \left( \sum_{i=1}^J W_i\% * t_i^2 \right) - \tau^2 \quad (A.5)$$

$$\theta_i = t_i / \tau \quad (\text{A.6})$$

$$E_{\theta i} = E_i * (\tau) \quad (\text{A.7})$$

$$\sigma_{\theta}^2 = \sigma^2 / \tau^2 \quad (\text{A.8})$$

where  $W_i\%$  = the mass fraction of particles collected at the drum outlet ( $W_i/W_T$ )

$W_i$  = the mass of particles collected at the drum outlet at time period  $\Delta t_i$ , lb

$W_T$  = the total mass of particles dumped into the drum as an impulse input, lb

$\tau$  = mean residence time, min

$E_i$  = exit age, 1/min

$E_{\theta i}$  = dimensionless exit age

$\theta_i$  = dimensionless time

$\sigma^2$  = variance

$\sigma_{\theta}^2$  = dimensionless variance

APPENDIX B

LISTING OF COMPUTER SOURCE PROGRAMS

```

10 '' C ***** ADBLOCK.BAS ***** C
20 '' CCCCCCCCCCCCCCCCCCCCCCCCCCCCCCCCCCCCCCCCCCCCCCCCCCCCCCCCC
30 '' C C
40 '' C TEMPERATURE DATA SAMPLING PROGRAM (ADBLOCK) IN C
50 '' C BASIC LANGUAGE WITH TEMPERATURE SENSORS (T-TYPE) C
60 '' C INTERFACED WITH MICROCOMPUTER ( IBM PC-AT ) C
70 '' C USING A/D CONVERTER (DT-2805 WITH DT-707-T BOARD) C
80 '' C DIFFERENTIAL AND UNIPOLAR INPUTS : 8 CHANNELS C
90 '' C C
100 '' C REF.: USER MANUAL FOR DT2801 SERIES FROM DATA C
110 '' C TRANSLATION, INC. C
120 '' C C
130 '' CCCCCCCCCCCCCCCCCCCCCCCCCCCCCCCCCCCCCCCCCCCCCCCCCCCCCCCCC
140 '' C
150 '' CCCCCCCCCCCCCCCCCCCCCCCCCCCCCCCCCCCCCCCCCCCCCCCCCCCCCCCCC
160 '' C C
170 '' C NOMENCLATURE C
180 '' C C
190 '' C ADL : A/D DATA IN LOW BYTES C
200 '' C ADH : A/D DATA IN HIGH BYTES C
210 '' C ADGAIN: SPECIFIED NO FOR GAIN C
220 '' C GAIN : THE GAIN VALUE OF A/D BOARD C
230 '' C I : SCANNING NO. C
240 '' C MV : MILI VOLTAGE C
250 '' C NCONV : CONVERSION NUMBERS C
260 '' C REFT : REF TEMPERATURE (F) C
270 '' C REF : CORRESPONDING REF VOLTAGE (MV) C
280 '' C T : READING TEMPERATURES (F) C
290 '' C TIME : SCANNING TIMES (MIN.) C
300 '' C C
310 '' CCCCCCCCCCCCCCCCCCCCCCCCCCCCCCCCCCCCCCCCCCCCCCCCCCCCCCCCC
320 DIM T#(50),ADL%(50),ADH%(50)
330 ''
340 '' -----
350 '' CREATE A DATA BANK FOR TEMPERATURES MEASUREMENTS
360 '' -----
370 OPEN "A:TFILE" FOR OUTPUT AS #1
380 CLOSE #1
390 ''
400 '' -----
410 '' SPECIFY ALL NECESSARY VARIABLES
420 '' -----
430 DEFINT A-Z
440 I=1 ' FIRST-TIME SCANNING
450 INPUT " START TIME (MIN) =" ;TIME
460 BASE.ADDRESS = &H2EC ' FOR THIS CASE
470 COMMAND.REGISTER = BASE.ADDRESS +1

```

```

480 STATUS.REGISTER      = BASE.ADDRESS +1
490 DATA.REGISTER      = BASE.ADDRESS
500 COMMAND.WAIT        = &H4
510 WRITE.WAIT          = &H2
520 READ.WAIT           = &H5
530 CCLEAR              = &H1
540 CCLOCK              = &H3
550 CSAD                = &HD
560 CRAD                = &HE
570 CSTOP               = &HF
580 PERIOD#             = 40000! ' FOR THIS BOARD
590 BASE.FACTOR#        = 4096  ' FOR 12-BIT BOARD
600 BASE.CHANNELS       = 8     ' FOR DIFFERENTIAL-END
610 ADGAIN=3           ' FOR GAIN SET AT 500
620 GAIN=500           ' FOR 0-20 MV RANGE
630 ''
640 '' -----
650 '' STOP AND CLEAR THE DT2801 SERIES BOARD
660 '' -----
670 ''
680 OUT COMMAND.REGISTER, CSTOP
690 TEMP = INP(DATA.REGISTER)
700 WAIT STATUS.REGISTER, WRITE.WAIT, WRITE.WAIT
710 WAIT STATUS.REGISTER, COMMAND.WAIT
720 OUT COMMAND.REGISTER, CCLEAR
730 ''
740 '' -----
750 '' SET CLOCK RATE : WAIT UNTIL THE DT-2805 BOARD
760 '' DATA IN FLAG IS CLEARED AND READY, FLAG IS SET,
770 '' THEN WRITE THE SET CLOCK PERIOD COMMAND BYTE
780 '' TO THE COMMAND REGISTER.
790 '' -----
800 ''
810 WAIT STATUS.REGISTER, WRITE.WAIT, WRITE.WAIT
820 WAIT STATUS.REGISTER, COMMAND.WAIT
830 OUT COMMAND.REGISTER, CCLOCK
840 ''
850 '' -----
860 '' DIVIDE PERIOD NO. INTO HIGH/LOW BYTES AND WRITE
870 '' BOTH BYTES TO THE DATA IN REGISTER, THEN WAIT
880 '' FOR A CLEAR DATA IN FULL FLAG BEFORE EACH WRITE.
890 '' -----
900 ''
910 PERIODH = INT(PERIOD#/256)
920 PERIODL = PERIOD# - PERIODH * 256
930 WAIT STATUS.REGISTER, WRITE.WAIT, WRITE.WAIT
940 OUT DATA.REGISTER, PERIODL
950 WAIT STATUS.REGISTER, WRITE.WAIT, WRITE.WAIT
960 OUT DATA.REGISTER, PERIODH
970 ''
980 '' -----
990 '' INPUT THE DESIRED A/D START CHANNEL, END CHANNEL,
1000 '' GAIN AND NUMBER OF CONVERSIONS BY USER.
1010 '' -----

```

```

1020 ''
1030 ADSCHANNEL=0 ' START CHANNEL NO.
1040 ADECHANNEL=7 ' END CHANNEL NO.
1050 ''
1060 PRINT " NUMBER OF CONVERSIONS TO ";
1070 INPUT " BE DONE ( 3-1000 )"; NCONV#
1080 IF NCONV# < 3 THEN GOTO 1060
1090 IF NCONV# > 1000 THEN GOTO 1060
1100 ''
1110 '' -----
1120 '' DO A SET A/D PARAMETERS COMMAND TO SET UP THE
1130 '' A/D BOARD. WAIT UNTIL THE DT-2805 BOARD DATA
1140 '' IN FULL FLAG IS CLEAR AND READY FLAG IS SET,
1150 '' THEN WRITE THE SET A/D PARAMETERS COMMAND
1160 '' BYTE TO THE COMMAND REGISTER.
1170 '' -----
1180 ''
1190 WAIT STATUS.REGISTER, WRITE.WAIT, WRITE.WAIT
1200 WAIT STATUS.REGISTER, COMMAND.WAIT
1210 OUT COMMAND.REGISTER, CSAD
1220 ''
1230 '' -----
1240 '' WAIT UNTIL THE DT-2805 BOARD DATA IN FULL FLAG
1250 '' IS CLEAR, THEN WRITE THE A/D GAIN BYTE TO THE
1260 '' DATA IN REGISTER.
1270 '' -----
1280 ''
1290 WAIT STATUS.REGISTER, WRITE.WAIT, WRITE.WAIT
1300 OUT DATA.REGISTER, ADGAIN
1310 ''
1320 '' -----
1330 '' WAIT UNTIL THE DT-2805 BOARD DATA IN FULL
1340 '' FLAG IS CLEAR, THEN WRITE THE A/D START
1350 '' CHANNEL BYTE TO THE DATA IN REGISTER.
1360 '' -----
1370 ''
1380 WAIT STATUS.REGISTER, WRITE.WAIT, WRITE.WAIT
1390 OUT DATA.REGISTER, ADSCHANNEL
1400 ''
1410 '' -----
1420 '' WAIT UNTIL THE DT-2805 BOARD DATA IN FULL
1430 '' FLAG IS CLEAR, THEN WRITE THE A/D END
1440 '' CHANNEL BYTE TO THE DATA IN REGISTER.
1450 '' -----
1460 ''
1470 WAIT STATUS.REGISTER, WRITE.WAIT, WRITE.WAIT
1480 OUT DATA.REGISTER, ADECHANNEL
1490 ''
1500 '' -----
1510 '' DIVIDE NCONVERSION NO. INTO HIGH AND LOW
1520 '' BYTES AND WRITE BOTH BYTES TO THE DATA IN
1530 '' REGISTER, WAIT FOR A CLEAR DATA IN FULL FLAG
1540 '' BEFORE EACH WRITE.
1550 '' -----

```

```

1560 ''
1570 NUMBERH = INT(NCONV#/256)
1580 NUMBERL = NCONV# - NUMBERH * 256
1590 WAIT STATUS.REGISTER, WRITE.WAIT, WRITE.WAIT
1600 OUT DATA.REGISTER, NUMBERL
1610 WAIT STATUS.REGISTER, WRITE.WAIT, WRITE.WAIT
1620 OUT DATA.REGISTER, NUMBERH
1630 ''
1640 '' -----
1650 '' START TO READ A/D COMMAND: WAIT THE DT-2805
1660 '' BOARD DATA IN FULL FLAG IS CLEAR AND READY FLAG
1670 '' IS SET, THEN WRITE THE READ A/D COMMAND BYTE
1680 '' TO THE COMMAND REGISTER.
1690 '' -----
1700 ''
1710 WAIT STATUS.REGISTER, WRITE.WAIT, WRITE.WAIT
1720 WAIT STATUS.REGISTER, COMMAND.WAIT
1730 OUT COMMAND.REGISTER, CRAD
1740 ''
1750 '' -----
1760 '' READ THE A/D DATA, HIGH AND LOW BYTES, INTO
1770 '' ARRAYS AND WAIT FOR A SET DATA OUT READY FLAG
1780 '' BEFORE EACH READ.
1790 '' -----
1800 ''
1810 FOR LOOP = 1 TO NCONV#
1820     WAIT STATUS.REGISTER, READ.WAIT
1830     ADL(LOOP) = INP(DATA.REGISTER)
1840     WAIT STATUS.REGISTER, READ.WAIT
1850     ADH(LOOP) = INP(DATA.REGISTER)
1860 NEXT LOOP
1870 ''
1880 '' -----
1890 '' WAIT UNTIL THE DT-2805 BOARD DATA IN FULL FLAG
1900 '' IS CLEAR AND READY FLAG IS SET, INDICATING
1910 '' COMMAND COMPLETION, THEN CHECK THE STATUS
1920 '' REGISTER ERROR FLAG.
1930 '' -----
1940 ''
1950 WAIT STATUS.REGISTER, WRITE.WAIT, WRITE.WAIT
1960 WAIT STATUS.REGISTER, COMMAND.WAIT
1970 STATUS = INP(STATUS.REGISTER)
1980 IF (STATUS AND &H80) THEN GOTO 2760
1990 ''
2000 '' -----
2010 '' CALCULATE AND PRINT ALL CONVERTED A/D VOLTAGES,
2020 '' PUT A FORMAT TO INDICATE FIRST AND LAST CHANNEL
2030 '' READINGS.
2040 '' -----
2050 ''
2060 FACTOR# = (10/BASE.FACTOR#) / (GAIN)
2070 NCHAN = ADECHANNEL - ADSCHANNEL + 1

```

```

2080 '' -----
2090 '' COMPUTE THE A/D READINGS IN VOLTS AND ALSO
2100 '' TRANSFORM INTO MILLI-VOLTS IN ORDER TO
2110 '' CALCULATE THE TEMPERATURES IN F.
2120 '' -----
2130 IF NCHAN < 1 THEN NCHAN = NCHAN + BASE.CHANNELS
2140 ''
2150 '' -----
2160 '' READ ROOM TEMPERATURES MANUALLY
2170 '' -----
2180 INPUT " REF. TEMP (c) AS THE ROOM TEMP. "; REFTC
2190 REFT = REFTC * 9/5 + 32 ' CONVERT FROM C TO F
2200 '' -----
2210 '' FOLLOWING EQUATION IS OBTAINED USING REGRESSION
2220 '' METHOD (REG) FOR T-TYPE THERMOCOUPLES; MV=f(T)
2230 '' MV = A*T^2 + B*T + C
2240 '' -----
2250 REF#=1.30874E-05*REFT^2+.0205856*REFT-.670943
2260 ''
2270 '' -----
2280 '' COMPUTE THE A/D READINGS IN VOLTS AND ALSO
2290 '' TRANSFORM INTO MILLI-VOLTS IN ORDER TO
2300 '' CALCULATE THE TEMPERATURES IN F.
2310 '' -----
2320 FOR L = 1 TO NCONV#
2330 DATA.VALUE# = ADH(L) * 256 + ADL(L)
2340 UNI.VOLTS# = DATA.VALUE# * FACTOR#
2350 MV# = UNI.VOLTS# * 1000 + REF#
2360 '' =====
2370 '' THE FOLLOWING EQUATION IS USED FROM
2380 '' MASTER'S WORK FOR T-TYPE THERMOCOUPLES
2390 '' T = A*MV^2 + B*MV + C
2400 '' =====
2410 T#(L) = -.81229947#*MV#^2 + 45.457*MV# + 32.64111
2420 '' =====
2430 '' PRINT THE RESULTS ON SCREEN
2440 '' =====
2450 PRINT USING "#####.##### (MV)"; MV#;
2460 PRINT USING "#####.#### (F)"; T#(L);
2470 IF (L MOD NCHAN) = 0 THEN PRINT
2480 IF (L MOD NCHAN) = 0 THEN PRINT
2490 NEXT L
2500 ''
2510 '' -----
2520 '' TO BUILD UP A DATA FILE FOR TEMPERATURES MEASURING
2530 '' -----
2540 OPEN "A:TFILE" FOR APPEND AS #1
2550 '' =====
2560 '' PRINT ALL THE RESULTS (TEMPERATURE PROFILES)
2570 '' ON THE DISK FOR THE PURPOSE OF FURTHER ANALYSIS
2580 '' =====
2590 PRINT #1, " CHAN. NO. FROM ";
2595 ADSCHANNEL; " TO "; ADECHANNEL
2600 FOR J = 1 TO L-1

```



```

2610         PRINT #1, " THE TIME SCANNING (MIN.)";TIME,
2615         "CONV. NO=";J,
2620         PRINT #1, " GAIN = ";GAIN , "REF TEMP(F)=";REFT,
2630         PRINT #1, " THE TEMP (F)="; USING
2635         "#####.#####"; T#(J)
2640     NEXT J
2650 CLOSE #1
2660 ''
2670 '' -----
2680 '' TO DECIDE WHETHER GOING ON NEXT SCAN OR NOT !
2690 '' -----
2700 INPUT " DO YOU LIKE TO DO NEXT SCAN ? 'Y' OR 'N'";B$
2710 IF B$ = "N" THEN GOTO 2910 ELSE GOSUB 2820: GOTO 460
2720 ''
2730 '' -----
2740 '' PRINT THE ERROR MESSAGE !!!
2750 '' -----
2760 PRINT
2770 PRINT " ERROR "
2780 PRINT
2790 GOTO 2910 ' TO QUIT THE JOB BECAUSE OF ERROR
2800 ''
2810 '' -----
2820 '' SUBROUTINE FOR NEXT SCANNING PREPARATION
2830 '' -----
2840 INPUT " THE CURRENT TIME (MIN.).... "; CTIME
2850 TIME = CTIME
2860 RETURN
2870 ''
2880 '' *****
2890 '' PROGRAM IS STOPED HERE !!!
2900 '' *****
2910 END

```

```

C ----- C
C ***** REG.FOR ***** C
C CCCCCCCCCCCCCCCCCCCCCCCCCCCCCCCCCCCCCCCCCCCCCCCCCCCCCCCCC C
C
C          REGRESSION FITTING PROGRAM (REG.FOR) C
C          USING 2 IMSL ROUTINES: RLFOTH AND RLDOPM C
C          Y = C(1)*X^2 + C(2)*X + C(3) C
C C
C CCCCCCCCCCCCCCCCCCCCCCCCCCCCCCCCCCCCCCCCCCCCCCCCCCCCCCCCC C
C ----- C
C
C          NOMENCLATURES C
C
C          A:  CONSTANTS USED FOR GENERATING THE C
C              ORTHOGONAL POLYNOMIAL C
C          B:  ADDITIONAL CONSTANTS USED FOR GENERATING C
C              THE ORTHOGONAL POLYNOMIAL C
C          C:  REGRESSION COEFFICIENTS OF FITTED POLYNOMIAL EQ. C
C              IN ASCENDING DEGREE ORDER C
C          ID: DEGREE OF THE ORTHOGONAL POLYNOMIAL C
C          MD: MAXIMUM DEGREE ALLOWED FOR THE FITTED EQ. C
C          N:  THE NUMBER OF DATA POINTS C
C          RSQ: CONTROLLING THE DEGREE OF THE FITTED EQ. C
C          S:  ERROR SUM OF SQUARES C
C          X:  TEMPERATURE (°F) C
C          Y:  VOLTAGE SIGNAL (MV) C
C ----- C
C
C ----- C
C          JOB CONTROL CARDS FOR USING MAINFRAME COMPUTER AT OSU C
C ----- C
C //U15158FC JOB (15158,123-45-6789),TIME=(0,5),CLASS=1, C
C //          NOTIFY=*,MSGCLASS=X C
C /*PASSWORD ? C
C /*ROUTE PRINT LOCAL C
C /*JOBPARM FORMS=9001, ROOM=C C
C //          EXEC FORTVCG C
C //FORT.SYSIN DD * C
C ----- C
C          MAIN PROGRAM C
C ----- C
C          OBTAIN A FITTING EQ. IN THE FORM OF Y=f(X) C
C          THE RANGE OF X IS ABOUT FROM 50-100 F C
C          (AROUND ROOM TEMPERATURES) C
C ===== C

```

```

      INTEGER N,MD,ID,IER
      REAL X(26),Y(26),RSQ,C(5),S(5),A(2),B(2)
      DOUBLE PRECISION P(52),T(12)
C -----
C SPECIFY ALL THE NECESSARY DATA
C -----
C
      X(1)=50.
      DO 10 I=1,25
          X(I+1)=X(I)+2.
10 CONTINUE
      DATA Y /.391,.435,.479,.523,.567,.611,.656,.7,.745,
$           .789,.834,.879,.924,.969,1.014,1.06,1.105,
$           1.151,1.196,1.242,1.288,1.334,1.38,1.426,
$           1.472,1.518/

      N=26
      RSQ=100
      MD=2
C -----
C CALL THE IMSL SUBROUTINE -- RLFOTH
C ( REGRESSION USING ORTHOGONAL POLYNOMIAL)
C -----
      CALL RLFOTH(X,Y,N,RSQ,MD,ID,P,C,S,A,B,IER)
C -----
C CALL THE IMSL SUBROUTINE -- RLDOPM
C ( DECODER FOR AN ORTHOGONAL EQ.)
C -----
      CALL RLDOPM(C,ID,A,B,T)
C =====
C PRINT THE RESULTS -- THE COEFFICIENTS OF FITTING
C POLYNOMIAL EQUATION
C =====
C
      WRITE(6,20) (C(I),I=1,3)
20 FORMAT(5X,'1ST COEFFICIENT (A)=' ,F10.3/5X,'2ND
$ COEFFICIENT (B)=' , F10.3/5X, '3RD COEFFICIENT
$ (C)=' , F10.3)
C *****
C PROGRAM STOP HERE !!!
C *****
      STOP
      END
C =====
C DATA ENTRY CARDS (IF ANY)
C =====
//GO.SYSIN DD *
//

```

```

C ***** MODEL.FOR *****C
C
CCCCCCCCCCCCCCCCCCCCCCCCCCCCCCCCCCCCCCCCCCCCCCCCCCCCCCCC
C
C          HEAT TRANSFER MODELING PROGRAM (MODEL.FOR) C
C          A SET OF 1ST ORDER DIFFERENTIAL EQS. WAS C
C          SOLVED BY DGEAR ROUTINES OF IMSL PACKAGE C
C
C          ----- PC VERSION ----- C
C
CCCCCCCCCCCCCCCCCCCCCCCCCCCCCCCCCCCCCCCCCCCCCCCCCCCCCCCC
C
C-----C
C
C          NOMENCLATURES C
C
C          A: HEAT TRANSFER AREA (ft2 ) C
C          C: HEAT CAPACITY OF PROP (Btu/lb °F) C
C          CW: HEAT CAPACITY OF SOYBEANS (Btu/lb °F) C
C          H: STEP SIZE OF INTEGRATION IN TIME SPACE C
C          M: MASS FLOW RATES OF PROP (lb/min.) C
C          METH: BASIC METHOD INDICATOR C
C          MITER: ITERATION METHOD INDICATOR C
C          N: NUMBER OF DIFFERENTIAL EQS. C
C          TOL: TOLERANCE C
C          U: HEAT TRANSFER COEFFICIENT (Btu/ft2 min °F) C
C          UALI: LUMPED HEAT LOSS AT INLET (Btu/min °F) C
C          UALO: LUMPED HEAT LOSS AT OUTLET (Btu/min °F) C
C          UAL: LUMPED HEAT LOSS ELSEWHERE (Btu/min °F) C
C          VB: MASS OF SOYBEAN AT EACH STAGE (lb) C
C          VM: LUMPED MASS OF PROP WITH OPERATED C
C          APPARATUS AT EACH STAGE (lb) C
C          X: ELAPSED TIME (MIN.) C
C          XEND: END-TIME OF INTEGRATION C
C          Y: TEMPERATURES OF PARTICLE SURFACE (°F) C
C          Y(1)-Y(13) FOR INTERPROP C
C          Y(14)-Y(26) FOR SOYBEANS C
C          YAIR: AIR TEMPERATURE (°F) C
C          YO: INLET TEMPERATURE OF INTERPROP (°F) C
C          YI: INLET TEMPERATURE OF SOYBEANS (°F) C
C          YPRIME: DERIVATIVES FOR Y C
C          W: MASS FLOW RATES OF SOYBEANS (lb/min) C
C
C-----C

```

```

C -----
C
C AN IMSL (DGEAR) SUBROUTINE OF PC-VERSION, CALLED
C 'DIFEQS.LIB' NEEDED TO BE LINKED WITH THIS MAIN PROGRAM.
C
C -----
C
C MAIN PROGRAM
C -----
C THE FOLLOWING PROGRAM IS SET FOR MODELING TEST #3 ONLY.
C THE USERS ARE ENCOURAGED TO CHANGE THE VARIABLES FOR
C DIFFERENT CASES ENCOUNTERED.
C *****
C
C $INCLUDE: 'IMSL'
C     INTEGER N, METH, MITER, INDEX, IWK(26), IER, I, J, K
C     REAL    Y(26), WK(962), X, TOL, XEND, H
C     EXTERNAL FCN, FCNJ
C
C
C -----
C SPECIFY ALL NECESSARY VARIABLES
C -----
C ALL THE DATA SHOWN HERE IS JUST A DEMONSTRATION
C AND YOU CAN CHANGE THEM AS YOU DESIRED.....
C
C =====
C DATA U, A, W, CW/17., 1.364E-03, .58, .49/
C N=26
C X=0.0
C Y0=180.
C YI=70.
C TOL=.001
C H=.0001
C
C =====
C CREATE A DATA FILE OF TEMPERATURES FOR ANALYSIS
C =====
C OPEN (6, FILE='TMODEL.DAT', STATUS='NEW')
C =====
C SPECIFY THE INITIAL CONDITIONS FOR PROP AND SOYBEAN,
C ADOPTED FROM STEADY STATE TEMPERATURE PROFILES OF PROP
C ON HEATING TEST WITHOUT INPUTTING SOYBEANS.
C =====
C DATA Y /117,113,109,105,102,99,97,94,92,90,88,86
C 1      85,13*70./
C -----
C PRINT THE INITIAL CONDITIONS
C -----
C WRITE(6,40) X, Y0, (Y(I), I=1,13)
C WRITE(6,45) (Y(I), I=14,26), YI
C
C =====
C SET UP THE SPECIFIC ALGORITHM WITH DGEAR (STIFFNESS)
C =====

```

```

METH=2
MITER=2
INDEX=1
C -----
C   A LOOP FOR INTEGRATION FROM X=0 TO X=XEND
C -----
      DO 30 K=1,100
        XEND=FLOAT(K)
C
C =====
C   CALL DGEAR ROUTINE
C =====
      CALL DGEAR(N,FCN,FCNJ,X,H,Y,XEND,TOL,METH,
1          MITER,INDEX,IWK,WK,IER)
      IF (IER.GT.128) GO TO 60
C =====
C   PRINT THE MODELING RESULTS OF TEMPERATURE PROFILES
C   FOR BOTH PROP AND SOYBEAN PHASES
C =====
      WRITE(6,40) X,Y0,(Y(I),I=1,13)
      WRITE(6,45) (Y(I),I=14,26),YI
40     FORMAT(1X,'TIME(MIN.)=',F9.2/(3X,14F6.1))
45     FORMAT((3X,14F6.1))
30     CONTINUE
      STOP
60     CONTINUE
C
C -----
C   END OF MAIN PROGRAM !!!
C -----
C
      STOP
      END
C -----
C   SUBPROGRAMS FOR USING WITH MAIN PROGRAM
C -----
      SUBROUTINE FCN(N,X,Y,YPRIME)
      INTEGER N
      REAL Y(N),YPRIME(N),X,M
C =====
C   SPECIFY ALL THE NECESSARY INPUTS
C =====
C   AGAIN THESE INPUT DATA ARE JUST FOR DEMONSTRATION
C   AND YOU CAN CHANGE THEM BASED ON YOUR NEEDS.....
C -----
      DATA U,A,W,CW,VM,C,M,Y0,YI/17.,1.364E-03,.58,.49,.4,
1         .24,1.25,180.,70./
      DATA UALI,UALO,UAL,VB,YAIR/0.4,0.03,0.03,.4,70./
C =====
C   A LOOP TO DEFINE THE INTEGRAL FORM:  $y'=f(x,y)$ 
C   --- INTERPROP PHASE ---
C =====

```

```

DO 10 I=2,12
10   YPRIME(I)=(1./(VM*C))*(W*CW*Y(I+14)+M*C*Y(I-1)-
1     W*CW*Y(I+13)-M*C*Y(I)-UAL*(Y(I)-YAIR))
1     YPRIME(1)=(1./(VM*C))*(W*CW*Y(15)+M*C*Y0-W*CW*Y(14)
1     -M*C*Y(1)-UALI*(Y(1)-YAIR))
1     YPRIME(13)=(1./(VM*C))*(W*CW*YI+M*C*Y(12)-
1     W*CW*Y(26)-M*C*Y(13)-UALO*(Y(13)-YAIR))
C =====
C     --- SOYBEAN PHASE ---
C =====
1     YPRIME(26)=(1./(VB*CW))*(U*A*Y(13)+W*CW*YI-
1     (W*CW+U*A*Y(26)))
C
DO 20 KJ=1,12
    J=26-KJ
20   YPRIME(J)=(1./(VB*CW))*(U*A*Y(J-13)+W*CW*Y(J+1)-
1     (U*A+W*CW)*Y(J))
C *****
C     END OF SUBPROGRAM-- FCN
C *****
    RETURN
    END
C -----
C     SUBPROGRAM OF FCNJ
C -----
    SUBROUTINE FCNJ(N,X,Y,PD)
    INTEGER N
    REAL Y(N),PD(N,N),X
C *****
C     END OF SUBPROGRAM -- FCNJ
C *****
    RETURN
    END

```

APPENDIX C

CALCULATIONS FOR OPERATING VARIABLES



The calculations for the mass volume of both the big particles (soybean) and the small particles (prop) in a variety of operating conditions are listed as follows:

$$m = 75 \text{ lb/hr} = 1.25 \text{ lb/min} ; M = 35 \text{ lb/hr} = 0.58 \text{ lb/min}$$

(1) for prop phase:

(i) drum speed operated at 2 rpm,  $\tau = 4.8$  mins:

$$V_m = \tau * m/N = (4.8) * (1.25) / 13 = 0.464 \text{ lb}$$

(ii) drum speed operated at 1 rpm,  $\tau = 8.7$  mins:

$$V_m = \tau * m/N = 0.8 \text{ lb}$$

(iii) drum speed operated at 0.5 rpm,  $\tau = 18$  mins:

$$V_m = \tau * m/N = 1.77 \text{ lb}$$

(iv) drum speed operated at 0.25 rpm,  $\tau = 38.3$  mins:

$$V_m = \tau * m/N = 3.7 \text{ lb}$$

(2) for soybean phase:

(i) conveyer at  $\Omega = 5.6$  rpm,  $\tau \cong 24/\Omega = 4.3$  mins:

$$V_M = \tau * M/N = (4.3) * (0.58) / 13 = 0.2 \text{ lb}$$

(ii) conveyer at 2.8 rpm,  $\tau \cong 8.6$  mins:

$$V_M = \tau * M/N = 0.38 \text{ lb}$$

(iii) conveyer at 1.86 rpm,  $\tau \cong 12.9$  mins:

$$V_M = \tau * M/N = 3.46 \text{ lb}$$

APPENDIX D

EXPERIMENTAL DATA GRAPHS

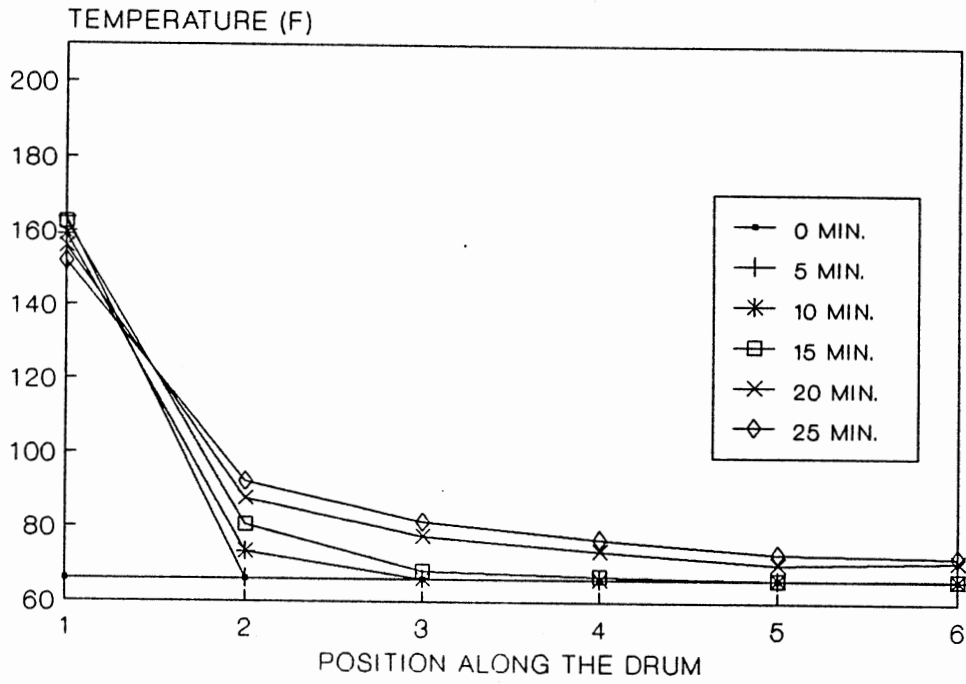


Figure 62. Experimental Temperature Profiles for Run #1

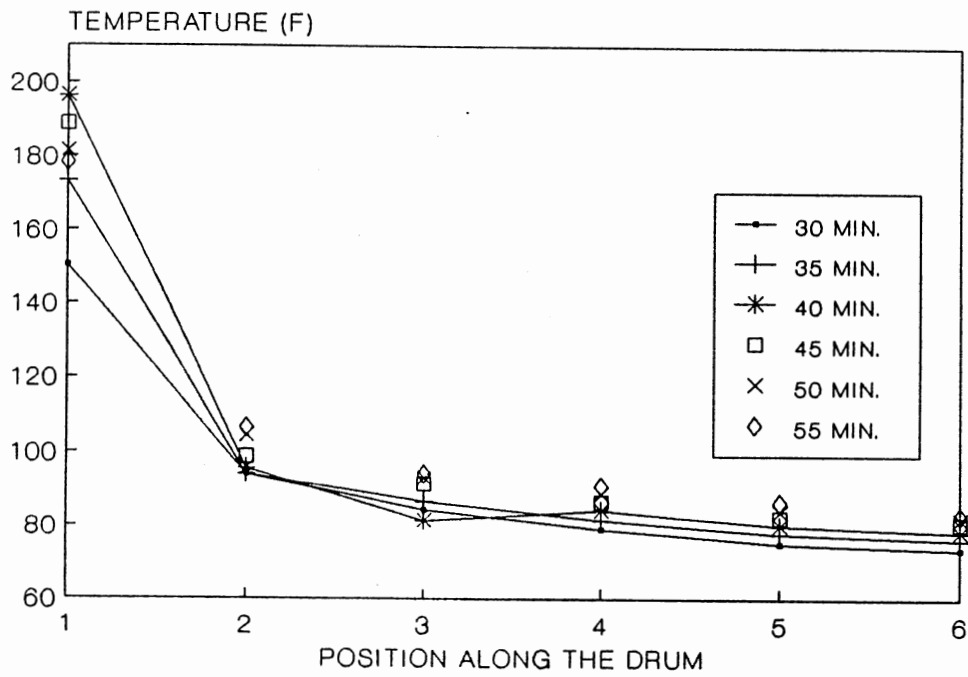


Figure 63. Experimental Temperature Profiles for Run #1

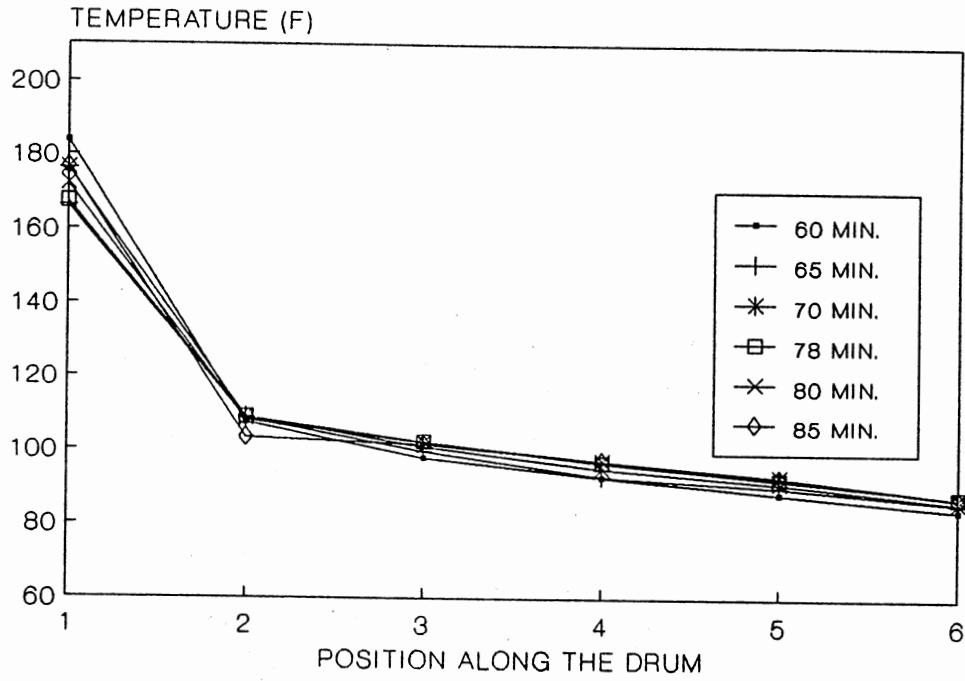


Figure 64. Experimental Temperature Profiles for Run #1

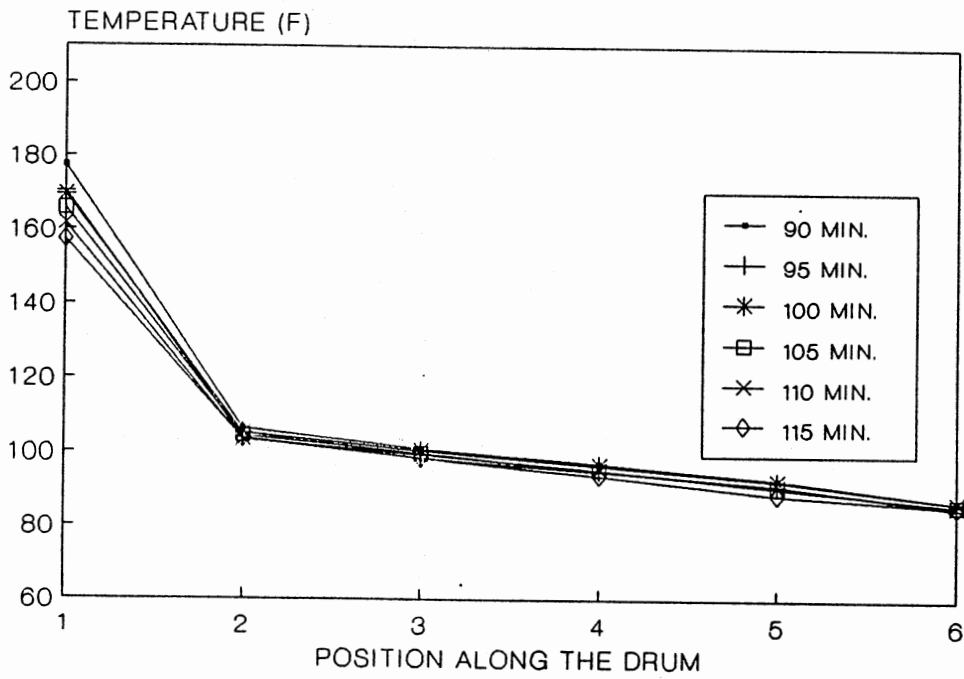


Figure 65. Experimental Temperature Profiles for Run #1

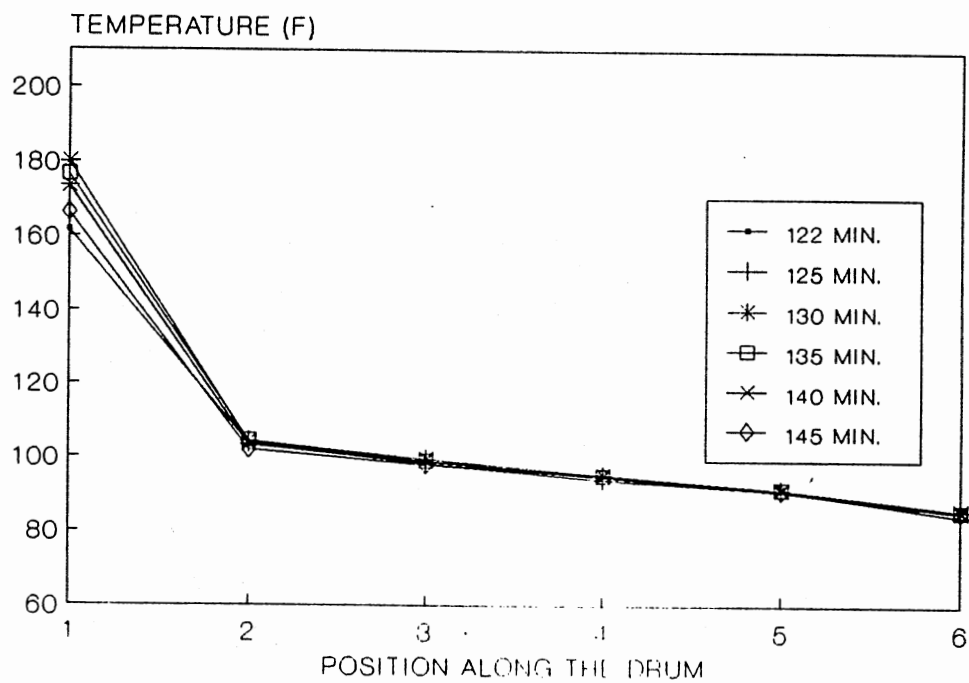


Figure 66. Experimental Temperature Profiles for Run #1

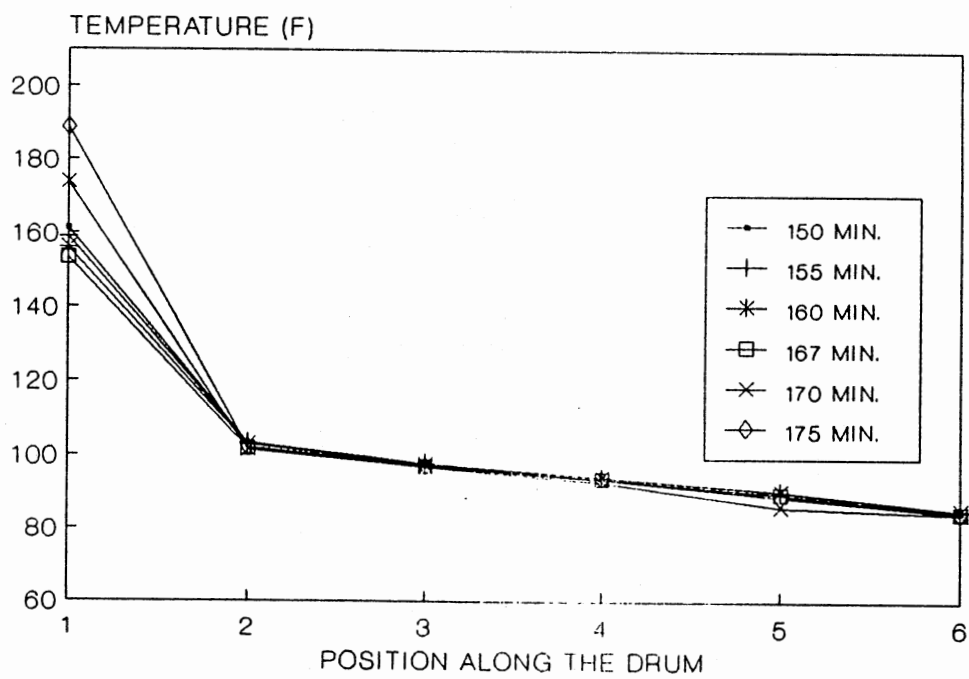


Figure 67. Experimental Temperature Profiles for Run #1

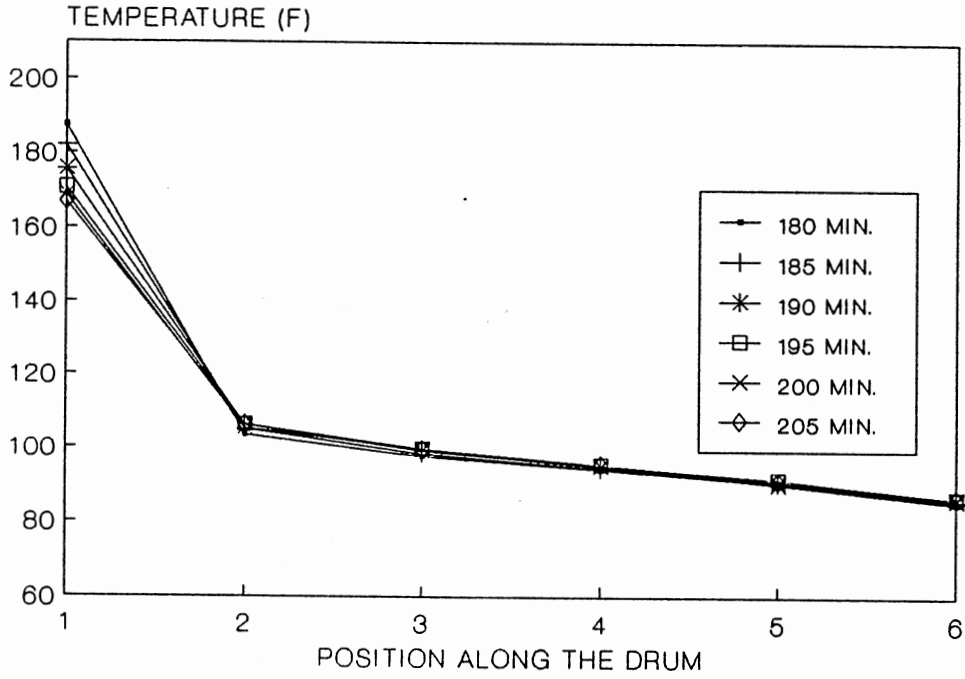


Figure 68. Experimental Temperature Profiles for Run #1

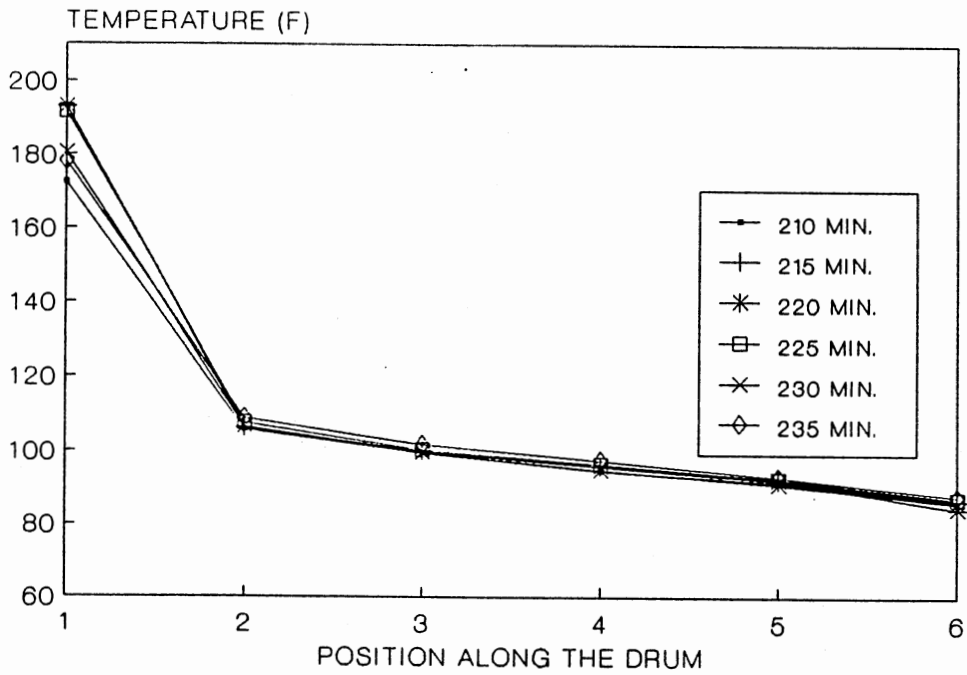


Figure 69. Experimental Temperature Profiles for Run #1

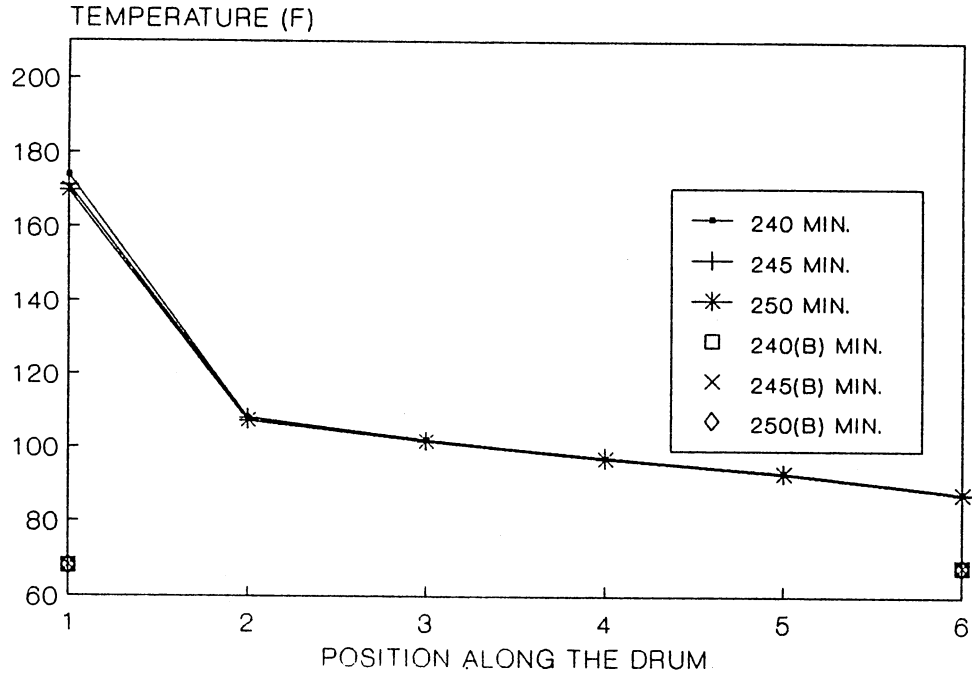


Figure 70. Experimental Temperature Profiles for Run #1

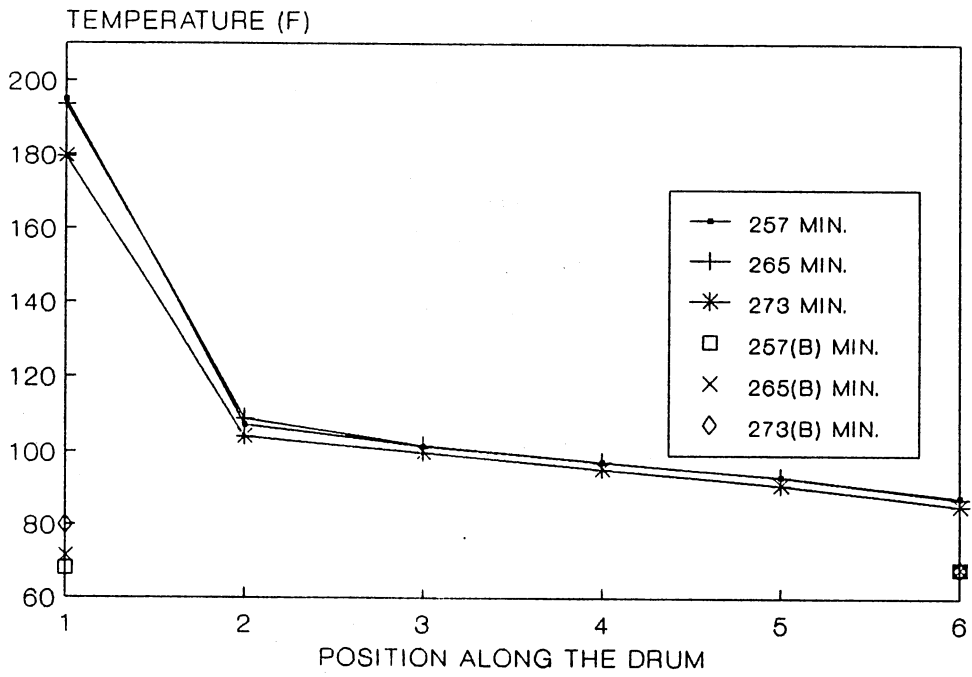


Figure 71. Experimental Temperature Profiles for Run #1

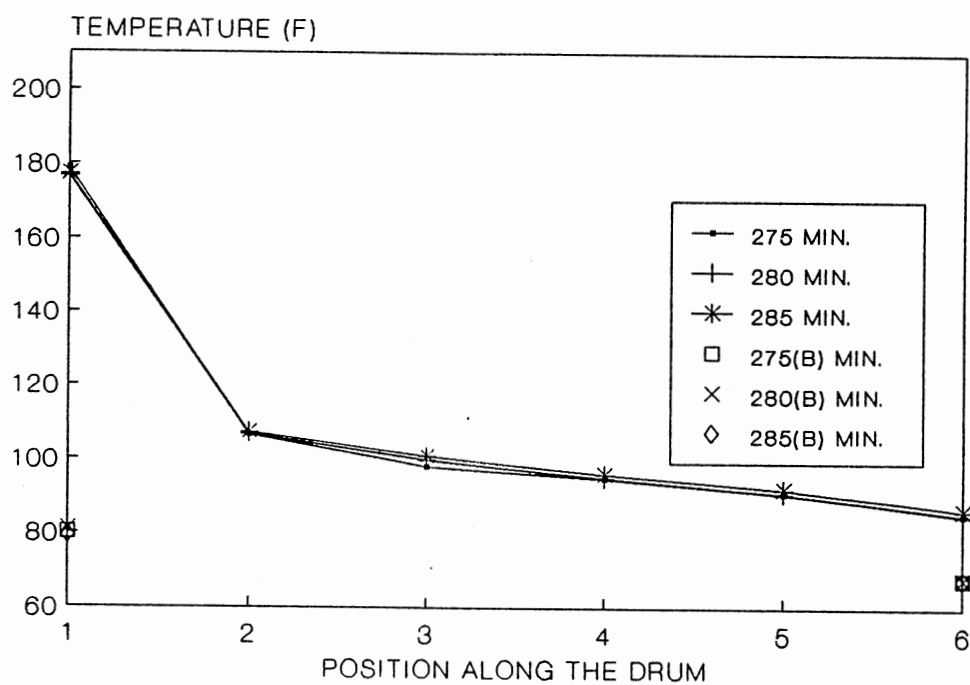


Figure 72. Experimental Temperature Profiles for Run #1

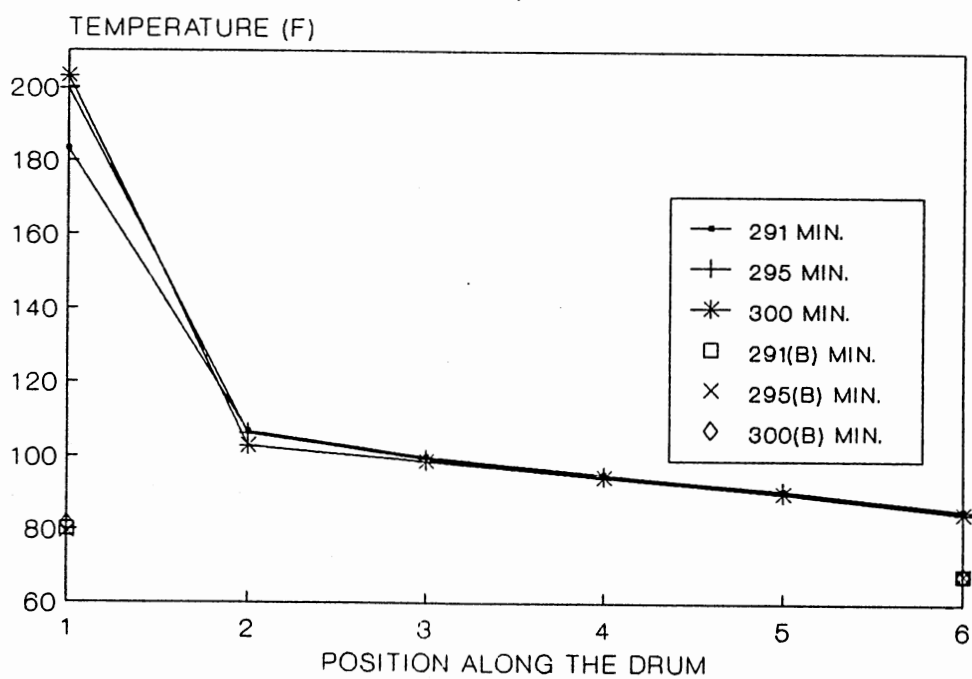


Figure 73. Experimental Temperature Profiles for Run #1



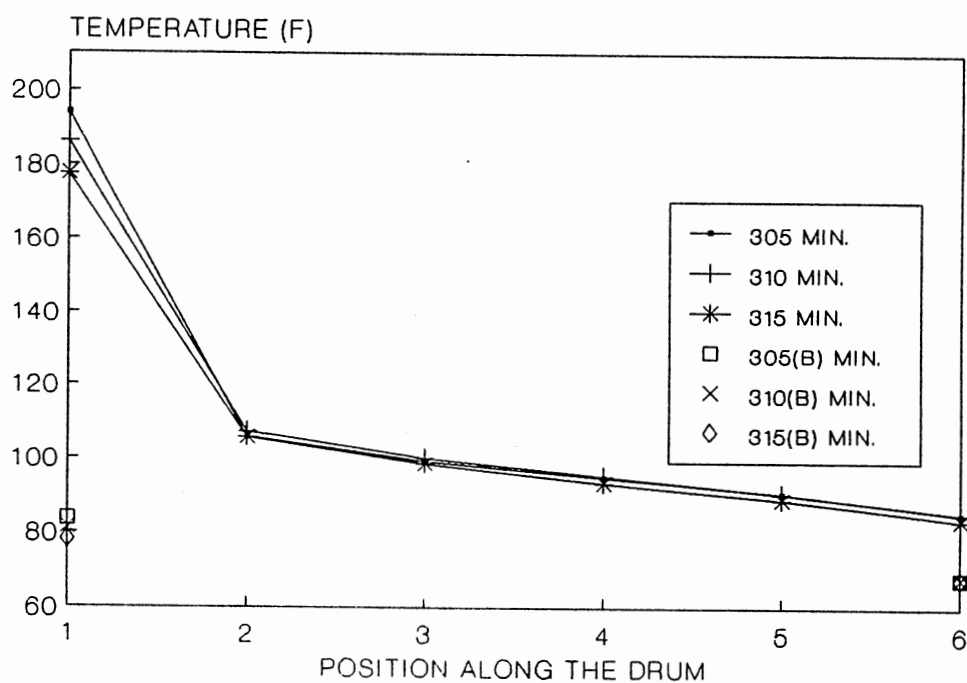


Figure 74. Experimental Temperature Profiles for Run #1

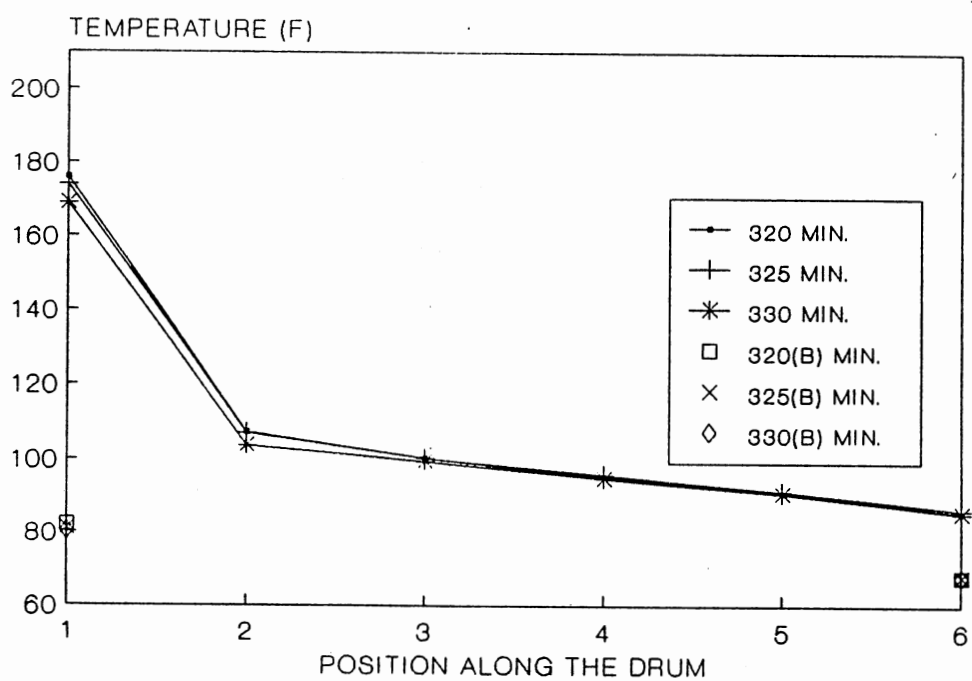


Figure 75. Experimental Temperature Profiles for Run #1

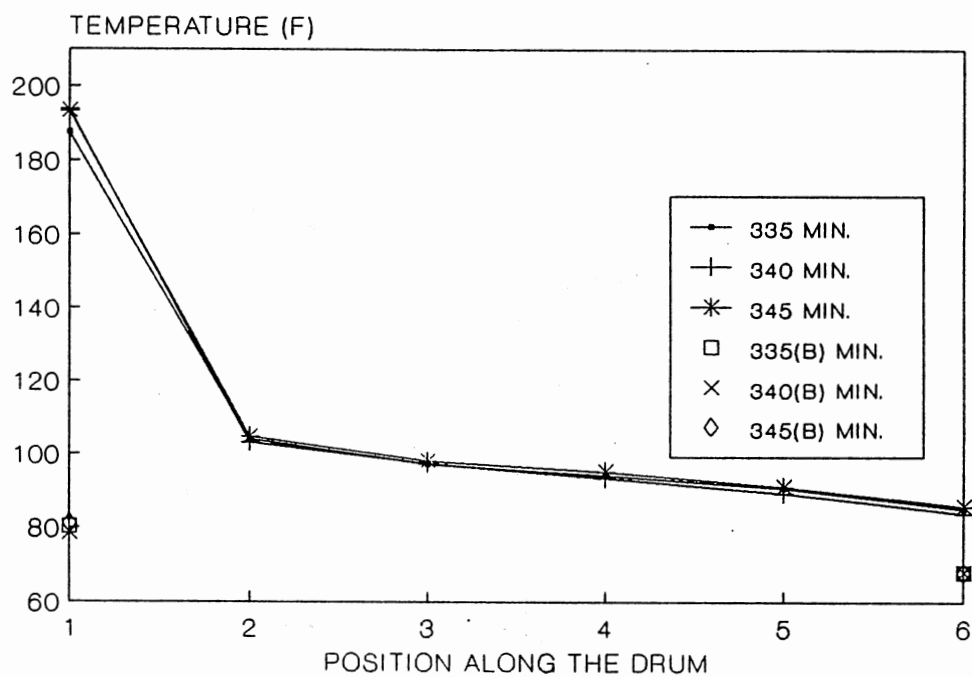


Figure 76. Experimental Temperature Profiles for Run #1

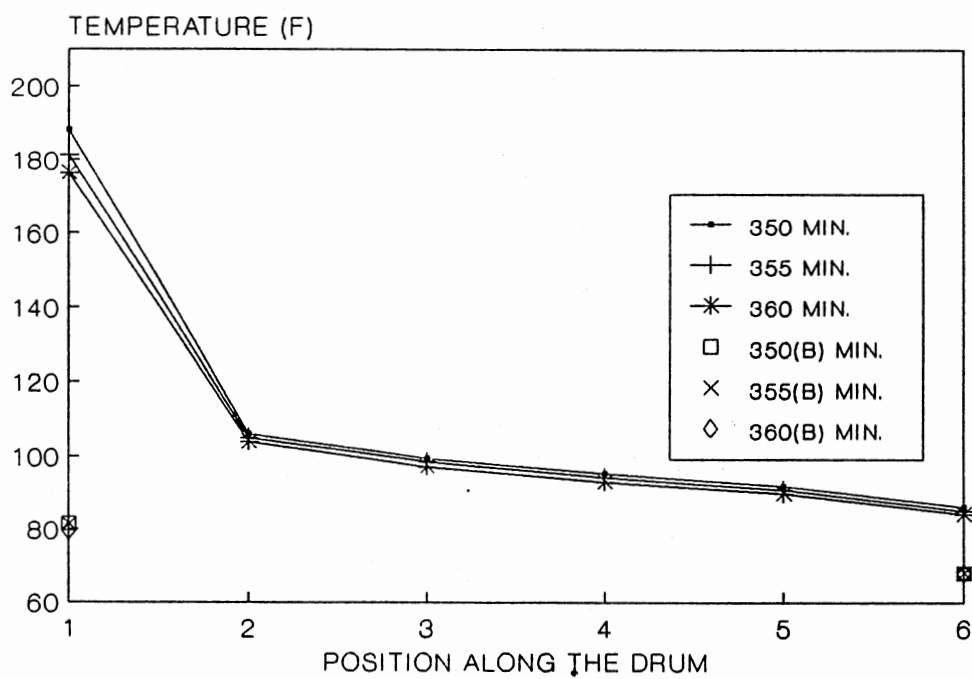


Figure 77. Experimental Temperature Profiles for Run #1

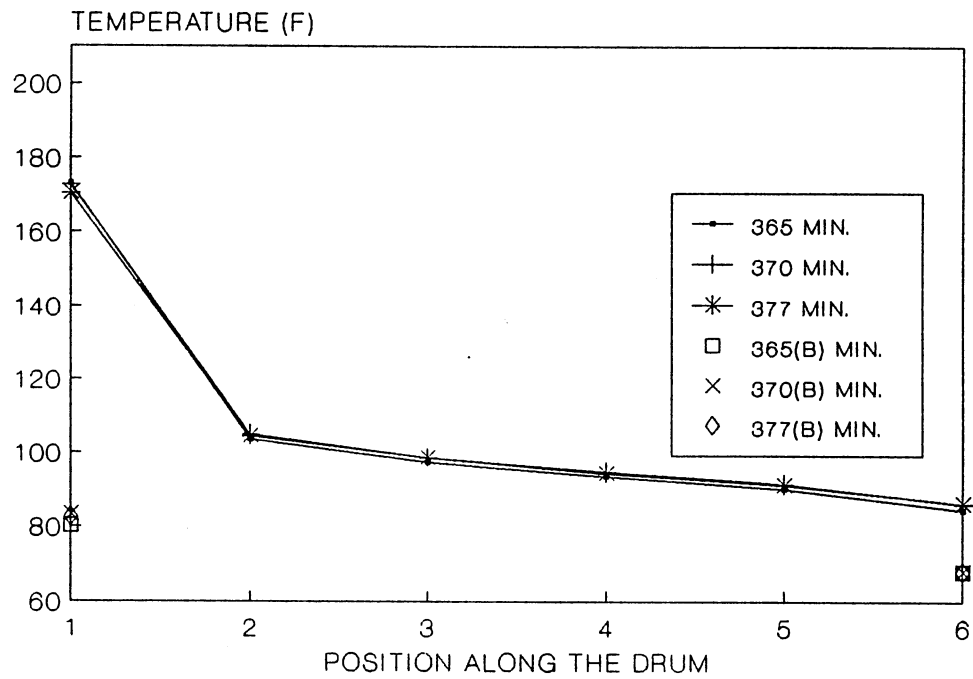


Figure 78. Experimental Temperature Profiles for Run #1

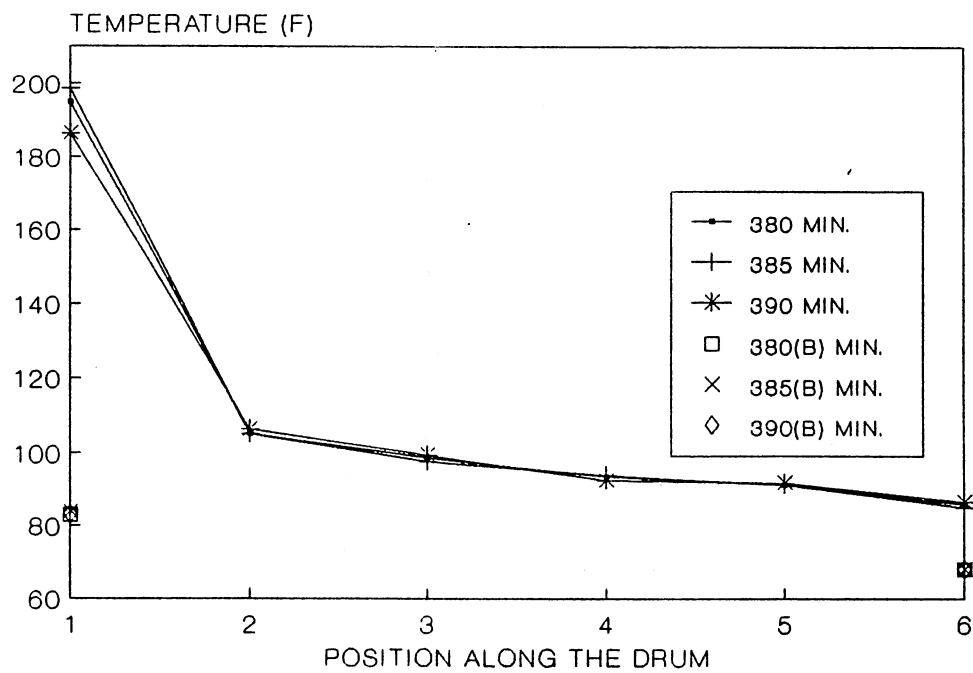


Figure 79. Experimental Temperature Profiles for Run #1

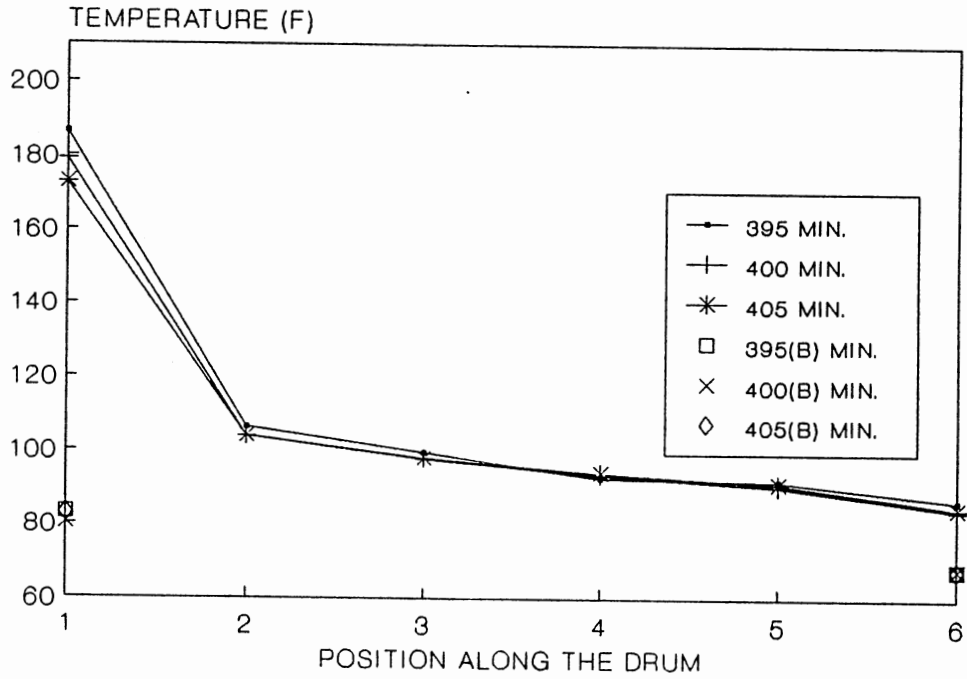


Figure 80. Experimental Temperature Profiles for Run #1

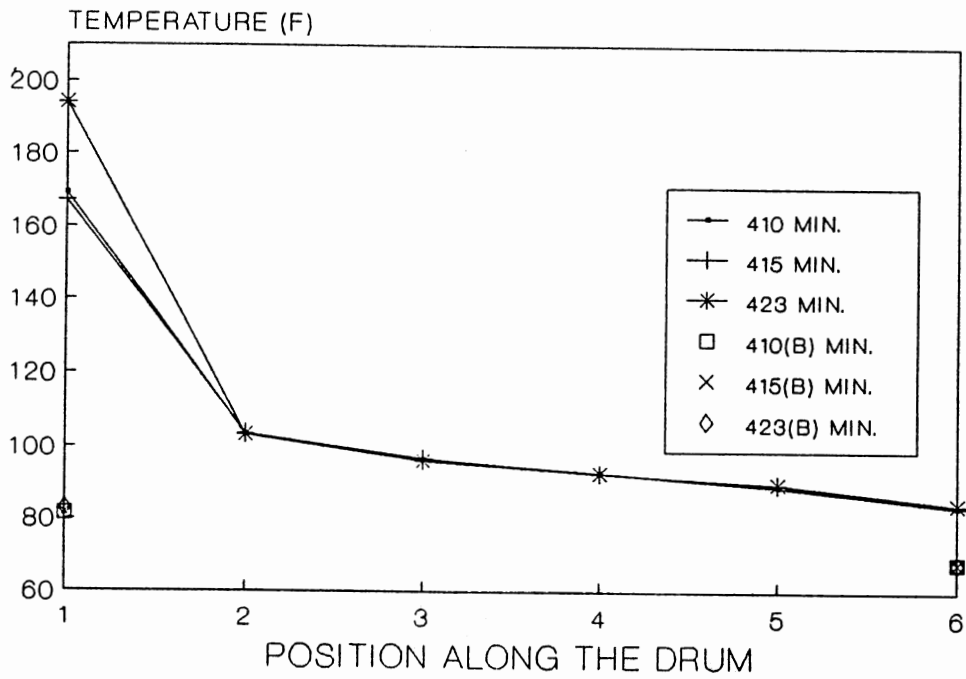


Figure 81. Experimental Temperature Profiles for Run #1

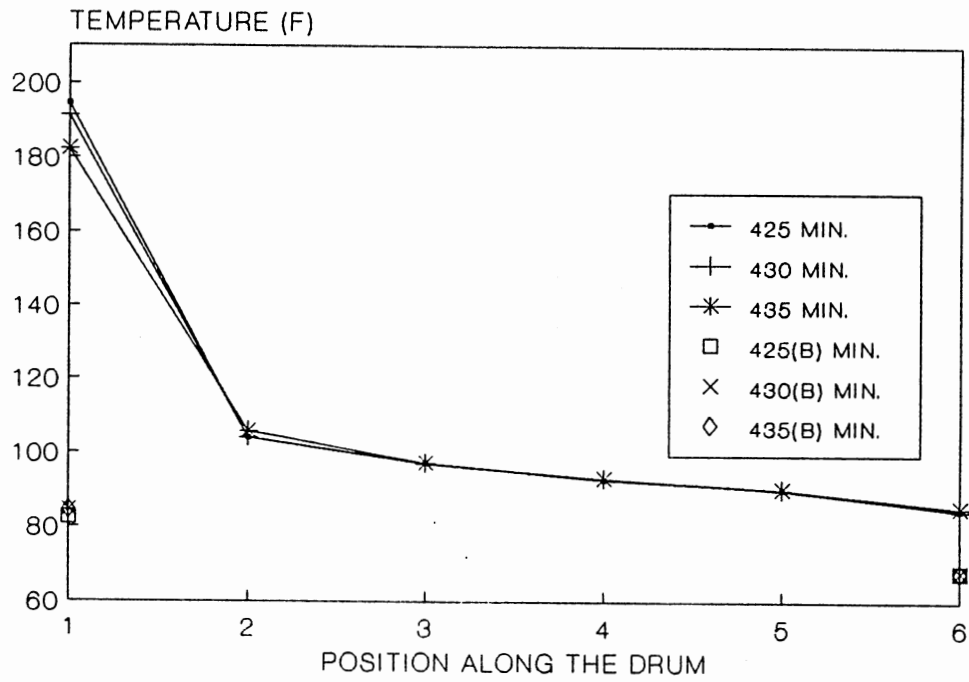


Figure 82. Experimental Temperature Profiles for Run #1

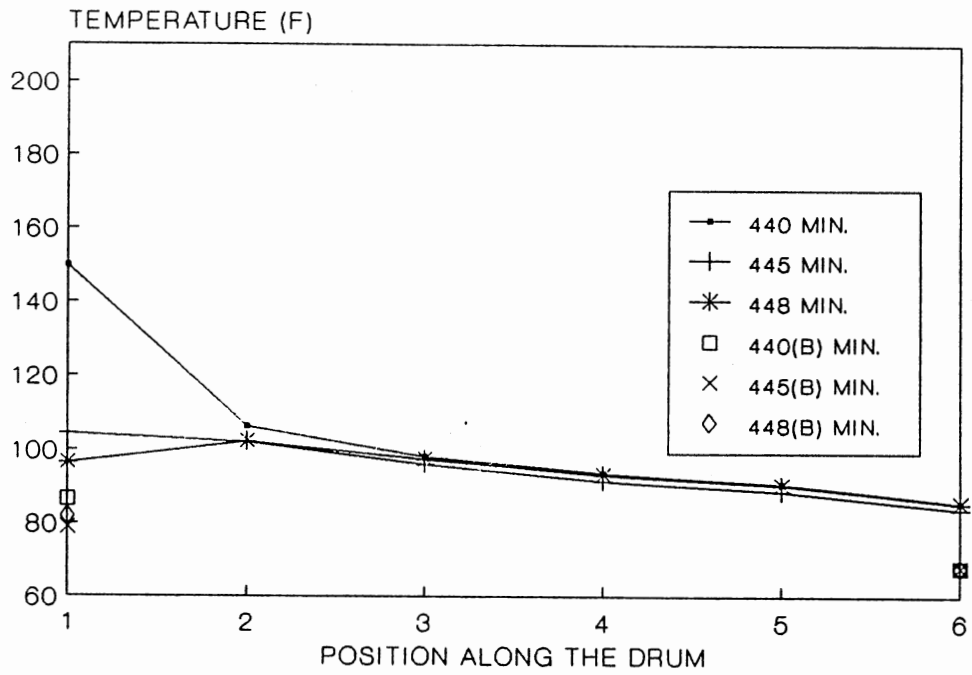


Figure 83. Experimental Temperature Profiles for Run #1

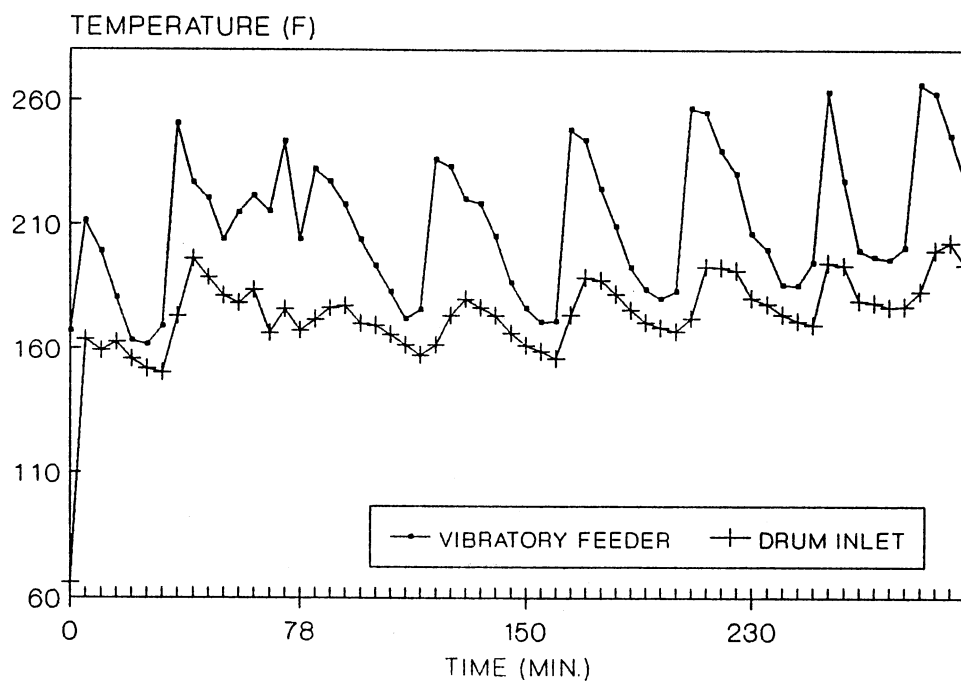


Figure 84. Experimental Temperature Profiles for Run #1

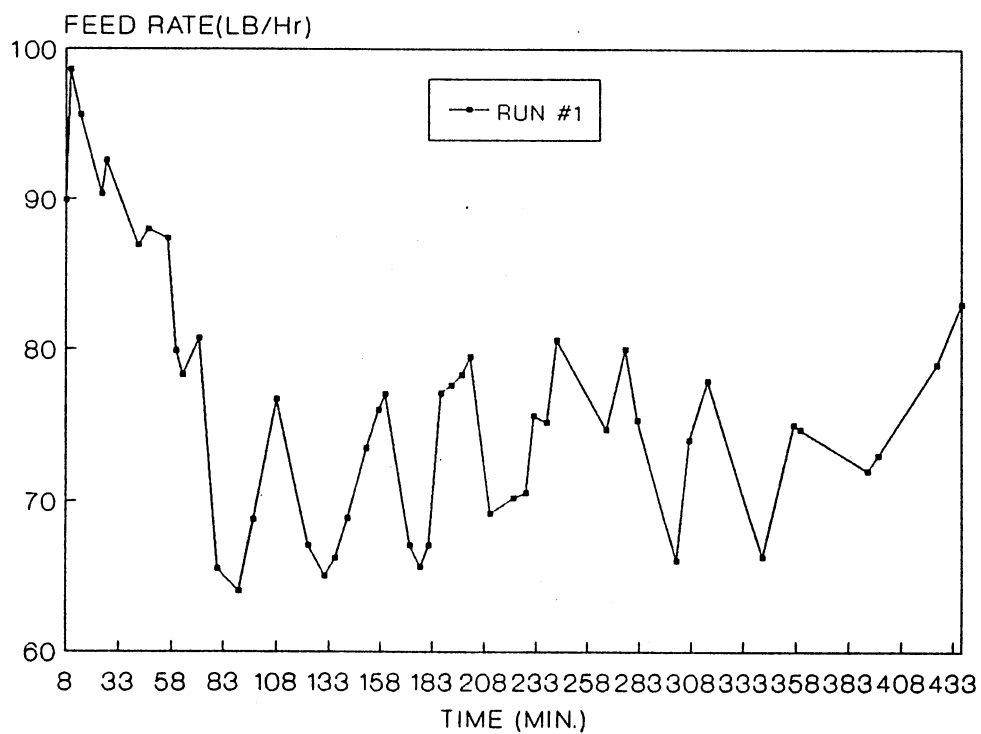


Figure 85. Feed Rates of Prop for Run #1

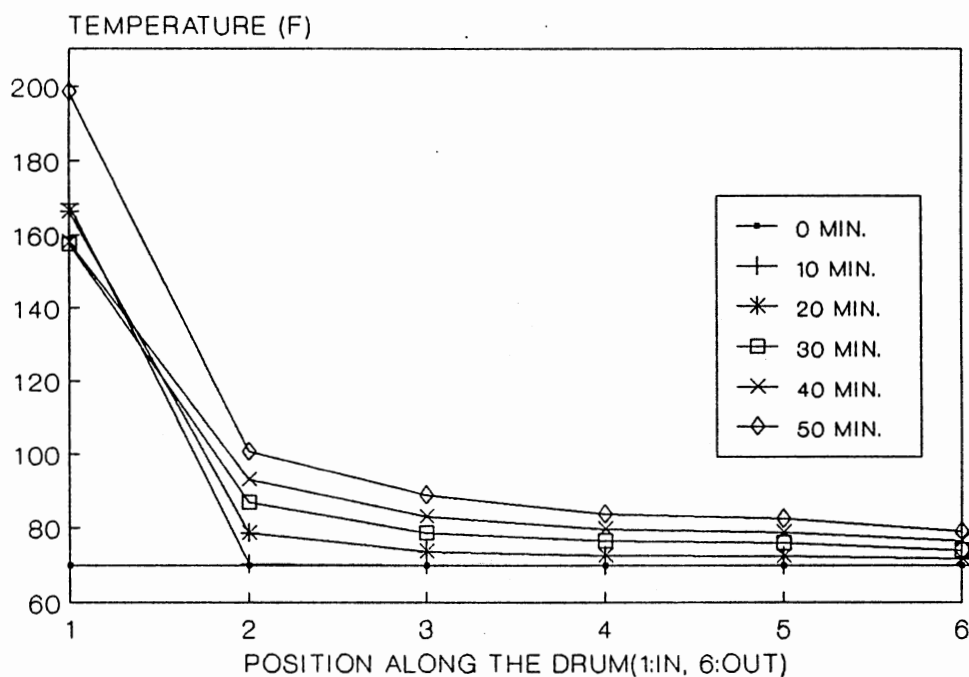


Figure 86. Experimental Temperature Profiles for Run #3

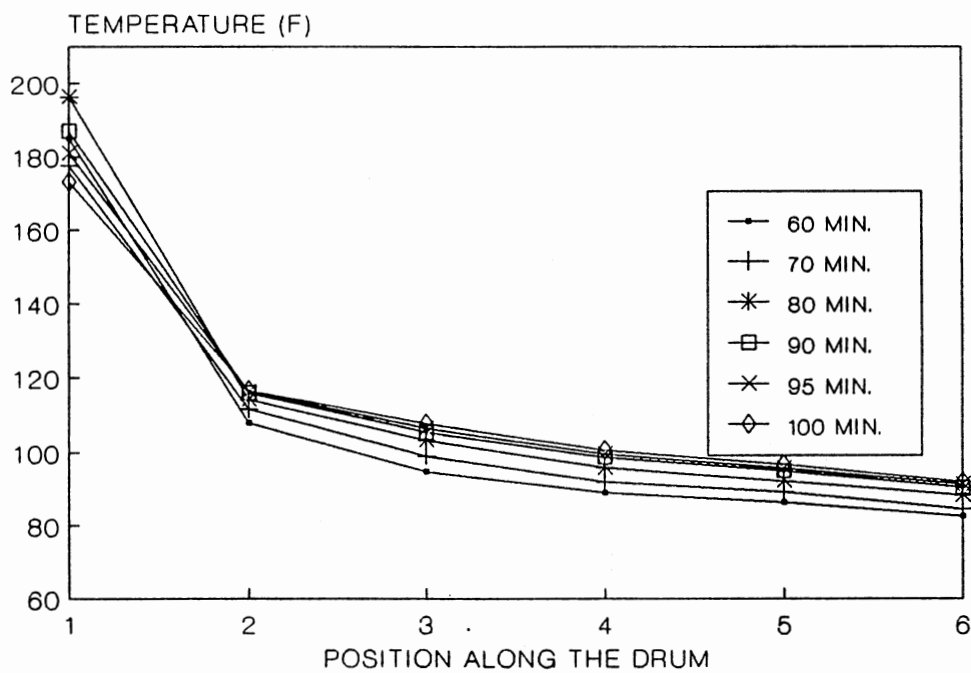


Figure 87. Experimental Temperature Profiles for Run #3

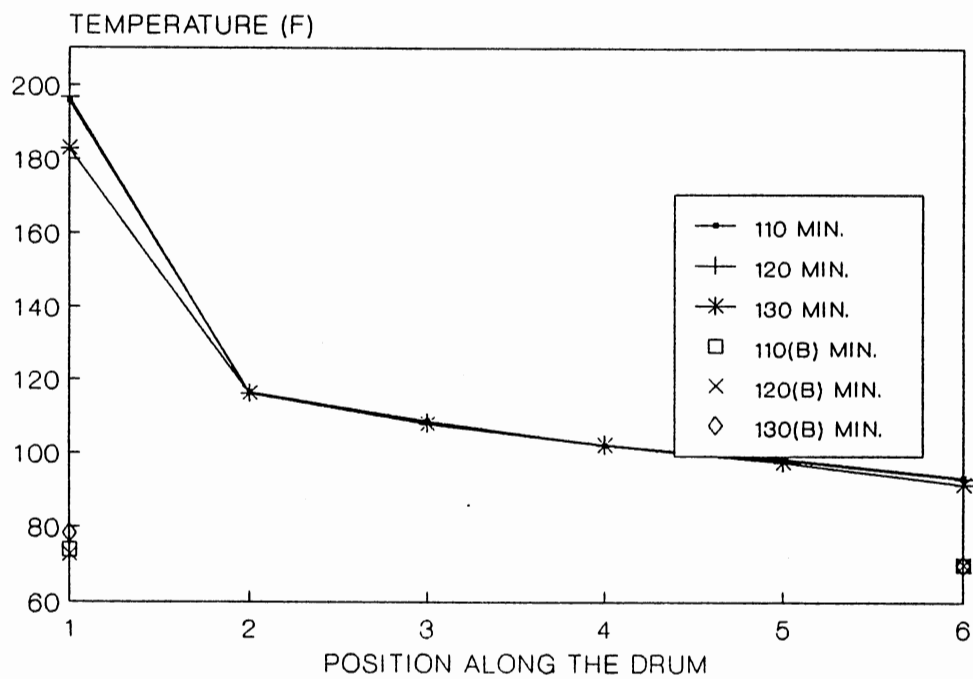


Figure 88. Experimental Temperature Profiles for Run #3

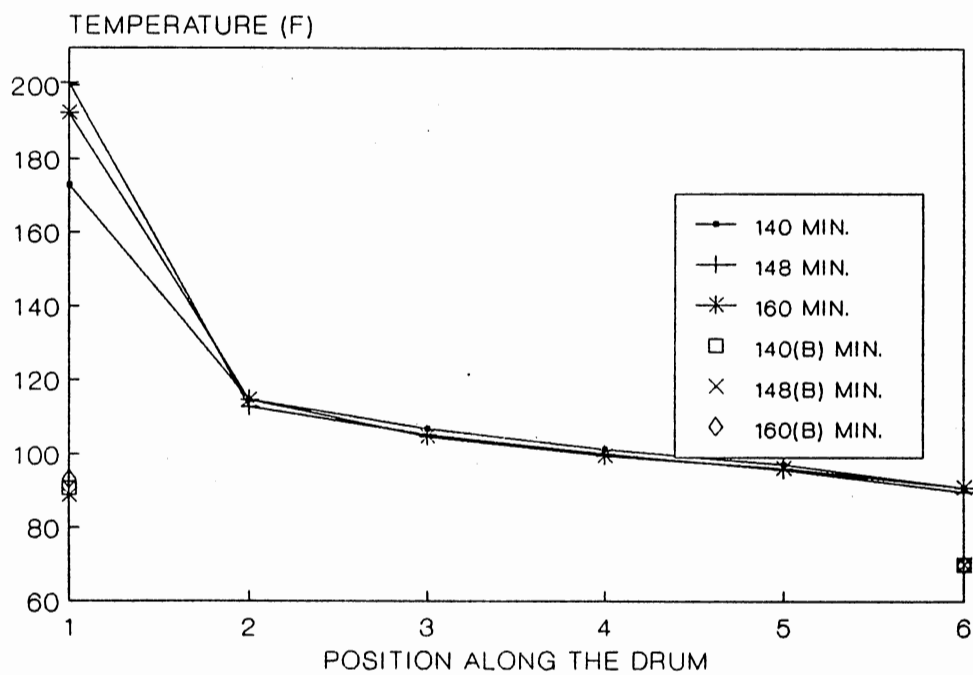


Figure 89. Experimental Temperature Profiles for Run #3



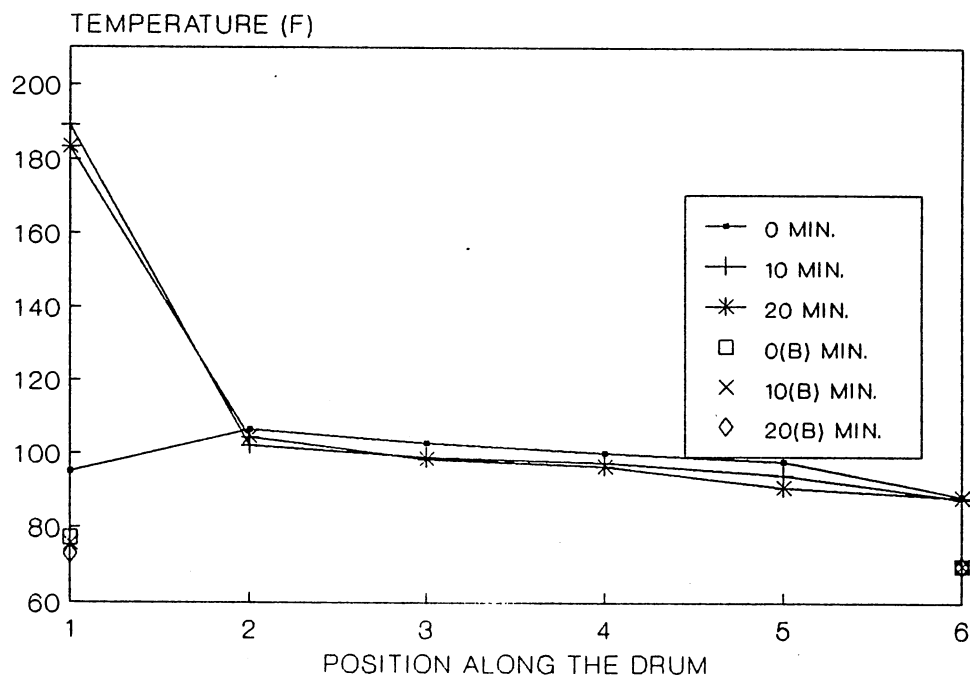


Figure 90. Experimental Temperature Profiles for Run #3

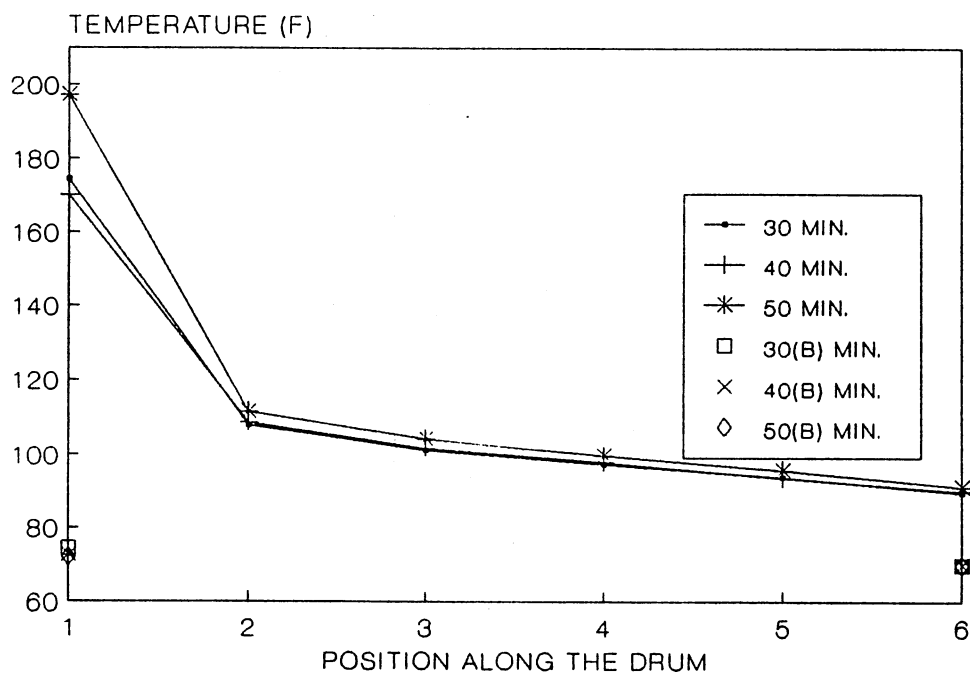


Figure 91. Experimental Temperature Profiles for Run #3

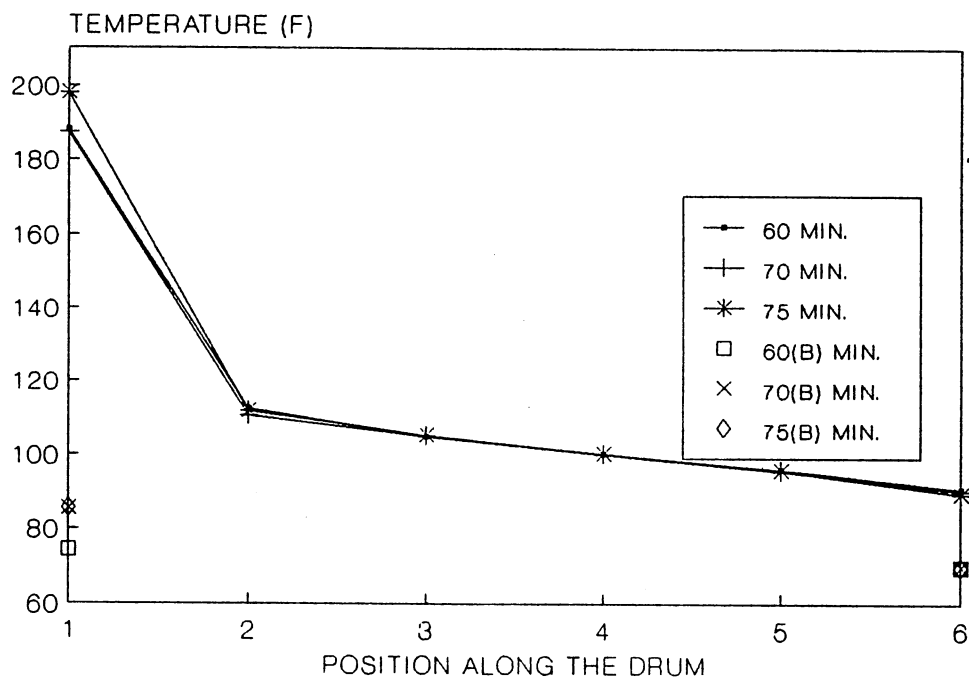


Figure 92. Experimental Temperature Profiles for Run #3

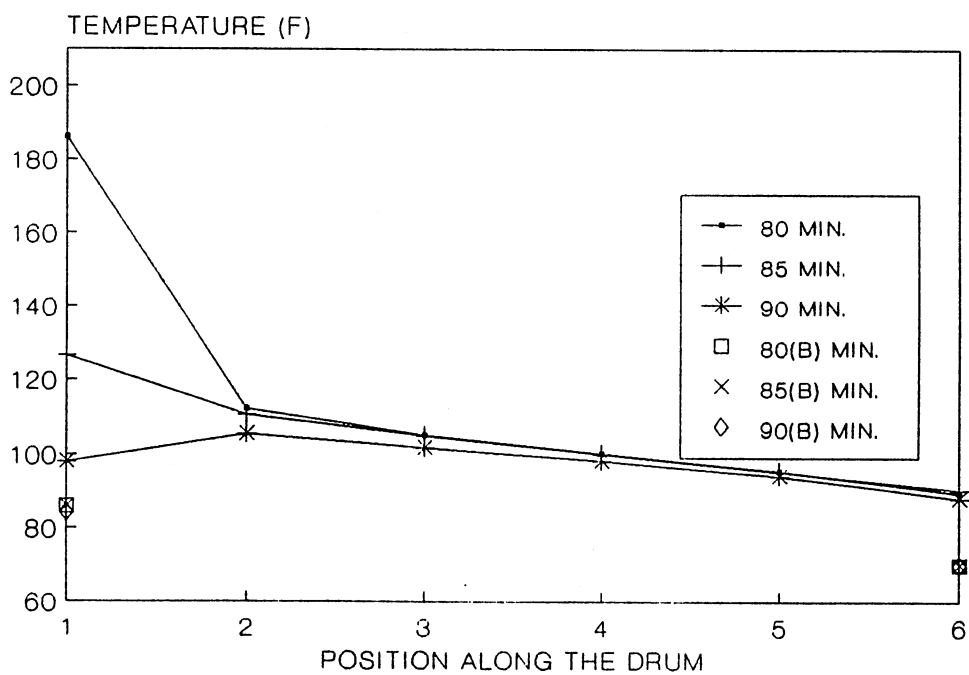


Figure 93. Experimental Temperature Profiles for Run #3

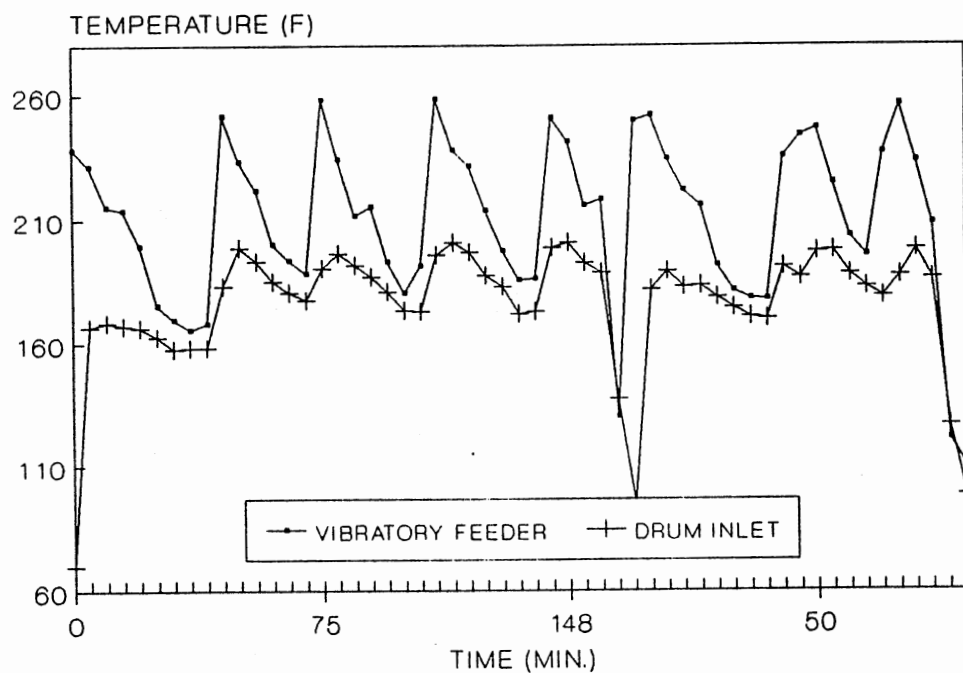


Figure 94. Experimental Temperature Profiles for Run #3

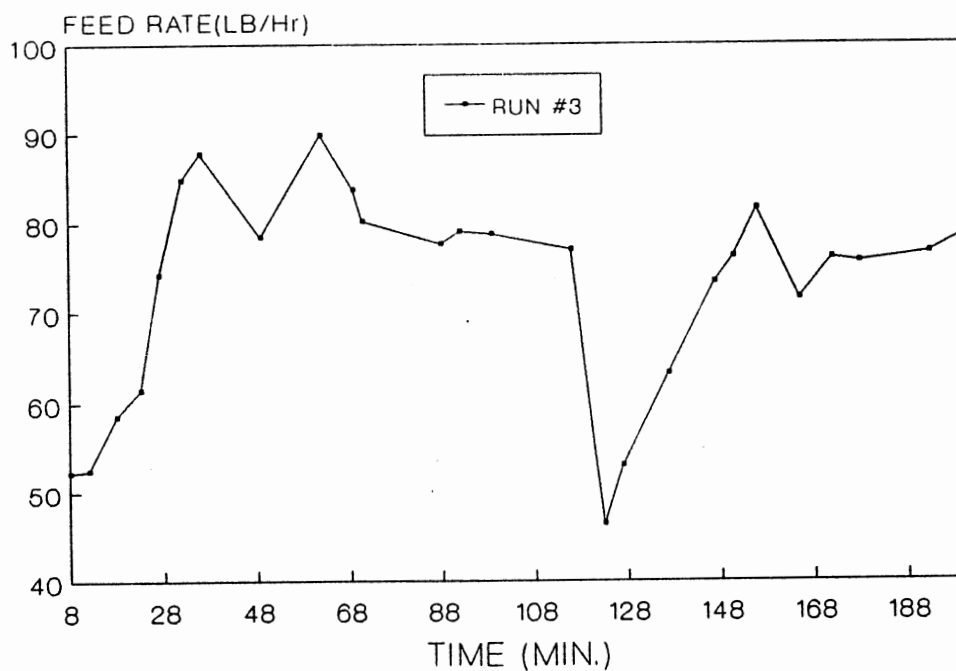


Figure 95. Feed Rates of Prop for Run #3

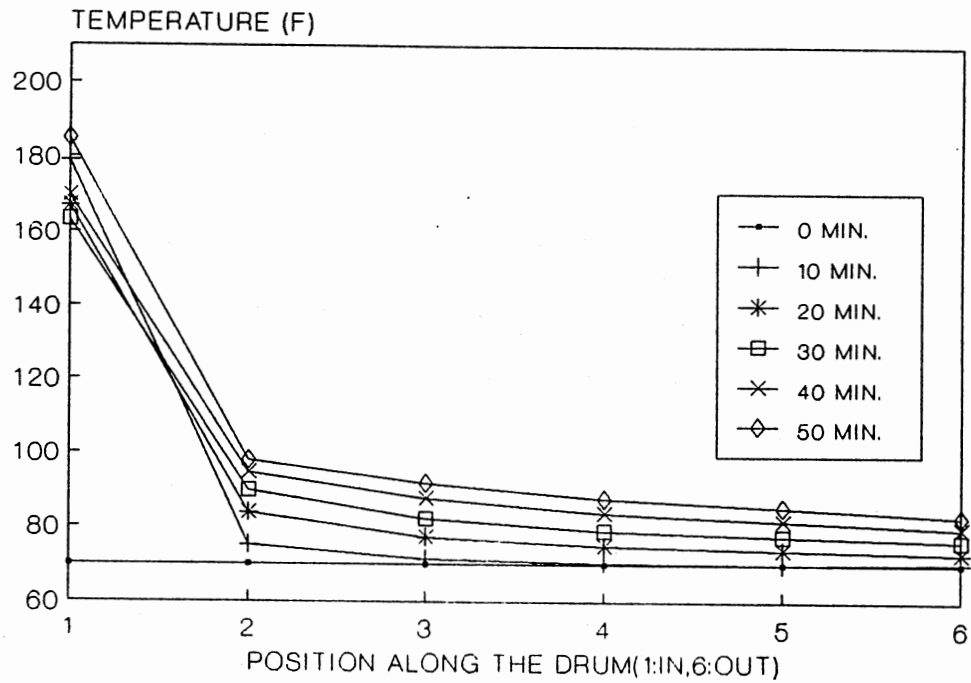


Figure 96. Experimental Temperature Profiles for Run #4

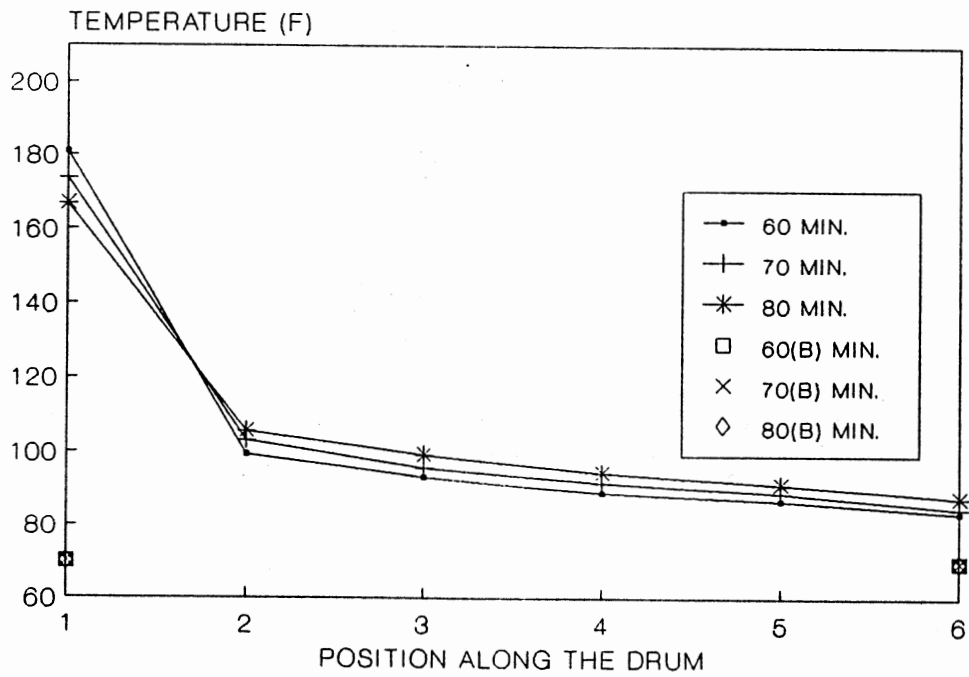


Figure 97. Experimental Temperature Profiles for Run #4

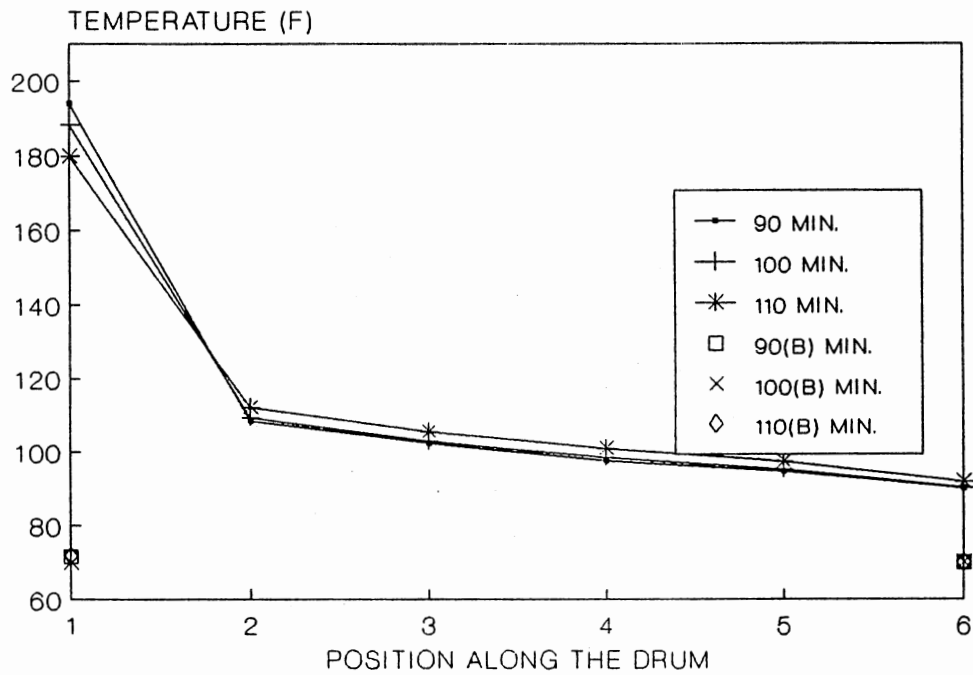


Figure 98. Experimental Temperature Profiles for Run #4

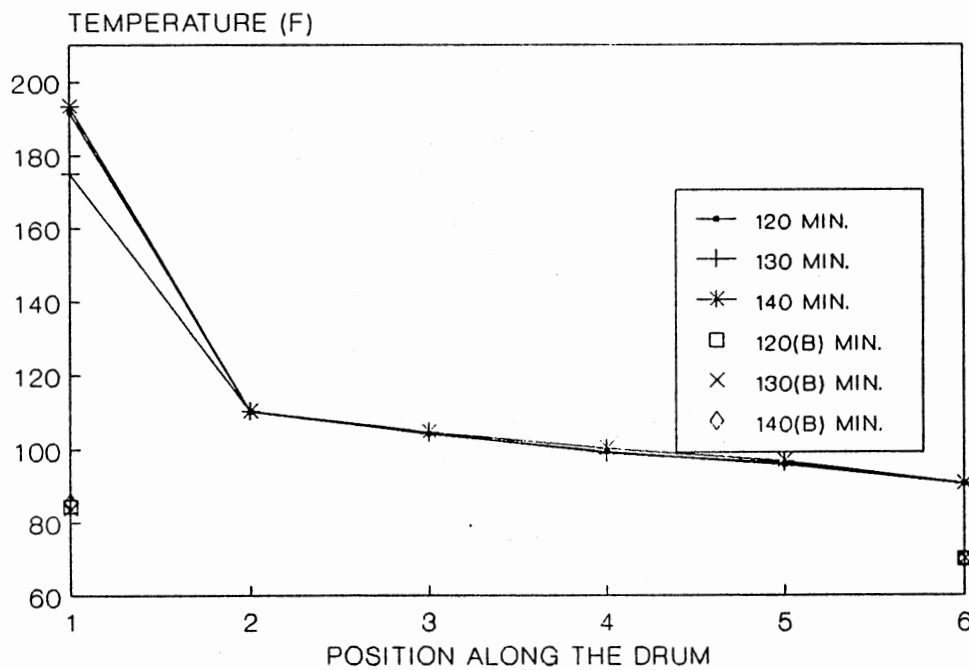


Figure 99. Experimental Temperature Profiles for Run #4

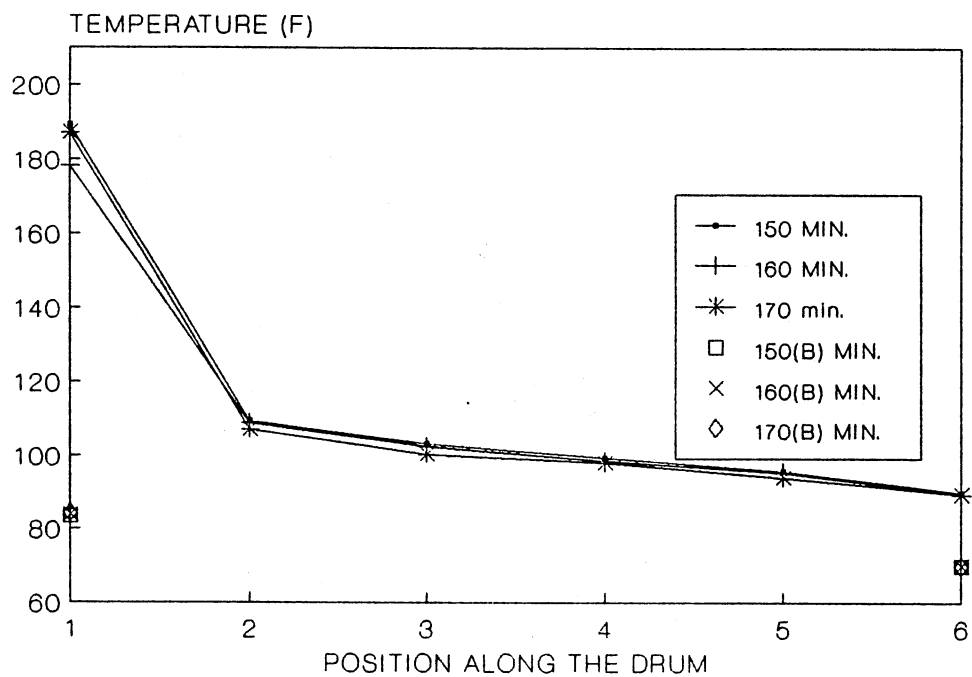


Figure 100. Experimental Temperature Profiles for Run #4

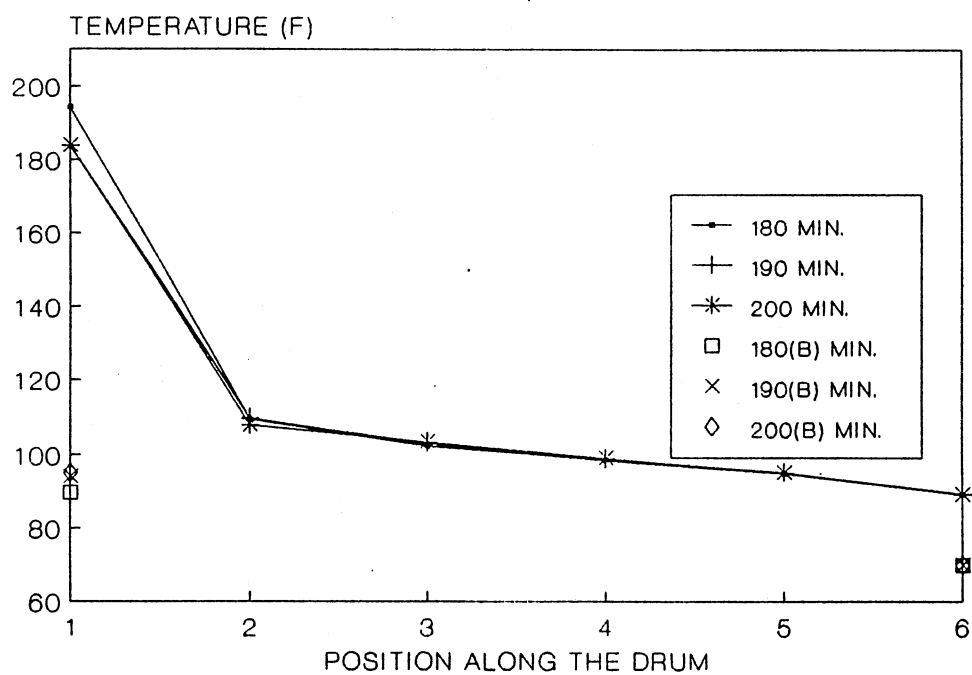


Figure 101. Experimental Temperature Profiles for Run #4

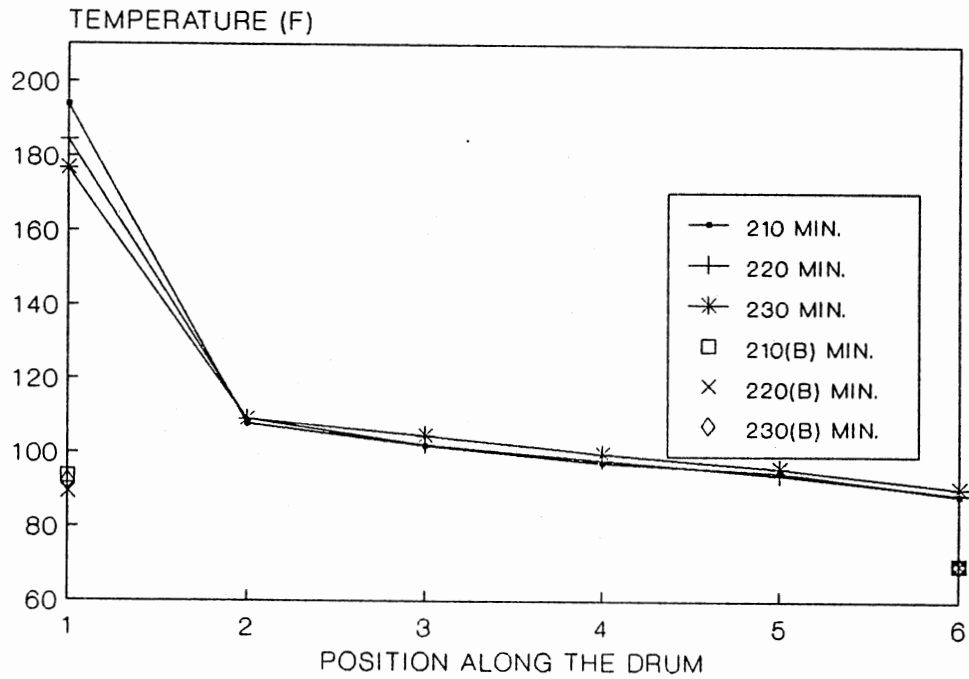


Figure 102. Experimental Temperature Profiles for Run #4

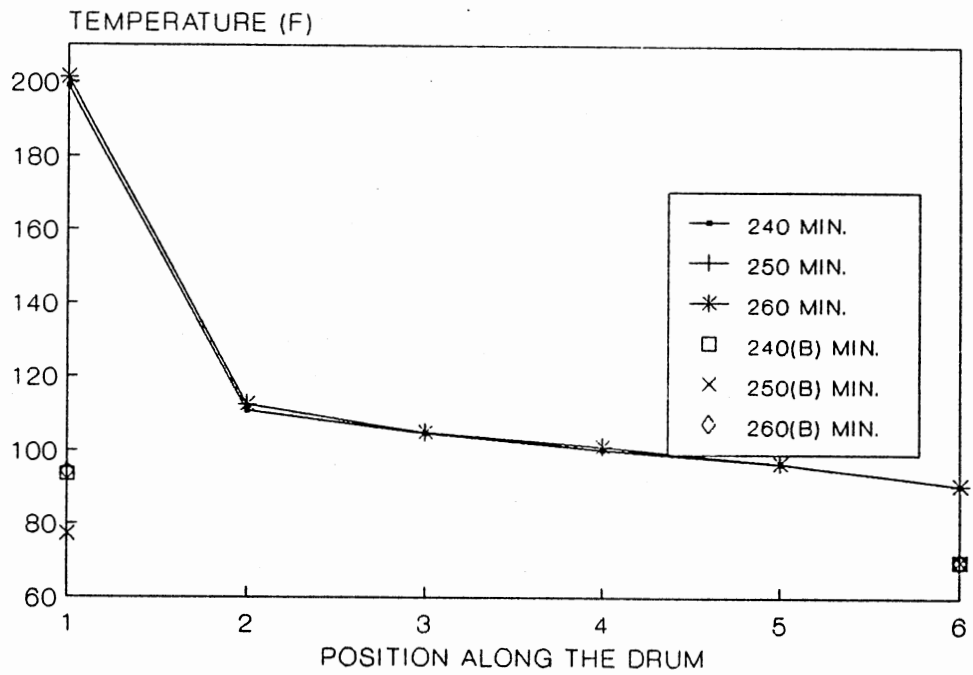


Figure 103. Experimental Temperature Profiles for Run #4

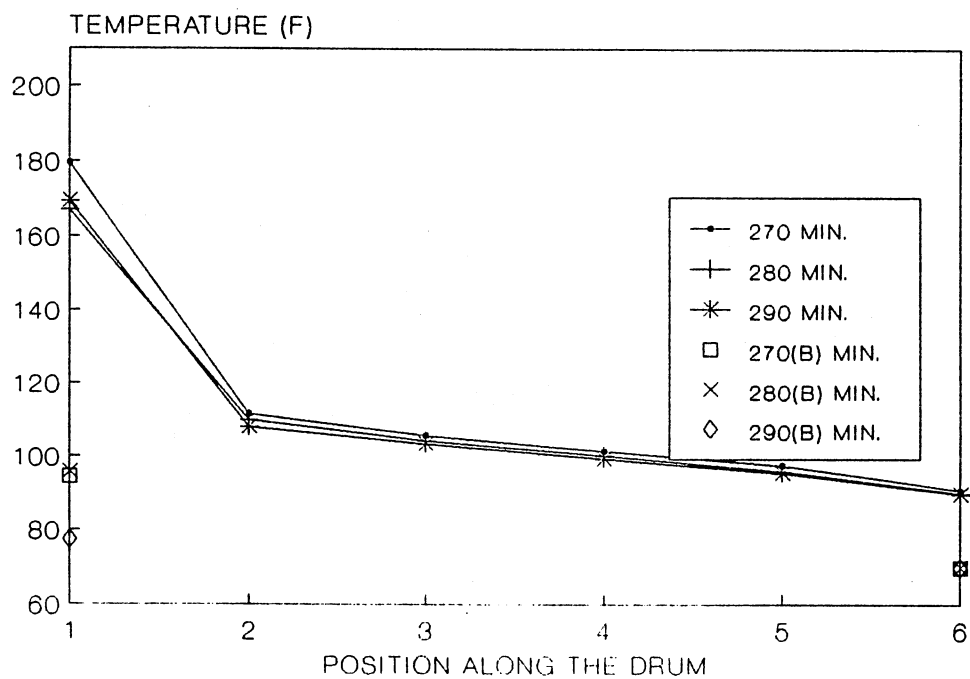


Figure 104. Experimental Temperature Profiles for Run #4

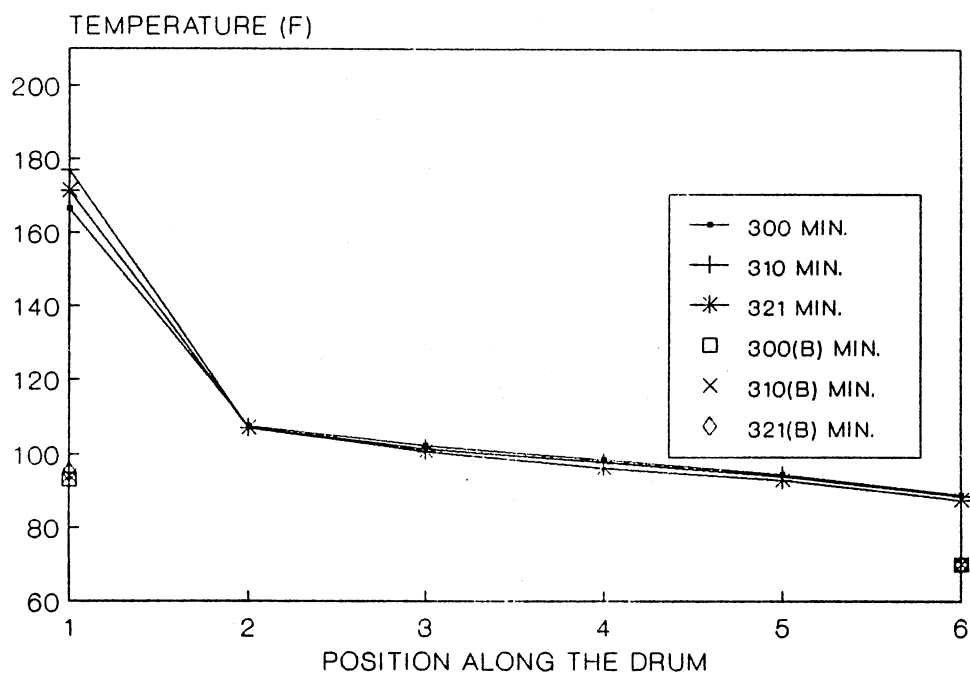


Figure 105. Experimental Temperature Profiles for Run #4



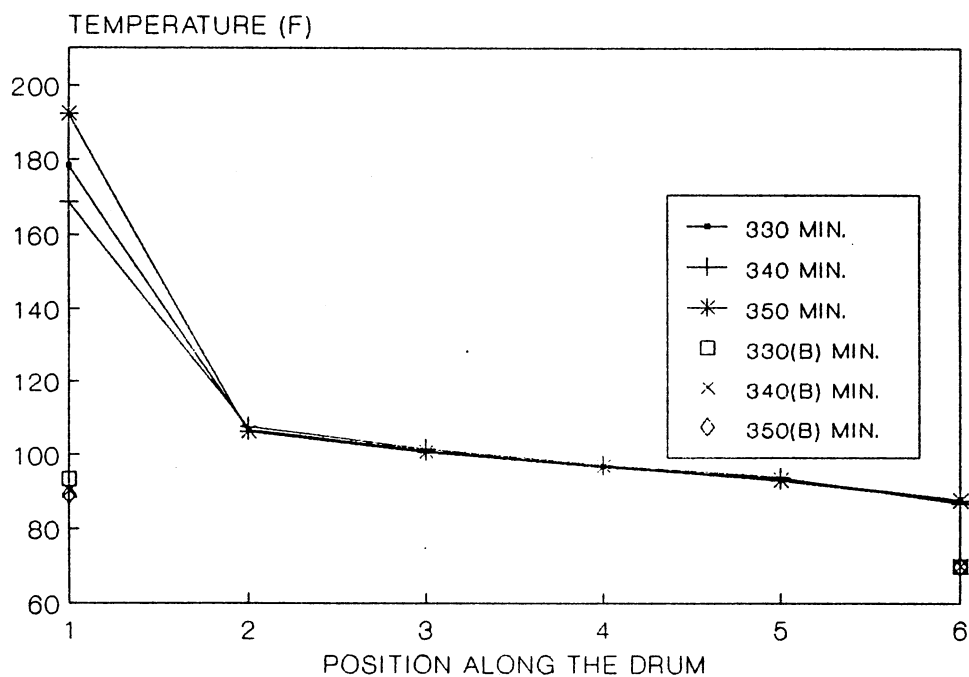


Figure 106. Experimental Temperature Profiles for Run #4

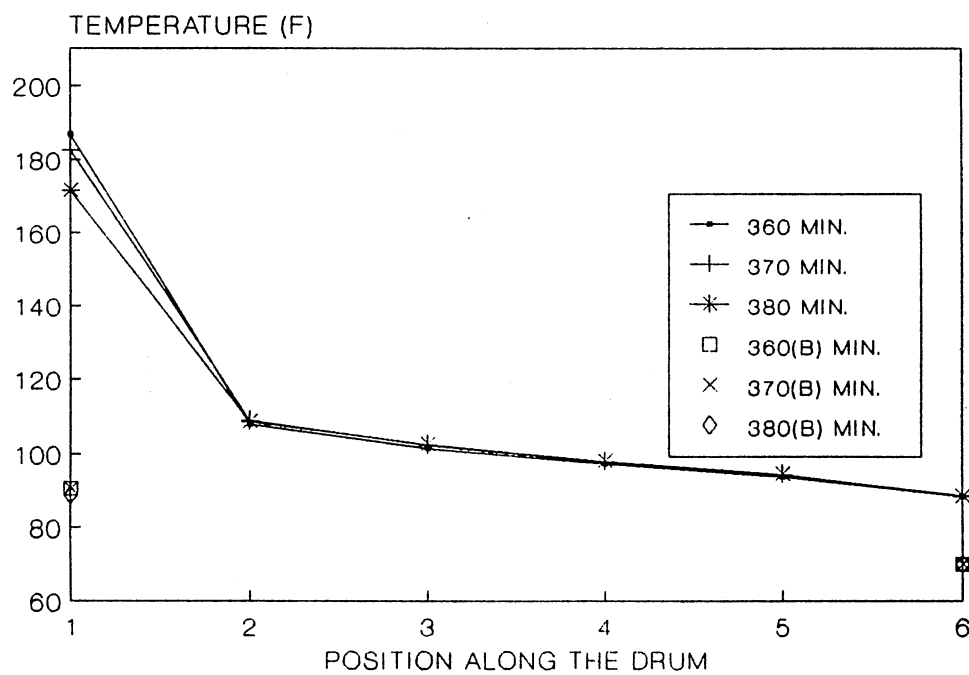


Figure 107. Experimental Temperature Profiles for Run #4

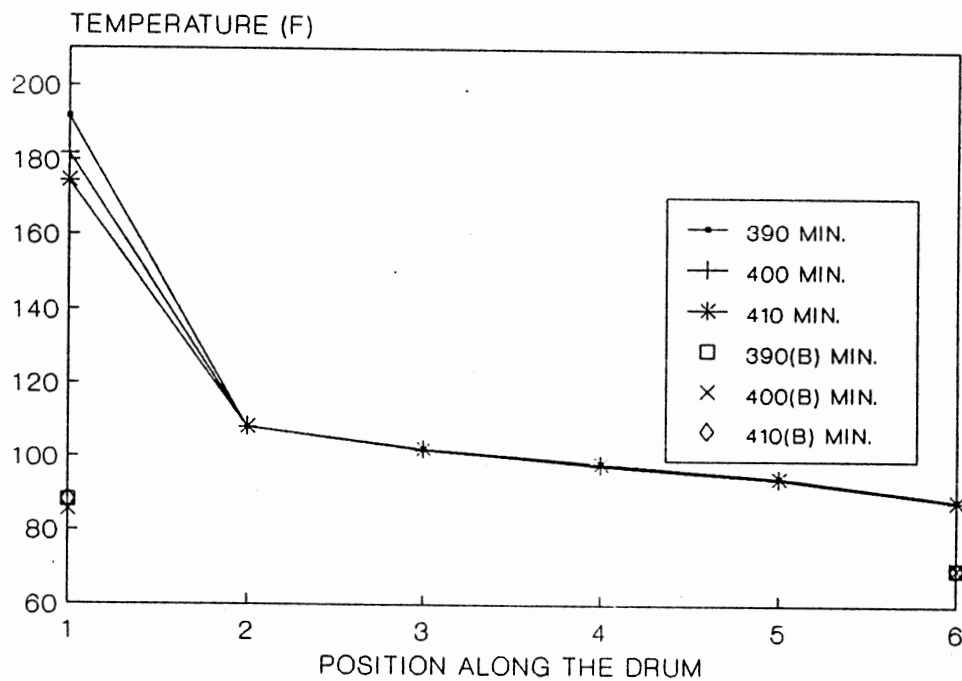


Figure 108. Experimental Temperature Profiles for Run #4

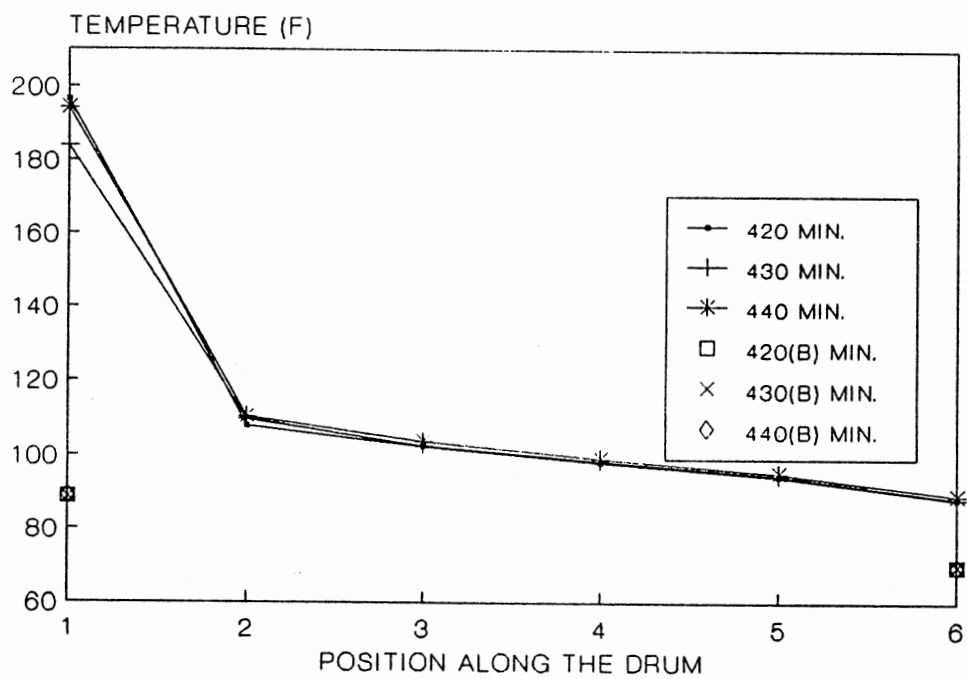


Figure 109. Experimental Temperature Profiles for Run #4

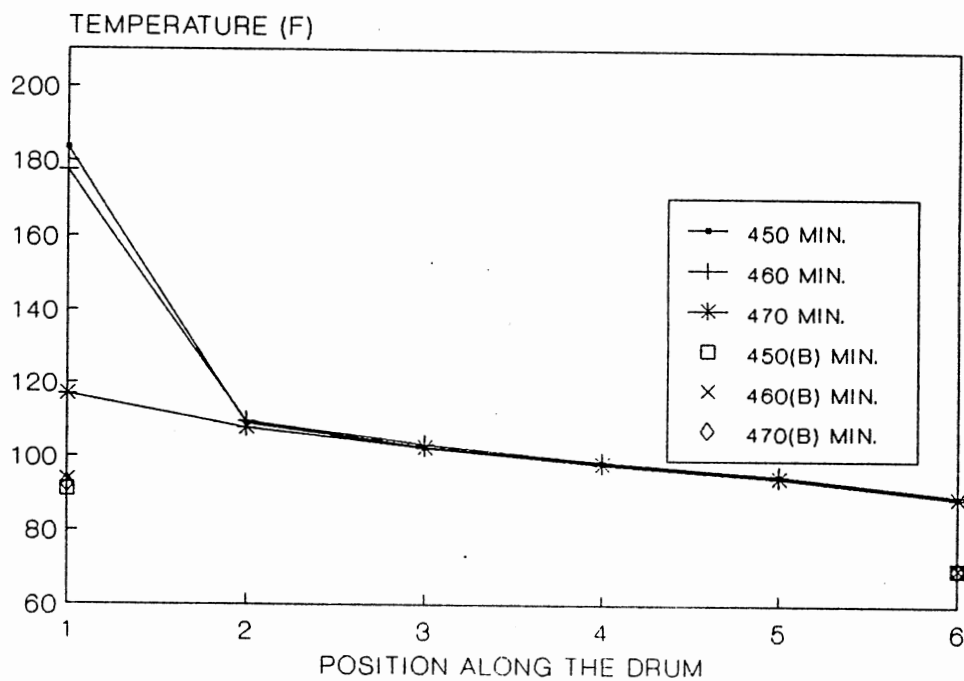


Figure 110. Experimental Temperature Profiles for Run #4

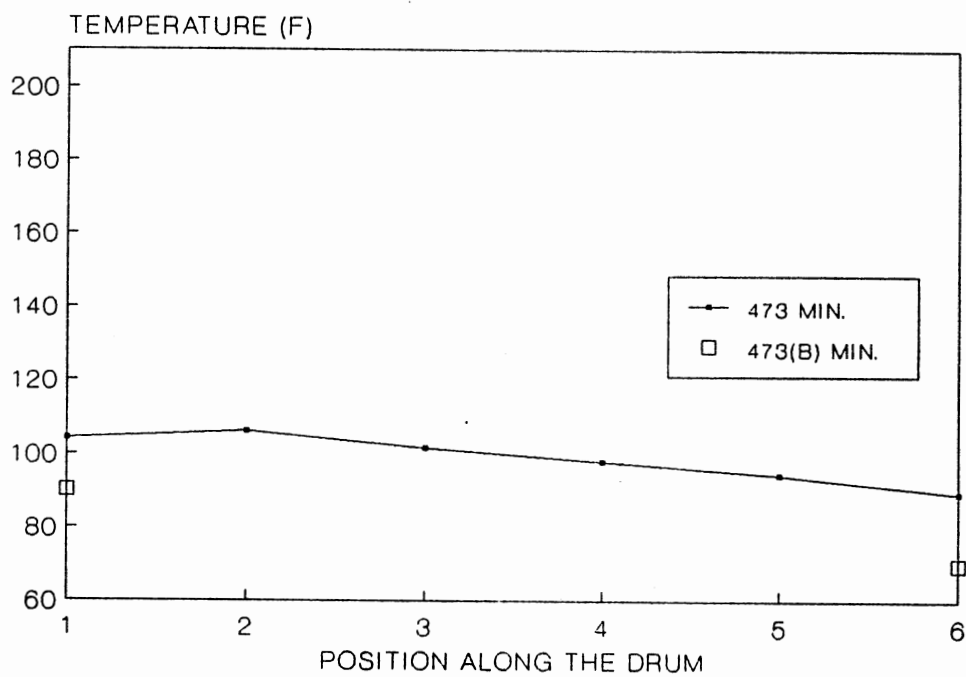


Figure 111. Experimental Temperature Profiles for Run #4

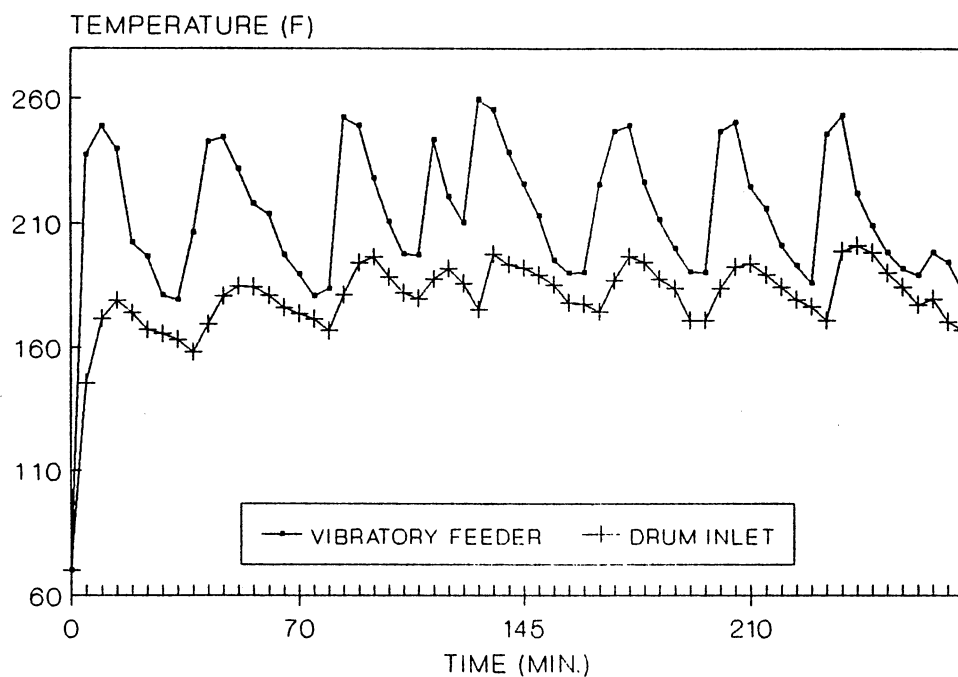


Figure 112. Experimental Temperature Profiles for Run #4

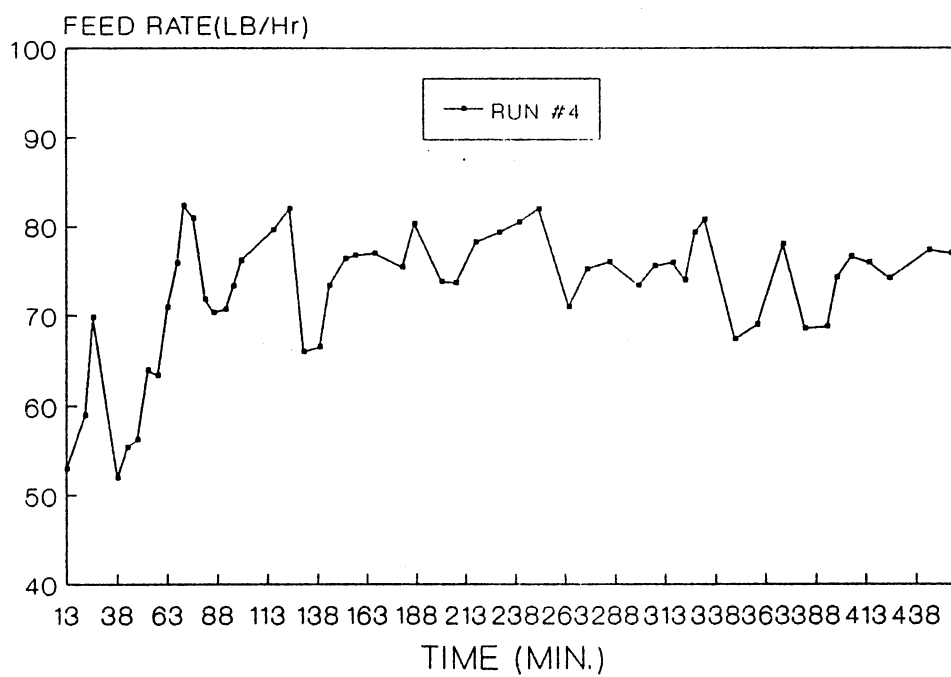


Figure 113. Feed Rates of Prop for Run #4

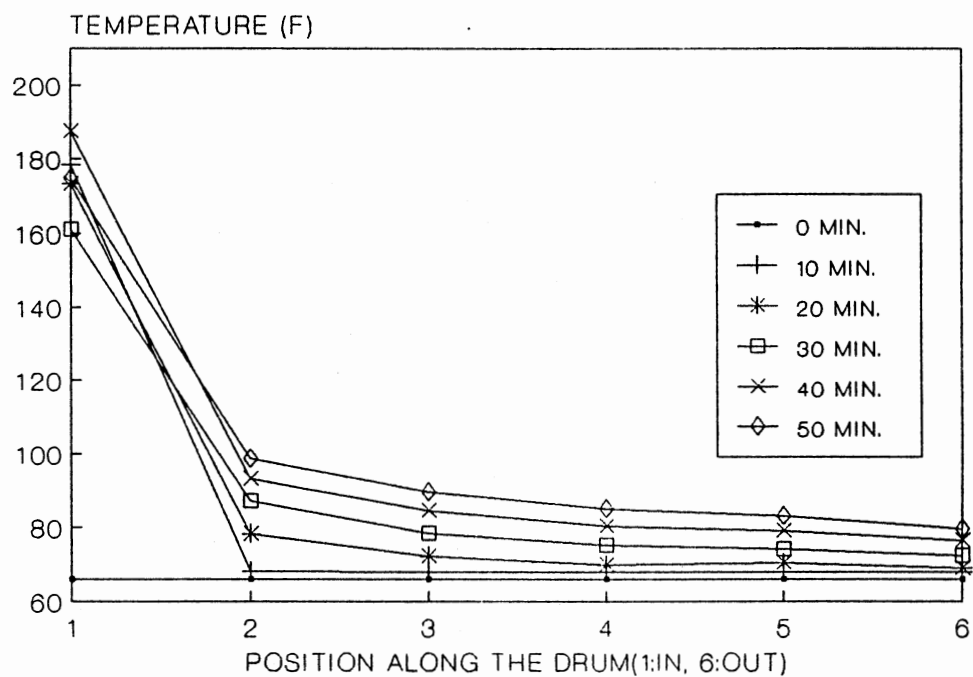


Figure 114. Experimental Temperature Profiles for Run #5

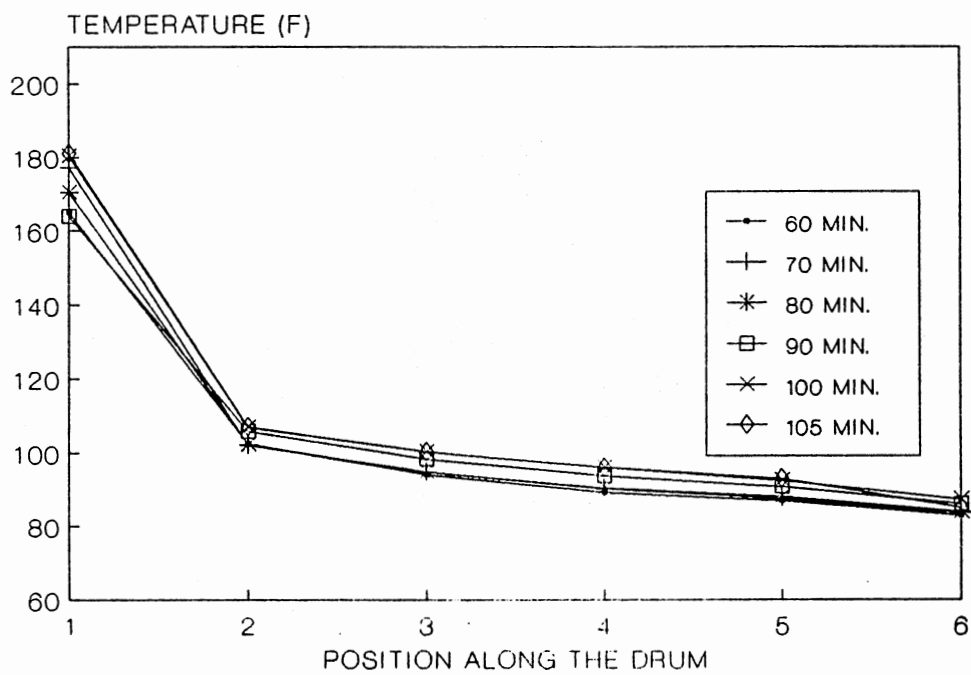


Figure 115. Experimental Temperature Profiles for Run #5

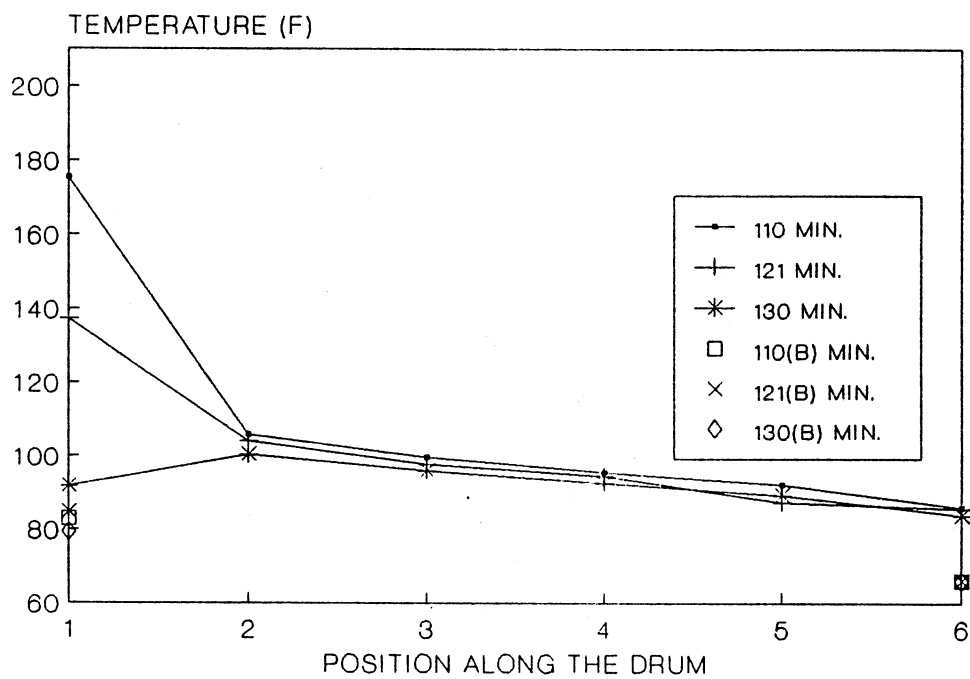


Figure 116. Experimental Temperature Profiles for Run #5

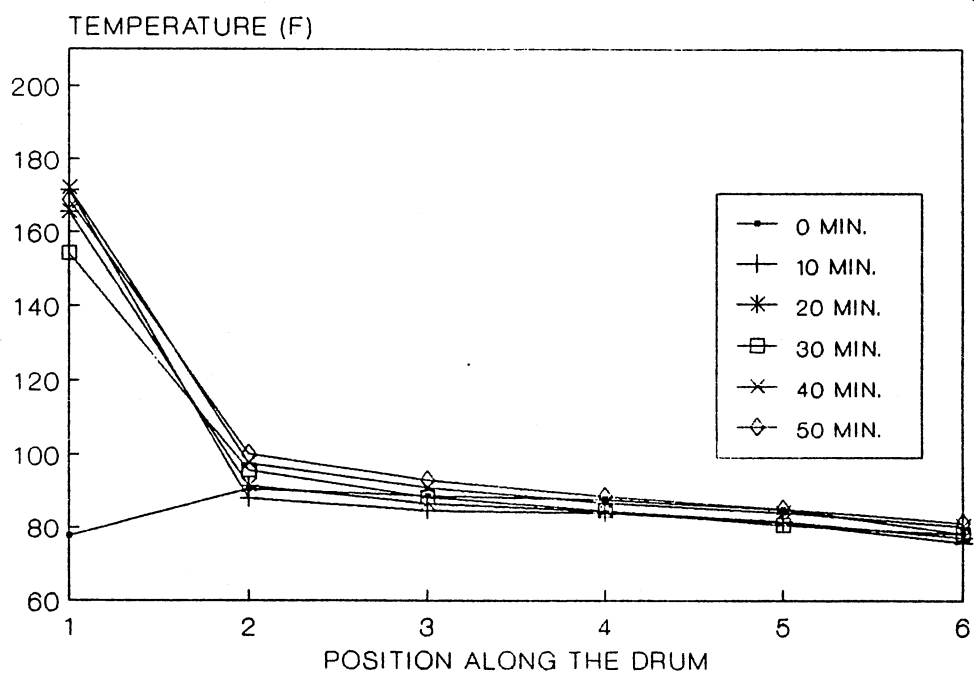


Figure 117. Experimental Temperature Profiles for Run #5

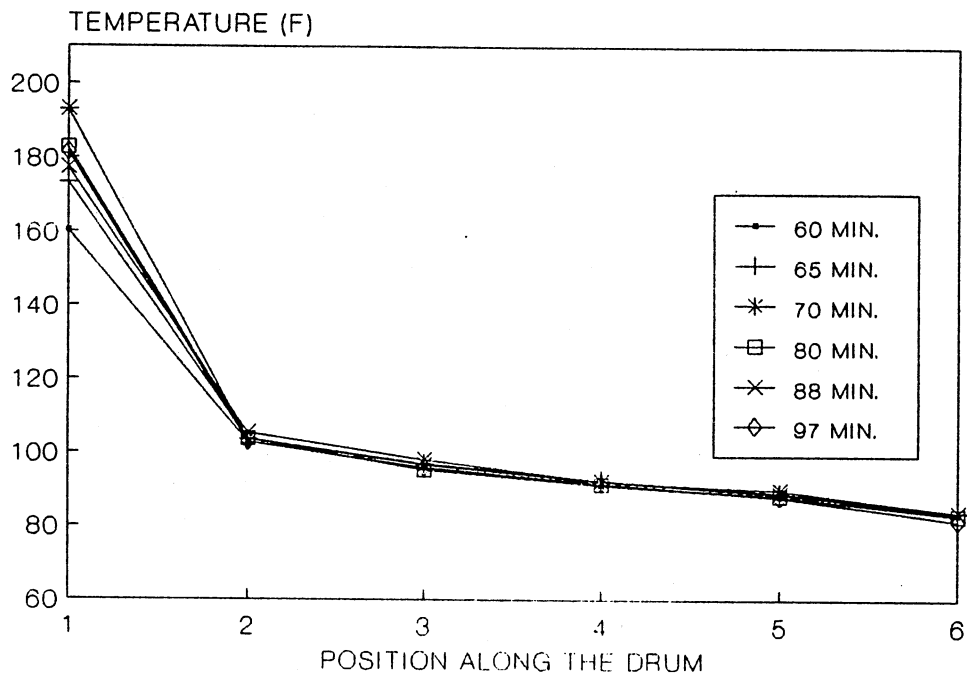


Figure 118. Experimental Temperature Profiles for Run #5

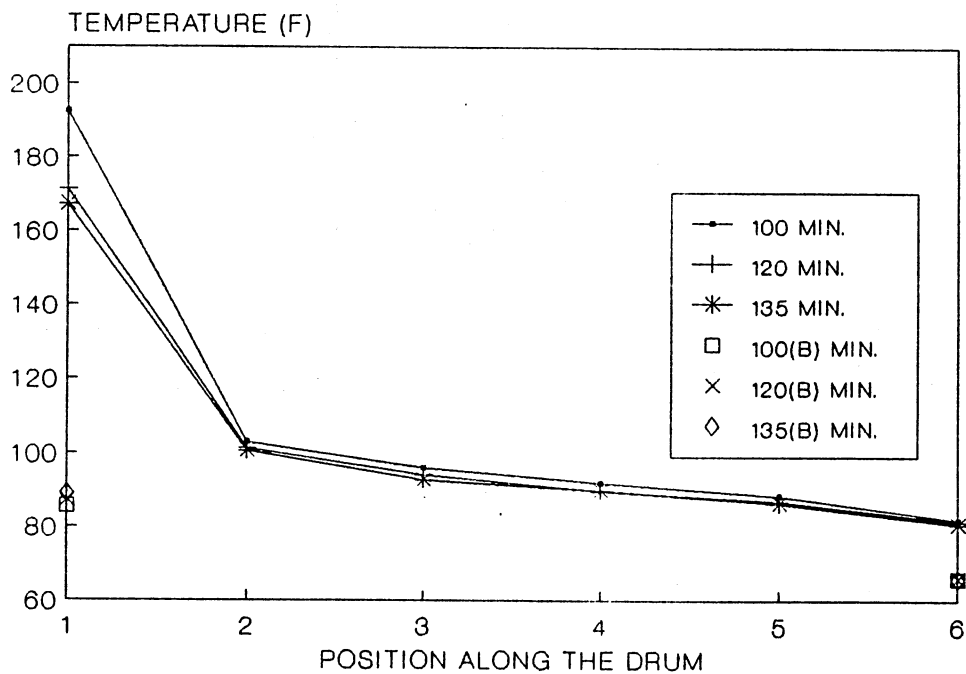


Figure 119. Experimental Temperature Profiles for Run #5

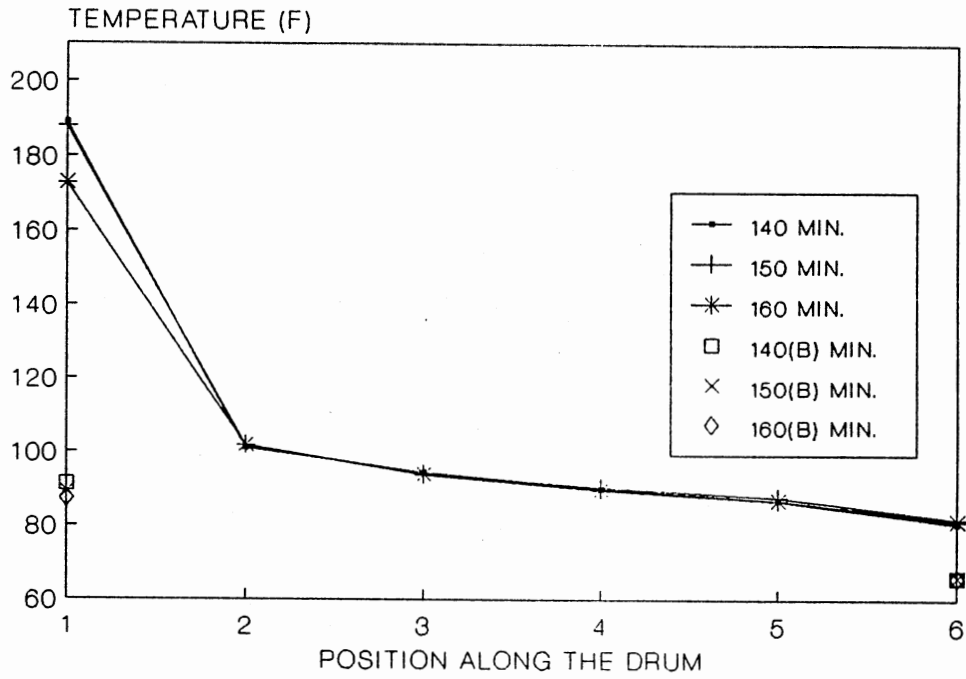


Figure 120. Experimental Temperature Profiles for Run #5

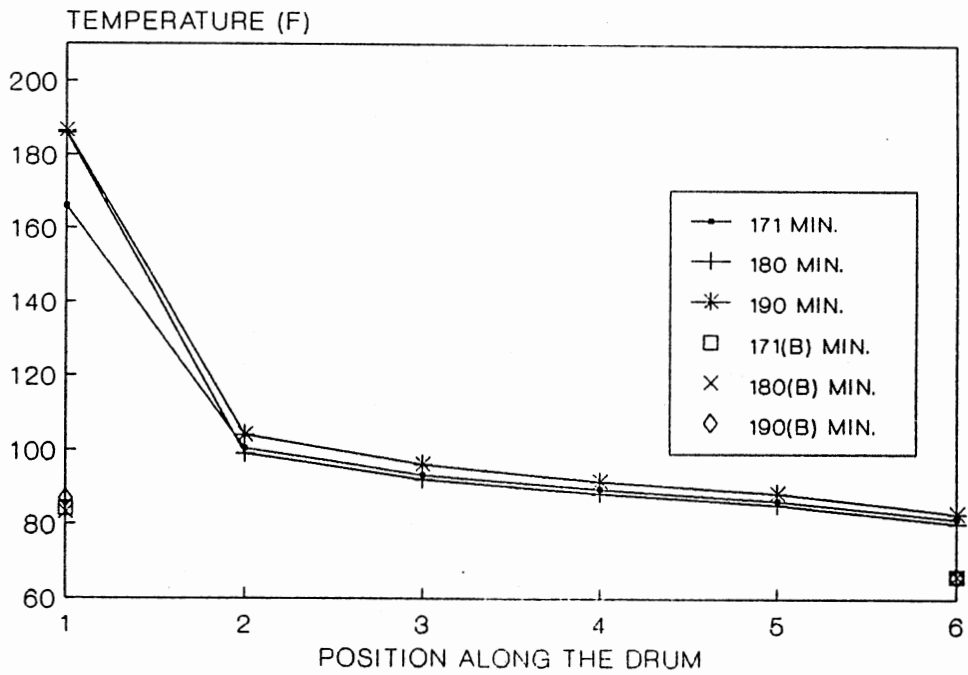


Figure 121. Experimental Temperature Profiles for Run #5



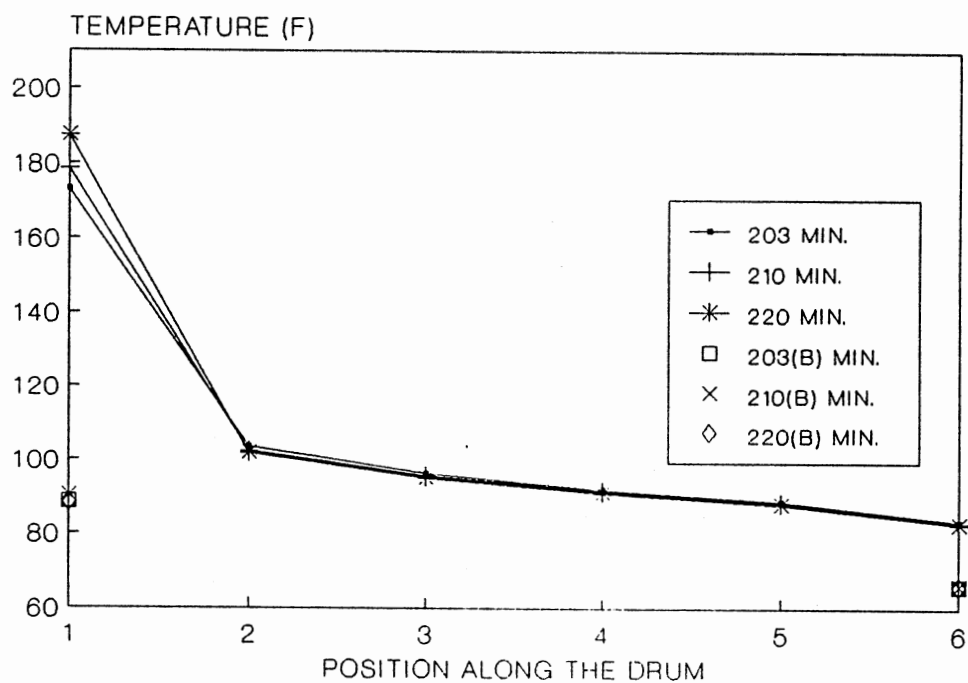


Figure 122. Experimental Temperature Profiles for Run #5

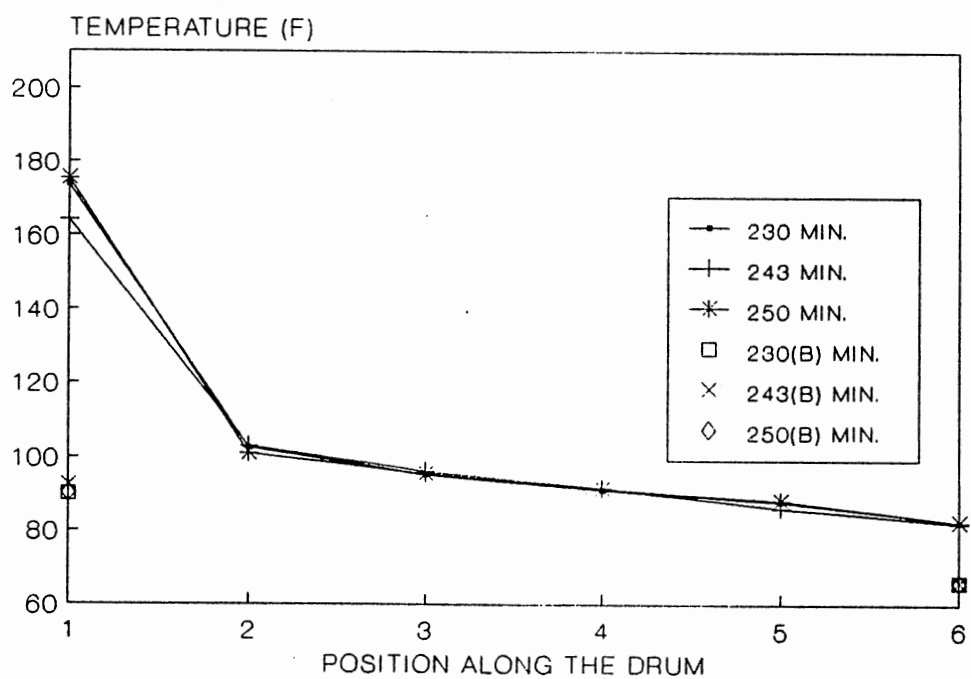


Figure 123. Experimental Temperature Profiles for Run #5

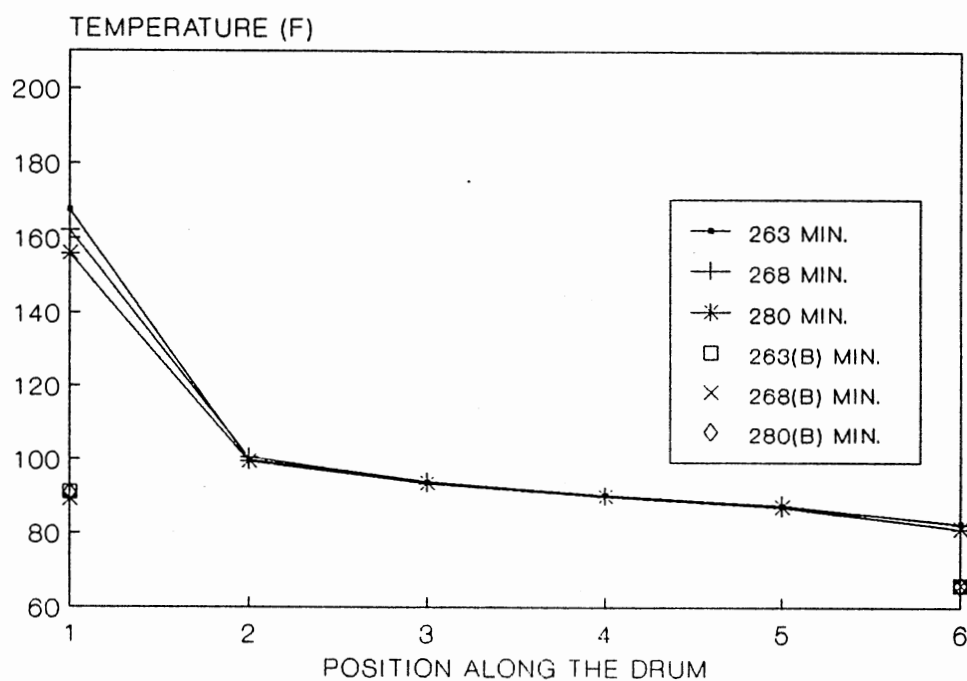


Figure 124. Experimental Temperature Profiles for Run #5

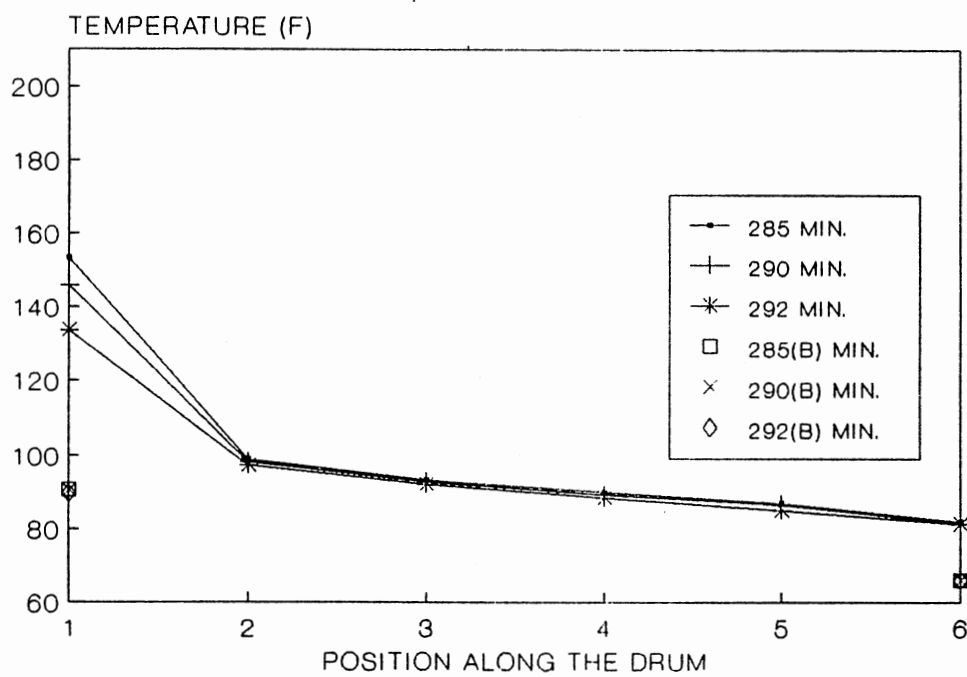


Figure 125. Experimental Temperature Profiles for Run #5

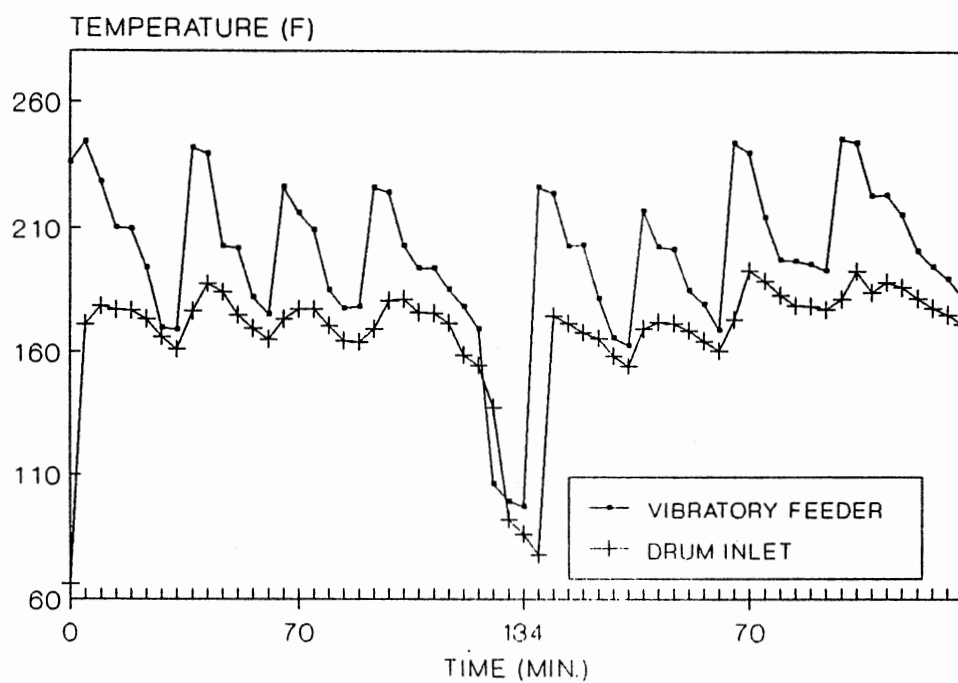


Figure 126. Experimental Temperature Profiles for Run #5

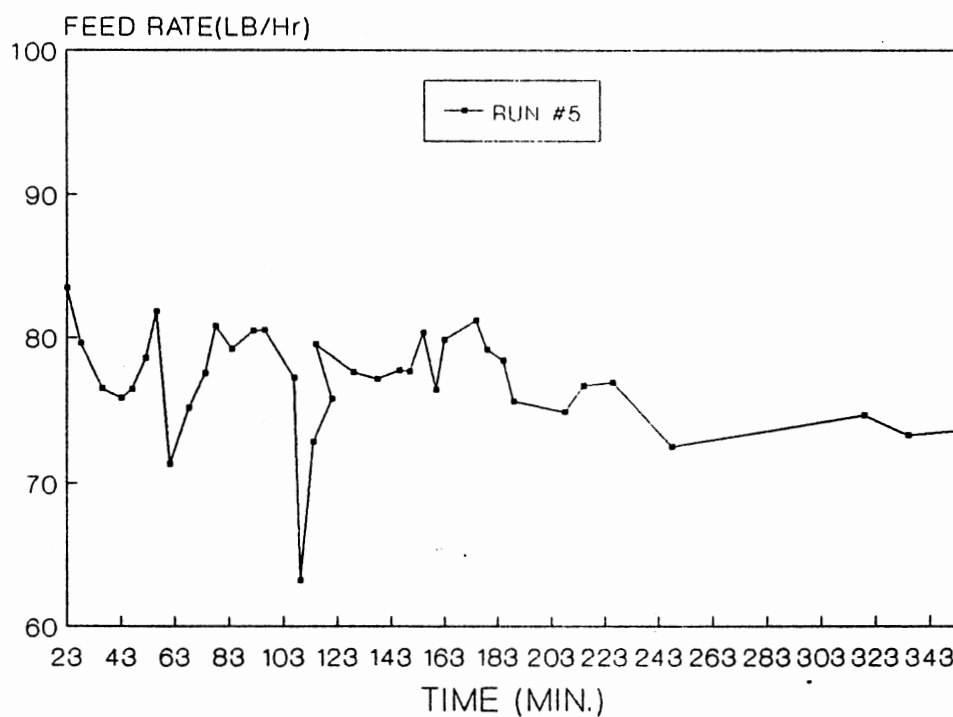


Figure 127. Feed Rates of Prop for Run #5

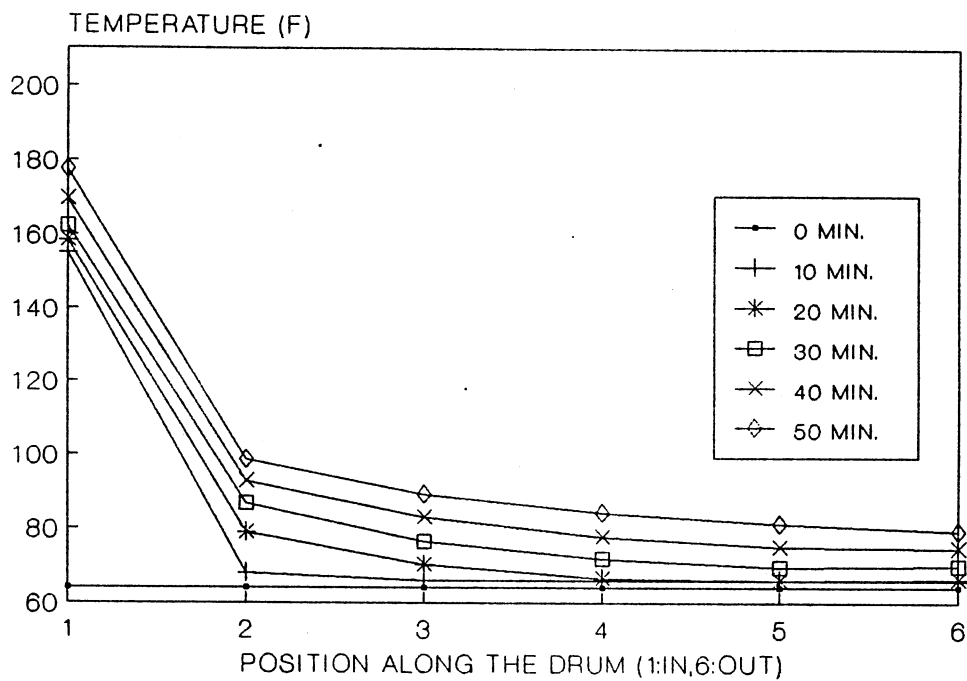


Figure 128. Experimental Temperature Profiles for Run #6

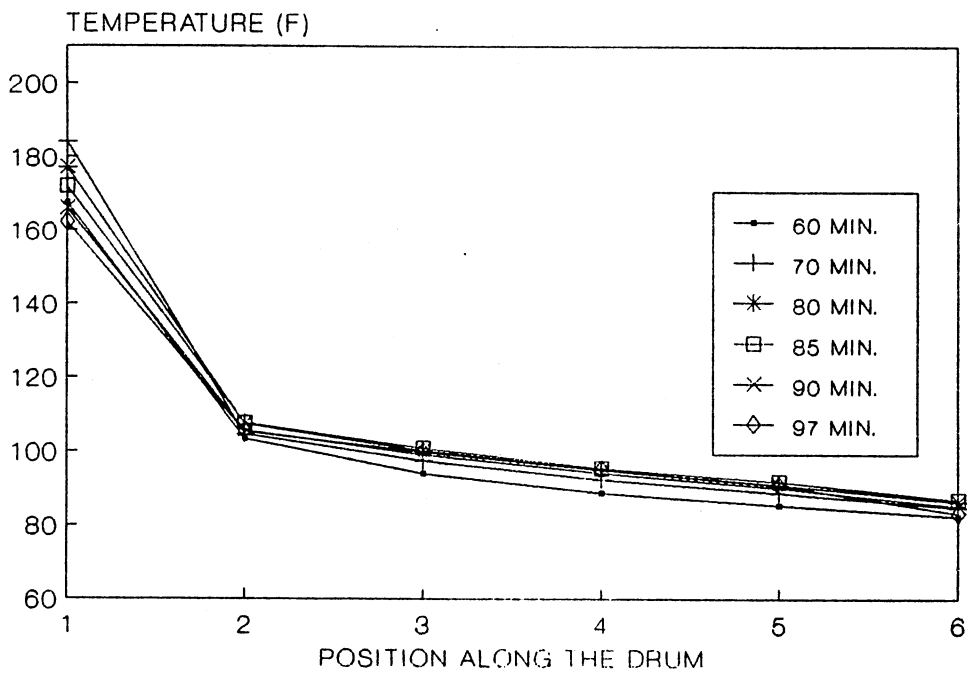


Figure 129. Experimental Temperature Profiles for Run #6

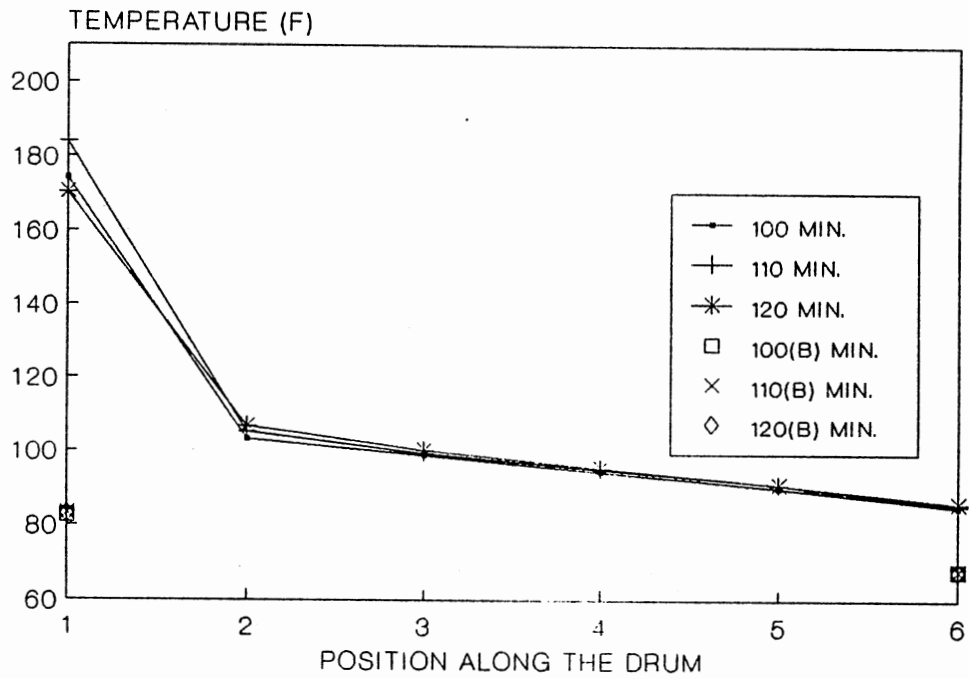


Figure 130. Experimental Temperature Profiles for Run #6

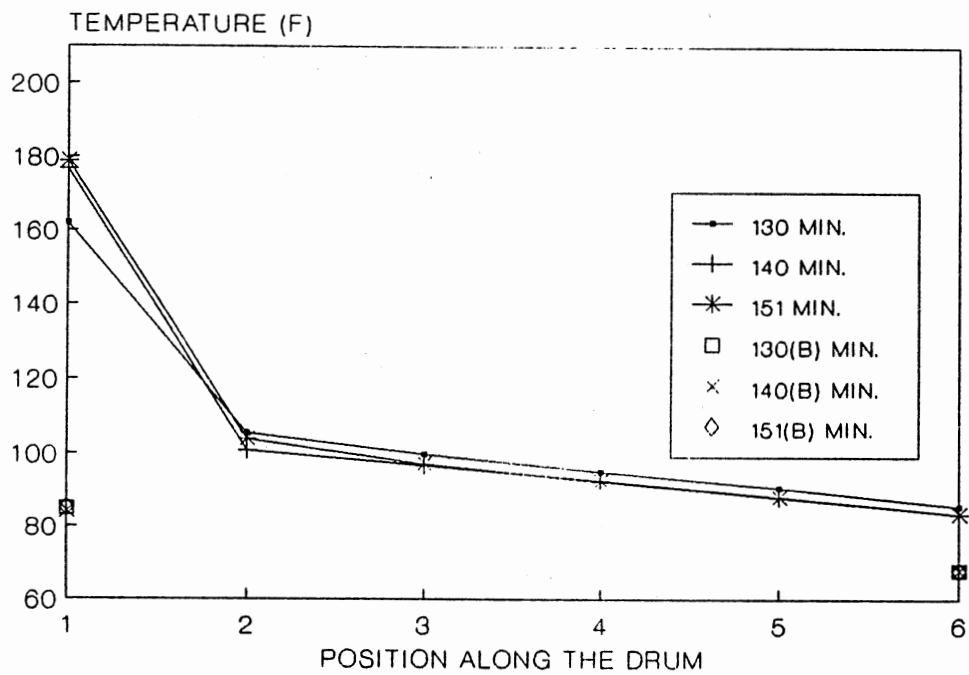


Figure 131. Experimental Temperature Profiles for Run #6

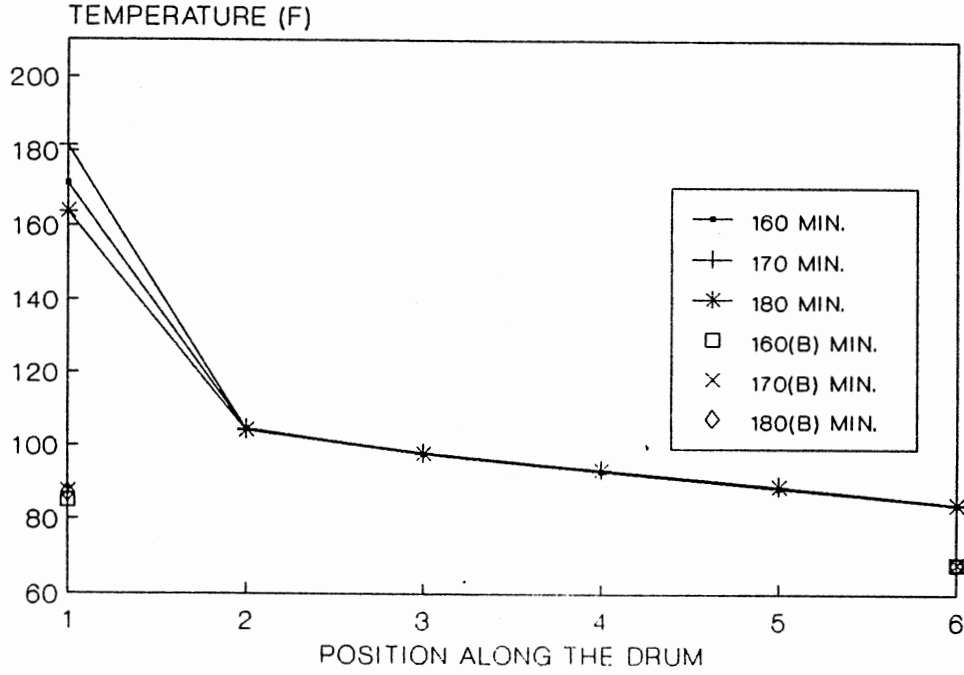


Figure 132. Experimental Temperature Profiles for Run #6

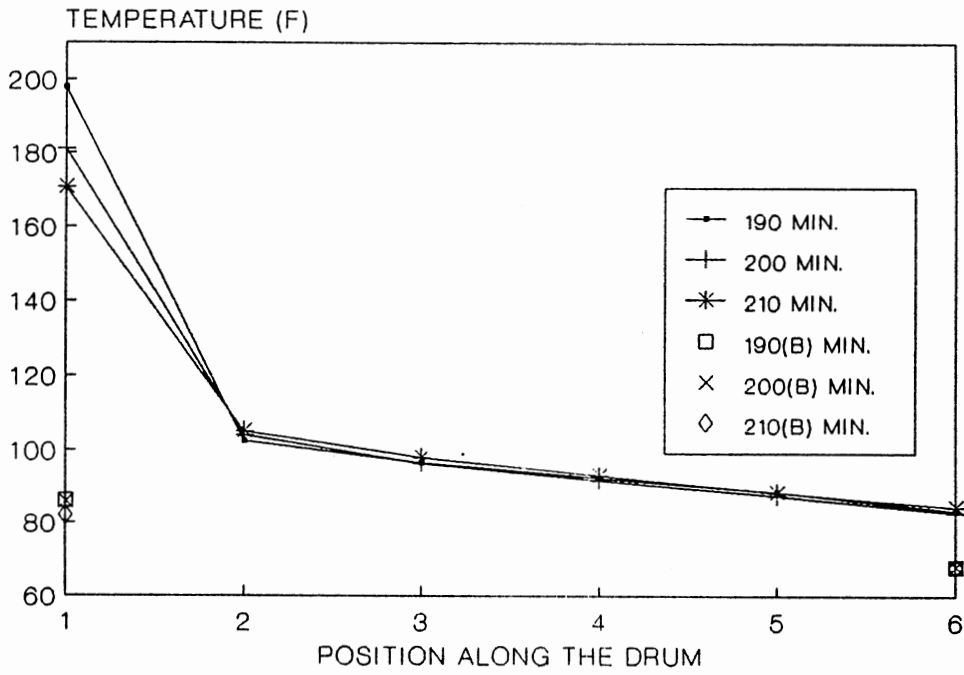


Figure 133. Experimental Temperature Profiles for Run #6

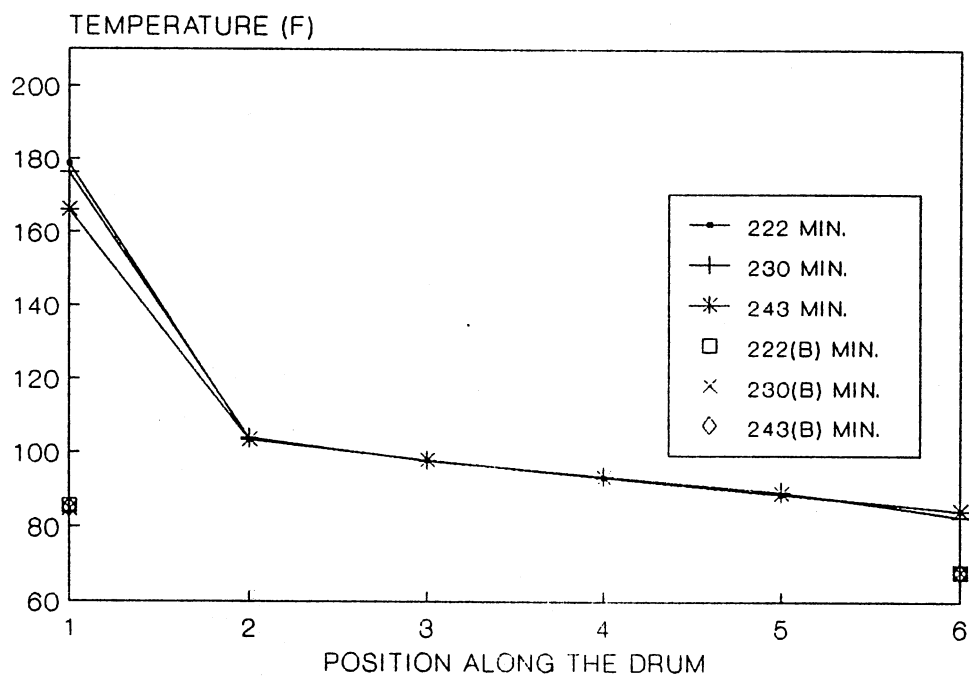


Figure 134. Experimental Temperature Profiles for Run #6

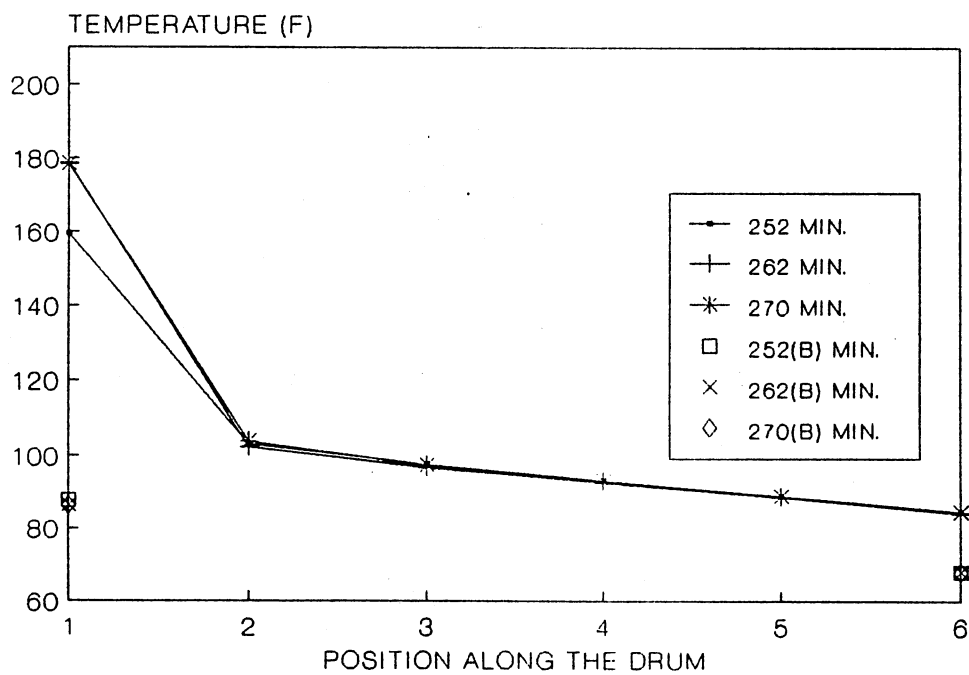


Figure 135. Experimental Temperature Profiles for Run #6

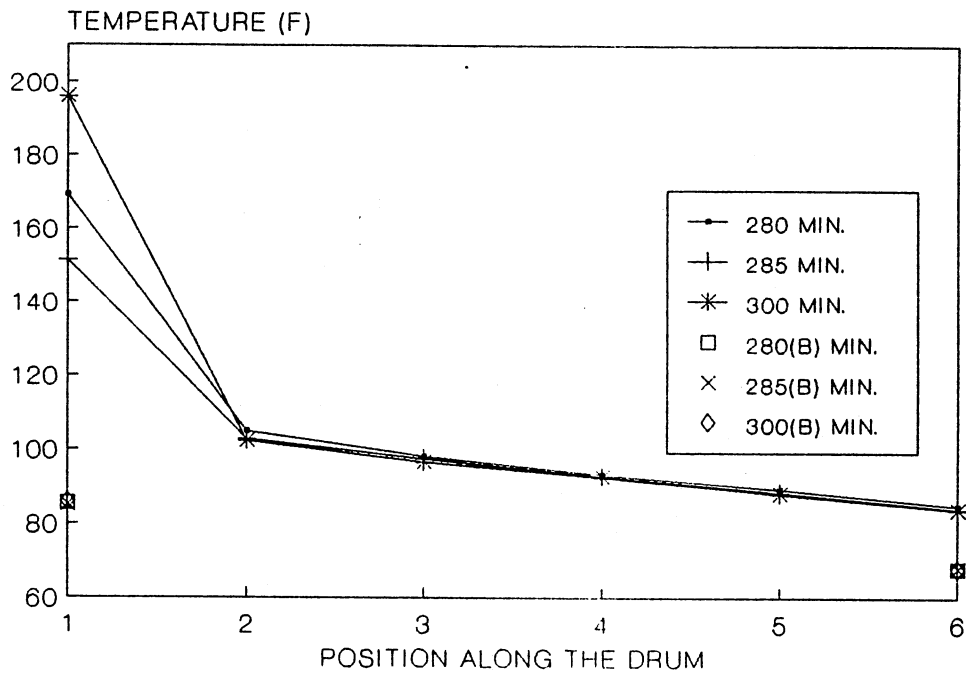


Figure 136. Experimental Temperature Profiles for Run #6

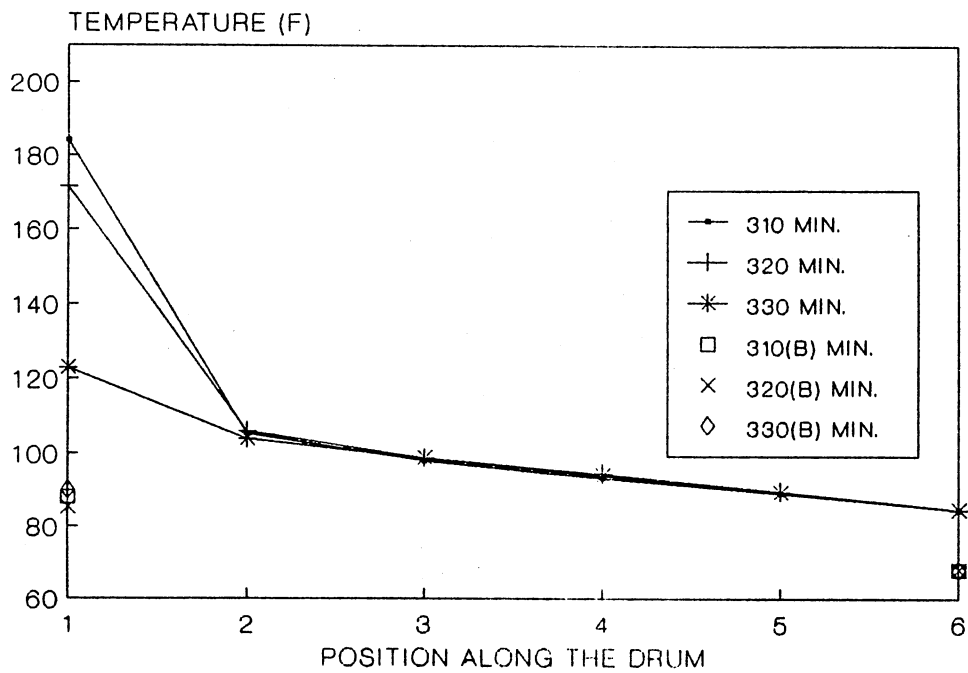


Figure 137. Experimental Temperature Profiles for Run #6



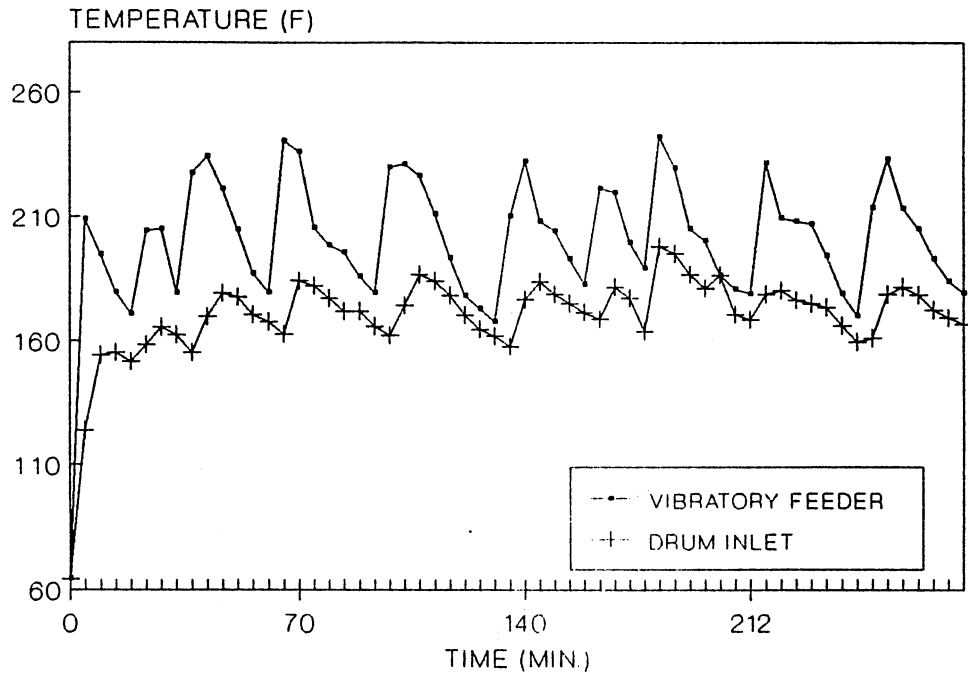


Figure 138. Experimental Temperature Profiles for Run #6

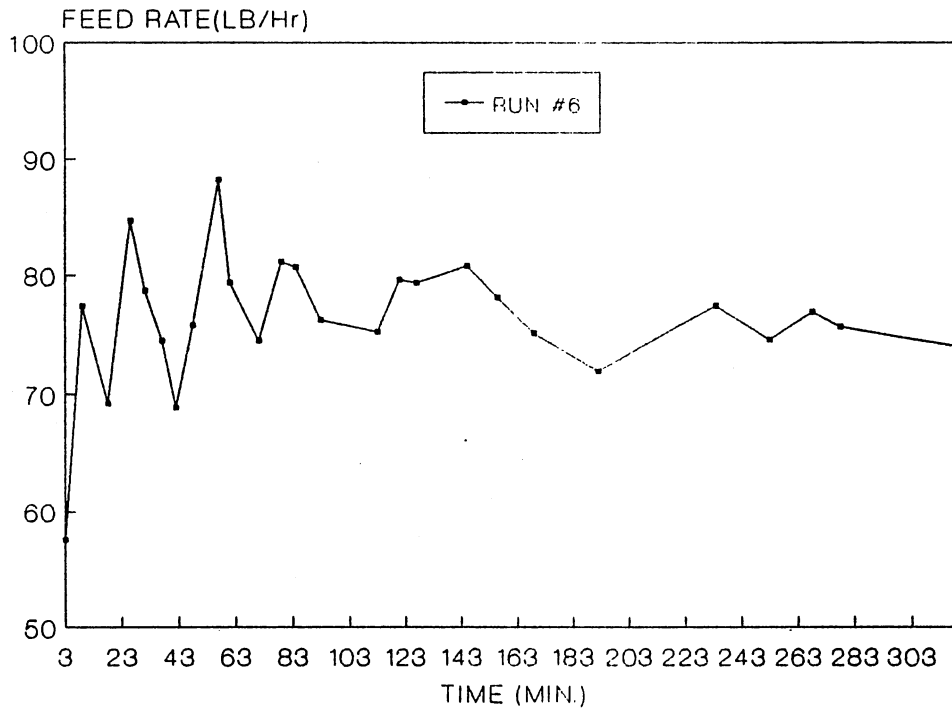


Figure 139. Feed Rates of Prop for Run #6

2  
VITA

Shyh-Jye Chern

Candidate For the Degree of  
Doctor of Philosophy

**Thesis:** EXPERIMENTAL DESIGN AND MODELING OF A CONTINUOUS  
COUNTERFLOW SOLID-SOLID HEAT TRANSFER PROCESS

**Major Field:** Chemical Engineering

**Biographical:**

**Personal Data:** Born in Ying Ko, Taiwan (ROC), Sep. 20,  
1957, the son of J. C. Chern and J. In. Chiu.

**Education:** Graduated from Chemical Engineering  
Department at National Taipei Institute of  
Technology, Taipei, Taiwan, in June 1978 with a  
Bachelor of Science in Chemical Engineering Degree;  
Received Master of Engineering in Chemical Engi-  
neering Degree from West Virginia Institute of  
Technology in May 1985; Completed Requirements for  
the Doctor of Philosophy Degree in Chemical  
Engineering at Oklahoma State University in July  
1989.

**Extracurricular Training:** Short Course on Micro-  
computer (1982).

**Professional Experience:** Assistant Engineer,  
Polymerization and Spinning Section, Hualon  
Chemical Textile Co., Taipei, Taiwan, June 1978 to  
June 1980; Design Engineer, Instrumentation and  
Control Division, Fu-Tai Engineering Consulting  
Co., June 1980 to July 1983; Graduate Teaching and  
Research Assistant, Chemical Engineering Depart-  
ment at West Virginia Inst. of Tech., December  
1983 to May 1985; Graduate Teaching and Research  
Assistant, Chemical Engineering Department at  
Oklahoma State Univ., August 1985 to July 1989.

**Professional Organization:** Honor Society of Phi-Kappa-  
Phi and Omega-Chi-Epsilon